Biochemical and structural analyses of two hyaluronan lyases

ZAINAB HUSSEIN ELMABROUK

PhD

2006

Biochemical and structural analyses of two hyaluronan lyases

ZAINAB HUSSEIN ELMABROUK

A thesis submitted in partial fulfilment of the requirements of the University of Northumbria at Newcastle for the degree of Doctor of Philosophy

Research undertaken in the school of Applied Sciences and in collaboration with York Structural Biology Laboratory at the University of York

October 2006

Abstract

Glycosaminoglycans are major components of the extracellular matrix, mostly in the form of proteoglycans. They are involved in a diversity of biological processes, ranging from cell signaling to blood coagulation. Hyaluronan and chondroitin sulphate comprise a biologically important subset of glycosaminoglycans. Hyaluronate lyases are glycosaminoglycan degrading enzymes that act as eliminases. They degrade hyaluronan the main polysaccharide component of the host connective tissues, thereby destroying the normal connective tissue structure and exposing the tissue cells to a variety of bacterial toxins.

Two members of family 8 polysaccharide lyases were cloned, expressed in *E. coli* and purified to homogeneity using immobilised metal affinity and gel filtration chromatography methods. The first lyase was SC1C2.15 (82.9 kDa) from the soil bacterium *Streptomyces coelicolor* A3(2). Characterisation of the *N*-terminal hexahistidine tagged protein revealed that the enzyme displayed hyaluronate lyase activity, and it exhibited activity toward hyaluronan, chondroitin-4 and 6-sulphate with the highest activity toward HA. The enzyme displayed an optimum activity at pH 5.2 against hyaluronan and 4.8 against chondroitin-4 and 6-sulphate and an optimum temperature at 57 °C. The kinetic parameters of the enzyme against sodium hyaluronan, potassium hyaluronan, chondroitin-4-sulphate and chondroitin-6-sulphate were determined in the absence and presence of calcium. Additionally, HPAEC analysis showed that the enzyme has an exolytic mode of action. The enzyme was crystallised and its three-dimensional structure solved at a resolution of 2.7Å. It was shown to be composed of two domains, an α-helical N-terminal catalytic domain and a β-sheeted C-terminal domain. Through site directed mutagenesis, it was found that amino acid residues Tyr253, His244 and Asn194 are crucial for the enzyme, as substitution of these amino acids with alanine resulted in the loss of activity of the enzyme toward all substrates, demonstrating that these residues are pivotal in the catalysis by the *Streptomyces coelicolor* hyaluronate lyase. Y253A and N194A were co-crystallised with hyaluronan disaccharide, hyaluronan tetrasaccharide, chondroitin-4-sulphate disaccharide and L-ascorbic acid 6-hexadecanoate. The complexes were bound in the cleft located on the N-terminal domain of the enzyme in front of the interface between the N-and C- terminal domains revealing that the active site (substrate-binding site) is found in the cleft. The α and β- domains of the *Streptomyces coelicolor* hyaluronate lyase were each cloned separately. Both subunits were expressed in insoluble form, and therefore both were refolded under denatured conditions. Characterisation of the N-terminal α-domain reveals the presence of small amounts of activity, representing approximately 10% of activity compared with the wild type enzyme, indicating that this domain is the functional domain of *Streptomyces coelicolor* hyaluronate lyase.

Another ORF hylA of *Streptococcus pyogenes* SF370 that encodes hyaluronate lyase was cloned using a ligase independent cloning system and hyper-expressed in *E. coli*. Biochemical characterization of HylA showed that the enzyme is active only toward hyaluronan. It worked most efficiently at pH and temperature of 6 and 47 °C respectively, with a K_m of 0.206 ± 0.01 mg ml^{-1} and a k_{cat} of 17.5 ± 0.56 s^{-1}. Moreover, the mode of action of the enzyme is endolytic as judged by analysis of digestion products by HPAEC. The enzyme was crystallised and sufficient quality diffraction data were derived enabling the determination of crystal parameters. Furthermore, four mutant proteins were generated via the mutagenesis strategy: Y327A, Y327F, N257A and H307A. These were expressed and purified in the same way as the native enzyme. The mutants Y327A, Y327F and N257A were completely inactive toward HA, while the mutant H307A showed very little activity against HA which was approximately 5 % of the level of activity of the wild type. The results of mutagenesis indicate that the enzymatic activity resides mainly within the N-terminal domain.

From family PL12, a gene coding for heparin sulphate lyase (Spy0628) was amplified from *Streptococcus pyogenes SF370* cloned, expressed in *E. coli* in the soluble form and purified to homogeneity. The enzyme was found to be inactive against heparin, heparan sulphate and all other glycosaminoglycans (hyaluronan, chondroitin-4 and 6-sulphate).

Table of Contents

List of Figures

List of tables

Declaration

I declare that the work contained in this thesis has not been submitted for any other award and that it is all my own work. The work was done in collaboration with the York Structural Biology Laboratory at the University of York

Name: Zainab Hussein Elmabrouk

Signature:

Date: October 2006

Acknowledgments

I would like to thank all the people who have contributed to this work.

In particular I am grateful to Professor Gary Black, my supervisor. I am very grateful for his support and encouragement. He has a wonderful energy and it has been great to be a part of his group. I wish to express unlimited appreciation to Dr Simon Charnock to whom I am thankful for his scientific guidance, encouragement, and friendly advice.

My thanks to all the present and former members of the A307group, in particular to the Obaidur Rahman, Mandy Lyall, Anna Lindsay, and Meng Zhang for giving me valuable advices, help and to top it all a wonderful scientific feeling to work in. My thanks to all of them for providing that great impression which makes me feel at home.

I would like to thank all the people who have contributed to this work from York Structural Biology Laboratory. In particular I am grateful to Dr Edward Taylor, Dr Florence Vincent, Dr Johan Turkenburg and Prof. Gideon Davies.

My apologies to all others who I have not mentioned by name I am thankful to them for the many ways they helped me. Finally, I would like to pay acknowledgment to the constant support of my family members, whose love can never be repaid.

Abbreviations

A	Alanine
Å	Angstrom
Amp^r	Ampicillin resistance
APS	Ammonium persulphate
ATP	Adenosine triphosphate
bp	base pair (s)
BPB	Bromophenol blue
BSA	Bovine serum albumin
C	Cytocine
C°	Degree Celsius
CFE	Cell free extract
Cm	Chloramphenicol resistance
CS	Chondroitin sulphate
CSS	Clear strategy screen
C-terminal	Carboxy terminal
3 D	Three dimensional
Da	Dalton
DMSO	Dimethyl sulphoxide
DNA	Deoxyribonucleic acid
DsDNA	Double stranded DNA
DNSA	Dinitrosalicyclic acid
DNTP	Deoxynucleotriphosphate
DS	Dermatan sulphate
DTT	Dithiothreitol
ECM	Extracellular matrix
EDTA	Ethylene diamine tetraacetic acid Disodium sal
F	Phenylalanine
g	Gram(s)
G	Guanidine
GAG	Glycosaminoglycan
GluA	Glucuronic acid
GH	Glycoside hydrolase
HA	Hyaluronan / Hyaluronic acid
HEPES	N-[2-Hydroxyethyl]piperazine-N-[2-ethanesulphonic acid]
HEWL	Hen egg white lysozyme
His tag	Hexahistidine tag
HPAEC	High performance anion exchange chromatography
HS	Heparan sulphate
IMAC	Immobilised metal affinity chromatography
IPTG	Isopropyl- β-D-Thiogalactopyranoside
Kan	Kanamycin resistance
kb	Kilobase pair (s)
k_{cat}	Turnover number
k_{cat}/k_m	Catalytic efficiency
kDa	Kilodalton
k_m	Michaelis-Menten constant
KS	Keratan sulphate
L	Litre(s)

LB	Luria-Bertani medium
M	Metre(s)
M	Molar
MA	Milliamps
MAD	Multiple anomalous difference
min	Minute(s)
Mm	Millimetre
Mr	Relative molecular mass
MW	Molecular weight
N	Asparagine
NAG	N-acetylglucosamine
N-terminal	Amino terminal
OD	Optical density at x nm
ORF	Open reading frame
P	Plasmid
PAGE	Plyacrylamide gel electrophoresis
PCR	Polymerase chain reaction
PEG	Polyethylene glycol
PL	Polysaccharide lyase
rpm	Revolution per minute
s	Second(s)
SDM	Site-directed mutagenesis
SDS-PAGE	Sodium dodecylsulphate polyacrylamide gel electrophoresis
T	Temperature
TAE	Tris-Acetate-EDTA
TEMED	N,N,N,N-tetramethylethylene diamine
Tet	Tetracycline resistance
T7 lac	lac operator just downstream of T7 promotor
Tm	Melting temperature
Tris	Tris(hydroxymethyl)aminomethane
UDP	Uridine diphosphate
UV	Ultraviolet
V	Volt(s)
Vmax	Maximium velocity
v/v	Volume per volume
W	Tryptophan
w/v	Weight per volume
x g	Times gravity
X-gal	5-bromo-4-chloro-3-indoyl- β-D-galactoside
Y	Tyrosine
α	Alpha
β	Beta
K	Kilo
M	Milli
μ	Micro
n	Nano
1°	Primary
2°	Secondary
3'	Three prime
5'	Five prime

Chapter 1 General introduction

Carbohydrates are the most abundant class of organic compounds found in living organisms. They play an enormous variety of functions in biological systems, such as energy storage, cellular signalling and recognition sites on cell surfaces. The structural and functional diversity of carbohydrates is reflected by an enormous group of enzymes implicated in their synthesis (glycosyltransferases), modification (carbohydrate esterases) and degradation (polysaccharide lyases and glycoside hydrolases) (Henrissat *et al.*, 2001). These enzymes are termed carbohydrate active enzymes and they are catalogued in a Carbohydrate-Active Enzyme database that has been created and maintained since1998 (http://afmb.cnmrs.fr/~cazy/CAZY/index.html). These enzymes are divided into various families based on the similarity of their amino acid sequences.

This introduction first describes the structure of connective tissues in animal cells. This is because the substrates of the hyaluronate lyases are hyaluronan and chondroitin sulphate, which are the major components of these connective tissues in addition to other types of glycosaminoglycans including dermatan sulphate, heparan sulphate, heparin and keratan sulphate. This introduction also describes the structure of these glycosaminglycans and then describes in detail the polysaccharide lyases and glycoside hydrolases that degrade them.

1.1 Animal Connective tissues

Connective tissues arise from embryonic tissue called the mesenchyma, which is derived from the mesoderm, an embryonic germ layer that gives rise to muscles, nerves, skeletal tissue and the lining of the body cavities. Mesenchyme is the stem tissue of all the connective tissues of the body (Caplan and Bruder, 2001; Chiquet-Ehrismann and

Tucker, 2004). It is considered the most abundant and widely distributed tissue in the animal body. The main function of connective tissue is to bind and support a variety of body structures and to fill the spaces between them (Chiquet-Ehrismann and Tucker, 2004). Therefore, it provides protection for vital organs and facilitate locomotion. It differs from epithelial tissue in the arrangement and variety of cells and in the amount and kinds of matrix found between cells. It has fewer cells and large amounts of extracellular matrix (ECM) (Section 1.2), which is composed of ground substance and fibres (Junquira *et al.*, 1998; Ross *et al.*, 2003).

1.1.1 Connective tissue types

The various connective tissues are generally classified according to their composition and the organisation of their extracellular and cellular components, as well as their functions.

1.1.1.1 Loose connective tissue

Loose connective tissue, also called areolar tissue, is the most widespread of all connective tissues in the body. It is characterised by sparse, loosely arranged thin fibres and an abundance of cells. Also ground substance is abundant and occupies more volume than the fibres. This tissue holds organs in place and attaches epithelial tissue to other underlying tissues. It is located around blood vessels and nerves and fills the spaces between intermuscular planes (Figure 1.1). The function of loose connective tissue is to increase the elasticity in tissues and organs and to allow the movement of nutrients, oxygen and waste between capillaries and tissue cells.

The primary location of loose connective tissue is beneath those epithelia that cover the body surface. Hence it represents the initial site in which antigens and other foreign

substances or organisms that penetrate epithelial surfaces can be challenged and destroyed. It is thus the site of inflammatory and allergic immune reactions. Therefore loose tissue blocks the spread of pathogenic organisms, except those which can digest the ground substance. The main cells in loose connective tissue are fibroblasts. They are responsible for the synthesis of fibres and produce a variety of substances including glycoproteins, proteoglycans and glycosaminoglycans into the extracellular space. Fibroblasts are active during reparative processes secreting proteins that are needed to repair the tissue damage. Also other cells are present in this tissue such as macrophages, mast cells and plasma cells. Macrophages arise from monocytes, which circulate in the blood. They migrate into the connective tissues where they differentiate into macrophages. The chief function of these cells is defensive via the ingestion of foreign bodies by phagocytosis. Mast cells are found throughout connective tissues but are concentrated near blood vessels. The most obvious substances contained in the vesicles of these cells are heparin and histamine. The mast cells help immune responses to antigens that activate the release of histamine and heparin. Plasma cells originate from B-lymphocytes, which produce antibodies. They present in large numbers in the connective tissues of intestinal mucosa (Junquira *et al.*, 1998; Ross *et al.*, 2003).

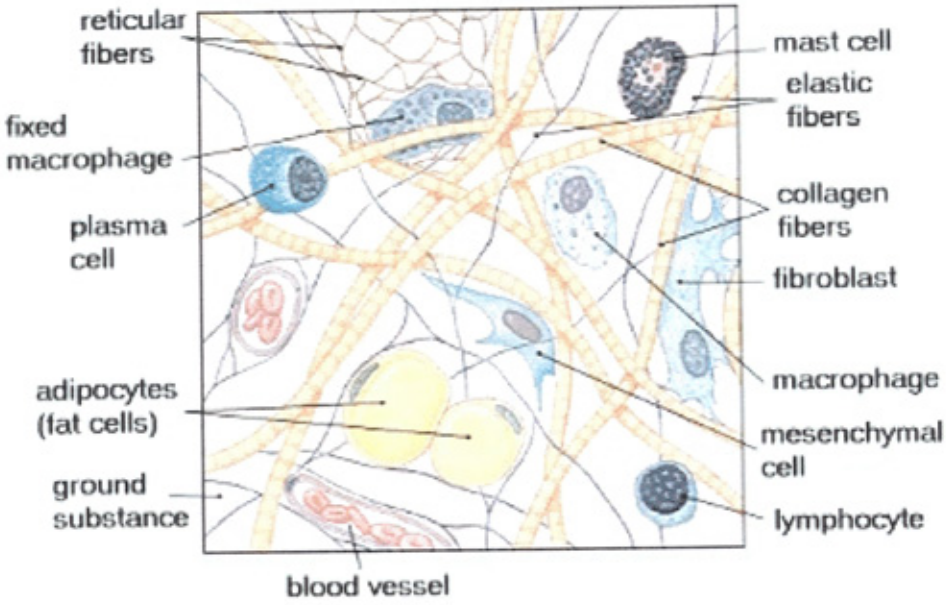

Figure 1.1 Loose connective tissue (taken from www.mhhe.com/biosci/ap/histology_mh/lossects.html).

1.1.1.2 Dense connective tissue

The predominant component of dense connective tissue is collagen fibres and it is the main fibres in the matrix of most connective tissues. Collagens are predominantly synthesised by fibroblasts, chondrocytes, myofibroblasts and osteoblasts (Bosman and Stamenkovic, 2003). They are synthesised as longer precursor protein called procollagens. Subsequently procollagens are converted by the action of enzymes at the plasma membrane into collagen molecules, which are then accumulated in the ECM space to form collagen fibrils that are responsible for the strength and integrity of connective tissue. Twenty different types of collagens (I - XX), have been identified to date which have different mechanical and functional preperties. They are classified by Roman numerals on the basis of their chronological discovery. The major fibrous collagens are collagen types I, II and III. Type I collagen is the most abundant structural

component in the skin, tendons and bones. The fibrils of this type are thick and closely packed. On the other hand type II collagen has thin fibres and is the most abundant protein in the cartilage. Type III collagen exists in many tissues; it is more abundant in wall of blood vessels and hollow intestinal organs (Bosman *et al.*, 2003; Rosso *et al.*, 2004). Type IV, VII, IX, X and XII are found associated with collagen fibrils or organised in the network as basal laminae (Rosso *et al.*, 2004). Types V and XI are minor components and locate mostly co-polymerised with collagen I and II, respectively (Bosman and Stamenkovic, 2003).

The classification of dense connective tissue depends on the orientation of fibres within the tissue. In dense irregular connective tissue, the fibres are arranged in bundles oriented in various directions to withstand stresses to which the structure can be subjected. This type is found in the dermis of the skin and forms a sheath like structure around bones and muscles. On the other hand, the fibres in regular dense connective tissues are arranged parallel to each other such as in tendons and ligaments (Junquira *et al.*, 1998; Ross *et al.*, 2003).

1.1.1.3 Adipose tissue

This form of connective tissue is essentially loose connective tissue containing large numbers of adipocytes supported by a collagen matrix. It is located around the kidneys, adrenals, mesenteries, under skin, grooves of the heart and bone marrow (Junquiera *et al.*, 1998).

1.1.1.4 Cartilage

Cartilage is a specialized form of connective tissue that lacks blood vessels, lymphatic vessels and nerve fibres. It is surrounded by a sheath of dense connective tissue called perichondrium, which contains nerves and lymphatic vessels (Kuettner, 1992). The

ECM of cartilage is composed of glycosaminglycans and proteoglycans, which interact with collagen and elastic fibres. These structural macromolecules give the cartilage its form and stability. Cartilage proteoglycans are composed of chondroitin 4-sulphate, chondroitin 6-sulphate and keratan sulphate that are covalently attached to core proteins. Articular cartilage is the connective tissue that covers ends of long bones in synovial joints, providing smooth articulation during joint movement. It lacks the perichondrium and is supplied by oxygen and nutrients from the synovial fluid through diffusion (Roughley and Lee, 1994; Knudson and Knudson, 2001). The specific structural organisation of articular cartilage matrix gives it biochemical characteristics such as elasticity and tensile strength, which give the cartilage its ability to absorb and distribute loads (Roughley and Lee, 1994; Buckwalter and Mankin, 1997; Huber *et al.*, 2000).

The pericellular environment of articular cartilage is characterized by the presence of large proteoglycans aggregates. Chondrocytes, the only cell types found in articular cartilage have CD44 receptor that interacts with hyaluronan (HA) (Knudson *et al.*, 1993) therefore binding proteoglycans to the cell. The pericellular environment has very little organised fibrillar collagens, but a high concentration of filamentous type VI collagen (Section 1.1.2.1) which also links to HA and interacts with the cell surface (Knudson and Knudson, 2001).

Cartilage is formed from type II collagen and aggregan. The interaction of aggregan with collagen and HA results in the organisation and stability of cartilage matrix. Aggregan is the most essential proteoglycan in the articular cartilage. It is a multimodular molecule expressed by chondrocytes. It is composed of about 100 chondroitin sulphate chains and some keratan sulphate chains with N- and O- linked oligosaccharides. Chondroitin sulphate chains account for the major function of

aggrecan due to its ability to bind huge amounts of water in ECM (Kiani *et al.*, 2002). The interaction between the aggrecan molecules and HA is stabilized by a glycoprotein called link protein which is a synthesised by the chondrocytes (Hardingham, 1979; Hedlund *et al.*, 1999). Aggrecan has essential role in mediating chondrocyte-chondrocyte and chondrocyte-matrix interactions via its ability to interact with HA.

1.2 Extracellular matrix

Most cells in multicellular organisms are surrounded by a complex mixture of non-living material known as the extracellular matrix. The ECM in vertebrates is composed of a mixture of structural and functional macromolecules that play an essential role in the maintenance of cell and tissue structure and function (Rosso *et al.*, 2004). ECM is made up of two classes of macromolecules. The first are high molecular weight carbohydrates that are composed of glycosaminoglycans portion covalently bound to a core protein. The core protein with the glycosaminoglycans attached is termed the proteoglycans. The other class of ECM macromolecule is fibres, which are large strands of protein insoluble in water. The fibrous protein is divided into two types: structural proteins such as collagen and elastin; and specialized proteins such as fibronectin (a glycoprotein which has binding sites for cells, glycosaminoglycans and collagen), vitronectin and laminin. The ability of a cell to proliferate, differentiate and function depends on the presence and maintenance of intact extracellular matrix (Hardingham and Fossang, 1992; Rosso *et al.*, 2004).

In addition the ECM promotes the regulation of cell behaviour, and the survival, development and communication of macromolecules such as collagen, elastin and fibronectin.

The ECM has three major functions. The first is to regulate cellular differentiation and metabolic functions. Secondly, it gives structural support for cells. Thirdly, it acts as a physical barrier or selective filter to soluble molecules (Adams and Watt, 1993).

1.2.1 Glycosaminoglycans

Glycosaminoglycans (GAGs) are a specific class of biological macromolecules, and they are the most abundant heteropolysaccharides in the body. They are unbranched polymer chains found in the ECM of tissues bound to structural proteins such as collagen, aggregated with other proteoglycans, or at cell surfaces as integral membrane proteoglycans (Ernst *et al.*, 1995; Vynios *et al.*, 2002).

GAGs are linear polysaccharides formed from variable numbers of repeating disaccharide units. They are synthesised as polymers consisting of repeated disaccharide units of hexosamine (D-galactosamine or D-glucosamine) and uronic acid (D-glucuronic acid or L-iduronic acid) (Jandik *et al.*, 1994; Calabro *et al.*, 2001; Vynios *et al.*, 2002). They differ in the type of disaccharide, degree of sulphation, and linkages between these disaccharides (Figure 1.2). Consequently, many different types of GAGs have been identified namely HA, chondroitin-4- and 6-sulphate, dermatan sulphate, keratan sulphate, heparin and heparan sulphate (Tkalec *et al.*, 2000) (Figure 1.2).

Table 1.1 Structure of Glycosaminoglycans (taken from web.indstate.edu/thcme/mwking/glycans.htm).

Structure	GAG	Localization
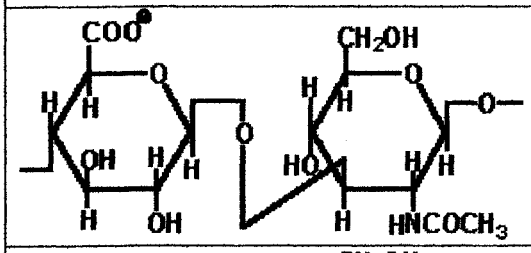	Hyaluronates: Composed of D-glucuronate + *N*–D-acetyl glucosamine linkage is β-(1, 3)	Synovial fluid, vitreous humor, ECM of loose connective tissue
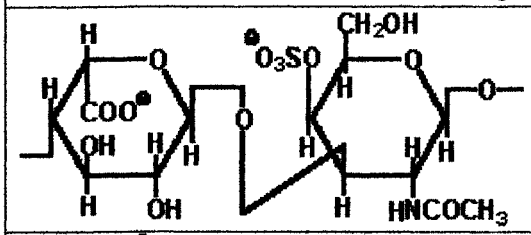	Dermatan sulphates: composed of L-iduronate (many are sulfated) + *N*–D-acetyl galactosamine -4-sulfate linkages is β-(1, 3)	Skin, blood vessels, heart valves
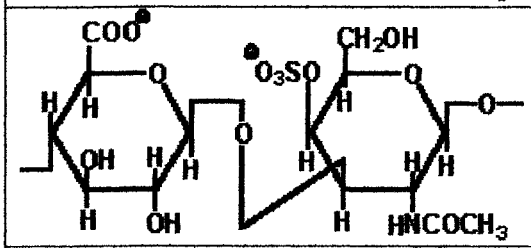	Chondroitin-4-sulphates: composed of D-glucuronate + *N*–D-acetyl galactosamine -4- or 6-sulfate linkage is β- (1, 3)	Cartilage, bone, heart valves
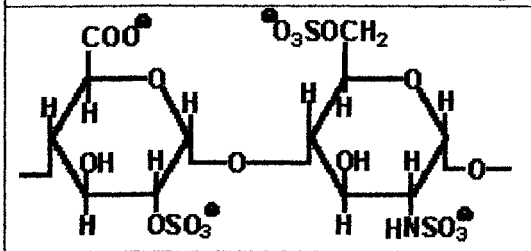	Heparin and Heparan sulfates:composed of D-glucuronate-2-sulfate (or iduronate-2-sulfate) + *N*-sulfo-D-glucosamine-6-sulfate linkage is β (1, 4) (heparans have less sulfate than heparins)	Basement membranes, components of cell surfaces Heparin is a component of intracellular granules of mast cells lining the arteries of the lungs, liver and skin
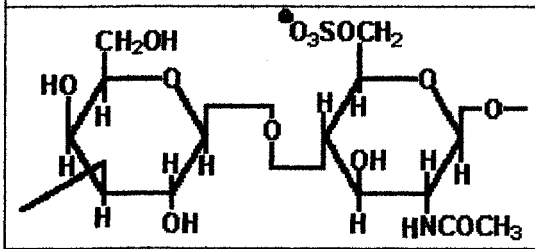	Keratan sulfates: composed of galactose + *N* –acetyl glucosamine-6-sulfate	Cornea, bone, cartilage aggregated with chondroitin sulfates

In their biosynthesis all GAGs except HA are covalently bound to core proteins, forming proteoglycans in the endoplasmic reticulum and Golgi apparatus. However, HA does not contribute to proteoglycan formation. The linkage of GAGs to the protein core involves a specific trisaccharide linker, which is composed of two galactose residues and a xylulose residue. The trisaccharide linker is bound to the protein core through O-glycosidic bond to the serine or threonine residue in the protein (Perrimon and Berufield, 2001; Varki *et al.*, 2003). The protein cores of proteoglycans are rich in serine and threonine residues, which allow multiple GAG attachment. The GAG chain is extended via the alternative addition of glucuronic acid and *N*-acetyl galactosamine to the non-reducing end (Iozzo, 1998; Vynios *et al.*, 2002).

GAGs have many functions which are important in the body, such as their ability to fill space and bind water molecules in the ECM. This function is critical to tissues such as the cornea and cartilage (Scott, 1992). Moreover, they afford structural integrity to cells and allow the migration of cells. Due to the high viscosity of GAGs they are perfect for lubricating fluid in the joints (Varki *et al.*, 2003). GAGs have a role in physiological processes such as glomerular permeability, neuron development, angiogenesis, and act as barriers to diffusion across basement membranes, and as anticoagulant coatings of blood vessels (Ernst *et al*, 1995).

Some proteoglycans have only one GAG chain, such as decorin, which is a chondroitin sulphate/-dermatan sulphate proteoglycan. Others may have more than 100 chains like aggrecan, which is a chondroitin sulphate/-keratan proteoglycan (Roughley and Lee, 1994).

Proteoglycans are widely distributed in animal tissues and are synthesised by nearly all types of cells. They are found on cell surfaces and inside the cells as well as in the ECM. For example, perlecan is a heparan sulphate proteoglycan found in the ECM; whereas serglycin is a heparin proteoglycan located inside the cell (Iozzo, 1998). Proteoglycans are most abundant in the connective tissues, especially in articular cartilage. The most abundant proteoglycan in articular cartilage is aggrecan, which is characterised by its ability to interact with HA to form large proteoglycan aggregates (Roughley and Lee, 1994; Knudson et al., 2000).

The variability of proteoglycans and their interaction with many molecules give them the ability to fulfil many functions such as mediating the binding of cells to the matrix, connecting the components of ECM together and playing a vital role in cell proliferation and migration. They also have an essential role in modulating the structure of skin and regulating its functions (Ruoslahti, 1989; Prathiba and Gupta 2000).

The structural variability of GAG chains contribute to the various roles of proteoglycans. For instance, the binding of heparan sulphate to proteins serves a variety of biological activities such as organogenesis in embryonic development, angiogenesis, regulation of blood coagulation, modulation of growth factor activities, and cell adhesion (Hardingham and Fosang, 1992; Salmivitra *et al.*, 1996; Rosenberg *et al.*, 1997).

Another example of protein-GAG interaction occurs in the corneal stroma where the core proteins of dermatan sulphate proteoglycan bind to collagen fibres. It has been suggested that self-association of DS controls the distance between collagen fibres, therefore enabling the crucial transparency of the cornea (Scott, 1992).

1.2.1.1 Keratan Sulphate

This is the only GAG which does not contain uronic acid. Keratan sulphate (KS) is a sulphated polylactosamine chain composed of alternating units of β 1,4- linked galactose (Gal) and β 1,3- linked N-acetyl-D-glucosamine, with O- sulphate groups at position C-6 of the Gal and/or N-acetyl-D-glucosamine units (Roughley and Lee, 1994; Funderburg, 2000). There are two types of KS which are different from each other in the type of glycosidic linkage on the protein core. An N- glycosidic linkage is typically present in cell bound glycoproteins and is characteristic of the corneal KS (KS I), while the O-glycosidic linkage usually exists in mucins and is characteristic of the cartilage KS (KS II). The molecular weight of KS is usually small, ranging from 10 –26 kDa in type I KS to approximately 5 kDa in type II (Ernst *et al.*, 1995; Vynios *et al.*, 2002).

1.2.1.2 Heparan sulphate and heparin

Heparan sulphate and heparin are sulphated GAGs which are composed of alternating units of β 1, 4- linked hexuronic acid and α 1,4-linked glucosamine. The glucosamine is mostly N-acetylated or N-sulphated. The hexuronic acid unit is either L-iduronic acid or glucuronic acid (Laurent and Fraser, 1992; Su *et al.*, 1996; Mao *et al.*, 2002). The sulphation may occur at carbon positions 2, 3 or 6 of glucosamine or at carbon 2 of the hexuronic.

Heparin is found in the granules of the connective tissue mast cells that line arterial walls (Esko and Lindahl, 2001). It has many functions in the body including the inhibition of blood coagulation, potentiation of angiogenesis and modulation of cellular proliferation (Watanabe *et al.*, 1998).

Heparin has a similar structure to heparan sulphate, but has more sulphated groups (Su *et al.*, 1996; Pope *et al.*, 2001; Esko and Lindahl, 2001; Mao *et al.*, 2002). Heparan

sulphate is found ubiquitously on cell surfaces and in the ECM covalently bound to a variety of different proteins forming heparan sulphate proteoglycans. Syndecans and glypicans are the main cell surface proteoglycans (Pope *et al.*, 2001; Franco *et al.*, 2001).

Heparan sulphate is involved in many biological processes such as cell-cell adhesion, cell matrix adhesion, lipoprotein metabolism, blood coagulation, tissue regeneration, and inflammation (Kuberan *et al.*, 2002). Furthermore, heparan sulphate controls the activity of growth factors and the cytokines that contribute to cell proliferation, migration and the production of matrix. The wide range of biological activities of heparan sulphate/heparin results from their specific interactions with different proteins, ligands and receptors (Yamada and Sugahara, 1998; Franco *et al.*, 2001).

1.2.1.3 Chondroitin sulphate and dermatan sulphate

Chondroitin sulphate (CS) and dermatan sulphate (DS) are sulphated GAGs which are considered the most common types of GAGs in ECM proteoglycans. They are composed of alternating units of β 1,3-linked hexuronic acid and β 1, 4-linked N-acetyl-D-galactosamine with a sulphated group position at C-4 and/or 6 at N-hexoseamine (Laurent and Fraser, 1992; Roughley and Lee, 1994; Pojasek *et al.*, 2001; Pojasek *et al.*, 2002; Mao *et al.*, 2002). Therefore, the name chondroitin 4-sulphate or chondroitin A is used if the sulphate groups are located at the C4 position of N-acetyl galactosamine; whereas are termed chondroitin 6-sulphate or chondroitin C if the sulphation occur at the C6 position of N-acetyl galactoseamine (Roughley and Lee, 1994; Pojasek *et al.*, 2001). The presence of sulphate groups at different locations in the CS chain results in the structural variability of the chain and consequently functional diversity (Nadanaka *et al.*, 1998). The sulphation of GAGs in CS chains is usually regular, with one sulphate

per disaccharide throughout the chain. This contrasts with heparan sulphate chains where sulphation is irregular.

The distribution of chondroitin 4-sulphate and chondroitin 6-sulphate differs in the cartilages of different human bones. For instance, equal amounts of chondroitin 4-sulphate and chondroitin 6-sulphate are found in the subarticular cartilages, whilst articular and vertebral body cartilages have only chondroitin 6-sulphate (Mourao *et al.*, 1976). Moreover adult cartilages comprise exclusively of chondroitin 6-sulphate. It has been suggested that chondroitin 4-sulphate is a crucial compound for the calcification process, whereas chondroitin 6-sulphate is important in the integrity of articular surfaces playing a secondary role in calcification processes (Mourao *et al.*, 1976; Rodrigues et al., 2005).

CS is found abundantly in ECM, and particularly in cartilage. It is also found in neural tissues and cell surfaces. It has an essential role in a variety of biological activities. For example, it holds water and nutrients and allows molecules to move through cartilage. Additionally, CS can decrease the level of cholesterol in the blood and prevent excessive blood clotting.

DS is also called chondroitin B. It is synthesised as CS chains, and then some of its glucuronic residues undergo epimerisation to iduronate through a change of the configuration of the carboxyl group at carbon 5 of the sugar ring. A polysaccharide is accordingly considered to be DS if some of its hexuronic acid units are idouronic acids; while it is considered to be CS if all the hexuronic acids are glucuronic acids (Malmstrom and Aberg, 1982; Laurent and Fraser, 1992; Mao *et al.*, 2002).

DS occurs predominantly in small proteoglycans with 2 to 8 side chains of 15-55 kDa, but CS is found in large aggregating protoeglycans with 20 to 100 GAG chains of 15-70 kDa (Ernst *et al.*, 1995).

1.2.1.3.1 Biosynthesis of chondroitin sulphate

The biosynthesis of CS occurs by the action of many membrane bound enzymes found in the endoplasmic reticulum and Golgi bodies (Salmivirtu *et al.*, 1996). The first step in the biosynthesis of CS is the addition of xylose to the OH serine residue in the core protein by xylosyl transferase. Subsequently, two Gal residues and glucuronic acid residue are added to form a tetrasaccharide structure. After that the polymerisation of chondroitin takes place in Golgi organelles by the alternating addition of N-acetyl-D-galactosamine and glucuronic acid, yielding repeating disaccharide regions. Two types of enzymes, designated N-acetyl galactosaminyl-transferase and glururonyl transferase catalyse the biosynthesis of CS (Sugumaran and Silbert 1990; Nadanaka 1999). The sulphation of N-acetyl-D-galactosamine residues takes place during the process of chain elongation via a specific sulphotransferase that gives sulphate groups at the carbon 4 or 6 position of N-acetyl-D-galactosamine (Sugumaran and Silbert 1990; Roughley and Lee, 1994; Nadanaka 1999).

1.2.1.4 Hyaluronic acid

HA is a major constituent of soft connective tissue and is a component of the ECM. It is also the main component of the microbial capsule of some pathogenic bacteria such as *Streptococcus pyogenes.* It is a non-sulphated GAG chain of variable length. HA is considerably larger than the other GAGs, with a chain length ranging from one hundred to several thousand disaccharides. HA is composed of repeating disaccharide units of glucuronic acid and N-acetyl-D-glucosamine that are linked by alternate β1-3 and β 1,

4-linkages (Itano and Kimata, 1996; Day and Sheehan, 2001). HA carries a high net negative charge from the carboxyl groups of the glucuronic acid residues, which in biological systems are associated with many mobile cations, such as Ka^{+}, Na^{+}, Mg^{2+} and Ca^{2+} forming a neutral salt (Laurent *et al.*, 1992).

HA is found in nearly all tissues throughout vertebrates. It may exist free, as in synovial fluid, or distributed with fibrous matrices as in skin and vitreous humor. The highest concentration is found in the synovial fluids of all joints, the vitreous body of the eye, amniotic fluid, hyaline cartilage and skin tissue (Fraser *et al.*, 1997; Csoka *et al.*, 2001). It is also found in other organs and tissues such as muscle, kidney, lung and brain, while blood serum contains the lowest concentration of HA (Fraser *et al.*, 1997).

Moreover, HA plays an important role in the integrity of tissue through its interaction with cells, collagen and other interstitial matrix components, and it is crucial for the stabilization of loose connective tissues (Fraser *et al.*, 1997). Therefore it has been suggested that removal of interstitial HA leads to an increase in tissue permeability (Coleman, 2002).

Furthermore, HA is involved in many physiochemical and biological processes such as space filling, lubrication, providing a hydrated matrix through which cells can migrate, wound healing, the development of cancer, and immune cell adhesion (Itano and Kimata, 1996; Day and Sheehan, 2001; Day and Prestwich, 2002). This is because HA binds to a large number of proteins that differ considerably in their affinity, specificity and cellular localisation (Day and Prestwich, 2002).

In addition, it has been established that HA increases in the early phase of tissue repair and accumulates in inflammation, edema, myocardial infarction, rheumatic joints, and

wound repair (Shyjan *et al.*, 1996; Fraser and Laurent 1997; Csoka *et al.*, 2001). Therefore, due to its involvement in so many diverse processes, HA can play a major role in both the normal and abnormal functions of cells.

Laurent *et al.* suggested in 1992 that excessive production of HA at the plasma membrane result in a slight loosening of the cells from the ECM, and consequently cell division occurs easily. Also, an increased amount of HA in the ECM is related to cell migration in embryogenesis, wound healing and tumour cell invasion. This is because its highly hydrated structure facilitates cell movement and migration (Brecht *et al.*, 1986; Knudson *et al.*, 1993).

One of the most typical properties of HA is its visco-elasticity in the hydrated state. Upon binding water, its volume increases by about 1000 fold compared to the non-hydrated state. In the hydrated state, the diffusion of electrolytes and proteins is significantly facilitated (Laurent *et al.*, 1996; Gerdin and Hallgren, 1997).

1.2.1.4.1 Receptors of HA

There are many receptors of HA on cell surfaces that direct the effect of HA and thus influence cell behaviour (Laurent and Fraser, 2000; Day and Prestwich, 2002). These receptors link to high molecular weight HA as well as with small fragments. One of these receptors is a receptor for HA mediated motility (RHAMM), which is found in many subcellular compartments such as mitochondria and cell surfaces. The binding of this receptor with HA plays an important role in activating signalling pathways (Bajorath *et al.*, 1998; Tammi *et al.*, 2002).

The other receptor which is considered the most common receptor for HA is CD44 (lymphocyte homing receptor). CD44 is a family of transmembrane glycoprotein and belongs to a group of HA–binding proteins called hyaladherins. CD44 appears in different forms. A short form is found on normal cells, and longer variants are found on motile cancer cells only (Knudson, 1996). A part of CD44 protrudes via the surface membrane into the cell cytoplasm, where it mediates the interaction with the cytoskleleton, the machinery for cell movement. The binding of CD44 receptors with HA has been documented to play a vital role in the process of tumor metastasis, promoting the formation of tumor embolisms which sequentially, increases the chances that the tumor cells would be trapped in the lungs (Zhang *et al.*, 1995; Stern *et al.*, 2001).

The interaction of HA with CD44 plays a fundamental role in cell adhesion to ECM components and is involved in the stimulation of proliferation, migration and angiogenesis. Furthermore, CD44 appears to perform an important function in the degradation of HA through pulmonary macrophages and other cells. The first step of this depolymerization is the attachment of HA to the cell surface. Then it enters the cell, carried into a lysosomal compartment, and eventually depolymerised by acid hydrolases (Underhill, 1992; Culty and Underhill, 1992).

The depolymerization of HA is essential in some tissues. For instance, an increased amount of HA in adult lung tissue could inhibit the exchange of blood and gas, and therefore it is necessary to eliminate HA from the system via macrophages (Fraser *et al.*, 1988; Underhill, 1992). It has also been demonstrated that CD44 has an essential role in embryonic morphogenesis and organogenesis through the localized degradation of HA (Underhill, 1992).

1.2.1.4.2 HA biosynthesis

HA biosynthesis occurs by the action of several membrane bound enzymes located at the cell membrane (Itano and Kimata, 1996; Shyjan *et al.*, 1996). The hyaluronan synthase enzyme is unique among known enzymes because it harbours the two glycosyltransferase activities required for HA polysaccharide production (Weigel *et al.*, 1997).

The synthesis of HA in streptococci is controlled by an operon composed of three different genes: *hasA, hasB* and *hasC*. *hasA* encodes hyluronate synthase, *hasB* encodes Uridine diphosphate (UDP)-glucose dehydrogenase and *hasC* encodes UDP-glucose pyrophosphorylase (Dougherty and van de Rijn, 1994; Crater and van de Rijn, 1995; Shyjan *et al.*, 1996; Alberti *et al.*, 1998). It has been demonstrated that *hasC* is not involved for HA synthesis suggesting that there is another source of UDP-glucose is available in the cell for HA production (Ashbaugh *et al.*, 1998).

The synthesis of HA occurs at the inner surface of the plasma membrane, unlike with other GAGs where it occurs in the Golgi body. The HA chain is produced by the alternate addition of glucuronic acid and N-acetyl glucosamine from their UDP derivative onto the reducing end of the chain through the effect of hyaluronate synthase. The non-reducing end of the growing chain extrudes into the extracellular space (Watanabe and Yamaguchi 1996; Kakehi *et al.*, 2003).

It has been reported that the synthesis of HA is increased in the interstitium during various disorders of joints especially, inflammation. Therefore, when the production of HA in connective tissues is increased, especially in and around the joints, this leads to increased elimination of HA in the circulation. Thus, the level of HA in the serum is enhanced (Gerdin and Hallgren, 1997; Laurent 1997).

1.2.1.4.3 The microbial capsule

Certain pathogenic bacteria produce a capsule made of an extracellular polysaccharide, which is considered a virulence factor. Due to the similarities between this microbial polysaccharide and the GAGs of the host, the antibody response to such bacteria is very weak. Consequently pathogenic bacteria with such a capsule can easily avoid the immune system (Bisno *et al.*, 2003).

Group A streptococci have an outer HA capsule which, along with the M protein, is considered to be an important virulence factor of this species. Group A carbohydrate antigen and the type-specific M-protein are attached to the bacterial cell wall and membrane (Figure 1.2). Both HA and M- protein give the streptococcal cell antiphagocytic properties (Moses *et al.*, 1997; Cunningham 2000).

The mucoid strains of group A streptococci cause more severe infections than non-mucoid strains. Wesseles *et al.* (1991) found that, in a capsular mutant, the resistance to phagocytosis is lost despite the presence of M protein and the virulence of these strains is significantly reduced in mice.

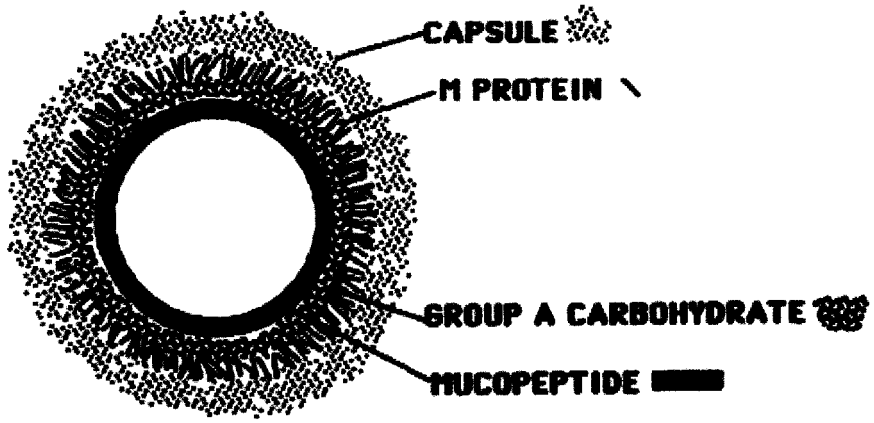

Figure 1.2 Diagram of the group A streptococcal cell
The cell is covered with an outer HA capsule and the group A carbohydrate, consisting of a polymer of rhamnose with *N*-acetylglucosamine side chains. Streptococcal M protein extends from the cell wall and is anchored in the membrane (taken from Cunningham 2000).

1.3 Carbohydrate-active enzymes classification

Carbohydrate active enzymes (CAZy) are classified into families according to the amino acid sequence similarities (Coutinho and Henrissat, 1999; Henrissat and Coutinho, 2000, http://afmb.cnrs-mrs.fr/CAZY). This present classification procedure is based upon hydrophobic cluster analysis (Henrissat, 1991; Henrissatand Bairoch 1996; Coutinho and Henrissat, 1999), a powerful amino acid sequence comparative technique that can detect structural similarities despite low primary amino acid similarities. A significant advantage of classification according to sequence similarities is that it allows logical grouping of enzymes of different EC numbers into polyspecific families and offers insights into the divergent evolution of enzyme families (Henrissat and Coutinho, 2000).. Conversley, some enzymes that can be grouped by function have been shown to belong to several distinct families and thus reflect convergent evolution (Henrissat, 1991; Davies and Henrissat, 1995; Campbell *et al.*, 1997, Henrissat and Davies, 1997; Coutinho and Henrissat, 1999). The CAZy server illustrates the modular structure of carbohydrate-active enzymes and has been produced to offer access to updated

classifications of polysaccharide lyases, glycoside hydrolyases, glycosyltransferases, carbohydrate esterases and carbohydrate-binding modules in families. Fundamental of this classification was the prediction that sequence determines structure, and thus useful structural, evolutionary and even mechanistic information can be derived from amino acid sequence alone (Campbell *et al.*, 1997; Henrissat and Davies, 1997; Davies, 1998; Davies and Henrissat, 2001). Accordingly, all members of a family share common properties that can be predicted if the property is determined for one or more of the family members.

The characteristic that makes these families especially valuable is that, despite accommodating different substrate specificities, they correlate with numerous structure-based properties of the enzymes, for instance important conserved fold and active site geometry. With the development of genome sequencing, this classification system has vast predictive power (Davies et al., 2005).

There are two classes of enzymes that cleave the glycosidic bond. The first class contains polysaccharide lyases. These cleave glycosidic bonds through the β-elimination mechanism. In contrast, the second class of enzymes that degrade glycosidic bonds is the glycoside hydrolases, which cleave the bond through a hydrolytic mechanism (Fietherie *et al.*, 1999; Li *et al.*, 2000).

1.3.1 Glycoside hydrolases

Over the past twenty years glycoside hydrolases have been extensively studied with an abundance of structural and biochemical data available. A naming system has been suggested for the sugar binding sites within glycoside hydrolases. This system depends on the naming of subsites from the point of enzymic cleavage. Accordingly, all the subsites toward the right of cleavage (i.e in the direction of the reducing end of the

substrate) are considered +1, +2 to +n are considered +1, +2 to +n whereas those toward the left of the site of cleavage (i.e in the direction of the non-reducing end of the substrate) are considered –1, –2 to –n (Davies *et al.*, 1997). Moreover, this system can be extended simply for use with polysaccharide lyases.

Glycoside hydrolyases cleave glycosidic linkages by a hydrolytic mechanism. This mechanism is further divided into inversion and retention mechanisms. Both mechanisms use a protonated carboxyl group from an acidic amino acid as the proton donor to the glycosidic oxygen, and an ionised carboxyl group as a catalytic base. The position of the catalytic base in relation to the proton donor differs. In the retention mechanism, the distance is about 5.5 Å, while in inverting enzymes it is about 10.5 Å (Rye and Withers, 2000; Henrissat and Coutinho, 2000; http://afmb.cnrs-mrs.fr/CAZY). In retaining enzymes the reaction proceeds by a double displacement mechanism, where the glycosidic bond is cleaved by proton donation. After that the water molecule activated by proton abstraction from the base starts a second nucleophilic attack upon the intermediate. On the other hand, inverting enzymes catalyse hydrolysis through a single displacement mechanism, in which the general acid-catalysed leaving group departure, whereas the general base-assistance to nucleophilic attack is by a water molecule from the opposite side of the sugar ring. The two catalytic residues of inverting enzymes are normally separated by ~ 10 Å between the catalytic base and sugar to allow the accommodation of the water molecule (Davies and Henrissat, 1995). The families of glycoside hydrolases that degrade GAGs are shown in Table 1.2.

Table 1.2: GH families that hydrolyase GAGs. Based on data derived from CAZy (http://afmb.cnrs-mrs.fr/CAZY/).

Family	Members	Known activity	Known mechanism	3-D structure
56	50	Hyaluronidase	Retaining	Fold $(\beta/\alpha)_7$
79	26	Heparanase/endo-β-glucuronidase	Retaining (Inferred)	Not available
84	31	Putative hyaluronidase/N-acetyl β-glucosaminadase	Unknown	Not available
88	41	Δα-4,5-unsaturated glucuronyl hydrolase	Unknown	$(\alpha/\alpha)_6$

1.3.1.1 Hyaluronidases

Hyaluronidase is a general term introduced to describe enzymes that degrade HA. The hyaluronidases are divided into three main groups (Figure 1.3), which have the same specificity but with different mechanisms of action. The first group is the hyaluronate-4-glycanohydrolyases (EC 3.2.1.35). This group includes the testicular type of hyaluronidase and the venoms of different snakes and insects. They cleave the β-N-acetyl-hexosamine (1→4) glycosidic bond in both HA and CS, yielding the tetra and hexasaccharides as end products (Menzel and Farr, 1998; Hynes and Walton, 2000; Kudo and Tu, 2001; Girish *et al.*, 2004). This type of enzymes are associated with both hydrolytic and transglycosidase activities (Girish *et al.*, 2004). In humans, hyaluronidase is found in many organs and body fluids; for instance, liver, testes, spleen, skin, kidney, uterus, placenta and sperm (Frost *et al.*, 1997; Csoka *et al.*, 1997; Csoka *et al.*, 2001). None of these enzymes have been comprehensively studied yet due to the difficulty of isolation, purification and activity assays, as well as their instability (Kreil, 1995).

The best-known hyaluronidase of eukaryotic is bovine testicular hyaluronidase. This has been extensively studied and is used in many medical fields such as ophthalmology,

orthopaedia and internal medicine (Menzel and Farr, 1998). The pH optimum of testicular hyaluronidase is dependent on the substrate used, hyaluronidase assay and incubation conditions (Gorham *et al.*, 1975; Otti *et al.*, 2003).

The second group (Figure 1.3) of hyaluronidases are hyaluronate-3-glycanohydrolases (EC 3.2.1.36), which are produced by leeches and some hookworms. The end products of these enzymes are also tetra- and hexa-saccharides.These enzymes cleave the β-1,3-glycosidic bond of HA, this group exhibit only hydrolytic activity (Menzel and Farr, 1998; Hynes and Walton, 2000; Girish *et al.*, 2004). Leeches produce hyaluronidase, which acts as a spreading factor facilitating the diffusion of other components that help the leech to obtain blood (Frost *et al.*, 1996; Csoka *et al.*, 1998).

Hyaluronidases break the glycosidic linkages of HA which are the most abundant mucopolysaccharide of the intercellular ground substance, consequently allowing the pathogens to penetrate and spread through host tissues. They cleave these bonds via a hydrolytic mechanism (section 1.3.1).

The third group of hyaluronidases (Figure 1.3) is bacterial hyaluronidases, more appropriately known as hyaluronate lyases (EC 4.2.2.1 or 4.2.99.1). These produce unsaturated disaccharides (Hynes and Walton, 2000; Girish *et al.*, 2004). It has been reported that bacteriophages isolated from some strains of bacteria such as *Streptococcus pyogenes* and *Streptococcus equi* also have hyaluronidases, which are not homologous with their bacterial enzymes (Hynes *et al.*, 1995). It has been documented that bacteriophage hyaluronidases degrade the HA capsules of bacterial host cells (Hynes *et al.*, 1995; Hynes and Walton, 2000). Moreover it appears that all the hyaluronidases found in prokaryotes are hyaluronate lyases (Smith *et al.*, 2005).

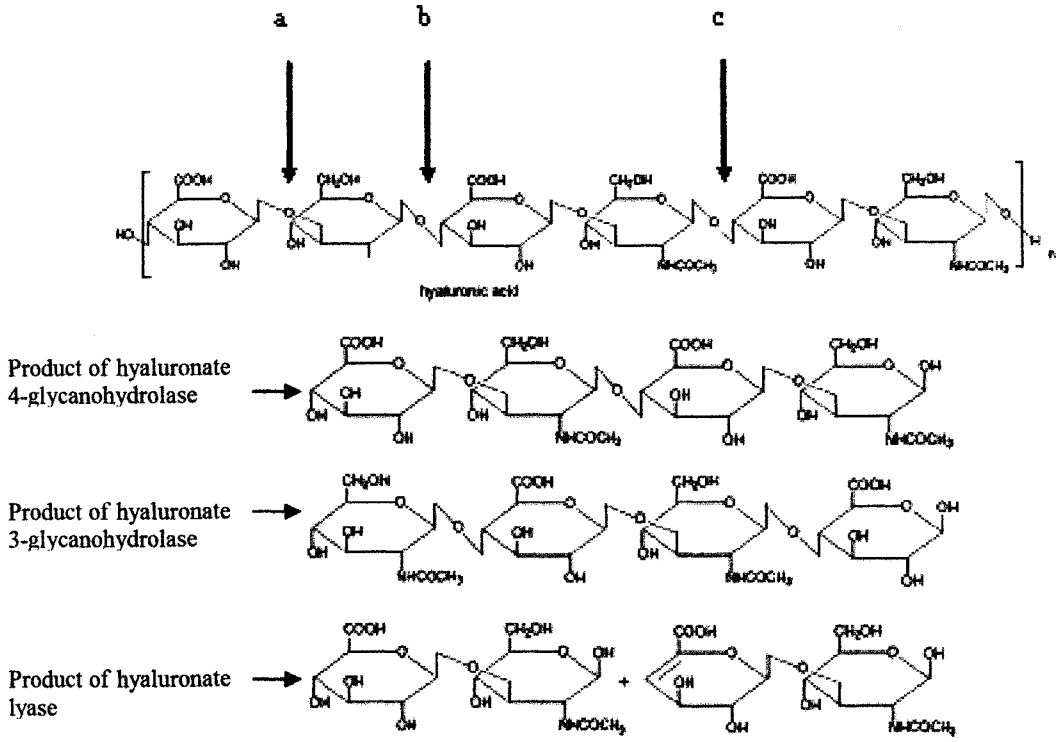

Figure 1.3 Classification of hyaluronidases (a, b, c represent the cleavage site of each enzyme) a, hyaluronate-3-glycanohydrolases degrade HA by cleavage of the 1,3-β-glycosidic bond. The main product is tetrasaccharide; b, hyaluronate-4-glycanohydrolyases degrade HA by cleavage of the 1,4-β-glycosidic bond producing tetrasaccharide as the main product. Both of them degrade HA by hydrolytic mechanism ; c, bacterial hyaluronate lyases degrade HA by cleavage of the 1,4-β-glycosidic bond by a β-elimination reaction producing unsaturated disaccharide as main product (adapted from Meyer, 1970 with some modification).

1.3.1.2 Heparin hydrolyases

Heparin hydrolases are endoglycosidases present in different places in the body such as macrophages, β and T-lymphocytes, fibroblasts and tumor cells. The function of these enzymes is to cleave heparan sulphate from proteoglycan core proteins and degrade them to small chains (Bame, 1983; Ernst *et al.*, 1995). It has been reported that heparin hydrolases release growth factors that are linked to extracellular heparan sulphate

proteoglycans and thus are involved in regulating cell growth and differentiation (Bame, 2001).

1.3.1.3 Keratanases

Since KS does not contain uronic acid, the only enzymes that can degrade this polysaccharide are hydrolyases. Keratanases split both the β-1,3 linkage at the reducing end of hexosamine and the β 1,4 bond at the non-reducing end of hexosamine (Ernst *et al.*, 1995).

1.3.2 Polysaccharide lyases

Polysaccharide lyases are classified into highly related families of enzymes, the members of which share primary sequence homology and also share structural similarities.The 18-polysaccharide families known are found as a part of a continuously updated carbohydrate-active enzyme database at http://afmb.curs-mrs.fr/~cazy/index.html. Polysaccharide lyases cleave glycosidic bonds, which are present in a variety of important components such as oligosaccharides, polysaccharides, glycoproteins, glycolipids and proteoglycans.

These enzymes cleave polysaccharide substrates which are anionic polymers producing unsaturated products at the non-reducing terminus. These lyases cleave the polymer chain by a β-elimination at 1,4 β or 1,4 α-linked bonds. This unsaturated bond, which absorbs energy in the UV range, is formed between C4 and C5 of the uronic acid residue. In contrast, the degradation products of glycoside hydrolases are saturated oligosaccharides (Sutherland, 1995).

There are 18 families of polysaccharide lyases, compared to 100 families of glycoside hydrolyases. This is because of restricted substrate specificity of the former, which need

a free carboxylate group at the C5 position of the sugar ring of their substrates (Greiling *et al.*, 1975; Fethiere *et al.*, 1999; Charnock *et al*, 2002).

Both pathogenic and non-pathogenic bacteria produce polysaccharide lyases. Non-pathogenic bacteria use these enzymes mainly to release carbon sources for growth rather than the invasion of plant and animal tissues as in the case of pathogenic bacteria (Linhardt *et al.*, 1986).
Another source of polysaccharide lyases are fungi, which use these enzymes for the degradation of plant polysaccharides (Linhardt et al., 1986).

It has been proposed that the mechanism of the action of polysaccharide lyase relies on three events in order to achieve catalysis. Firstly the negatively charged uronic acid moieties attached to the C5 of each saccharide unit are neutralized by positive charges to allow substrate binding. Then a proton is abstracted from the C5 of the saccharide occupying the +1 subsite and a proton is donated to the glycosidic oxygen, resulting in bond cleavage and the formation of a double bond between the C4 and C5 of the saccharide occupying the +1 subsite (Gacesa, 1987; Capila *et al.*, 2002; Charnock *et al*, 2002).

The 3D structure of polysaccharide lyases has been reported for enzymes from polysaccharide families 1, 3, 5, 6, 8, 9 10 and 16 from the use of X-ray crystallography. The structures have revealed three catalytic module topographies. The (α/α) barrel (Figure 1.4B) is observed in families 5 and 8, which include hyaluronate lyase (Li *et al.*, 2000; Li and Jedrzejas, 2000), xanthane lyase (Hashimoto *et al.*, 2001), chondroitin AC lyase and chondroitin ABC lyase. Others have a β-helix topology (Figure 1.4A) as observed in families 1, 3, 6 and 9 such as pectate lyases, pectin lyases, chondroitinase B

and rhammoglucuroman lyases (Huang *et al.*, 1999, http://afmb.curs-mrs.fr/~cazy/index.htm1) and a triple-stranded β-helical structure (Figure 1.4C) that is observed in family 16 (Smith *et al.*, 2005).

Five families of polysaccharide lyases can degrade GAGs. These are families 6, 8, 12, 13 and 16 (Table 1.3).

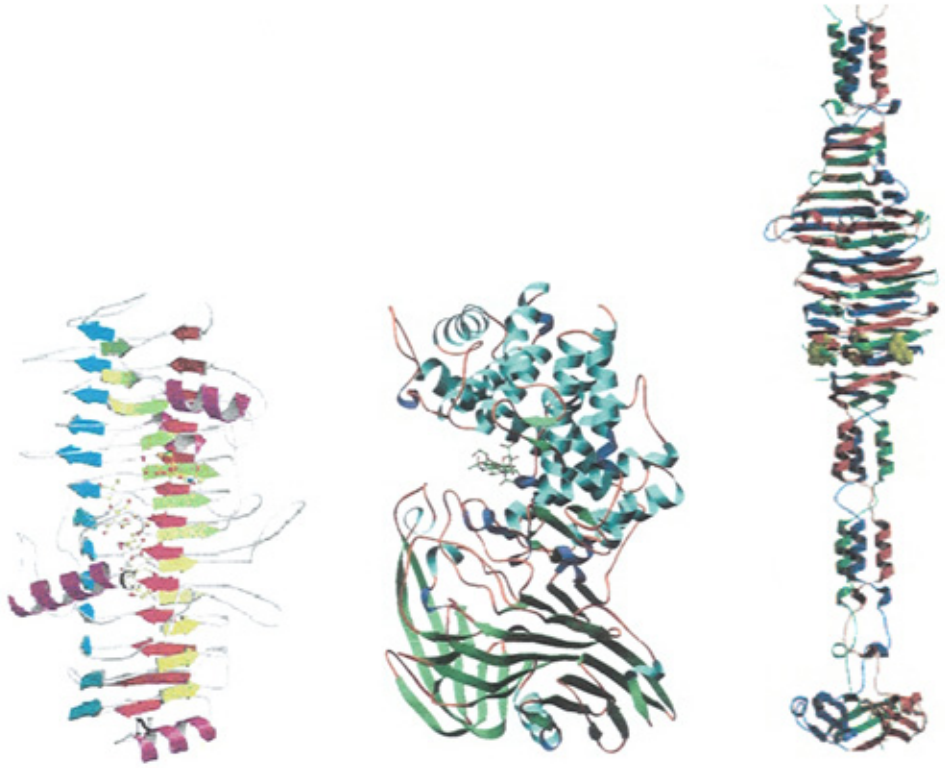

Figure 1.4 The topology of polysaccharide lyases A) β-helix topology (taken from Huang *et al.*, 1999); B) (α/α) barrel topology (Taken from Jederzejas *et al.*, 2002), C) Triple stranded β-helix (Taken from Smith *et al.*, 2005).

Table 1.3 PL families that degrade GAGs. Based on data derived from CAZy (http:// afmb.cnrs-mrs.fr/CAZY).

Family	Members	Known activity	Representatives	3-D structure	Reference
6	4	Chondroitinase B, Alginate lyase	*Flavobacterium heparinum*	β-helix	Huang *et al.*, 1999
8	78	Hyaluronate lyase, Chondroitin ABC lyase, Chondroitin AC lyase, Xanthane lyase	*Flavobacterium heparinum* *Streptococcus pneumoniae*	α+β domain	Fethiere *et al.*, 1999 Li *et al.*, 2000
12	18	Heparin-sulphate lyase	*Flavobacterium heparinum*	Not available	Su *et al.*, 1996
13	2	Heparin lyase		Not available	
16	26	Hyaluronate lyase	*Streptococcus pyogenes*	Triple stranded β-helix	Smith *et al.*, 2005

1.3.2.1 Polysaccharide lyase family 6

This is a relatively small family encoding only 4 open reading frames from different organisms (Table 1.2). One of these enzymes is chondrotinase B from *Flavobacterium heparinum*. This is the only enzyme among chondroitinases which cleaves only one substrate, as it has been found to be active only against DS. According to Huang *et al.* (1999), chondroitinase B has the right-handed parallel β-helix topology (Figure 1.4 A) as in the case of pectate lyases. Co-crystallised chondroitinase B with DS disaccharide gave insights into the active site and to the possible residues that are important in the substrate binding and catalysis (Huang et al., 1999). Biochemical characterisation has shown that the enzyme has a broad pH optimum ranging from 6.8 to 8 (Huang *et al.*, 1999) and the K_m and k_{cat} for the enzyme are 4.6 μM and 190 s^{-1} respectively (Pojasek *et al.*, 2001). Through using site directed mutagenesis, Pojserak *et al.* in 2002 mutated the residues that are important in the catalysis. They found that the mutation of Lys250 resulted in complete elimination of the activity of the enzyme, suggesting that its role is in stabilising the carbanion intermediate. However, mutated His277 and Glu333 resulted in decreased activity. Thus it was proposed that both residues act in the abstraction of a proton from C-5 of the galactosamine.

1.3.2.2 Polysaccharide lyase family 8 (PL 8)

PL 8 is considered the second largest family of polysaccharide lyases, encoding 78 open reading frames from different organisms. Hyaluronate lyases are the main class of enzymes dominating this family with 39.7 % of the open reading frames classified with this activity. Known activities of this family are hyaluronate lyase,

chondroitin ABC lyase, chondroitin AC lyase, heparin lyase and xanthan lyase (http://afmb.curs-mrs.fr/~cazy/index.html).

1.3.2.2.1 Xanthane lyases

Xanthan lyases belong to family 8 of polysaccharide lyase. Xanthan lyases are produced by many species of bacteria including *Bacillus* sp. GL1 (Hashimoto *et al.*, 2001; Hashimoto *et al.*, 2003) and *Paenibacillus alginolyticus* XL-1 (Ruijssenaars *et al.*, 2000).

Xanthan lyase degrades xanthan gum an extracellular heteropolysaccharide produced by many strains of plant pathogenic bacteria such as *Xanthomonas campestris* (Ruijssenaars *et al*, 2000; Hashimoto *et al.*, 2001; Hashimoto *et al.*, 2003; Hsu *et al.*, 2004). It is composed of a main cellulosic chain to which are attached trisaccharide side chains formed from one glucuronyl and two mannosyl residues (Ruijssenaars *et al.*, 2000; Hashimoto *et al.*, 2001; Hashimoto *et al.*, 2003). Xanthan gum is widely used as a thickening or stabilizing agent in the food and pharmaceutical industries (Hsu *et al.*, 2004).

Xanthan lyases are synthesised as a precursor form which is 99 kDa in size, then processed into a mature form of 75 kDa after the removal of signal peptide and a C-terminal sequence. Furthermore xanthan lyase acts exolytically on the side chain of the polysaccharide and releases pyruvylated mannose, in contrast to the other polysaccharide lyases which cleave the glycosidic bond in the main chain of their substrates (Ruijssenaars *et al.*, 2000; Hashimoto *et al.*, 2001; Hashimoto *et al.*, 2003).

The biochemical characterisation of xanthan lyase has shown that the pH optimum of this enzyme is 5.2 and its optimum temperature is 50 °C. This enzyme is highly specific toward xanthan, and does not cleave HA or chondroitin. The structure of xanthan lyase has been solved at 2.3 Å resolution. The structure of the enzyme is generally the same as that of the family 8 lyases for hyaluronate and chondroitin AC, but some differences were observed in the loop structure over the cleft (Hashimoto *et al.*, 2003).

1.3.2.2.2 Hyaluronate lyases

Hyaluronate lyases have been identified in both Gram-positive and Gram-negative bacteria and these bacteria are often pathogenic. For instance, pathogenic bacteria that produce hyaluronate lyase include *Streptococcus pneumonia* (Jedrzejas *et al.*, 1998; Li *et al.*, 2000; Li *et al.*, 2001), *Streptococcus agalactiae* (Lin *et al.*, 1994; Baker *et al.*, 1997; Li and Jedrzejas, 2001), *Streptococcus pyogenes* (the subject of this thesis and which will be described in the results and discussion chapter), *Streptococcus suis* (Allen *et al.*, 2004), *Streptococcus intermedius* and *Streptococcus constellatus* (Takao, 2003), *Peptostreptococcus* species (Tam and Chan, 1985), *Propionibacterium acnes* (Ingham *et al.*, 1979) and *Staphylococcus aures* (Abramson and Friedman, 1969; Rautela and Abramson, 1973). Moreover these enzymes are synthesised by soil bacteria like *Streptomyces coelicolor* (the subject of this thesis), *Streptomyces hyaluronolyticus* (Price *et al.*, 1997; Maccari *et al.*, 2004) and *Streptomyces griseus*.

Some hyaluronate lyases are very specific, such as hyaluronate lyase of *Streptomyces hyaluronolyticus* (Ohya and Kaneko, 1970; Price *et al.*, 1997), which is specific only

against HA and does not degrade chondroitin or chondroitin sulphate or any other GAGs. Other hyaluronte lyases are non-specific, degrading both HA and CS, for instance, the hyaluronate lyases of *Streptococcus pneumonia, Streptococcus agalactiae* (Jedrzejas *et al.*, 2002) and *Peptostreptococcus* (Tam and Chan, 1985) degrade chondroitin 4 and 6-sulphate.

Hyaluronate lyases cleave HA chains through a β-elimination mechanism resulting in the formation of double bond at the non-reducing end: a property shared by all polysaccharide lyases. It is involved in the cleavage of the β-1,4 glycosidic bond between N-acetyl-D-glucosamine and D-glucuronic acid (Figure 1.5). As a consequence of this function it facilitates host tissue invasion by bacteria leading to the increased permeability of tissue, which plays an important role in infections (Ponnuraj and Jedrzejas, 2000).

It has been shown that all hyaluronate lyases of PL 8 that have been characterised, act exolytically making an initial random cut in the HA chain, followed by processive release of unsaturated disaccharides as in the case of *Streptococcus pneumonia* (Jedrzejas *et al.*, 1998a, b; Jedrzejas, 2000; Li *et al.*, 2000; Kelly *et al.*, 2001; Nukui *et al.*, 2003), *Streptococcus agalactiae* (Pritchard *et al.*, 1994; Pritchard *et al.*, 2000; Jedrzejas *et al.*, 2002), *Peptostreptococcus* species (Tam and Chan, 1985) and *Streptococcus intermedius* and *Streptococcus constellatus* (Takao *et al.*, 1997; Takao, 2003).

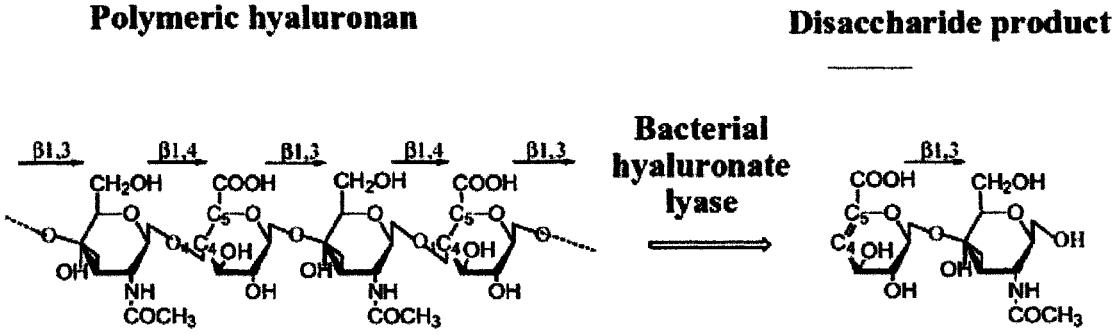

Figure 1.5: Degradation of HA by exolytic bacterial hylauronate lyase Hyaluronate lyases degrade HA by cleavage of the 1,4-β-glycosidic bond by a β-elimination reaction producing unsaturated disaccharide product (2-acetamido-2-deoxy-3-*O*-(β-*D*-gluco-4-enepyranosyluronic acid)-*D*-glucose) (taken from Akhtar and Bhakuni, 2004). Hyaluronan is built from alternating units of glucuronic acid (GlcUA) and *N*-acetylglucosamine (GlcNAc).

Table 1.4 Biochemical characterization of hyaluronate lyases from various sources. Abbreviations: HA Hyaluronan, C4S chondroitin-4-sulphate, C6S chondroitin-6-sulphate.

Organism	Molecular weight (kDa)	PH Optimum	Temperature Optimum	k_m mg ml^{-1}	k_{cat} µmol. min mg	Mode of action	Reference
Streptococcus pneumoniae	83	5.5-6		0.09		Exolytic	Jedrzejas *et al.*, 1998; Li *et al.*, 2000
Streptococcus agalactiae	92	6.3	40 °C	8×10^{-4}		Exolytic	Ozegowski *et al* in 1994; Pritchard *et al.*, 1994; Rodig *et al.*, 2000; Mello *et al.*, 2002
Streptococcus dysagalactiae	117	5.8-6.6	37 °C	53 µM	1,610	Exolytic	Hamai *et al.*, 1989
Streptococcus suis		5.5				Exolytic	Allen *et al.*, 2004
Streptococcus intermedius	117					Exolytic	Takao, 2003
Streptococcus constellatus	120	6.2					Takao, 2003
Peptostreptococcus	160	HA 7.2 C4S 7.6 C6S 8.0	46 °C	HA 0.14 C4S 1.4 C6S 2.6	HA 400 C4S 30 C6S 30	Exolytic	Tam and Chan, 1985
Staphylococcus aureus	84	4.8-6					Abramson and Friedman, 1969; Rautela and Abramson, 1973

1.3.2.2.3 Chondroitin lyases

Chondroitin lyases are produced by many species of either soil or intestinal bacteria. These include *Flavobacterium columnare* G4 (Takegawa *et al.*, 1991), *Arthroebacter aurescens* (Hiyama and Okada, 1975; Hiyama and Okada 1976; Lunin *et al.*, 2004), *Flavobacterium heparinum* (Hiyama and Okada, 1975; Hiyama and Okada 1976; Michelacci *et al.*, 1987; Tkalec *et al.*, 2000; Pojasek *et al.*, 2001) and *Proteus vulgaris* (Yamagata *et al.*, 1968; Thurston *et al.*, 1975; Hamai *et al.*, 1997, Huang *et al.*, 2003). These enzymes catalyse the cleavage of the glycosyl oxygen bonds between N-acetyl galactosamine and either D-glucuronic acid or L-iduronic acid. In family 8 of the polysaccharide lyases there are two types of chondroitin lyases; AC lyases and ABC lyases.

It has been shown that AC lyase from *Flavobacterium heparinium* does not degrade DS (Hiyama and Okada, 1976). However, Huang and his colleagues reported that AC lyase from *Flavobacterium heparinium* splits the glycosidic bond on the non-reducing terminal of uronic acid of chondroitin-4-sulphate, chondroitin-6-sulphate, HA and DS. It degrades DS only at 1-4 linkages where D-glucuronic acid is present but not L-iduronic acid (Huang *et al.*, 2001). Conversely, chondroitin AC lyase of *Arthrobacter aurescens* degrades chondroitin-4-sulphate, chondroitin-6-sulphate and HA, but is unable to cleave DS (Lunin *et al.*, 2004). Surprisingly, it has been demonstrated that *Arthrobacter aurescens* AC lyase possesses higher activity toward HA than either chondroitin-4-sulphate or chondroitin-6-sulphate (Lunin *et al.*, 2004). They found that k_{cat} for HA is about two times that of chondroitin-4 or 6-sulphate (Table 1.6). Also, this enzyme has more affinity toward HA than other types of

GAGs (Table 1.5). It was also shown that the AC lyase of *Arthrobacter aurescens* degrades chondroitin-6-sulphate faster than it does chondroitin-4-sulphate, whereas the AC lyase of *Flavobacterium heparinium* has more affinity toward chondroitin-4-sulphate than to chondroitin-6-sulphate (Hiyama and Okada 1976). On the other hand, Pojasek and his co-workers reported that *Flavobacterium* AC lyase has a slight preference for chondroitin-6-sulphate over chondroitin-4-sulphate. The enzyme has a K_m of 0.6 μM and a k_{cat} of 480 s^{-1} towards chondroitin-6-sulphate, whereas, with chondroitin-4-sulphate the K_m and k_{cat} are 0.8 μM and 234 s^{-1}, respectively (Pojasek *et al.*, 2001). The relative activities of chondroitinase either ABC lyase or AC lyase against HA, chondroitin-4-sulphate, chondroitin-6-sulphate and DS are shown in Table 1.5.

The ABC lyase of *Flavobacterium heparinium* degrades DS, chondroitin-4-sulphate and chondroitin-6-sulphate but does not cleave HA, while the ABC lyase of *Proteus vulgaris* degrades HA in addition to DS, chondroitin-4-sulphate and chondroitin-6-sulphate (Lunin *et al.*, 2004). There are many conflicting theories regarding the mechanism of action of ABC lyase of *Proteus vulgaris*. Yamagata *et al.* (1968) suggested that the only product of ABC lyase activity on chondroitin-4-sulphate is the disaccharide, whilst Sanderson and co-workers found that the degradation of chondroitin-4-sulphate with this enzyme produced equal amounts of disaccharide, tetrasaccharide and hexasaccharides (Sanderson *et al.*, 1989). On the other hand, it has been shown that the ABC lyase has endolytic action toward chondroitin-6-sulphate or DS and exolytic action against chondroitin-4-sulphate. More recently, it was reported that *Proteus vulgaris* produces two types of chondroitin lyase: ABC lyase I and II (Hamai *et al.*, 1997). These enzymes have different modes of action.

ABC lyase I acts endolytically and produced disaccharides and tetrasaccharides; and conversely ABC lyase II acts exolytically and has more affinity toward oligosaccharides (Hamai *et al.*, 1997).

Chondroitin lyases have different biochemical characteristics. For instance, the pH optimum varies from 5.5 to 8. ABC lyase from *Proteus vulgaris* has different pH optima for the degradation of GAGs. The pH optima for unsulphated chondroitin, HA and CS are 6.2, 6.8 and 8, respectively (Ernst *et al.*, 1995). Also, it has been found that the pH optimum of ABC I for chondoitin-6-sulphate varied with different buffers. It has a pH optimum of 7 with a 50 mM sodium phosphate buffer, while with a 50 mM Tris buffer the optimal activity was observed at pH 8.0; but this difference was not detected with DS (Prabhakar *et al.*, 2005).

Different chondroitinases have different optimum temperatures ranging from 30 °C for *Flavobacterium heparinium* AC lyase (Michelaeci *et al.*, 1987), to 50 °C for *Arthroebacter aurescens* AC lyase (Hiyamn and Okada, 1975; Lunin *et al.*, 2004), to 75 °C for ABC lyase of *Bacillus* species (Ernst *et al*, 1995).

Furthermore, previous studies involving the effect of various divalent cations have found that the AC lyase of *Arthroebacter aurescens* was activated by Co, Ca, Mg and Ba (Table 1.6), but was completely inhibited by Pb, Cu, Fe, Sn and Hg (Hiyamn and Okada, 1977). In the same way, AC lyase of *Flvobacterium heparinium* was stimulated by Mn, Ca, Mg, and Ba but inhibited by Zn, Fe and Cu (Yamagata *et al.*, 1968).

Table 1.5 Relative activity of AC lyases and ABC lyases against various GAGs. HA, hyaluronan; C4S, chondroitin-4-sulphate; C6S, chondroitin-6-sulphate; DS, dermatan sulphate.

	C4S	C6S	DS	HA	References
ABC lyase of *Proteus vulgaris*	100% 100%	100% 60%	40% 34%	2% 60%	Yamagata *et al.*, 1968, Thurston *et al.*, 1975
ABC lyase of *Flavobacterium heparinum*	100%	100%	100%	0%	Yamagata *et al.*, 1968, Michelacci *et al.*, 1987
AC lyase of *Flavobacterium heparinum*	100%	86 %	0%	188%	Hiyama and Okada, 1976
AC lyase of *Arthrobacter aurescens*	100 %	110 %	0 %	320 %	Hiyama and Okada, 1976

Table 1.6 Biochemical characterization of chondroitin AC lyasee and ABC lyases from various sources. Abbreviations: HA Hyaluronan, C4S chondroitin-4-sulphate, C6S chondroitin -6-sulphate, DS Dermatan sulphate.

Organism	Molecular weight (kDa)	Inhibitors	Activators	pH Optimum	Temperature Optimum	k_m mg ml^{-1}	k_{cat} s^{-1}	Mode of action	Reference
Arthrobacter aurescens AC lyase	75-80	Fe, Sn, Cu, Pb	Mg, Ca, Ba	6	50 °C	HA 0.082 C4S 0.196 C6S 0.196	HA $2.7x10^{-3}$ C4S $1.42x10^{3}$ C6S $1.7x10^{-3}$	Exolytic	Hiyama and Okada, 1975; Hiyama and Okada 1976; Lunin *et al.*, 2004
Flavobacterium heparinium AC lyase	70-75	Zn, Cu Fe Fe, Ca, Mg, Ba	Mg, Ca, Ba, Mn	6-7.5	30 °C	C6S 0.6 µM C4S 0.8 µM	C6S 480 C4S 234	Endolytic	Hiyama and Okada, 1975; Hiyama and Okada 1976; Michelacci *et al.*,1987; Pojasek *et al.*, 2001
Proteus vulgaris ABC lyase	118	Zn, heparin	Mg, Mn	7.9-8.3	37 °C	C4S 1.5 µM C6S 1.2 µM DS 2.5 µM	5200 ± 1300 min^{-1} 37000 ± 6500 27000 ± 2500	Endolytic	Yamagata *et al.*, 1968, Thurston *et al.*, 1975; Huang *et al.*, 2003; Prabhakar *et al.*, 2005
Flavobacterium heparinium ABC lyase	>70	Ca, PO		-	30 °C				Yamagata *et al.*, 1968; Michelacci *et al.*, 1987
Aureobacterium	81	Hg, Zn, Fe, Cu		7.5	37 °C			Endolytic	Takegawa *et al.*, 1991

1.3.2.2.4 Biochemical characteristics of polysaccharide lyase family 8 enzymes

Several enzymes from PL 8 have broad specificity, and some have broad pH optima (Tables 1.4 and 1.6). For example, the hyaluronate lyases of *Staphylococcus aureus* and *Streptococcus dysglactiae* have wide pH optima of 4.8-6 (Abramson and Friedman, 1969; Rautela and Abramson, 1973) and 5.8 to 6.6 (Hamai *et al.*, 1989) respectively. The pH optima for chondroitin AC or ABC lyases (6-8.3) are slightly higher than those of hyaluronate lyases, which range from 4.8 to 7.6 (Tables 1.4 and 1.6). Furthermore, some of the enzymes have different pH optima with different substrates; these include the hyaluronate lyase of *Peptostreptococcus* sp (Tam and Chan, 1985) and the ABC lyase of *Proteus vulgaris* (Yamagata *et al.*, 1968).

The effect of divalent cations on PL 8 varies considerably. Some enzymes have an absolute requirement for calcium for catalysis, as in the case of the hyaluronate lyase of *Streptococcus pneumoniae* (Jedrzejas *et al.*, 1998a; Ponnuraj and Jedrzejas, 2000; Jedrzejas *et al.*, 2002). Some lyases of this family appear to be less affected by the presence and concentration of divalent cations. However, hyaluronate lyase of *Streptococcus agalactia* has a preference for magnesium over calcium (Ozegowski *et al.*, 1994). On the other hand, no absolute requirement for divalent ions for catalysis was found with the hyaluronate lyases from *Streptomyces coelicolor* or *Streptococcus pyogenes* (this project).

1.3.2.2.5 Sequence homology within polysaccharide lyase family 8

The emergence of completely sequenced bacterial genomes has led to a rapid increase in the number of open reading frames encoding putative enzymes that interact with carbohydrate either via synthesis or degradation. The sequence comparison of *Streptomyces coelicolor* with other lyases of PL 8 shows an identity of 20 % to *Streptococcus pneumoniae* hyaluronate lyase, 18 % to *S Streptococcus agalactiae*, 21.8 % to S *Streptococcus pyogenes* hyaluronate lyase and 39.8 % to *A. aurescens* AC lyase. The multiple sequence alignment of some members of family 8 (Figure 1.6) illustrate the presence of some highly conserved amino acids that are likely to play a role in substrate binding and catalysis. As shown in Figure 1.6, about 16 amino acid residues are conserved in most PL 8 lyases. This indicate that the sequence similarity of the family 8 enzymes is low but that a few amino acid residues are highly conserved in all enzymes and these residues are not clustered together in the sequence but end up forming the active site after protein folding.

The work of Fietherie *et al.* (1999) and Li *et al.* (2000) has suggested the importance of tyrosine, asparagine and histidine residues in catalysis. Subsequent site directed mutagenesis of these amino acids in *Streptococcus pneumoniae* (Li *et al.*, 2000; Kelly *et al.*, 2001; Jedrzejas *et al.*, 2002) and *Streptococcus agalactia* (Li and Jedrzejas, 2001) has resulted in the complete elimination of catalytic activity in the case of tyrosine and reduction to only 6 % and 12 % in the case of asparagine and histidine respectively. Therefore these results indicate that tyrosine, asparagine and histidine are responsible for proton abstraction and donation (Li *et al.*, 2000). This sequence alignment suggests that

these amino acids might be selected for site directed mutation in both *Streptomyces coelicolor* and *Streptococcus pyogenes*.

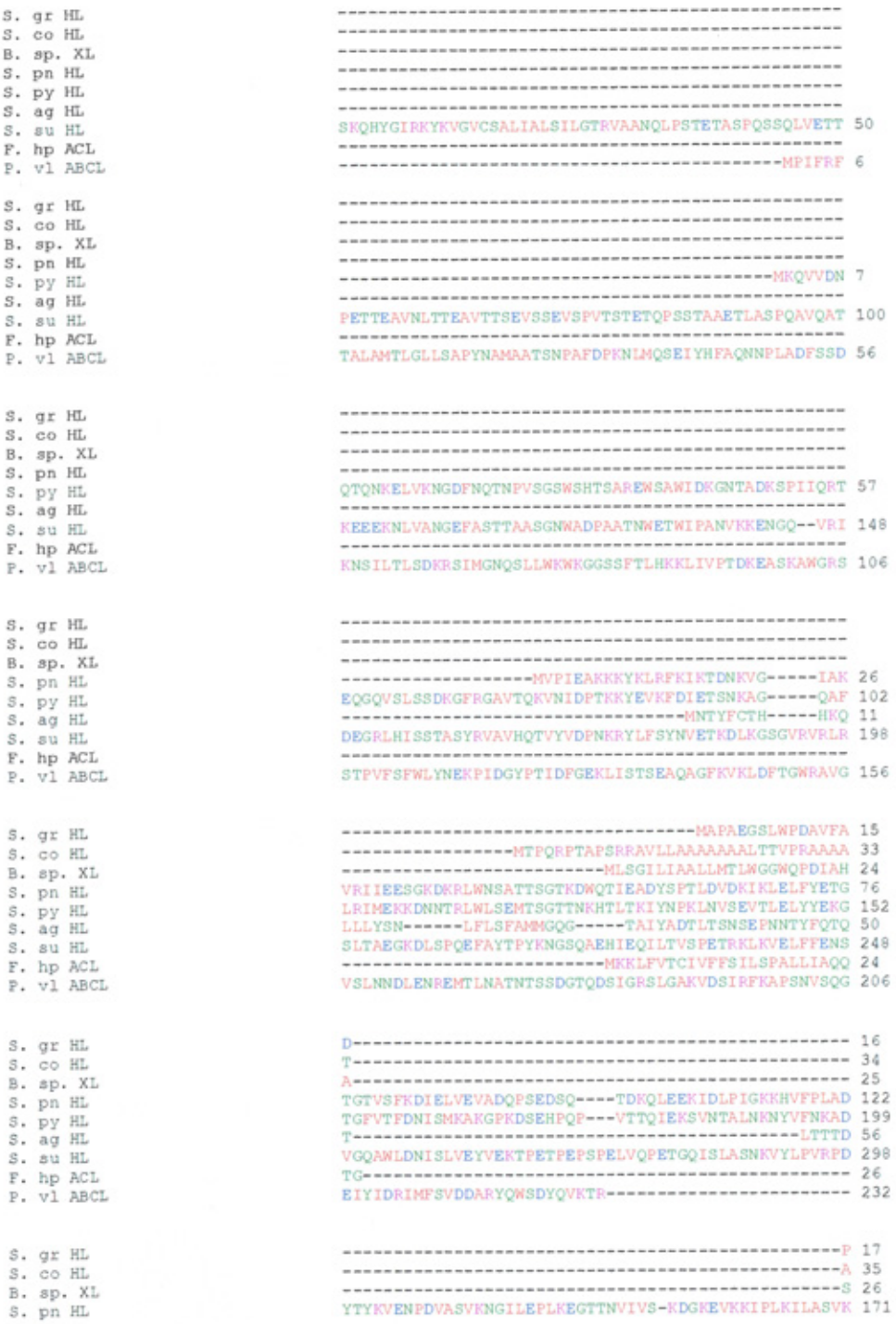

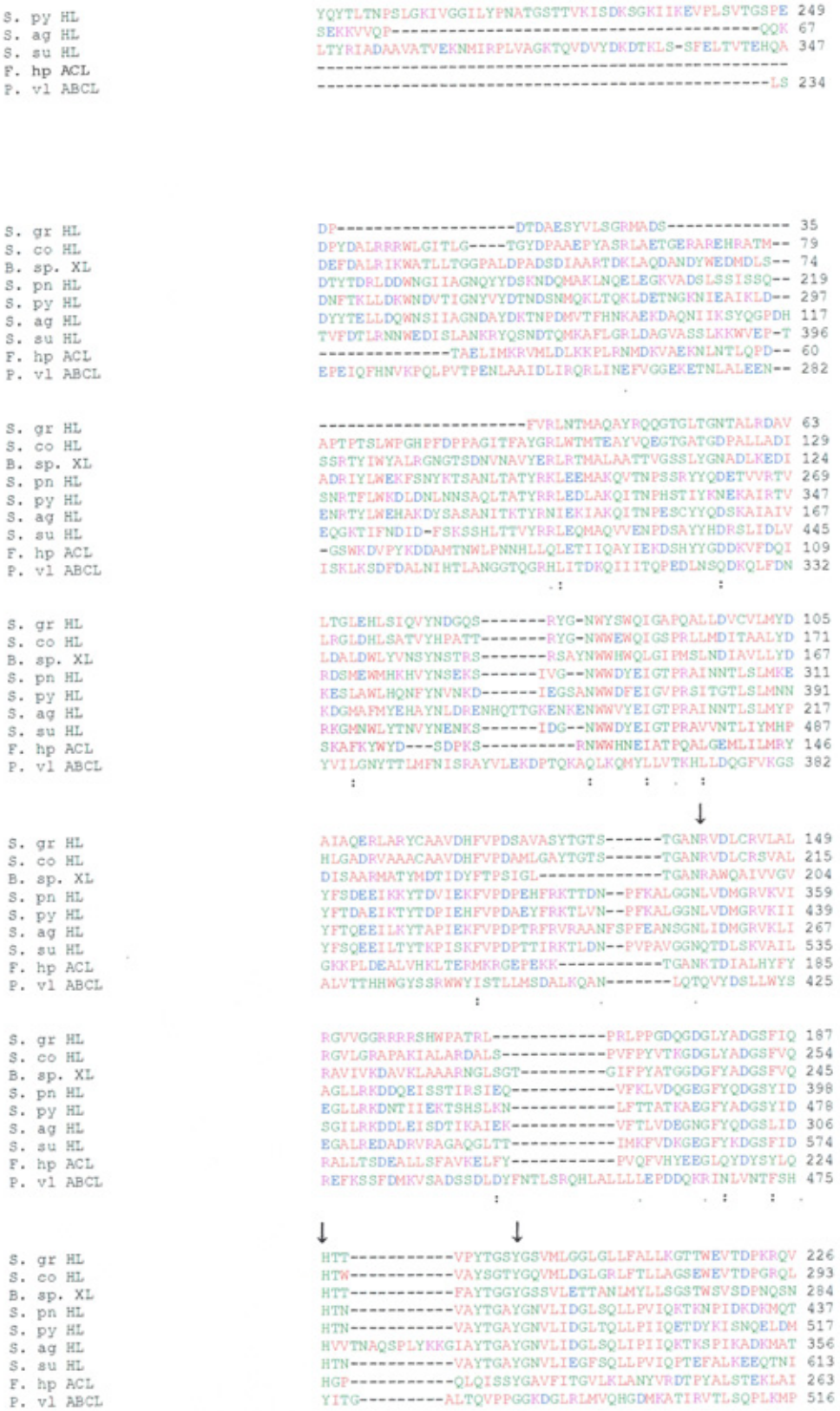
S. py HL
S. ag HL
S. su HL
F. hp ACL
P. vl ABCL
S. gr HL
S. co HL
B. sp. XL
S. pn HL
S. py HL
S. ag HL
S. su HL
F. hp ACL
P. vl ABCL
S. gr HL
S. co HL
B. sp. XL
S. pn HL
S. py HL
S. ag HL
S. su HL
F. hp ACL
P. vl ABCL
S. gr HL
S. co HL
B. sp. XL
S. pn HL
S. py HL
S. ag HL
S. su HL
F. hp ACL
P. vl ABCL
S. gr HL
S. co HL
B. sp. XL
S. pn HL
S. py HL
S. ag HL
S. su HL
F. hp ACL
P. vl ABCL

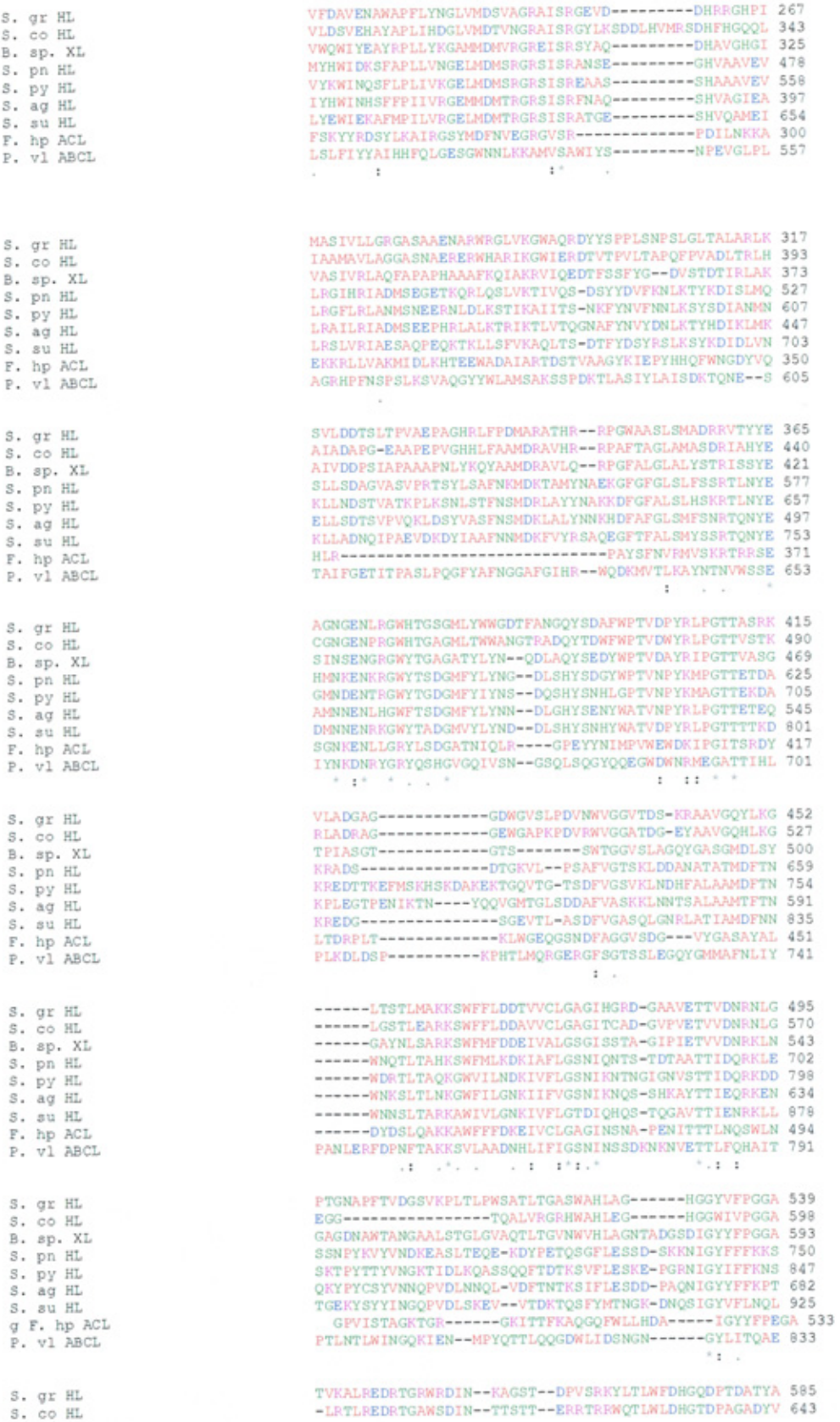
S. gr HL
S. co HL
B. sp. XL
S. pn HL
S. py HL
S. ag HL
S. su HL
F. hp ACL
P. vl ABCL
g F. hp ACL

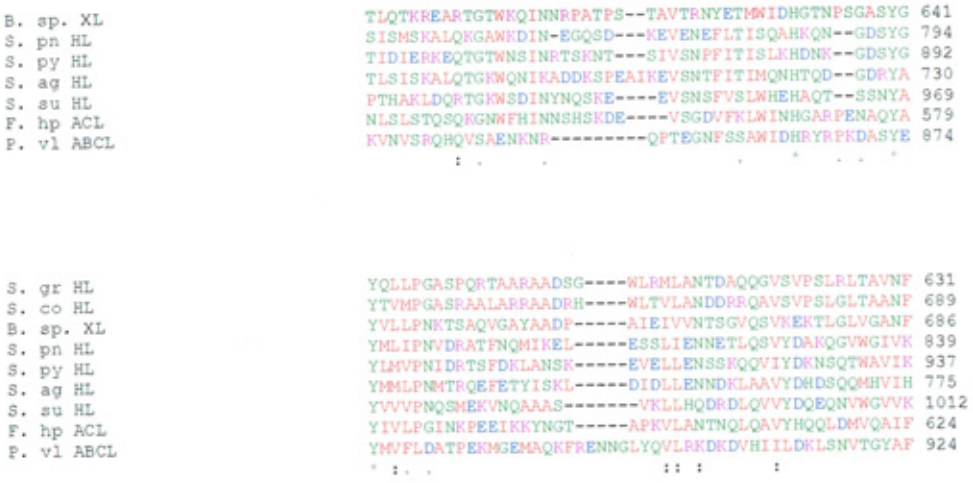

Figure 1.6 Multiple sequence alignment of PL 8

The three residues, Tyr264, Asp205 and His255, which have been shown to be involved in catalysis are marked by arrow heads above the sequence. The alignment was performed using ClustalW. From top to the bottom: (*S. gr* HL) hyaluronate lyase of *Streptomyces griseus*; (*S. co* HL) hyaluronate lyase of *Streptomyces coelicolor*; (B. sp. XL) xanthan lyase of *Bacillus* sp. GL1; (S. pn HL) hyaluronate lyase of *Streptococcus pneumoniae*; (S. py HL) hyaluronate lyase of *Streptococcus pyogenes*; (S. ag HL) hyaluronate lyase of *Streptococcus agalactiae*; (*S. su* HL) hyaluronate lyase of *Streptococcus suis*; (F. hp ACL) chondroitinase AC from *Flavobacterium heparinium*; (P. vl ABCL) chondroitin ABC lyase from *Proteus vulgaris*. Sequence was colored according to residue properties: red, hydrophobic; magenta, Basic positively charged; blue, Acidic negatively charged; green, hydroxyl + Amine + basic-Q.

1.3.2.2.6 Structural comparison of polysaccharide lyase family 8

The GAGs enzymes of this family have some sequence similarities and also share structural similarities. Most of these enzymes are apparently non-specific, acting on different GAGs but with different affinities.

The three-dimensional structures of seven enzymes of PL 8 have been determined. These are the chondroitin AC lyase of *F. heparinium* (Fethiere *et al.*, 1999; Capila *et al.*, 2002), hyaluronate lyase of *S. pneumoniae* (Jedrzejas *et al.*, 1998b; Li *et al.*, 2000; Jedrzejas *et al.*, 2002), hyaluronate lyase of *S. agalactiae* (Jedrzejas and Chantalat, 2000;

Ponnuraj and Jedrzejas 2000; Li and Jedrzejas, 2001), xanthan lyase of *Bacillius* sp. (Hashimoto *et al.*, 2003), chondroitin ABC lyase I of *P. vulgaris* (Huang *et al.*, 2003), hyaluronate lyase of *S. coelicolor* (discussed in this thesis) and chondroitin AC lyase of *A. aurescence* (Lunin *et al.*, 2004).

The enzymes of PL 8 share a common barrel fold with an $(\alpha/\alpha)_5$ topology and they have elongated clefts (transverse along the enzyme molecule). Within this cleft the substrate binds and catalysis take place. However, the number of helices in these enzymes differs (Li *et al.*, 2000; Ponnuraj and Jedrzejas 2000; Li and Jedrzejas, 2001; Jedrzejas *et al.*, 2002).

Some of these enzymes, such as chondroitin AC lyase of *F. heparinium* (Fethiere *et al.*, 1999); xanthan lyase of *Bacillius* species (Hashimoto *et al.*, 2001; Hashimoto *et al.*, 2003), and hyaluronate lyase *S. pneumoniae* (Li *et al.*, 2000; 2001), are composed of two domains. In the N-terminal α-domain, also called the catalytic domain, a cleft is located. The other domain is the C-terminal β domain which is rich in β-sheets (Figure 1.8). Other enzymes, such as the hyaluronate lyase from *S. agalactiae* (Li and Jedrzejas, 2001; Mello *et al.*, 2002), and chondroitin ABC lyase I of *P. vulgaris* (Huang *et al.*, 2003) are composed of three domains: the N-terminal small β domain; the middle α-domain; and the C-terminal β domain (Figure 1.8). The structure of the N-terminal β domain in *P. vulgaris* resembles the carbohydrate-binding domain of xylanases and glucuronases (Huang *et al.*, 2003). The middle domain, which is a catalytic domain, and the C-terminal β-domain, have the same structure as the hyaluronate lyase of *S. pneumoniae* and AC lyase of *F. heparinium* and *A. auresues* domains. The α and β-

domains of PL 8 are connected together through one flexible peptide linker of various lengths (Li *et al.*, 2000) which enables both domains to move with respect to each other. This movement facilitates the catalytic cleft to widen and narrow in order to accommodate substrate binding before catalysis. However, in the cases of *S. agalactiae* (Li and Jedrzejas, 2001; Mello *et al.*, 2002) and *P. vulgaris* (Huang *et al.*, 2003) there are two peptide linkers, one of which connects βI-domain to the α-domain and another which connects the α-domain to the βII-domain.

It was found that the mode of substrate binding is almost similar in *S. pneumoniae* hyaluronate lyase, *F. heparinium* AC lyase and *A. aurescens* AC lyase when they are compared between inactive *S. pneumoniae* mutant Y408F complexed with HA oligosaccharide, and Y243F of *F. heparinium* complexed with chondroitin tetrasaccharide.

The catalytic residues of ABC lyase I are the same as those of AC lyase and hyaluronate lyases of *S. pneumoniae* and *S. agalactiae*, in spite of the low level of sequence identity between the catalytic domain of ABC lyase and the other enzymes (Huang *et al.*, 2003).

Recently, a mechanism for *S. pneumoniae* involving proton acceptance and donation has been suggested (Li *et al.*, 2000; Ponnuraj and Jedrzejas, 2000; Kelly *et al.*, 2001; Jedrzejas *et al.*, 2002). The first step in this proposed mechanism involves the binding of the substrate to the catalytic cleft of the enzyme, followed by the neutralization of the carboxyl group of the C5 glucuronate moiety of HA by Asn345. Next, the C5 proton is removed by His399 to form a double bond between C4 and C5. After that Tyr408

donates a proton resulting in the breaking of the glycosidic bond (Figure 1.7). Ultimately the product, which is a disaccharide, leaves the active site, while the catalytic residues balance protons via exchange with water (Li *et al.*, 2000; Li *et al.*, 2001; Li and Jedrzejas, 2001; Ponnuraj and Jedrzejas, 2000).

Lunin and his collaborators proposed that Tyr242 of *A. aurescens* AC lyase and its equivalents in other lyases of PL 8 has the ability to act as a general base instead of His233 due to its location at a suitable distance from the C5 atom of the +1 glucuronic acid. His233 and its equivalents in other lyases are located far from (~ 4 Å) the C5 atom of the +1 glucuronic acid, and therefore it is highly unlikely that His233 acts as a general base. Thus its function might be implicated in decreasing the pKa of Tyr242, resulting in the deprotonation of its hydroxyl group and priming it for the role as a general base (Lunin *et al.*, 2004).

Moreover, Prabhakar and co-workers agree, suggesting that His501 of *P. vulgaris* ABC lyase has a vital role in proton extraction during catalysis as the mutation of this amino acid resulted in abolishing the activity of the derivative enzymes completely (Prabhakar *et al.*, 2005). This is in contrast to the H399A mutant of *S. pneumoniae* hyaluronate lyase, which retained 12 % of its activity (Li *et al.*, 2000; Kelley *et al.*, 2001). Tyr508, which is located near the glycosidic oxygen of the substrate, has a possible role in protonating the leaving group. The proximity of Arg560 to the C-5 proton of the uronic acid makes this amino acid suitable for the stabilization of the carbanion intermediate produced during catalysis (Prabhakar *et al.*, 2005).

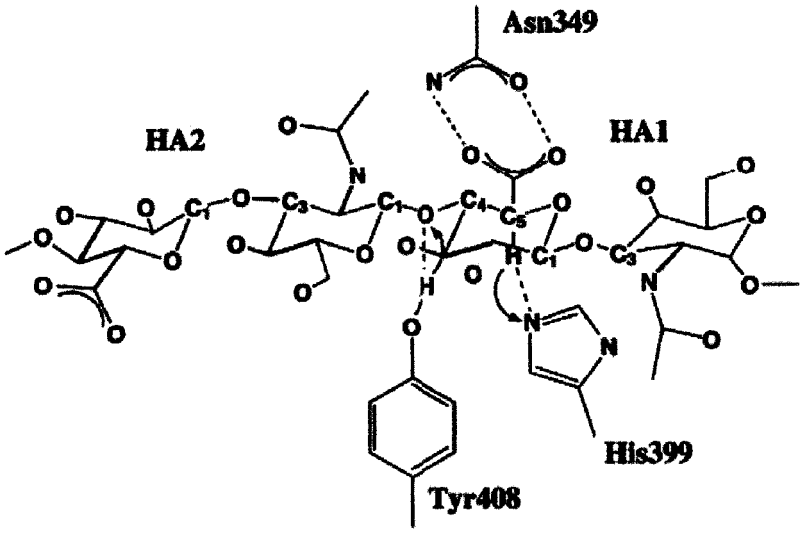

Figure 1.7 Mechanism of hyaluronan degradation by *S. pneumoniae* (adapted from Jedrzejas *et al.*, 2002).

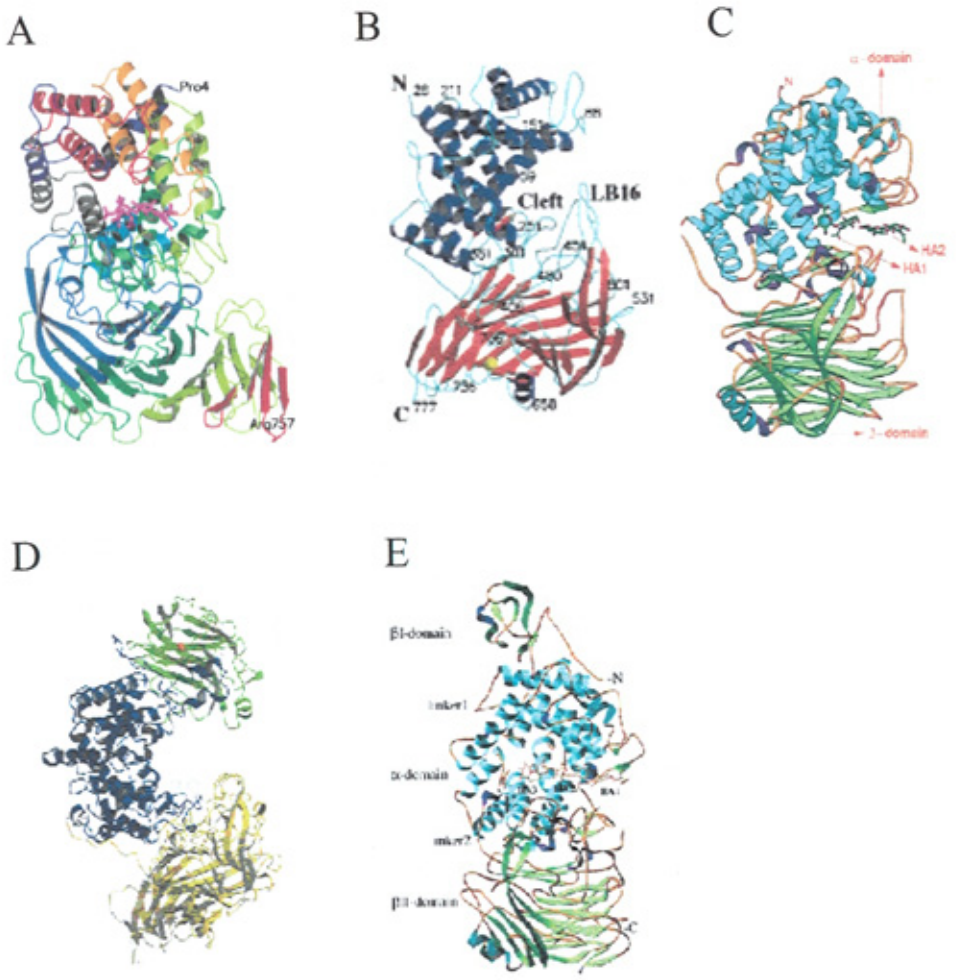

Figure 1.8 Three-dimensional structures of polysaccharide degrading enzymes of PL 8. A) *A. aurescence* AC lyase (Lunin *et al.*, 2004); B) *Bacillus* sp. xanthan lyase (Hashimoto *et al.*, 2001); C) *S. pneumoniae* hyaluronate lyase (Li *et al.*, 2000); D) *P. vulgaris* ABC lyase (Huang *et al.*, 2003); E) *S. agalactiae* hyaluronate lyase (Li and Jedrzejas, 2000).

1.3.2.3 Polysaccharide lyase family 12

PL 12 comprises 18 open reading frames. The known activity of this family is heparin lyases, and no 3D structure is available for this family. Biochemical information for this family is also limited to only three types of heparin lyases that have been isolated and biochemically characterized from *F. heparinium*, namely: heparinases I, II and III also called heparin lyases I, II and III (Yang *et al.*, 1985; Lohse and Linhardt, 1992; Su *et al.*, 1996; Yamada and Sugahara, 1998). It has been shown that heparin lyase I degrades heparin, heparin lyase II is active against both heparin and heparan sulphate whereas heparin lyase III degrades mainly heparan sulphate (Yang *et al.*, 1985; Lohse and Linhardt, 1992; Su *et al.*, 1996)

These enzymes split the α-1,4- glucosaminidic bonds of the heparan sulphate and heparin chain resulting in the formation of a double bond at the non-reducing terminal of uronic acid. Yamada and Sugahara (1998) have shown that heparin lyase I cleaves the glucosaminidic bonds linked to 2- sulphated glucuronic and iduronic acid residues of the hexosamine unit. Heparin lyase II cleaves nearly all the α-glucosaminide linkages in both heparan sulphate and heparin independently of O- and / or N-sulphation. This enzyme is able to degrade not only N-sulphate or N-acetylate but also non-substituted polymers. On the other hand, heparin lyase III is active on the low sulphated regions in both heparin and heparan sulphate, thus it prefers to act on heparan sulphate rather than on heparin. Also, it has more affinity towards polymeric heparan sulphate than heparan sulphate oligosaccharides. Heparin lyase III splits the glucosaminidic bond of glucosamine (N-sulphate or N-acetylate α-1,4- glucuronic acid) (Yamada and Sugahara, 1998).

According to the work of Lohse and Linhardt (1992), the mechanism of action of all heparin lyases is endolytic. The pH optimum of heparin lyases I, II and III are 7.3, 6.9 and 7.6, respectively in the presence of 0.1 M NaCl. Conversely, Yang *et al.* (1985) reported that the pH optimum of heparin lyase I is 6.5 in the presence of 0.1 M NaCl. The optimum temperature is 35 °C for heparin lyase I, 40 °C for heparin lyase II and 45 °C for heparin lyase III. Moreover, Lohse and Linhardt demonstrated that the activity of heparine lyase I is increased by increasing the concentration of salt while the activity of both heparin lyase II and III is decreased. The K_m and k_{cat} of heparin lyases I, II and III are: 17.8 ± 1.5 and 219 ± 3.48, 57.7 ± 6.56 and 16.7 ± 0.555, and 29.4 ± 3.16 μm and 141 ± 3.88 μmol min^{-1} mg^{-1} protein, respectively (Lohse and Linhardt, 1992).
The digestion of heparin by these enzymes results in the formation of different products due to differences in the substrate specificities of these enzymes. Consequently, these enzymes are used to elucidate the primary structure of heparin and heparan sulphate from a variety of proteoglycans, cells or tissues (Ernst *et al.*, 1996).

1.3.2.4 Polysaccharide lyase family 16

This family was first classified as glycoside hydrolase family 69, and comprises 26 open reading frames of bacteriophage hyaluronidases that infect different strains of *Streptococcus pyogenes*. However, after the characterization of some enzymes from this family it was found that the mechanism of action of these enzymes was lytic rather than hydrolytic (Baker *et al.*, 2002; Smith *et al.*, 2005). Therefore, this family was reclassified as polysaccharide lyase family 16 (PL 16) (Smith *et al.*, 2005). PL 16 contains three characterized enzymes from *S. pyogenes* bacteriophage H4489A (Baker *et*

al., 2002), *S. pyogenes* SF370 (Smith et al., 2005) and *S. pyogenes* bacteriophage 10403 (Mishra *et al.*, 2006). It was found that these enzymes degrade only HA, and they are unable to degrade chondroitin, chondroitin-4-sulphate or chondroitin-6-sulphate (Baker *et al.*, 2002; Smith *et al.*, 2005; Mishra *et al.*, 2006). Accordingly, it is suggested that the role of these enzymes is to assist the phage in accessing the cell wall of the bacterial host through the digestion of the surrounding HA capsule.

PL 16 hyaluronate lyases have low molecular weights (Mishra *et al.*, 2006), in contrast to PL 8 hyaluronate lyases that have high molecular weight ranges from 77-121 kDa (Baker *et al.*, 2002) and they show very low amino acid sequence homology with bacterial hyaluronate lyases (Mishra *et al.*, 2006). On the contrary to the hyaluronate lyases of PL 8, which are characterized by a high turnover number (8600 s^{-1} for group B streptococci), the HylP of *S. pyogenes* bacteriophage H4489A and HylP1 of *S. pyogenes* SF370 have low turnover values of 4.9 and 7.2 ± 0.9 s^{-1}, respectively. The mechanism of action of both enzymes is endolytic, producing a mixture of oligosaccharides with a predominance of hexamers and octamers as end products in the case of the HylP1 of *S. pyogenes* SF370, while the main end product of HylP of *S. pyogenes* bacteriophage H4489A is a tetramer (Baker *et al.*, 2002; Smith *et al.*, 2005).

Recently the 3D structure of HylP1 of *S. pyogenes* SF370 has been solved. It was found that the structure of HylP1 is comprises three intertwined polypeptide chains. The N-terminal domain of HylP1 contains a mixed globular α/β capping region. The middle part of the enzyme is comprises triple-stranded β-helix that creates an unequal triangular cylinder (Smith *et al.*, 2005). It was found that the active site of Hylp2 of *S. pyogenes*

bacteriophage 10403 is found in the C-terminal domain of the enzyme. This fragment has been isolated and found to be functionally active (Mishra *et al.*, 2006).

1.4 Value of analysing GAG active enzymes

Enzymes which degrade GAGs may provide a tool for the preparation of novel therapeutic agents, since the structural data for some of these enzymes have been obtained allowing the identification of important residues involved in catalysis and substrate recognition. Therefore the introduction of mutations in these residues will allow a better understanding of how these enzymes work, which will consequently help in the design of inhibitors.

Hyaluronidases could be widely used in a variety of therapeutic aspects. It is known that the degradation of HA by hyaluronidases results in an increase in membrane permeability, and decreases the viscosity of and helps the diffusion of injected fluids. Therefore, these enzymes may be a valuable tool in medicine as they may be used to increase the speed of absorption, to improve the effectiveness of local anaesthesia and to prevent tissue destruction resulting from the intramuscular and subcutaneous injection of fluids (Frost *et al.*, 1996; Menzel and Farr, 1998).

Moreover, these enzymes could be used as a means of producing large quantities of oligosaccharides which may be used in the medical field instead of HA, as these fragments are more favourable. This is because the presence of the double bond in such oligosaccharides is essential in protecting the epidermis of humans against UV induced

oxidation damage. Also oligosaccharides can penetrate the skin more easily than HA, which has a high molecular weight (Kuhn *et al.*, 2003).

It is becoming increasingly clear that HA oligosaccharides can induce a variety of biological processes such as angiogenesis. Misra et al. (2003) showed that HA oligosaccharides (12 mers) suppress the development of breast cancer, probably through disturbing the binding between CD44 tumour cells and the endogenous HA produced by tumour cells.

In addition, it has been suggested that oligosaccharides of size 4-16 disaccharide could be used in vaccinations against tumours or viral antigens due to the increased activation of immune responses (Termeer *et al.*, 2000).

It has been shown that certain sizes of HA oligosaccharides control the expression of heat shock protein 72 (Hsp72), by increasing the activation of heat shock factor 1 (HSF1) under stress conditions, which suppresses the degeneration of synovial cells in an arthritis model (Xu *et al.*, 2002). Also, it has been documented that low molecular weight fragments of HA stimulate the expression of genes implicated in the inflammatory response, such as genes for chemokines and cytokines (Xu *et al.*, 2002).

1.5 Hyaluronidase inhibitors

Selective and potent inhibitors of hyaluronidases are needed in order to study the role of HA and HA degrading enzymes in physiological and pathophysiological processes. Furthermore, inhibitors of enzymes which degrade HA could be used as drugs in

combination with antibiotics in antibacterial therapy. Recently it has been reported that vitamin C has an inhibitory effect on *S. pneumoniae* hyaluronate lyase, but the inhibitory effect was weak upon this enzyme and there was no effect on bovine testicular hyaluronidase (Li *et al.*, 2001). More recently, based on the structural information available for *S. pneumoniae* hyaluronate lyase in complex with vitamin C, it has been suggested that the introduction of lipophilic chains in position 6 of vitamin C such as in L-ascorbic acid-6-hexacanoate, may lead to a greater inhibitory effect. Consequently the effect of L-ascorbic acid-6-hexacanoate on *S. pneumoniae* hyaluronate lyase and bovine testicular hyaluronidase has been determined, and it was found that this compound has a strong inhibitory effect on both enzymes of about 1500 times stronger than vitamin C in inducing the inhibition (Botzki *et al.*, 2004). Also, Okorukwu and Vercruysse (2003) found that saccharic acid, which is an analogue of ascorbic acid, displayed strong inhibition upon bacterial hyaluronate lyase and did not affect the stability of HA substrate. This is unlike vitamin C, which degrades HA.

1.6 Objectives

Since there is no information available on ORF *sc1c2.15* of the soil bacterium *Streptomyces coelicolor* A3(2) that encodes a putative hyaluronate lyase of family 8, polysaccharide lyases, the first part of this project aims to clone, express, purify and characterise this putative gene product biochemically and structurally, in order to obtain an insight into its substrate specificity and catalytic mechanism. Subsequently, based on its three-dimensional structure, different mutants of the enzyme will be generated using site directed mutagenesis and co-crystallisated with different substrates in order to identify the amino acid residues that interact with these ligands.

It is well known that hyaluronate lyases of pathogenic bacteria constitute one of the virulence factors that assist bacteria in spreading deeply through human tissues and causing several diseases. Therefore, the goal of the second part of the project is to study the chromosomal gene of *Streptococcus pyogenes* that is responsible for hyaluronate lyase expression. ORF hylA of the human pathogenic bacterium *Streptococcus pyogenes* SF370 from the same family has been cloned, expressed, purified and characterised.

It is obvious from a review of the literature regarding family 12 of polysaccharide lyases that there remain lots of unanswered questions concerning their mode of action, the elucidation of the 3D structure and identification of key catalytic residues within the active site to further understand the ligand specificity and protein/ligand interactions of this family of enzymes. Consequently, ORF spy0628 from *Streptococcus pyogenes*

SF370 encodes putative heparin lyase has been cloned, expressed, purified and characterised.

Chapter 2 Materials and Methods

2.1: Materials

2.1.1 Chemicals, enzymes and kits

2.1.1.1: Antibiotics

Ampicillin and kanamycin were dissolved in sterile deionised water, while chloramphenicol and tetracycline were dissolved in 50 % (v/v) ethanol. The antibiotics were then diluted with media to final concentrations as shown in Table 2.1.

Table 2.1: Stock and final concentrations of antibiotics in media.

Antibiotic	Stock concentration	Final concentration($\mu g\ ml^{-1}$)
Ampicillin (SIG)	10 mg ml^{-1}	100
Chloramphenicol (SIG)	34 mg ml^{-1}	34
Kanamycin (SIG)	10 mg ml^{-1}	50
Tetracyclin (SIG)	6.25 mg ml^{-1}	12.5

2.1.1.2: Enzymes

All enzymes, buffers and reaction co-constituents were kept at -20 °C.

Table 2.2: Enzymes and Co-constituents. A list of buffer recipes used for each enzyme is given in Appendix IC.

Enzyme	Suppliers	Co-constituents
Pfu DNA polymerase	Promega	$MgCl_2$, reaction buffer
Platinium *Pfx* DNA polymerase	Invitrogen Corp	$MgCl_2$, reaction buffer
Kod DNA polymerase	Invitrogen Corp	$MgCl_2$, reaction buffer
Restriction enzymes	Promega	BSA, reaction buffer
T4 DNA Ligase	New England Biolabs	Reaction buffer
Hen egg white lysosyme	Fisher	None
RibonucleaseA	Sigma	None

2.1.1.3: Kits

All kits and components were stored at room temperature, except the cell re-suspension buffer of the plasmid purification kits, which was maintained at 4 °C. A list of components of each kit is shown in Appendix I E.

Table 2.3: List of various kits used

Kit	Suppliers
Nucleo Spin Extract 2 in 1 kit	Macherey-Nagel
QIA prep Spin Miniprep kit	Qiagen, Hilden
QIA quick Gel Extraction Kit	Qiagen, Hilden
Quik Change Site-Directed mutagenesis kit	Stratagene

2.1.2: Bacterial strains and vectors

2.1.2.1: Bacterial strains

All bacterial strains were maintained at –80 °C in 25 % glycerol (v/v).

Table 2.4 *E. coli* strains used in this study

E.coli strain	Relevant product	Application
E.coli TOP10		Cloning host
E. coli Bl21 (DE3)	ompT, λ-prophage- T7-polymerase	Hyper expression of protein
E. coli BL21 (DE3) pLysS	ompT, λ-prophage- T7-polymerase, pLysS, cat	Hyper expression of protein
E. coli BL21 Origami B	ompT, λ-prophage- T7-polymerase, PLysS, cat	Hyper expression of protein
Rosseta pLysS	ompT, λ-prophage- T7-polymerase, pLysS, cat	Hyper expression of protein

Different strains of *E coli* were used in this work in order to express the proteins in soluble active form, for instance Rosseta pLysS was used to enhance the expression of proteins that contain codons rarely used in *E. coli* BL21(DE3). Another strain, *E. coli* BL21 Origami B that has mutations in both the thioredoxin reductase and glutathione reductase genes, was used as it greatly enhances disulfide bond formation in the cytoplasm and is recommended for the expression of proteins that require disulfide bond formation for proper folding. It has been suggested that the expression in Origami produces more active protein with pET-32 vectors, since the thioredoxin fusion tag further enhances the formation of disulfide bonds in the cytoplasm (Prinzet al., 1997). Tuner strains are mutants of BL21 that enable adjustable levels of protein expression throughout all cells in a culture. By adjusting the concentration of IPTG, expression can be regulated from very low level expression up to the fully induced expression levels commonly associated with pET vector. Lower level expression may enhance the solubility and activity of difficult target proteins.

2.1.2.2: Vectors

For the cloning of PCR products pGEM® -T Easy (PRO) and pCR®-Blunt were used, and pET- 28a, pET–22b and pET–32c (NOV) were used for the subsequent expression of cloned open reading frames. Cloning and expression vectors maps are located in Appendix II of this work.

Table 2.5: Vectors used for cloning and gene expression.

Plasmid	Properties	Supplier
PET-22b	Amp^r,T7 lac, $lacI^q$	Novagen
PET-28a	Kan^r, T7 lac, $lacI^q$	Novagen
PET-32c	Amp^r,T7 lac, $lacI^q$	Novagen
pGEM® -T Eas	Amp^r,T7 lacZ	Promega
pCR®- Blunt	Kan^r, T7 la	Invitrogen

2.1.3: Oligonucleotides (MWG)

2.1.3.1: For amplification of SC1C2.15

Fwd: 5' CAT ATG GCC ACC GCC GAC CCC TAC 3'

Rev: 5' CTC GAG GCT GAG AGT CAC CTC ACA TTC 3'

Rev Stop: 5' GGA TCC TCA GCT GAG AGT CAC CTC 3'

2.1.3.1.1: For amplification of alpha domain

Fwd: 5' CAT ATG GCC ACC GCC GAC CCC TAC GAC GCC 3'

Rev: 5' CTC GAG GGC GGC CTC GCC GGG GGC 3'

Rev Stop: 5' GGA TCC TCA GGC GGC CTC GCC GGG GGC 3'

2.1.3.1.2: For amplification of beta domain

Fwd: 5' CAT ATG GGA CAC CAC CTC TTC GCG 3'

Rev: 5' CTC GAG GCT GAG AGT CAC CTC ACA TTC 3'

Rev Stop: 5' GGA TCC TCA GCT GAG AGT CAC CTC ACA TTC 3'

2.1.3.1.3: For creation of SC1C2.15 mutants

The primer sequences below were used for the construction of site directed mutants of SC1C2.15; mutation in bold.

Y253A

Fwd: 5' GCC TAC TCG GGG ACG **GCG** GGC CAG GTC ATG 3'

Rev: 5' CAT GAC CTG GCC **CGC** CGT CCC CGA GTA GGC 3'

N194A

Fwd: 5' CC ACC GGC GCC **GCG** CGC GTC GAC C TG 3'

Rev: 5' CAG GTC GAC GCG **CGC** GGC GCC GGT GG 3'

H244A

Fwd: 5' GGC TCC TTC GTC CAG **GCG** ACC TCG GTC GCC 3'

Rev: 5' GGC GAC CGA GGT **CGC** CTG GAC GAA GGA GCC 3'

2.1.3.2: For amplification of hylA

Fwd: 5' CAC CAC CAC CAC ATG GCC GAT ACA CTG ACT TCA AAT TCA GAA CC 3'

Rev: 5' GAG GAG AAG GCG CGT TAT TGT TGA TTT TGC CTG ACA GGA TGA GG 3'

2.1.3.2.1: For creation of HylA mutants (mutation in bold).

Y327A

Fwd: 5' C AT T GCT TAC ACT GGA GCT **GCG** GGT AAT GTG CTT AT A GAT GG C 3'

Rev: 5' GCC ATC TAT AAG CAC ATT ACC **CGC** AGC TCC AGT GTA AGC AAT G 3'

Y327F

Fwd: 5' GGC ATT GCT TAC ACT GGA GCT **TTC** GGT AAT GTG CTT ATA GAT GGC 3'

Rev: 5' GCC ATC TAT AAG CAC ATT ACC **GAA** AGC TCC AGT GTA AGC AAT GCC 3'

N207A

Fwd: 5' CCT TTT GAA GCC AAT AGC GGA **GCG** TTA ATT GAT ATG GGG CGT G 3'

Rev 5' CAC GCC CCA TAT CAA TTA ACG CTC **CGC** TAT TGG CTT CAA AAG 3'

H307A

Fwd: 5' GAC GGT TCT TTA ATT GAT **GCG** GTG GTT ACT AAC GCT CAA AGT CC 3'

Rev: 5' GG ACT T TG AGC GTT AGT AAC CAC **CGC** ATC AAT TAA A

GA ACC G TC 3'

2.1.3.3: For amplification of *Spy0628*

Fwd: 5' CAT ATG TTT TTT GCC TTC GCA CGC 3'

Rev: 5' CTC GAG GTG TTT CAA TCG AAT AAT CTC 3'

Rev Stop:5' GGA TCC TTA GTG TTT CAA TCG AAT AAT CTC 3'

2.1.4: Media and buffers

2.1.4.1: Media for culturing *E.coli*

2.1.4.1.1: Liquid media

2.1.4.1.1.1 LB-Media (Luria Bertani)

Tryptone (OX)	10	$g\ L^{-1}$
Yeast extract (OX)	5.0	$g\ L^{-1}$
NaCl (SIG)	10	$g\ L^{-1}$

pH 7.0

2.1.4.1.1.2 NZY Broth

NZ (casein hydrolysate) (OX)	10	$g\ L^{-1}$
Yeast extract (OX)	5	$g\ L^{-1}$
NaCl (SIG)	5	$g\ L^{-1}$
$MgSO_4$ 1 M (SIG)	1.0	$ml\ L^{-1}$

pH 7.0

2.1.4.1.1.3 NZY^+ Broth

NZY^+ broth was used for the recovery of transformed chemically competent cells. The broth was made by the addition of 0.45 ml of supplement (stored at 4 °C) to 10 ml of NZY broth using sterile vessels and pipette tips.

2.1.4.1.1.4 NZY (supplement)

1 M $MgCl_2.H_2O$	12.5	ml $45ml^{-1}$
1 M $MgSO_4.H_2O$	12.5	ml $45ml^{-1}$
20 % (w/v) glucose	20.0	ml $45ml^{-1}$

Filter sterilised

2.1.4.1.2: Solid media

For the preparation of agar plates LB media was supplemented with agar (bacteriological agar N°1) 2g 100 ml^{-1}. Agar was then made soluble by autoclaving the media, and poured into Petri dishes once the media had cooled to 50 °C.

2.1.4.1.3: Selective media

In addition to the presence of the appropriate antibiotic in the media, isopropylthio-β,D-galactoside (IPTG) was added to *E. coli* strains carrying pET plasmid to induce transcription of the recombinant gene. Also, in order to detect the insertional inactivation of β-galactosidase gene in recombinant plasmids, 5-bromo-4-chloro-3-indoyl-β-D-galactoside (X-Gal) was added to the solid media with IPTG (Blue/white selection). The stock and final concentrations of IPTG and X-Gal are shown in table 2.6.

Table 2.6 Stock and final concentrations of IPTG and X-Gal.

Compound	Stock concentration	Final concentration
IPTG	24 mg ml^{-1}	240 μg ml^{-1}
X-Gal	40 mg ml^{-1}	80 μg ml^{-1}

2.1.4.2: Media for culturing *Streptococcus pyogenes*

Todd Hewitt	36.4	g L^{-1}
Yeast extract	2.0	g L^{-1}
Glycine	20.0	g L^{-1}

2.1.4.3: Buffers

2.1.4.3.1: For isolation of plasmid DNA

2.1.4.3.1.1: <u>STET buffer</u>

Sucrose	80	g L^{-1}
Triton X-100	50	ml L^{-1}
EDTA 0.5M, pH8	100	mlL^{-1}
Tris	6.06	g L^{-1}

2.1.4.3.2: For agarose gel electrophoresis of DNA fragments

2.1.4.3.2.1 <u>DNA loading buffer</u> (6x)

Sucrose	4.0	g 10 ml^{-1}
Bromophenol blue	0.025	g 10 ml^{-1}

2.1.4.3.2.2 <u>TAE running buffer</u> (50x)

Tris-base	242	g L^{-1}
Glacial acetic acid	57.1	ml L^{-1}
0.5 M EDTA, pH 8	100	ml L^{-1}

This buffer was diluted to 1x with deionised water prior to use in the preparation of agarose gels and use as reservoir buffer in gel tanks.

2.1.4.3.2.3 TE buffer

0.5 M Tris-HCl, pH 7.5	20	ml L^{-1}
0.5 M EDTA, pH 8	2.0	ml L^{-1}

2.1.4.3.3: For preparation of compotent *E.coli* cells

2.1.4.3.3.1 FSB buffer (Transformation solution)

1 M potassium acetate, pH 7.5	1.00	ml L^{-1}
(pH adjusted with acetic acid)		
$MnCl_2$-$4H_2O$	890	mg L^{-1}
$CaCl_2$-$2H_2O$	150	mg L^{-1}
KCl	750	mg L^{-1}
Hexamminecobalt chloride	80	mg L^{-1}
100 % (v/v) glycerol	10	ml L^{-1}
deionised water	80	ml L^{-1}

Sterilized by filtration

2.1.4.3.3.2 $MgCl_2$-$CaCl_2$ solution

$MgCl_2$	3.25	g 200 ml^{-1}
$CaCl_2$	0.588	g 200 ml^{-1}
$CaCl_2$	2.90	g 200 ml^{-1}

2.1.4.3.4: For uronic acid assay

120 mM sodium tetraborate / 80 % sulphuric acid (H_2SO_4)

100 mg ml meta-hydroxydiphenyl in dimethyl sulphoxide

2.1.4.3.5: For protein analysis and purification

2.1.4.3.5.1 SDS- PAGE running buffer10 x (Stock)

Running buffer was made up at 10 x stock concentration and diluted to 1 x before use.

Tris	30.3	g L^{-1}
Glycine	144	g L^{-1}
SDS	10	g L^{-1}

The pH of the Tris-HCl and glycine was adjusted to 8.8 in a volume of ~ 900 ml prior to the addition of SDS.

2.1.4.3.5.2 SDS-PAGE sample buffer

60 mM Tris-HCl, pH6.8	0.6	ml 10 ml^{-1}
50 % (v/v) Glycerol	5.0	ml 10 ml^{-1}
10 % (w/v) SDS	2.0	ml 10 ml^{-1}
14.4 mM B-Mercaptoethanol	0.5	ml 10 ml^{-1}
0.1 % (w/v) Bromophenol blue	1.0	ml 10 ml^{-1}
deionised water	0.9	ml 10ml^{-1}

Stored at -20 °C in 0.5 ml aliquots.

2.1.4.3.5.3 Solublising SDS-PAGE sample buffer

SDS-PAGE sample buffer	7.6	ml
Urea	2.4	g

Stored at 4 °C

2.1.4.3.5.4 12% (w/v) Acrylamide resolving gel components

40% (v/v) solution (37.5:1 acrylamide: bisacrylamide)	3.0 ml	
Buffer B*	2.5	ml

deionised water	4.0	ml
10 % (w/v) ammonium persulphate	50	µl
TEMED	10	µl

***Buffer B**

2M Tris-HCl, pH8.8	75	ml 100 ml^{-1}
10% SDS	4	ml 100 ml^{-1}

2.1.4.3.5.5 4 % (w/v) Acrylamide stacking gel components

40 % (v/v) solution (37.5:1 acrylamide : bisacrylamide)		0.5 ml
Buffer C*	1.0	ml
deionised water	2.5	ml
10 % (w/v) ammonium persulphate	30	µl
TEMED	10	µl

***Buffer C**

1 M Tris-HCl, pH 6.8	50	ml 100 ml^{-1}
10 % (w/v) SDS	4.0	ml 100 ml^{-1}

2.1.4.3.5.6 Protein size standard

High molecular weight range (SIG) (M.W. 36, 45, 55, 66, 84, 97, 116 and 205 kDa)

Low molecular weight range (SIG) (M.W. 20, 24, 29, 36, 45, and 66 kDa)

Lyophilised standards (SIG) were reconstituted with 100 µl of deionised water to give a final concentration of ~2.0-3.5 mg ml^{-1}, which was aliquoted into 4 µl amounts and stored at –20 °C. A list of proteins used to produce the appropriate sized bands is given

in the Appendix I (Table ID).

2.1.4.3.5.7 Coomassie blue gel stain solution

Coomassie Brilliant Blue R250	1	$g\ L^{-1}$
Acetic acid glacial	100	$ml\ L^{-1}$
Methanol	450	$ml\ L^{-1}$

2.1.4.3.5.8 Coomassie gel destain solution

Acetic acid glacial	100	$ml\ L^{-1}$
Methanol	100	$ml\ L^{-1}$

2.1.4.3.6 For purification of His-tagged proteins

2.1.4.3.6.1 Starting buffer (20mM HEPES, 0.5M NaCl, 10mM Imidazole)

HEPES	4.77	$g\ L^{-1}$
NaCl	29.2	$g\ L^{-1}$
Imidazole	0.68	$g\ L^{-1}$

pH 7.4

2.1.4.3.6.2 Elution buffer (20mM HEPES, 500mM imidazole)

HEPES	4.77	$g\ L^{-1}$
Imidazole	34.0	$g\ L^{-1}$

pH 7.4

2.1.4.3.7: Gel filtration buffer

10 mM Tris HCl, 200 mM NaCl, pH 8

Tris-base	3.03	$g\ L^{-1}$
NaCl	11.7	$g\ L^{-1}$

pH 8

2.1.5 Reagents for Bradford's assay

Bovine serum albumin (BSA) was made at a concentration of 10 mg ml^{-1} and stored at – 20 °C, for subsequent dilution in assay. Bradford Reagent (Brilliant blue G in phosphoric acid and methanol) was stored at 4 °C.

2.1.6 Protein crystallization screens

The solutions used for crystal development are given in the Appendix III.

2.1.7 HPAEC chemicals

All HPAEC chemicals were degassed by vacuum prior to use.

0.1 M NaOH

NaOH (47 % (v/v) solution FIS CHEM)	8.5	ml L^{-1}

1.3 M NaCl (in 0.1 M NaOH)

NaOH (47 % (v/v) solution FIS CHEM)	8.5	ml L^{-1}
NaCl (FIS CHEM)	76	g L^{-1}

2.1.8 DNSA reagents

3,5-Dinitrosalic	10	g L^{-1}
Phenol	2	g L^{-1}
NaOH	10	g L^{-1}
Sodium sulphite	0.5	g 10 ml^{-1}
Glucose	2	g 10 ml^{-1}

2.1.9 Dialysis

Dialysis of substrates or proteins was achieved in cellulose membrane tubing (size 25 mm x 16 mm; retains >90 % Cytochrome C [M.W. 12400 Da]; Sigma) and secured with dialysis tubing closures. Dialysis of oligosaccharides was accomplished in cellulose ester membrane tubes (size 16 mm x 10 mm) and secured with dialysis tubing closures. The molecular weight cut off from these tubes ranged from 100 to 100,000 Daltons and they were packaged wet in 0.1 % (w/v) sodium azide as a preservative.

2.1.9.1 Preparation of dialysis tubing

The dialysis tubing was cut into pieces of suitable length and boiled for 10 min in a large volume in deionised water. The tubing was then rinsed thoroughly inside and outside with deionised water, then stored at 4 °C in deionised water. However, the dialysis tubes for oligosaccharides were cut into pieces according to the volume of each fraction (1cm ml^{-1}) and they were prepared by soaking them in a large volume of deionised water for about 30 min at room temperature (without boiling) to remove the sodium azide preservative agent. The tubes were then rinsed several times thoroughly inside and outside with deionised water.

2.1.9.2 Preparation of dialysed substrates

Sodium hyaluronate from the fermentation of streptococci (Fisher UK), potassium hyaluronate from umbilical cord (Sigma brand, Sigma-Aldrich, Gillingham UK), choindroitin-4-sulphate from bovine trachea (Fluka brand, Sigma-Aldrich, Gillingham UK) and choindroitin-6-sulphate from shark cartilage (Fluka brand, Sigma-Aldrich, Gillingham UK) were used. Each substrate (1g) was added to 100 ml of deionised water and autoclaved. This solution was then stirred for 5 h at room temperature with 50 mM EDTA, pH 8. Precipitates were then removed by centrifugation for 15 min at 14000 x g

and supernatants were subsequently dialysed three times in 4 L against 18.2 MΩ/cm water overnight. The dialysed substrates were then aliquoted in 20 ml volumes into Petri dishes, frozen at –20 °C, lyophilised overnight and stored at room temperature for future use. Prior to kinetic analysis, the substrate was redissolve in deionised water.

2.1.9.3 Preparation of dialysed protein

For dialysis of refolding proteins, after purification of α and β domains through immobilised metal affinity chromatography (IMAC), the fractions containing the refolding proteins were subjected to dialysis in cellulose membrane tubing (Section 2.1.9.1) against 50mM Tris-HCl, pH8 containing different concentrations of urea (section 2.2.3.7).

2.1.9.4 Preparation of dialysed oligosaccharides

The fractions of oligosaccharides purified through the gel filtration P-6 column (section 2.2.4.4) were transferred into separate dialysis tubes (one tube for each peak) and dialysed three times in 5 L deionised water, stirred for 1h, 2 h and overnight at room temperature. The dialysed fractions were then aliquoted into separate Petri dishes frozen at –80 °C, lyophilised for 2-3 days and then resuspended in 500 µl of deionised water .

2.2 Methods

2.2.1 Microbiology methods

2.2.1.1 Sterilisation

Unless stated otherwise, all solutions and apparatus were sterilised by autoclaving (Appendix D1) at 121 °C, with a pressure of 1.05 bar for 20 min. Solutions that could not be autoclaved were filter sterilised through a 0.2 µm Ministart® filter unit (Sartorius), attached to a suitable sterile syringe (Plastipak®, Becton Dickinson).

2.2.1.2 Growth of bacteria harbouring plasmid

2.2.1.2.1 Growth of bacteria for standard/crude plasmid purification

For high copy number plasmid, *E. coli* TOP10 was grown in 28 ml universals containing 5 ml of LB media (Section 2.1.4.1.1.1). For low copy number plasmid, *E. coli* was grown in 250 ml conical flasks containing 25 ml of LB media supplemented with the appropriate antibiotic, the resistance gene which was encoded on the plasmid to be purified. The cultures were inoculated from an agar plate, glycerol stock or liquid culture using a sterile wire loop, and grown overnight at 37 °C with orbital shaking at 200 rpm.

2.2.1.2.2 Growth of bacteria for starter cultures

E. coli strains TOP10, BL21, Tuner, Rosseta pLysS and Orgami B(DE3), and were grown in 28 ml sterile glass universals containing 5 ml LB media (section 2.1.4.1.1.1) supplemented with the appropriate antibiotic, the resistance gene for which was encoded on the plasmid carried by the cells. The cultures were inoculated from an agar plate, glycerol stock or liquid culture using a sterile wire loop, and grown overnight at 37 °C with orbital shaking at 150 rpm.

2.2.1.2.3 Growth of bacteria for the expression and subsequent purification of protein

In order to test the small-scale expression of proteins, once the recombinant plasmids were obtained and transformed into expression strains, a small-scale expression test was conducted to identify the optimal condition for protein production. 5 ml LB (section 2.1.4.1.1.1) containing the appropriate antibiotic was inoculated with a fresh single bacterial colony and incubated overnight at 37 °C with shaking at 200 rpm in a 28 ml

universal tube. 25 ml of pre-warmed LB medium in a 250 ml flask was inoculated with a 0.25 ml of overnight culture, supplemented with the appropriate antibiotic, and incubated at 37°C with shaking (200 rpm) until the OD_{600} reached 0.6. Then induction by the addition of IPTG to a final concentration of 1 mM.. The cells were then grown overnight using various temperatures (4°C, 20°C and 30°C). Subsequently 1ml of each sample was taken and the cells were pelleted resuspended in 300 µl of starting buffer, lysed by ultra-sonification, centrifuged at 20,000 x g to obtain cell free extracts, to 20 µl of each cell free extract 5 µl of loading buffer was added and then 20 µl run on a SDS-PAGE gel (section 2.2.3.1) and visualized by Coomassie blue staining to determine levels of protein expression.

Once the conditions were optimized for protein expression, the large-scale production of recombinant proteins from *E. coli* was carried out by culturing cells at the previously optimized conditions. 10 ml of LB media were inoculated with a fresh single bacterial colony and incubated overnight at 37 °C with shaking at 200 rpm in a 28 ml universal. After that, 10ml of the overnight culture was aseptically transferred into 1 L of pre-warmed LB media supplemented with the appropriate antibiotic and incubated at 37 °C with shaking (200 rpm) until the culture reached an OD_{600} of ~0.6, and checked by aseptically transferring 1 ml of culture to a cuvette and reading the OD in a spectrophotometer previously zeroed with LB media. Once the OD attained 0.6, the culture was then induced by the addition of IPTG to a final concentration of 1 mM. After induction, the culture was incubated either at 30 °C (for native HylA protein, and its mutants) or 20 °C (for native SC1C2.15 protein, its mutants and truncated alpha and beta proteins) or 4 °C (for truncated alpha and beta proteins) with overnight shaking at 100 rpm.

2.2.1.3 Plating bacteria

Prior to plating, LB agar plates were surface dried in an oven at 65 °C for 10 min. A glass spreader was sterilised by immersion in 70 % (v/v) ethanol, followed by the removal of excess ethanol by passing it quickly through a blue Bunsen flame, and used to spread 200 µl of bacterial suspension evenly over the surface of the agar. When all the liquid had been absorbed into the agar, the plate was incubated inverted at 37 °C for ~ 16 h.

2.2.1.4 Preparation of chemically competent cells of *E. coli* strains

Cells were rendered competent for transformation by either the $CaCl_2$ method (Cohen *et al.*, 1972) or the Hanahan method (Hanahan, 1983). The $CaCl_2$ method commenced with the inoculation of a single colony of the required strain of *E. coli* TOP10, BL21 (DE3) Tuner, Rosseta pLysS or Origami BL21 (DE3) from an agar plate into 5 ml of LB media to make a starter culture. After overnight growth, the starter culture was used to inoculate 50 ml of LB media in a 250 ml conical flask by an addition of 1 % (v/v) ionculum. The culture was then allowed to grow at 37 °C with shaking at 200 rpm up to an OD_{600} of 0.35; at this point the culture was placed on ice for 30 min. After incubation on ice, the culture was pelleted by centrifugation at 2700 x g for 10 min at 4 °C and the supernatant discarded. The cell pellet was then re-suspended (by gentle vortex) in 15 ml of ice-cold $MgCl_2$-$CaCl_2$ solution (80 mM $MgCl_2$, 20 mM $CaCl_2$) (section 2.1.4.3.3.2), and incubated on ice for a further 10 min, prior to re-centrifugation at 2700 x g for 10 min at 4 °C and the supernatant was discarded. The cell pellet was re-suspended (by gentle vortex) in 1 ml of ice-cold 0.1 M $CaCl_2$ solution. Finally, the cells were placed on ice, and at this point the cells were ready to use.

The other method, which is also used to make chemically competent *E. coli* cells is the Hanahan method. This method started with the inoculation of 50 ml LB with 0.5 ml of an overnight culture of the appropriate strain. Cells were grown at 37 °C with shaking at 200 rpm up to an OD_{600} of 0.4-0.5. The cells were then placed on ice for 30 min. After incubation on ice, the cell suspension was harvested by centrifugation at 2000 x g for 10 min at 4 °C and the supernatant discarded. The cells were suspended in 4 ml of ice cold FSB solution (section 2.1.4.3.3.1) and incubated on ice for 15 min. Cells were resuspended in 720 µl FSB-buffer following centrifugation at 2000 x g, at 4 °C for 10 min. Cells were chilled on ice and 26 µl of DMSO was added drop by drop. Cells were then incubated on ice for another 15 min prior to the addition of another 26 µl of DMSO, again drop by drop. Cells were left on ice until used or stored at –70 °C.

2.2.2 DNA Methods

2.2.2.1 General DNA methods

2.2.2.1.1 Isolation of genomic DNA from gram-positive bacterial culture

One colony of *S. pyogenes* was inoculated into 25 ml of Todd Hewitt media (section 2.1.4.2) and incubated at 37 °C overnight without shaking.

0.5 ml of the overnight culture was pelleted in a 1.5 ml micro-centrifuge tube at 14000 x g for 5 min and the supernatant was discarded, then 300 µl of 20 mM Tris/HCl pH 6.8, 3 µl of 100 mM $MgCl_2$ and 0.3 µl of 500 U ml^{-1} mutanolysin were added to the pellet and resuspended by vortex and incubated at 37 °C for 1 h. Cells were pelleted at 14000 x g for 5 min and supernatant discarded. 300 µl of lysis buffer (50 mM NaCl, 2.5 mM EDTA, 30 mM Tris /Hcl pH 8) and 25 mg ml^{-1} lysozyme was added to re-suspend the pellet and incubated at 37 °C for 30 min. The cells were pelleted again at 14000 x g, the supernatant was discarded and the permeabilised cells were resuspended in 300 µl of cell lysis solution and incubated at 80 °C for 5 min.

1.5 µl of RNase A solution was added to the cell lysate and the sample was mixed by inverting the tube 25 times, then incubated at 37 °C for 60-90 min.

In order to precipitate the protein, the sample was cooled to room temperature and 100 µl of protein precipitation solution was added to the cell lysate, vortexed for 20 sec, and incubated on ice for 60 min, then centrifuged at 14000 x g for 5 min.

The supernatant containing DNA was poured into a sterile 1.5 ml micro-centrifuge tube containing 300 µ l of 100 % isopropanol (v/v) and the sample was mixed by gentle inversion 50 times and centrifuged at 14000 x g for 3 min. The supernatant was discarded. The pellet was washed with 700 µl of 70 % (v/v) ethanol prior to centrifugation at 14000 x g for 3 min, then washed again with 700 µl of 100 % (v/v) ethanol and centrifuged for 2 min. After that, the sample was desiccated for 15 min in order to remove any latent ethanol, prior to re-suspension of the pellet in 50 µl of TE buffer and stored overnight at 4 °C.

2.2.2.1.2 Polymerase chain reaction (PCR)

Five different protocols were used. All reactions were analysed by running a 10 µl aliquot on an 1 % agarose gel.

2.2.2.1.2.1 Protocol 1 (for the amplification of *sc1c2.15*)

Primers (Section 2.1.3.1) were designed to provide recognition sites for restriction endonucleases upstream and downstream of the target sequence (section 2.1.3.1). These engineered sites allowed the open reading frame (ORF) to be inserted into a pET expression vector in frame. Two PCR products of the same gene were amplified from the cosmid 1C2, which contains a 42210 bp fragment of *Streptomyces coelicolor* A3(2) chromosomal DNA carrying coding sequence (CDS) *sc1c2.15* (synonym SCO5534). Cosmid 1C2 was kindly provided by Helen Kieser of the John Innes Centre, Norwich,

UK. One difference between the two reverse primers used was that one contained a stop codon and the other did not (see section 2.1.3.1); hence the two different PCR products produced were called Stop and No Stop respectively. The stop PCR product was used for subsequent cloning into pET-28a or pET-22b vectors so that the encoded products contained an N-terminal His tag or no tag, respectively, while the No stop PCR product was used for cloning into the pET-22b vector so that the encoded product contained C-terminal His tag. Also, each PCR product has a different annealing temperature for amplification. The reaction for the amplification of the *sc1c2.15* is shown in Table 2.7.

Table 2.7 Reaction components for PCR (protocol 1). A recipes for Pfx reaction buffer is given in the Appendix I (Table Ica).

Tube component	Volume added	Final concentration in PCR reaction
Sterile water	39 µl	
Forward primer 12.5 µM	1.5 µl	0.3 µM
Reverse primer 12.5 µM	1.5 µl	0.3 µM
Pfx reaction buffer 10 x	5 µl	1 x
Cosmid IC2 (contains 42210 bp fragment of *S. ceolicolor* chromosomal DNA) 0.1 µg μl^{-1}	1 µl	0.002 µg μl^{-1}
dNTPs 25 mM (each)	0.4 µl	0.2 mM (each)
Pfx polymerase (3 U μl^{-1})	0.5 µl	0.03 U μl^{-1}

The Eppendorf MasterCycler™ machine was then programmed to proceed as shown in Table 2.8.

Table 2.8 Reaction conditions for PCR (protocol 1)

Temperature (°C)	Duration (min: sec)	Cycles
94.0	02:00	Initial denaturation
94.0	00:15	5
1° annealing temperature	00:30	
68.0	02:00	
94.0	00:15	25
2° annealing temperature	00:30	
68.0	02:00	
68.0	10:00	Final extension
10.0	Continuous	

2.2.2.1.2.2 Protocol 2 (for the amplification of α- and β- domains)

The DNA sequence encoding the α and β domains of *sc1c2.15* was amplified from a pET-28a recombinant containing the entire *sc1c2.15* gene. Two PCR products encoding each domain were amplified. One product had a stop codon in the reverse primer (Section 2.1.3.1.1; 2.1.3.1.2), and the other product had a no stop codon, and hence the PCR products were named stop and no stop and they have different annealing temperatures for amplification.

The reaction for the amplification of the DNA sequence encoding the α and β domains is shown in Table 2.9.

Table 2.9 Reaction components for PCR (protocol 2). For the recipe of the Pfx reaction buffer (10 x) refer to Appendix I (Ica).

Tube component	Volume added	Final concentration in PCR reaction
Sterile water	40.1 µl	
Forward primer 12.5 µM	1.5 µl	0.3 µM
Reverse primer 12.5 µM	1.5 µl	0.3 µM
Pfx reaction buffer 10 x	5 µl	1 x
pET-28a-*sc1c2.15* template 21.5 ng μl^{-1}	1 µl	5 ng μl^{-1}
dNTPs 25 mM (each)	0.4 µl	0.2 mM (each)
Pfx polymerase (3 U/µl)	0.5 µl	0.03 U μl^{-1}

The PCR machine was then programmed to proceed as shown in Table 2.10.

The primary (1°) annealing and secondary (2°) annealing temperatures for amplification of the stop PCR product encoding the α domain were 56.2 °C and 65.8 °C respectively, and the 1° and 2° annealing temperatures for the non-stop were 57.8 °C and 64.9 °C respectively. For amplification of the PCR product encoding the β domain the 1° and 2° annealing temperatures for the stop PCR product were 56.2 °C and 65.8 °C respectively, and the 1° and 2° annealing temperatures for the non-stop were 57.8 °C and 64.9 °C, respectively.

Table 2.10 Reaction conditions for PCR (protocol 2).

Temperature (°C)	Duration (min:sec)	Cycles
94.0	02:00	First denaturation
94.0	00:15	5
1° annealing temperature	00:30	
68.0	01:18	
94.0	00:15	25
2° annealing temperature	00:30	
68.0	02:00	
68.0	10:00	Final extension
10.0	Continuous	

After the PCR had cooled to 10 °C, 10 µl was removed and run on an agarose gel to check if the amplification had worked.

2.2.2.1.2.3 Protocol 3 (for the amplification of *hylA*)

The ORF *hylA* was amplified from genomic DNA (Section 2.2.2.1.1) of *S. pyogenes* SF370 using the York Structural Biology Laboratories Ligase Independent Cloning (LIC) vector pET-YSBLIC (kindly provided by Mark Fogg). Vector pET-YSBLIC does not require the use of restriction enzymes, and therefore there is no need to provide the primers with recognition sites for restriction endonucleases. Primers were designed using the web site http://seq.yeastgenome.org/egi-bin/web-primer with an optimum melting temperature of 65 °C, optimium primer length of 35 bases and optimum GC

content of 50 %. After that, LIC specific ends were added to the 5' end of the forward and reverse primer. This LIC - annealing depends on the use of exonuclease properties of a DNA polymerase to create cohesive ends. This was achieved by incubation of the purified PCR product with T4 DNA polymerase in the presence of dATP. The 3' to 5' exonuclease activity of the enzyme removes nucleotide residues from both 3' ends of the PCR product nucleotides until it encounters the dATP present in the reaction mix. At this instant, the 5' to 3' polymerase activity of the enzyme counteracts the exonuclease activity to stop additional deletion. This generates 5' specific single stranded overhangs at both ends of the insert complementary to overhangs in the linearised LIC vector which was incubated with T4 DNA polymerase in the presence of dTTP.

A combination of T4 DNA polymerase treated insert and vector are subsequently annealed within ten minutes prior to transformation. The complementarity of the single stranded regions ensures that the insert and vector stay annealed during the transformation process and ligation arises as a result of the action of the DNA repair enzymes in the host cell (Bonsor et al., 2006).

The reaction for the amplification of the *hylA* is shown in Table 2.11.

Table 2.11: Reaction components for PCR (Protocol 3).
The recipe for the KOD reaction buffer (10 x) is given in Appendix

Tube component	Volume added	Final concentration in PCR reaction
Sterile water	34 µl	
Forward primer 20 µM	1 µl	0.4 µM
Reverse primer 20 µM	1 µl	0.4 µM
Reaction buffer 10 x	5 µl	1x
Template DNA 0.1 µg μl^{-1}	1 µl	0.002 µg μl^{-1}
dNTPs 25mM (each)	5 µl	0.3 mM (each)
$MgSO_4$ 25 mM	2 µl	1 mM
KOD Hot Start polymerase (3 U μl^{-1})	1 µl	0.06 U μl^{-1}

Then the PCR machine was programmed to proceed as shown in Table 2.12.

Table 2.12: Reaction conditions for PCR (Protocol 3).

PCR Cycle	Temperature (°C)	Duration (min:sec)	Cycles
Initial denature	94.0	02:00	1
Denature	94.0	00:30	35
Anneal	45	00:30	
Extension	72	02:24	
Final extension	72	03:00	1
Hold	4	N	

45 µl of PCR reaction was cleaned using the Qiagen PCR clean up kit (section 2.2.2.1.9).

9 µl of purified PCR product was made up to a volume of 20 µl by addition of the component listed in Table 2.13, then treated with T4 polymerase

Table 2.13 PCR product LIC T4 polymerase reaction. For the recipe of the T4 polymerase reaction buffer (10 x) refer to Appendix I.

Component	Volume	Final concentration
Purified PCR product	9 µl	
T4 polymerase reaction buffer 10 x	2 µl	1 x
dATP (100 mM)	0.5 µl	2.5 mM
DTT (100 mM)	1 µl	5 mM
T4 polymerase 2.5 U μl^{-1}	0.4 µl	0.05 U μl^{-1}
Sterile water	6.1 µl	

Once the reaction mix was complete, the tube was given a pulse in a microcentrifuge, prior to incubation at 22 °C for 30 min followed by incubation at 75 °C for 20 min. The DNA was then used for annealing into LIC vector.

2.2.2.1.2.3.1 LIC Annealing

The prepared target insert was combined with the prepared LIC vector by incubation for 10 min at room temperature (20-22 °C). Then 1 µl of 100 mM EDTA was added. After mixing, the reaction was left at room temperature for 10 min prior to transformation into chemically competent *E. coli* TOP10 cells (section 2.2.1.4).

2.2.2.1.3 Site-directed mutagenesis (SDM) protocol

2.2.2.1.3.1 Protocol A (for the creation of SC1C 2.15 mutants)

For the creation of SC1C2.15 site directed mutants, a pET-28a clone containing *sc1c2.15* was used as a template (p*sc1c2.15*-28a). Primers were constructed according to section 2.1.3.1.3. The reaction for the amplification of the p*sc1c2.15*-28a mutants is shown in Table 2.14.

Table 2.14: Reaction components for PCR of site-directed mutants (Protocol A). For the recipe of Pfu reaction buffer (10 x), refer to the Appendix I (Table ICc).

Tube component	Volume added	Final concentration in PCR reaction
Sterile water	41µl	
Forward primer 125 ng μl^{-1}	1µl	2.5 ng μl^{-1}
Reverse primer 125 ng μl^{-1}	1µl	2.5 ng μl^{-1}
Pfu reaction buffer 10 x	5µl	1 x
pET 28a- SC1C 2.15 template 21.5 ng μl^{-1}	0.5 µl	0.5 ng μl^{-1}
dNTPs 25 mM (Each)	0.5µl	0.25 mM (each)
Pfu polymerase (3 U μl^{-1})	1 µl	0.06 U μl^{-1}

The PCR machine was then programmed to proceed as shown in Table 2.15.

Table 2.15: Reaction conditions for PCR of site-directed mutants (Protocol A).

Temperature (°C)	Duration (min)	Cycles
95.0	00:30	1
95.0	00:30	16
55	01:00	
68.0	15.24	
10.0	Continuous	

2.2.2.1.3.2 Protocol B (for the creation of HylA mutants)

For the production of HylA site directed mutants, a pET-28a clone containing *hylA* was used as a template. Primers were constructed according to section 2.1.3.2.1.

The reaction of the amplification of the hylA mutants is given in Table 2.16.

Table 2.16: Reaction components for PCR (protocol B). The recipe of Pfu reaction buffer (10 x) is given in the Appendix IC (Table 1Cc).

Tube component	Volume added	Final concentration in PCR reaction
Sterile water	41µl	
Forward primer 125 ng µl^{-1}	1µl	2.5 ng µl^{-1}
Reverse primer 125 ng µl^{-1}	1µl	2.5 ng µl^{-1}
Pfu reaction buffer 10 x	5µl	1x
PET-28a-*hylA* template 21.5 ng µl^{-1}	0.5 µl	0.5 ng µl^{-1}
dNTPs 25 mM (Each)	0.5µl	0.25 mM (Each)
Pfu polymerase (3 U µl^{-1})	1 µl	0.06 U µl^{-1}

The PCR machine was then programmed to proceed as shown in Table 2.17.

Table 2.17: Reaction conditions for PCR (protocol 5).

Temperature (°C)	Duration (min)	Cycles
95.0	00:30	1
95.0	00:30	16
55	01:00	
68.0	15.36	
10.0	Continuous	

2.2.2.1.4 Restriction digests

All restriction endonuclease (New England Biolabs) digests were performed according to the manufacturer's instructions. In order to cut the DNA five units of enzyme were added for each 1 μg of DNA at 37 °C for > 1.5 h. BSA was added to the reaction mix at a final concentration of 0.1 mg ml^{-1}, and the appropriate reaction buffer (Appendix I) was also added to a final concentration of 1x. Care was taken when preparing digests that the glycerol concentration did not exceed 10 % (v/v) in the final reaction, in case enzyme specificity was affected.

The restriction endonucleases used to cut the plasmids/vectors are given in Table 2.18. A list of restriction endonucleases used in this study and corresponding reaction buffers are given in Appendix IC (Table ICb and 1Cc). The digested samples were then subjected to agarose gel electrophoresis (section 2.2.2.1.5). The required DNA fragment was recovered from the gel using a NucleoSpin® Extract 2 in 1 kit and used for ligation (sections 2.2.2.1.8 and 2.2.2.1.12 respectively).

Table 2.18: Restriction endonucleases used to cut plasmids/vectors. A list of the composition of reaction buffers is given in Appendix IC (Table ICb and ICc).

Plasmid/Vector	Restriction endonuclease
p*sc1c2.15*: Stop	*Nde*I / *Bam*HI
No stop	*Nde*I / *Xho*I
α-domain: Stop	*Nde*I / *Bam*HI
No stop	*Nde*I / *Xho*I
β-domain: Stop	*Nde*I / *Bam*HI
No stop	*Nde*I / *Xho*I
pET-28a	*Nde*I / *Bam*HI
pET-22b	*Nde*I / *Bam*HI
	or *Nde*I / *Xho*I
pET-32c	*Nde*I / *Bam*HI

2.2.2.1.5 Agarose gel electrophoresis

Agarose gels were prepared by heating agarose in 1 x TAE (section 2.1.4.3.2.2) buffer until all of the particles of agarose had completely dissolved. The amount of agarose added depended on the size of the gel to be cast. All gels in this study were 1 % (w /v) agarose in a total volume of 30 ml, except those gel cast for preparative purposes which were made in a volume of 50 ml in order to give the wells a greater capacity.

The solution was then allowed to cool down to ~ 60 °C prior to pouring the solution into a mini-gel casting tray (avoiding bubbles). The appropriate sized comb was then inserted into the solution. For analytical purposes a 12-toothed comb able to hold 15 µl in each well was used, and for preparative purposes a 5-toothed comb able to hold 50 µl in each well was used. Then the gel was allowed to set for >30 min.

The comb was removed when the gel had completely hardened, and the gel tray was placed horizontally in an agarose gel electrophoresis tank and then submerged in 1 x TAE buffer (section 2.1.4.3.2.2). Samples were then prepared by the addition of 2 µl of loading buffer (bromophenol blue 6x; section 2.1.4.3.2.1), and then the mixture was loaded slowly into the wells using a Gilson pipette. Also, 6 µl of an appropriate size standard was loaded into an unoccupied well in order to determine the size of electrophorised DNA fragments. The apparatus was then connected to a power supply at 100 milliamps, 200 volts, for approximately 40 min to ensure good separation of DNA fragments.

2.2.2.1.6 Visualisation of DNA and photography of agarose gels

After electrophoresis, the gel was stained by submersion in 10 µg ml^{-1} ethidium bromide solution for 10 min on a flat bed orbital shaker, shaking at 40 rpm. For analytical gels the ethidium bromide was re-used until staining became weak; however preparative gels used fresh ethidium bromide each time After staining, the gel was washed extensively with distilled water prior to visualisation over an ultraviolet (UV) light source produced

by the gel documentation system (Bio-Rad Gel Doc 2000 using Quantity One software). Hard copies of the gel picture were produced using a Mitsubishi Video Copy Processor (Model P91 attached to the gel doc system), with Mitsubishi thermal paper (K65HM-Œ/ High density type, 110 mm x 21 m).

2.2.2.1.7 Preparation of plasmid DNA (pDNA)

2.2.2.1.7.1 Large scale preparation of plasmid DNA

A large amount of DNA was achieved using the Qiagen plasmid kit as detailed below. One colony of *E. coli* harbouring the plasmid to be prepared (pET-28a, pET-22b or pET-32c) was inoculated from a fresh plate into 500 ml LB media containing the appropriate concentration of antibiotic and incubated overnight at 37 °C with vigorous shaking.

The bacterial cells were harvested by centrifugation at 5445 x g for 15 min at 4 °C and the supernatant discarded. The pellet was resuspended in 10 ml of buffer P1 (cell resuspension buffer). 10 ml of buffer P2 (lysis buffer) was then added and the sample was mixed gently and incubated at room temperature for 5 min. 10 ml of chilled buffer P3 (neutralisation buffer) was added and mixed gently and then incubated on ice for 20 min. Precipitated material was then separated by centrifugation at 20000 x g for 30 min at 4 °C. The supernatant which contained the plasmid DNA was centrifuged again at 20000 x g for 15 min at 4 °C and the supernatant retained. After equilibration of the Qiagen-tip 500 with 10 ml buffer QBT, the supernatant was transferred to the Qiagen-tip and allowed to enter the resin by gravity flow. Subsequently, the Qiagen tip was washed twice with 30 ml of buffer QC and then the DNA was eluted with 15 ml buffer QF and collected in sterile universal. In order to precipitate the DNA, 10.5 ml of 100 % (v/v) isopropanol was added to the eluted DNA, mixed well and then centrifuged at 15000 x g for 30 min at 4 °C. The supernatant was discarded carefully and the DNA pellet was washed first with 70 % and then with 100 % ethanol. Both washes were

performed by centrifugation at 15000 x g for 10 min and in each case the supernatant was discarded carefully. Finally the DNA pellet was air dried for 15 min and then re-dissolved in TE buffer (Section 2.1.4.3.2.3) and stored at –20 °C until use.

2.2.2.1.7.2 Standard preparation of pDNA

The purification of plasmid DNA from transformed *E. coli* strain TOP10 (section 2.2.1.2.1.) was achieved using a QIA prep Spin Miniprep kit (section 2.1.1.3). A 3 ml volume of bacterial cell culture (section 2.2.1.2.1) was pelleted in a 1.5 ml micro-centrifuge tube by repeated centrifugation at 14000 x g for 60 sec, and the supernatant discarded. The pellet was then pulsed and residual supernatant removed with a yellow tip attached to a Gilson pipette. The pellet was then resuspended by vortexing in 250 µl of buffer P1 (cell re-suspension buffer). 250 µl of buffer P2 (cell lysis buffer) was then added and the sample was mixed by gentle inversion 5-6 times, prior to incubation at room temperature for 5 min. 350 µl of buffer N3 (precipitation of proteins and chromosomal DNA) was then added to the sample, and the sample was again mixed by gentle inversion 5-6 times. Precipitated material was then separated by centrifugation at >17,900 x g for 10 min, and the supernatant was retained and applied to the QIAprep spin® filter tube placed into a 2 ml receptacle centrifuge tube. The DNA was then loaded onto the filter by centrifugation at >10000 x g for 1 min and the flow-through discarded, and washed with 500 µl of PB buffer, followed by an additional wash with 750 µl of PE buffer (50 % (v/v) ethanol). Both washes were performed by centrifugation at >10000 x g for 1 min and in each case the flow-through discarded. Prior to elution, the empty QIAprep spin filter tube and receptacle were centrifuged at >10000 x g for 2 min in order to remove any residual ethanol. Finally the QIAprep spin filter tube was transferred into a sterile 1.5 ml micro-centrifuge tube and the DNA was eluted from the

filter by centrifugation at >10000 x g for 1 min after the addition of 50 µl of EB buffer (elution buffer) to the centre of each QIAprep spin column.

2.2.2.1.7.3 Preparation of pDNA for sequencing

For the preparation of pDNA for sequence analysis, the standard preparation of pDNA method was used (section 2.2.2.1.7.2), with some additions. The elution step was performed twice from the filter by the addition of 2 x 100 µl of sterile deionised water pre-warmed to 70 °C in a water bath. The DNA was then concentrated by lyophilisation overnight in a freeze drier unit, and then sterile water was added to give a final concentration of 1µg. This method of elution gave a yield of DNA high enough for sequence analysis.

2.2.2.1.7.4 Crude preparation of pDNA for the screening of putative blue / white recombinants

A 3 ml volume of bacterial cell culture (section 2.2.1.2.1) was pelleted in a 1.5 ml micro-centrifuge tube by repeated centrifugation at 14000 x g for 1 min. The pellet was then pulsed and residual supernatant removed with a yellow tip attached to a Gilson pipette. The pellet was then re-suspended by vortex in 150 µl of STET buffer (section 2.1.4.3.1.1) and 10 µl of 10 mg ml^{-1} lysozyme was added to lyse the cells. Samples were then mixed by gentle inversion 5-6 times and incubated at room temperature for 15 min. The sample was then boiled for 40 sec and centrifuged at 14000 x g for 15 min immediately after removal from the water bath. The viscous pellet was then removed using a yellow tip and discarded. 150 µl of 100 % (v/v) isopropanol was added to the remaining supernatant and the sample mixed, and incubated at –20 °C for 1 h to allow precipitation of DNA. Upon removal from –20 °C the sample was immediately centrifuged at 14000 x g for 5 min and the supernatant discarded. The pellet was then pulsed and residual supernatant removed with a yellow tip attached to a Gilson pipette.

The pellet was then washed with 500 µl of ethanol prior to centrifugation at 14000 x g for 3 min. After discarding the supernatant, the pellet was then pulsed and the residual supernatant removed with a yellow tip attached to a Gilson pipette. Finally, the sample was dried for 10 min in order to remove any latent ethanol, prior to re-suspension of the pellet in 30 µl of TE buffer (section 2.1.4.3.2.3).

2.2.2.1.8 Agarose gel purification

Prior to removal of the fragment, the gel was 'briefly' visualised under low intensity UV and the location of the fragment to be excised was etched using a clean scalpel. The section of gel containing the fragment was then excised using a scalpel, and inserted directly into a pre-weighed micro-centrifuge tube. The tube was then re-weighed and the weight of the gel slice it contained was then calculated. For every 100 mg of agarose gel, 300 µl of QG buffer was added to the tube. The gel was then dissolved by incubation at 50 °C for 10 min with a brief vortex every 2-3 min. Once dissolved, 100 µl of isopropanol was added for every 100 mg of gel, and then the sample was loaded into a QIAprep spin filter tube and placed into a 2 ml collection tube. The sample was then centrifuged at ~17900 x g for 60 sec, and the flow-through discarded. After that, 500 µl of QG buffer was added to the sample in the QIAprep spin filter column and centrifuged for one min. The sample was then washed by the addition of 750 µl of buffer PE, which was centrifuged at 17900 x g for 60 sec and the flow-through discarded. The wash step was repeated prior to centrifugation at ~17900 x g for 60 sec of the empty QIAprep spin filter tube, in order to remove any residual ethanol from the filter. The QIAprep spin filter tube was then transferred into a sterile 1.5 ml micro-centrifuge tube, 30 µl of EB buffer was added to the centre of the filter membrane, and the column was left to stand for 1 min. The sample was then centrifuged at 17,900 x g for 60 sec. The filter was then discarded and the eluted DNA retained for subsequent use. To check the purification

had worked, 2 µl was removed from the eluted sample and made up to 10 µl with water, and ran on the agarose gel as described in section 2.2.2.1.5.

2.2.2.1.9 PCR clean up

Purification of PCR was achieved using a MinElute PCR purification kit. 200 µl of PB buffer was added to the 40 µl of PCR sample (5 volumes of buffer for 1 of the PCR volume). After mixing, the sample was then loaded into a MinElute column which was placed in a 2 ml collection tube and centrifuged at 17900 x g for 60 sec, and the flow-through was discarded. The sample was then washed by the addition of 750 µl of buffer PE and centrifuged at 17900 x g for 1 min and the flow-through discarded. The washing step was repeated, prior to centrifugation of the empty MinElute column and collection tube for 1 min, in order to remove any residual ethanol from the filter. The MinElute column was then transferred into a sterile 1.5 ml micro-centrifuge tube and 10 µl of buffer EB was added to the centre of the filter membrane. The column was left to stand for 1 min. The sample was then centrifuged at 17900 x g for 60 sec. To check the purification had worked, 2 µl was removed from the eluted sample, made up to 10 µl with water and run on the agarose gel as described in section 2.2.2.1.5.

2.2.2.1.10 Spectrophotometric quantification of DNA

Plasmid DNA was quantitatively determined by preparing a dilution of DNA in a 70 µl total volume. The dilution was transferred to a 100 µl quartz cuvette and scanned in a UV vis spectrophotometer (previously zeroed with water) between the wavelengths of 200 and 300 nm. Optimal wavelength for the absorbance of DNA was thought to be 260 nm. The optical density (OD) of the DNA solution was also measured at 280 nm to check for contamination with proteins. An OD_{260} of 1.0 is equivalent to approximately

50 μg ml^{-1} DNA. The concentration and purity of the DNA was determined as detailed below.

[double-stranded DNA] μg/μl = (A_{260}) x 50 x dilution/1000

DNA purity ratio = (A_{260}) / (A_{280})

The ratio of A_{260} / A_{280} of pure DNA solutions should range between1.8-2.0.

2.2.2.1.11 A-tailing DNA

In preparation for ligation into the pGEM-T® Easy, A-overhangs were synthesised on the DNA fragment as follows. 7μl of purified PCR product (section 2.2.2.1.9) was made up to a 10 μl reaction volume by the addition of the components listed in Table 2.19.

Table 2.19: Reaction components of the A-tailing procedure. For the composition of Taq DNA polymerase reaction buffer (10 x) refer to the Appendix I (Table ICc).

Component	Volume	Final concentration in A-tailing reaction
Purified PCR product	7 μl	
Taq DNA polymerase reaction buffer 10 x	1 μl	1
$MgCl_2$ (25 mM)	0.5 μl	1.25 mM
dATP (4 mM)	0.5 μl	0.2 mM
Taq DNA polymerase 5 U μl^{-1}	1 μl	0.5 U μl^{-1}

After mixing the reaction components, the tube was given a pulse in a microcentrifuge, prior to incubation in a 70 °C water bath for 30 min. The DNA was then used for ligation into pGEM-T® Easy vector (Table 2.5).

2.2.2.1.12 Ligation of DNA

For all ligations, a 2:1 insert to vector ratio was required. Concentrations were determined by running samples on an agarose gel using the analysis tool of the Bio-Rad Gel Doc 2000 using Quantity One™ software.

2.2.2.1.12.1: Ligation into pGEM-T® Easy vector

The ligation of cohesive termini generated from A-tailing blunt PCR products (Section 2.2.2.1.11) into linearised pGEM-T® Easy vector (Table 2.5) was performed by the addition of the components listed in Table 2.20.

Table 2.20: Reaction components for ligation into pGEM-T® Easy vector. The composition of Rapid ligation buffer is given in Appendix I (Table ICb and ICc)

Component	Volume
pGEM-T® Easy vector (dephosphorylated; Lab stock)	1µl (50 ng)
2x rapid ligation buffer (PRO)	5 µl
A-tailed PCR product (section 2.2.2.1.8)	3 µl (33 ng)
T4 DNA ligase (3 U μl^{-1}) (PRO)	1 µl

After the addition of the reaction components, the ligation was incubated at 16 °C overnight prior to transformation into TOP10 cells.

2.2.2.1.12.2 Ligation into pCR-Blunt® vector

Ligation of blunt-ended PCR products (Sections 2.2.2.1.2.1 and 2.2.2.1.2.2) into linearised pCR-Blunt® (Table 2.5) was performed by the addition of the components listed in Table 2.21. A 10:1 molar insert to vector ratio was used.

Table 2.21: Reaction components for ligation into pCR -Blunt® vector. The composition of Rapid ligation buffer is given in Appendix I (Table ICb and ICc).

Component	Volume
pCR-Blunt® vector (linearised; 25 ng)	1µl
10 x ligation buffer (with ATP)	1µl
Blunt PCR product (50 ng)	5µl
Deionised water	2µl
T4 DNA Ligase (4U μl^{-1})	1µl

This reaction was then incubated at 16 °C overnight prior to transformation into TOP10 chemically competent cells.

2.2.2.1.12.3 Ligation into pET vector

Table 2.22: Reaction components for ligation into pET vector

Component	Volume
pET vector cut with appropriate REs	100ng
10 x ligation buffer (NEB)	2 µl
Fragment cut from pGEM-T® /pCR®-Blunt vector and gel purified (100 ng; section 2.2.2.1.5)	2 µl (3 fold molar ratio more than cut vector)
Deionised water	13 µl
T4 DNA Ligase (3 U μl^{-1})	1 µl

After the addition of reaction components, the ligation was incubated at 16 °C overnight prior to transformation into TOP10.

2.2.2.1.13 Transformation into *E. coli* TOP10, BL21 (DE3), BL21Tuner, BL21 pLysS and BL21 Orgami

Transformations were performed using prepared competent cells (section 2.2.1.4) in 50 µl aliquots. 2.5 µl of ligation was added and mixed gently with a pipette tip and incubated with cells on ice for 30 min. The cells were then transferred to a water bath at 42 °C and heat shocked for 90 sec, and then incubated on ice for 2 min. After that, the cells were recovered by the aseptic addition of 200 µl of NZY+ enrichment broth (Sections 2.1.4.1.1.2; and 2.1.4.1.1.3), and incubated at 37 °C for 45 min.

Recovered cells were then aseptically plated on media supplemented with antibiotic appropriate for the plasmid. Plates were then incubated at 37 °C overnight to allow the growth of bacterial colonies.

2.2.2.1.14 Colony PCR screening for successful of hylALIC

2-4 colonies were selected from each plate (section 2.2.2.1.13) and were transferred using a sterile pipette tip into separate 0.5 ml PCR tubes containing 50 µl of autoclaved deionised water. After mixing gently with the pipette tip, 0.5µl from the water / cell suspension was taken immediately from each tube and added to a grided plate containing 50 µg ml^{-1} km. Also 4.5 µl of water/cell suspension was added to 1 ml LB media, in order to keep the cells fresh until after colony PCR verification. The plate and the tubes which contained 4.5 µl of water/cell suspension were incubated at 37 °C overnight, the tubes incubated by shaking. The 1 ml culture corresponding to positive results from colony PCR was used to inoculate 10 ml of LB media to make plasmid DNA (section 2.2.2.1.7.2).

The remaining 45 µl of water/cell suspension was heated at 95 °C for 5 min in a thermocycler (PCR machine) to disrupt the cells, followed by spinning them down at 14000 x g for 2 min. The supernatants were transferred to fresh tubes. Then 10 µl from each supernatant was added separately to fresh PCR tubes, then the other component of the PCR reaction was added as described in table 2.23. The PCR conditions used were as follows: 94°C for 2 min, followed by 35 cycles of denaturation at 94 °C for 30 s, annealing at 45 °C for 30 s, and extension at 72 °C for 2 min and finally one cycle of final extension at 72°C for 3 min.

Table 2.23 Reaction components for colony PCR screen for successful inserts.

Component	Volume	Final concentration
Cell / water supernatant	10 µl	
Forward primer	1 µl	0.4 µM
Reverse primer	1 µl	0.4 µM
dNTP's (25 mM)	0.4µl	0.4 µl
Taq DNA polymerase reaction buffer 10 x	5 µl	1 x
$MgCl_2$ (25 mM)	2.5µl	1.25 µM
Taq polymerase 5U μl^{-1}	1µl	0.1 U μl^{-1}
Sterile water	29.1 µl	

2.2.2.1.15 Construction of mutant plasmids of SC1C2.15 and hylA by site directed mutagenesis (SDM)

SDM was performed according to the Stratagene instruction manual for the QuikChange™: Site-Directed Mutagenesis Kit (Catalog #200518).

Mutant primers (sections 2.1.3.1.3; and 2.1.3.2.1) with a length of 25-45 bases and GC contents ≥ 40% were designed with the mutation in the centre of the primer and a Tm (melting temperature) of ≥ 78 °C. The Tm for each primer was determined as follows:

Tm = 81.5+0.41 (%GC)-675 / N -% mismatch

Key: % GC = Percentage of guanine and cytosine residues in the primer

N = Primer length in bases

% mismatch = Percentage of the primer non complementary at the point of mutation

Mutant plasmid was then generated by PCR (sections 2.2.2.1. 3.1; and 2.2.2.1. 3.2 for protocols A and B respectively). The PCR template was then digested with 1 µl of *Dpn*I (10 U μl^{-1}) restriction enzyme and incubated at 37 °C for 1 h. The *Dpn*I endonuclease was used as it is specific to methylated and hemimethylated DNA which is not found in the newly synthesized daughter strands and hence helps to digest the non mutated parental strands and select mutated DNA. The *Dpn*I treated DNA was then transformed into *E. coli* TOP10 (section 2.2.2.1.13). The plasmid DNA was made (section

2.2.2.1.7.2) from one of the transformants and sent to MWG BIOTECH, the mutations were confirmed by sequencing.

2.2.3 Protein methods

2.2.3.1 SDS-PAGE electrophoresis

SDS-PAGE gels were poured between two clean glass plates of dimensions 10.1 × 7.2 and 10.1 × 8.2 cm separated by a 1 mm spacer ridge on the larger of the two plates. The plates were clamped together and checked to ensure that the bottoms were flush, prior to securing the gel with vertical downward pressure in a casting stand on a rubber gasket. The components for the resolving gel (section 2.1.4.3.5.4) were then added and poured into the space between the plates, until the solution was approximately 2 cm below the top of the smallest plate. A small volume of water was carefully layered over the top of the resolving gel so that it did not dry out while polymerisation was occurring. Once the resolving gel was polymerised, the water was removed from the top of the gel by absorbing with filter paper. After that the components of the stacking gel were added (section 2.1.4.3.5.5), mixed and transferred to the top of the small plate. A 10-toothed comb was then immediately inserted into the gap between the plates, moving some of the un-polymerised stacking gel. The stacking gel was then allowed to set for about 30 min. Then the comb was removed, leaving well-defined sample wells, which were then rinsed with water. The gel was then placed vertically into an electrophoresis apparatus. SDS-PAGE 1 x running buffer (section 2.1.4.3.5.1) was then poured into the tank. Samples were then prepared by the addition of 5 µl of SDS-PAGE loading buffer (section 2.1.4.3.5.2) to 20 µl of sample. Also 8µl of SDS-PAGE loading buffer was added to the standards, which contained various proteins of known molecular weight and run alongside the samples to enable size estimation after staining. The samples and size standard were then pulsed briefly prior to boiling for 2 min. Subsequently the

samples and standards were centrifuged at 14000 x g for 1 min and 20 µl of all samples and 12 µl of standards were loaded into the wells using a Hamilton syringe. The apparatus was then connected to a power supply at 120 milliamps, 200 volts. Once the current was applied to a gel, all the negatively charged proteins migrated toward the anode at the base of the gel. Larger proteins migrated more slowly than smaller proteins. When protein bands reached the bottom of the gel, migration was stopped by turning off the electrical field. The gel was then removed from the plates and stained.

2.2.3.1.1 Visualisation of protein bands and photography of SDS-PAGE gels

After electrophoresis, the gels were removed from the plates and placed in Coomassie blue stain for 15 min with gentle shaking followed by immersion in de-staining buffer overnight at room temperature with moderate shaking until the bands were visible. The gels were then photographed using a gel documentation system (Bio-Rad Gel Doc 2000 using Quantity One™ software). Hard copies of the gel picture were produced using a Mitsubishi Video Copy Processor (Model P91 attached to the gel doc system), with Mitsubishi thermal paper (K65HM-Œ/ High density type, 110 mm x 21 m).

2.2.3.2 Isolation of cell free extract (CFE)

To obtain cell free extract, induced cells were firstly concentrated by centrifugation for 10 min at 5500 x g. After that the supernatant was discarded and the cells were re-suspended in 5-10 ml of starting buffer (section 2.1.4.3.6.1). Cells were then lysed in 5 ml volumes by sonication on ice at amplitude 15 for 1 min in 10 sec bursts with intervals of 10 seconds. The lysate was then decanted into centrifuge tubes and centrifuged at 4 °C for 30 min at 24000 x g. The soluble fraction was then transferred into a plastic universal and maintained on ice as a cell free extract.

2.2.3.3 Protein purification

Recombinant proteins used in this study were purified using immobilised nickel metal affinity and gel filtration chromatography methods. In all cases, the purity of the protein was assessed by SDS-PAGE (Section 2.2.3.1). Immobilised metal affinity chromatography (IMAC) was used to purify recombinant proteins under native conditions, which contained a stretch of 6 Histidine residues (His_6 tag) at the N-terminus or C-terminal). The metal affinity matrix used was Sepharose™ chelating fast flow resin.

2.2.3.4 Affinity purification using a fast flow Ni column

In order to purify protein by IMAC, a Sepharose chelating fast flow resin was used. For the high yield purification of protein using the automated FPLC® system gradient elution technique, the column was prepared by adding ~50 ml Sepharose™ chelating fast flow resin to a column (C 16/20; Amersham Bioscience) of the dimensions 1.6 cm internal diameter (i.d.) x 20 cm length (L). The column adapters were securely attached and the column was connected to the FPLC® system. Once connected, 1 M $NiSO_4$ solution was passed through the resin using the peristaltic pump until all the resin was a uniform colour. The column was then washed by passing through ~ 200 ml of starting buffer using a peristaltic pump. Once the column had been equilibrated, CFE (10-20 ml) was then loaded onto the column using a peristaltic pump. The column was then washed with 100 ml of starting buffer (section 2.1.4.3.6.1) at a flow rate of 5 ml min^{-1} by the FPLC gradient pump. Finally the protein was eluted at a flow rate of 5 ml min^{-1} using a linear gradient of imidazole (elution buffer; section 2.1.4.3.6.2) extending from 10 mM to 500 mM. The position of the target protein was determined by monitoring A280 using an inline UV spectrometer connected to the FPLC, and samples were collected in 5 ml volumes on a fraction collector. To confirm purity, a 20 µl aliquot

from each 5 ml fraction thought to contain the target protein was analysed by SDS-PAGE (section 2.1.4.3.5; section 2.2.3.1) and the pure fractions pooled.

2.2.3.5 Concentration and buffer exchange of protein

The concentration of protein was performed at 4 °C by centrifugation at 4000 x g in 30 kDa Vivaspin 6 ml cut-off concentrator units (Viva Science). After concentrating all the fractions containing the protein to about 1 ml, 10 mM Tris/HCl buffer pH 8 was added to the concentrated protein in a 30-kDa cut-off concentrator and washed three times by centrifugation.

2.2.3.6 Gel filtration chromatography

Gel filtration is a simple chromatographic method for separating molecules according to size. Different gels have pores with a different controlled range of sizes and act as molecular sieves separating molecules by differences in size. The gel matrix contains several porous beads with an eluant in between. The largest molecules in the sample will not be able to enter the pores in beads but will pass between them and thus will be eluted first, whereas smaller molecules that have access to the pores will be eluted later.

Purified protein from an affinity chromatography column was exchanged by concentration (Section 2.2.3.5) into gel filtration buffer (Section 2.1.4.3.7). The gel filtration column, of dimension 1.6 cm internal diameter x 60 cm length and with a bed volume of 120 ml was prepared by equilibration (using the FPLC® system) at a volume flow rate of 1 ml min^{-1} with 120 ml of gel filtration buffer. A sample of 0.5 ml was then loaded onto the column and eluted over 120 min with gel filtration buffer running at 1 ml min^{-1}. The elution point of the target protein was identified by A 280 (Figure VD, appendix V) using the inline UV spectrophotometer, and samples were collected on a

fraction collector in 5 ml volumes. To confirm purity, a 20 µl aliquot from each 5 ml fraction thought to contain the target protein was analysed by SDS-PAGE (section 2.2.3.1) and the pure fractions pooled.

2.2.3.7 Protein refolding

After centrifugation of the cells for 10 min at 5500 x g (section 2.2.3.2) and discarding the supernatant, the cells were re-suspended in starting buffer, sonicated and then centrifuged again at 24000 x g for 40 min at 4 °C. Subsequently, the cell free extracts were discarded and insoluble cell extract was solublised in starting buffer containing 8 M urea to denature the proteins. N-terminally tagged proteins were then purified by immobilised metal chromatography under denature conditions. The denatured protein was then placed in dialysis tubing (section 2.1.8.1) and sealed in the tubes with clamps. The dialysis tubes were then immersed in the refolding solutions sequentially, for > 5 h at 4 °C in 4 L volumes of 50 mM Tris-HCl pH 8.5 containing decreasing concentrations of urea of 6, 5, 4, 3, 2, 1, 0.66, 0.33 and 0 M urea solution. All the solutions were kept in 5 L beakers at a temperature of 4 °C during storage and while being used. The dialysed protein was then centrifuged at 18000 x g for 5 min to remove any insoluble material, and a 20 µl aliquot of the soluble fraction was run on an SDS-PAGE gel.

2.2.3.8 Determination of protein concentration

The concentration of proteins in the solutions was estimated with the assistance of the Bradford reagent (BioRad; Bradford, 1976).

Determination by the Bradford method involved the construction of 10 dilutions of BSA in 500 µl aliquots ranging from 1-10 µg ml^{-1}. 500 µl of Bradford's solution was then added to each dilution, and mixed. Each standard was then measured in a plastic cuvette at 595 nm against a blank containing 500 µl of water mixed with 500 µl of Bradford's

solution. A standard curve was then constructed (Figure 2.1). Dilutions of the protein to be determined were then made in 500 µl volumes and measured after the addition of Bradford's solution in the same way as the standards. Those values that fell on the standard curve were used to calculate protein concentration, using the following equation:

Protein concentration mg ml^{-1} = (concentration obtained from the curve) x (dilution of sample) / 1000

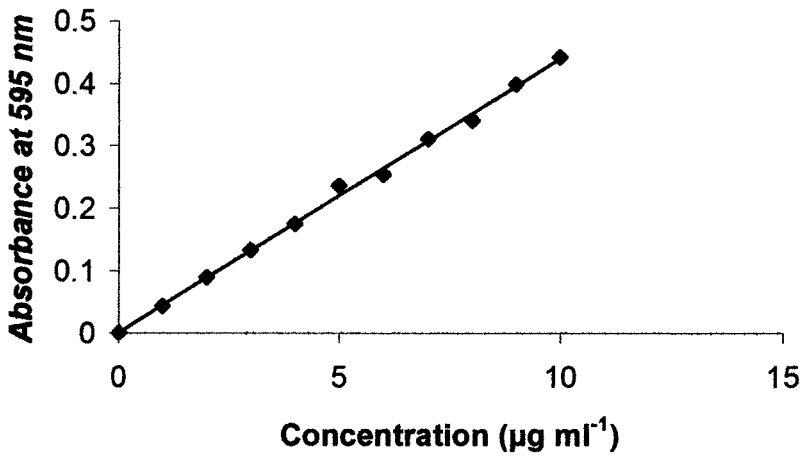

Figure 2.1: Standard curve for the Bio-Rad Bradford's protein assay
The curve was generated by the addition of 0, 1, 2, 3, 4, 5, 6, 7, 8, 9 and 10 µg.ml BSA in 500 µl deionosed water to 500 µl Bradford's reagent.

2.2.3.9 Crystallisation: the hanging drop method

Crystallisation was performed according to the vapour diffusion method. Crystal screening was performed in 24-multi well plates (Falcon ® Multiwell™ 24 well Becton Dickinson) into which 0.5 ml of crystallisation buffer (Appendix III) was aliquoted into each well. Wells were then greased around the rim using vacuum grease dispensed from a syringe. Cover slips were silanised by pre-treatment with Aqua Sil solution (HAMP RES), then dried and polished with a silk scarf prior to the addition of protein drops.

1 µl of protein was added to 1 µl of crystallisation buffer (removed from the well) on a cover slip to form a 2 µl drop. The cover slip was then inverted and sealed above the appropriate well. This method was repeated for all crystallisation buffers (Appendix III). The plates were then marked properly and incubated at 22 °C.

The conditions in which crystals were grown were then optimised in order to obtain crystals of good quality. This was achieved by varying the concentrations of buffer and salt. Once native crystals had grown, then the same conditions were used to set the crystals of mutant forms of the enzyme.

After the crystals had grown, acryoprotectant was produced by soaking each crystal in 1 µl of crystal growth buffer (mother liquor) and one drop of 25 % (v/v) glycerol. Then the samples were harvested in a rayon fibre loop and frozen in liquid nitrogen.

2.2.3.9.1 Crystal screening

The crystals were screened at the York Structural Biology Laboratory (YSBL) by X-ray to determine diffraction quality prior to data collection. Data collection was achieved using a 345 mm Mar Research image-plate detector on a Rigaku rotating anode RU-200 X-ray generator, with a Cu target operating at 50 kV (100 MA) and focusing X-ray optics (MSC). The quality of the crystal was judged by the diffraction pattern. This work was performed by Dr E. Taylor at YSBL.

2.2.3.9.2 Data collection

Data were collected by Dr E. Taylor and Dr Johan Turkenburg on the European Synchroton Radiation Facility (ESRF) from single crystals at 100 K with a D-14.2 and an ADSC Quantum-4 charge-coupled device detector. The cell index and collection strategy was determined using Mosflm (Leslie, 1992).

All data were processed with the HKL suite (Otwinowski and Minor, 1997) or Mosflm (Leslie, 1992). All other computing was undertaken using the CCP4 suite (Collaborative Computational Project Number 4) unless otherwise mentioned. Where appropriate data merging and reduction was undertaken in SCARLA or SCALEPACK. The SCPL8 structure of was solved by molecular replacement program AMORE using the pdb 10JM as a search module. A Rfree of 5% of the total reflections were maintained for cross validation before module building this set was used to monitor the module at various stages of refinement for the weighting of geometrical and temperature factor restraints. QUANTA and X-FIT (Accelrys) or COOT (ref) were used to make manual corrections to the module between cycles of REFMAC (Murshudov et al., 1997). Solvent molecules were added using X-SOLVATE and checked manually. The structure was validated using PROCHECK (Laskowski et al., 1993) prior to pdb deposition. The structure coordinated and details have be deposited with the macromolecular structure data base (This work was performed by Dr Edward Taylor, Dr Florence Vincent, Dr Johan Turkenburg and Prof. Gideon Davis laboratory at YSBL).

2.2.4 Assay Methods

2.2.4.1 Biochemical characterization of the enzymes

All enzyme assays were carried out in triplicate and the mean values were presented on graphs with error bars to represent the range for each data set. The same aliquot of purified enzyme was used in the kinetic experiments.

2.2.4.1.1 Standard assay at 232 nm

Equal concentrations (2.66 mg ml^{-1}) of dialysed HA, chondrotin-4-sulphate and chondroitin-6-sulphate were measured at different pHs of 100 mM sodium acetate

buffer. The rate of substrate degradation was measured by monitoring the increase of absorbance at 232 nm at 37 °C as shown in Tables 2.24 and 2.25.

Table 2.24 Standard reaction components for reactions containing HA. The enzyme was diluted in 10 mM Tris-HCl, pH 8, then 2.4 μg was added.

Component and stock concentration	Concentration in final reaction
HA (2.66 mg ml^{-1})	1 mg ml^{-1}
Sodium acetate buffer (100 mM) pH 5.2	20 mM
NaCl 1M	40 mM
BSA 2.5mg ml^{-1}	0.1mg ml^{-1}

Table 2.25 Standard reaction components for reactions containing Chondroitin-4 or 6- sulphate. The enzyme was diluted in 10 mM Tris-HCl, pH 8, then 2.4 μg and 4.8 μg was added respectively.

Component and stock concentration	Concentration in final reaction
Chondroitin sulphate (2.66 mg ml^{-1} for both 4-sulphate and 6-sulphate) (2.66 mg ml^{-1})	1 mg ml^{-1}
Sodium acetate buffer (100 mM) pH 5.2	20 mM
NaCl 1M	40 mM
BSA 2.5 mg ml^{-1}	0.1 mg ml^{-1}

All reactions were performed in a total volume of 500 μl, and all components except the enzyme were pre-warmed to 37 °C. Reactions were then performed thus: the substrate was first added to the buffer, NaCl and BSA were then added. The mixture was then transferred directly to a 0.5 ml quartz cuvette pre-warmed to 37 °C in a heated holder within a spectrophotometer pre-zeroed against water at 232 nm. The reaction was started by the addition of the enzyme. Data were then collected over a 1 min time course by observing an increase in absorbance at 232 nm (Figure VA Appendix V) due to the

formation of a double bond by β-elimination and analysed using Vision 2000 software to determine initial velocity.

2.2.4.1.1.1 Determination of K_m, k_{cat} and specific activity

For the determination of the kinetic parameters of SC1C2.15 against dialysed HA, chondroitin-4-sulphate and chondroitin-6-sulphate, varying substrate concentrations between 0.125-2 mg ml^{-1} (final concentration) were chosen and reactions were performed as detailed in section 2.2.4.1.1 (Tables 2.24 and 2.25).
Specific activities for dialysed HA, chondroitin-4-sulphate and chondroitin-6-sulphate were determined under standard assay conditions by the measurement of an initial reaction rate at saturating substrate concentration.

For the determination of the kinetic parameters of HylA, the same procedure was followed except that the analysis was carried out in 100 mM of sodium acetate buffer pH 6 and 0.1mg ml^{-1} BSA without NaCl and the substrate concentrations range was 0.1-0.8 mg ml^{-1} final concentration.

2.2.4.1.1.1.1 Calculation of K_m, K_{cat} and K_{cat} / K_m

Calculation of K_{cat} required the use of extinction coefficient for the double bond formed at the non-reducing end of the polysaccharide; this value was taken as 5500 $M^{-1} \cdot cm^{-1}$.
K_m was calculated by reciprocalising the X intercept in the Line-weaver Burk plot to give K_m in mg ml^{-1}.
K_{cat} is calculated through attaining a value of V_{max}

K_{cat} (s^{-1}) :

$\Delta A_{232} / \epsilon = C$

$$C / 2000 \times 10^6 / (\text{Total protein added mg}) = V_{max}\ U / mg)$$

V_{max} x MW of enzyme in grams / 60 = k_{cat}

Key: ΔA_{232} = Change in absorbance per 1 min

ϵ = Extinction coefficient of the double bond (5500 $M^{-1}.cm^{-1}$

C = moles of product produced per min per L

U = µmoles of product produced per min

K_{cat} is calculated by first using the Beer-Lambert law ($C = \Delta A / \epsilon$) to calculate C. C is expressed as: moles of product produced per min per L. However the reaction volume is only 500 µl therefore C is divided by 2000 to give: Moles of product produced per min per 500 µl. This value is then multiplied by 10^6 to convert into µ Moles of product produced per min per 500 µl this is defined as U. U is then divided by the total amount of enzyme added to the assay (mg). This gives the value for V_{max} which is: units of enzyme activity per min per mg. V_{max} is then converted from µmoles of product produced per min per mg into µmoles of product produced per min per µmoles by multiplied by the molecular weight of enzyme in mg. µmoles of product produced per min per µmoles is then converted into µmoles of product produced per second per µmole by dividing by 60. This gives the value for K_{cat}. (Appendix VI, tables VIA, B, C and D).

Specificity constants (s^{-1} ml mg^{-1}) were determined by dividing K_{cat} by K_m.

2.2.4.1.1.2 Determination of optimum pH

For the determination of the optimum pH of SC1C2.15, sodium acetate buffers of pH 4, 4.4, 4.8, 5.2, 5.6, 6, 6.4, 6.8 7 and 7.6 were used with 1mg ml^{-1} (final concentration) of different substrates plus 40 mM NaCl, and 0.1mg ml^{-1} BSA. For the dialysed HA and

chondroitin-4-sulphate 2.4 μg of SC1C2.15 (diluted in 10 mM Tris-HCl) was added. For chondroitin-6-sulphate, 4.8 μg of SC1C2.15 was added.

For the determination of the optimum pH of HylA, sodium acetate buffers of pH 4, 4.8, 5.2, 5.6, 6, 6.5, 7 and 8 were used with 1mg ml^{-1} (final concentration) of dialysed HA and 0.1mg ml^{-1} BSA without NaCl.

2.2.4.1.1.3 Determination of optimum temperature and thermostability of SC1C2.15 and hylA

The optimum temperature for SC1C2.15 and HylA was determined under the standard assay conditions given in section 2.2.4.1.1, except that the temperature of the reaction components and the heated cuvette holder was altered to a range of temperatures of 27, 37, 47, 57, 67 and 77 °C.

The thermostability of SC1C2.15 and HylA was assessed by pre-incubating the enzyme at 27, 37, 47,57 and 67 °C for 20 min prior to assaying the samples under standard conditions (section 2.2.4.1.1).

2.2.4.1.1.4 Determination of optimum $CaCl_2$ concentration and divalent ion requirement

Optimum $CaCl_2$ concentration was determined using the standard assay conditions except that the concentration of $CaCl_2$ varied for each assay, ranging from 0-4 mM (0, 0.1, 0.2, 0.4, 0.8, 1, 2 and 4). 1.2 μg of SC1C2.15 diluted in 10 mM Tris-HCl was added to all assays.

The effect of divalent cations on the activity of both enzymes was assessed using the standard reaction conditions (section 2.2.4.1.1). The divalent ions $CaCl_2$, $BaCl_2$, $MgCl_2$, $MnCl_2$, $NiCl_2$ and $CoCl_2$ were all tested at a final concentration of 2 mM.

2.2.4.2 Mode of action of SC1C2.15 and HylA by HPAEC

To analyse the reaction products of the SC1C2.15 and HylA by HPAEC, 19.2 μg of SC1C2.15 was used against HA and chondroitin-4-sulphate and 38.4 μg against chondroitin-6-sulphate in a total volume of 4 ml. The digestions were set at 37 °C under the standard assay conditions, except that 2 mg ml^{-1} of each substrate was added to the reaction as a final concentration. For HylA, 24 μg was used against HA also in a total volume of 4 ml under the standard assay conditions. Prior to the addition of the enzyme 300μl of reaction was removed as a zero time sample and boiled for 5 min. After the addition of the enzyme, six 300μl aliquots were removed from the reaction at time intervals of 5, 10, 20, 40, 80 and 160 min and inactivated by boiling for 5 min. To prevent the peeling of unsaturated oligosaccharides, 100 μl of sodium borohydride was added to each sample. Samples were then loaded, and eluted sequentially from a CarboPac PA1 column (250 mm x 4 mm) as described by Midura *et al.*, 1994 and Lauder *et al.*, (2000). The samples were loaded onto a completely automotive HPAEC system (under the control of Dionex PeakNet 5.1 software) using an auto-sampler. Samples were loaded onto the system using a 200 μl loop, at 1ml min^{-1} using a system pressure of ~2500 psi. De-gassed solutions (section 2.1.7; containing 0.1 M NaOH), mixed using a gradient pump, were then used to elute oligosaccharides using a linear gradient. Elution was at 1ml min^{-1}; a 12 min isocratic period of 98 %(v/v) eluent 0.1 M NaOH and 2 % (v/v) eluent 1.3 M NaCl in 0.1 M NaOH was followed by a linear gradient of 2 - 46 % eluent D over 50 min; 46 - 87 % eluent D over 8 min, 87 -100 % eluent D over 6 min was followed by a 4 min isocratic phase of 100 % eluent D. Eluted oligisaccharides were detected by a UV detector at a wave length of 232 nm. All data processing was performed through Dionex PeakNet 5.1 software.

2.2.4.3 Preparation of large scale of oligosaccharides

A large scale digest was performed consisting of 2 mg ml^{-1} HA, 40mM sodium acetate buffer pH 6 and 0.1mg ml^{-1} BSA as a final concentration, then 120 µg of HylA was added. The enzymatic digestion was performed at 37 °C for different time points to achieve products of different sizes. Also for SC1C2.15 a large digest was performed with chondroitin-4-sulphate in a reaction contained 2 mg ml^{-1} of substrate, 40 mM sodium acetate buffer pH 4.8, 40 mM NaCl and 0.1mg ml^{-1} BSA as a final concentration and the enzyme was then added to the final concentration of 4.8 µg. 0.3 ml of each sample was analysed by HPAEC. A 20 min time point digest for HylA produced the broadest range of digestion products, and this digest was chosen to purify the HA oligosaccharides. For SC1C2.15, 10 and 20 min were chosen for purification through a gel filtration P-6 column. The digests were freeze dried for 2-3 days, and then each digest was dissolved in 0.5 ml of 0.5 M NaCl.

2.2.4.4 Purification of oligosaccharides through gel filtration column

The digestion products (section 2.2.4.3) of both enzymes (SC1C2.15 and HylA) were then size separated using a Bio-Rad gel filtration P-6 column (170 x 1.5 cm) packed with bio-gel™ P2 polyacrylamide gel. This column was used to purify the digestion products of HA and chondroitin sulphate with HylA and SC1C2.15 respectively (Figures VE and VF, appendix V). The column was first prepared by equilibration (using the FPLC® system) with 0.5 M NaCl at a volume flow rate of 0.1ml min^{-1} for 2 days. A sample of 0.5 ml of digestion products was then loaded onto the column and eluted at a flow rate of 0.1ml min^{-1} in 0.5 M NaCl. Fractions were collected every 20 min at a flow rate of 0.1 ml min^{-1}. Peaks were detected by measuring the absorbance of fractions at 232 nm using an inline UV spectrometer connected to the FPLC, and samples were collected in 2 ml volumes on a fraction collector.

2.2.4.5 Determination of uronic acid

The uronic acid content for each oligosaccharide was then determined according to the method of Van den Hoogen *et al.* (1998). 40 µl of sample (each peak) was added to each well of a microtiter plate followed by the addition of 200 µl of concentrated sulphuric acid (H_2SO_4) containing 120 mM sodium tetraborate. After mixing, the plate was placed in an incubator for 1 h at 80 °C. After allowing to cool to room temperature, 40 µl of m-hydroxydiphenyl solution (section 2.1.4.3.4) was added and left for 15 min at room temperature. The absorbance was red at 570 nm. The fractions that contained high concentrations of uronic acid were dialysed.

2.2.4.6 Preparation of oligosaccharide fractions

After purification of the oligosaccharides through a P-6 gel filtration column (section 2.2.4.4), the fractions were pooled into separated dialysis tubes (sections 2.1.9 and 2.1.9.4) and dialysed 3 times in 18.2 MΩ cm^{-1} H_2O, stirred for 1 h, 2 h and overnight at room temperature to remove residual NaCl. Then the dialysed fractions were aliquoted into Petri-dishes, frozen at –80 °C, and freeze-dried for 2-3 days. Each plate was then re-suspended in 0.5 ml of deionised water, and transferred into pre-weighed micr-centrifuge tubes. 100 µ l of each fraction along with 100 µl of NaBH4 and 200 µl of deionised water was loaded into HPAEC in order to check the purity of each sample; the remainder was lyophilised and stored at –20 °C to use for crystallization.

2.2.5 3,5-Dinitrosalicylic acid (DNSA) reducing sugar assay

The reducing sugar content of solutions was determined spectrophotometrically using DNSA. In order to determine whether or not vitamin C can inhibits the enzymatic activity of *S. pyogenes* hyaluronate lyase, the effect of various concentrations of vitamin

C was examined. 0.69 μg of HylA diluted in 10 mM Tris / HCl and 1 mg ml^{-1} BSA (final concentration) was added to 1 mg ml^{-1} dialysed sodium hyaluronate, 20 mM sodium acetate buffer pH 6 and vitamin C (0 – 24 mM, final concentration) and mixed by vortex then 150 μl aliquots removed at various time points (0. 5, 10 and 20 min) and added to 150 μl DNSA reagent (1 % (w/v) DNSA, 0.2 % (v/v) phenol, 1 % (w/v) NaOH, 0.002 % (w/v) glucose, 0.05 % (w/v) NaSO) to terminate the reaction. For 0 time, 150 μl of the reaction mixture was removed prior to the addition of the enzyme. After that the tubes were boiled for 20 min, placed on the ice for 10 min and equilibrated to room temperature before reading the absorbencies. The absorbance was determined at 570 nm in a 96-well plastic microtitre plates (200 μl of each reaction was measured) using a plate reader. Standard curve was determined for each concentration of vitamin C which produced each time an assay was carried out. The standard curves were generated by the addition of 0-2 mg ml^{-1} of glucose (Final concentration; 10 mg ml^{-1} stock concentration) to 0 – 24 mM vitamin C (Final concentration) to 20 mM sodium acetate buffer pH 6 and 1 mg ml^{-1} dialysed sodium hyaluronate to a final volume of 150 μl. DNSA reagent (150 μl; section 2.1.8) was added to the standard curve and processed in the same way as the enzyme assays. All assays were carried out at 37 °C.

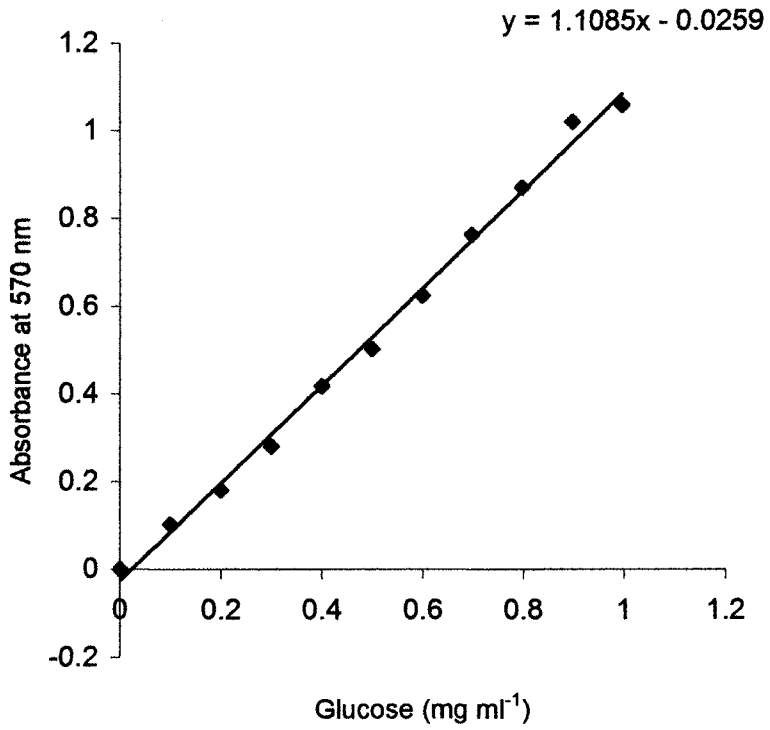

Figure 2.2 typical standard curve for DNSA assays. The curve was generated by the addition of 0, 0.1, 0.2, 0.3, 0.4, 0.5, 0.6, 0.7, 0.8, 0.9 and 1.0 mg ml^{-1} glucose (final concentration) to 1 mg ml^{-1} HA, 20 mM sodium acetate buffer and 0 – 24 mM Vc (final concentration) in a total volume of 150 µl. DNSA reagent (150 µl) was added, the tubes boiled for 20 min and placed on ice for 10 min. The tubes were equilibrated to room temperature before the A_{570} of solution was determined.

Chapter 3 Results: biochemical characterisation and crystallisation studies of a *Streptomyces coelicolor* A3(2) hyaluronate lyase

3.1 Introduction

Streptomycetes belong to the Actinomycete family. Actinomycetes produce about two-thirds of known antibiotics which are produced by microorganisms, and about 80% of those are synthesised by streptomycetes (Pieperberg, 1993). Streptomycetes can metabolise several compounds such as sugars, amino acids, aromatic compounds and alcohols through the secretion of extracellular hydrolytic enzymes.

Streptomycetes are found in different habitats such as soil, the sediments of lakes, rivers and marine environments. They have a complex life cycle involving the growth of substrate mycelia in the initial phase, followed by the development of aerial mycelium and finally conversion to spores (Pieperberg, 1993). The mycelial stage is sensitive to dryness, whereas the spores exhibit resistance to low nutrient and water availability (Karagouni et al., 1993), hence streptomycetes can live in soil for a long time.

Streptomyces coelicolor is a member of the Actinomycetes family, which also include *Myobacterium tuberculosis* and *Corynebacterium diphtheriae*. *Streptomyces coelicolor* is a Gram-positive bacterium which belongs to the sporoactinomycetes group. It is characterized by high guanine-cytosine content of its DNA, which results in a highly biased codon usage (http://www.sanger.ac.uk/Projects/S_coelicolor/). It is ubiquitous in complex soil environments, possesses a considerable range of metabolic processes, and has the ability to perform various biotransformations. Therefore, it is an important organism in the recycling of carbon in the environment.

Additionally *Streptomyces coelicolor* A3(2) strain has the largest bacterial genome sequenced to date at 8,667,507 base pairs (bp), long and containing about 7825 predicted genes, 819 of which are predicted to encode secreted proteins (Bentley *et al.*, 2002). It has been extensively studied due to its ability to produce many valuable products such as anti-cancer drugs and immunosuppressive agents that are important for both medical and industrial science antibiotics (Baltz, 1998; Bentley *et al.*, 2002).

S. coelicolor A3(2) has a linear chromosome like other members of streptomycetes. Its chromosome is divided into a central core region which constitutes about half of the chromosome which stretches from position 1.5 Mb to 6.4 Mb (Appendix V, Figure VB). This core includes all the genes that are important for cell division, DNA replication, transcription and translation. The other regions are a pair of chromosome arms; one arm is located between position 0 Mb and 1.5 Mb and is designated a leading arm. The other arm is called the trailing arm and it is found from position 6.4 Mb onwaeds. These regions contain the genes that are not important to the viability of the organism. The central core of *S. coelicolor* A3(2) is similar to the whole chromosome of the two pathogenic actinomycetes *Myobacterium tuberculosis* and *Corynebacterium diphtheriae* at the level of individual gene sequence. Accordingly, it seems that they arise from the same ancestor (Bentley *et al.*, 2002).

Several plasmids have been found in streptomyces species, the majority of which are self-transmissible fertility factors. Both linear and circular, low- and high copy- number plasmids are incorporated into the chromosomes. The first circular plasmid identified in *S. coelicolor* A3(2) was SCP2, a conjugative low-copy-number plasmid of 31 kb. It is present in one to four copies per chromosome (Bibb *et al.*, 1977). Three functional

regions on SCP2 involved in replication, stability and transfer of the plasmid have been recognized (Haug *et al.*, 2003).

SCP1 is a huge linear molecule of 350 kb with long terminal inverted repeats of about 80 kb on both ends (Kinashi and Murayama, 1991; Bentley *et al.* 2004). It is present in various forms in *S. coelicolor* strains as an autonomous replicating plasmid. It has been determined that SCP1 has a copy number of approximately four, demonstrating that the total amount of SCP1 in a single cell is about one-fifth that of the chromosomal DNA (Kinashi and Murayama, 1991). SCP1 carries genes for extracytoplasmic function sigma factors, antibiotic biosynthesis, and genes for spore-associated proteins (Bentley *et al.*, 2004).

S. coelicolor A3(2) produces many polysaccharide lyase enzymes that are able to degrade different types of polysaccharide chains. For instance it produces pectate lyase, pectin lyase, rhamnogalacturonan lyase, and the glycosaminoglycan-degrading enzymes; chondroitinase and hyaluronate lyase (based on data derived from CAZy: http://afmb.cnrs-mrs.fr/CAZY).

3.2 Glycosaminoglycans (GAGs)

GAGs are ubiquitous molecules expressed both on cell surfaces and in the ECM. On the basis of their disaccharide composition, different classes of GAGs have been identified as mentioned previously (section 1.2.1). They are negatively charged heterogenous polymers, and play an important role in various biological processes such as the lubrication and cushioning of joints, organization of cellular adhesion and motility, and modulation of cell signals (Jandik *et al.*, 1994; Rye and Withers, 2004).

HA is a large non-sulphated GAG, which is considered a major component of the ECM and connective tissues. It is produced by almost all tissues of vertebrates as well as by some species of bacteria such as *Streptococcus zooepidemicus*, *Streptomyces hyalurolyticus* and *Streptococcus pyogenes* (Menzel and Farr, 1998). It comprises several thousand repeats of disaccharide units of D-glucuronic acid (β-1,3) and N-acetyl-D-glucosamine (β–1,4) (Jedrzejas *et al.*, 1998). HA carries a negative charge, and consequently it can attract a large amount of water. Because of this it creates space between cells and loose tissues (Laurent *et al.*, 1996; Fraser *et al.*, 1997). HA produces a viscous solution that gives cells a soft and elastic bed to grow on as well as a medium of communication between cells through interaction with specific cell surface receptors (Li and Jedrzejas, 2001).

CS is another component of the ECM and is structurally closely related to HA (Table 1.1). It is a ubiquitous sulphated GAG composed of repeating units of β-1,3-D-glucuronic acid and β-1,4-N-acetyl-D-galactosamine (Fethiere *et al.*, 1999; Csoka *et al.*, 2001). The sulphation of CS occurs at positions 4 and 6 of galactosamine, producing chondroitin-4-sulphate and chondroitin-6-sulphate, respectively. Also, sulphation infrequently occurs at position 2 of uronic acid (Fethiere *et al.*, 1999).

It has been reported that CS plays an essential role in different biological processes including anticoagulation, osteoarthritis adhesion, differentiation, migration and proliferation (Ernst *et al.* 1995; Pojasek *et al.*, 2002). Therefore the degradation of CS by GAG degrading enzymes influences these cell processes. CS can bind a considerable amount of water and consequently can protect and cushion the surrounding structure. It is located in the ECM and on the cell surfaces of most tissues (Nadanaka *et al.*, 1998).

3.3 Results

The primary aim of the work undertaken in this chapter is to investigate the biochemical properties and structural analysis of SC1C2.15 of *S. coelicolor* A3(2). SC1C2.15 belongs to polysaccharide lyase family 8. This family includes 78 ORFs, only a few of which have been characterised biochemically and structurally. The optimum pH, optimum temperature, mode of action, effect of divalent cations, substrate specificity and absolute kinetic parameters (K_m and k_{cat}) of this enzyme were determined. Also the three dimensional structure of the native enzyme and its mutant form in complexes with different substrates were determined.

The results illustrate that the ORF *sc1c2.15* of *S. coelicolor* which encodes a putative lyase was successfully cloned and expressed in *Escherichi coli*. ORF SC1C2.15 was shown to be catalytically active on the substrate HA, chondroitin-4-sulphate and chondroitin-6-sulphate, and it was completely inactive toward dermatan sulphate, heparin sulphate and heparan sulphate. Characterisation of the N-terminally hexahistidine tagged SC1C2.15 revealed an optimum pH of 5.2 against potassium hyaluronate and 4.8 against chondroitin-4-sulphate and chondroitin-6-sulphate. The highest amount of activity of the enzyme was achieved at 57 °C. The values of the kinetic parameters K_m and k_{cat} were determined for different substrates in the absence and presence of calcium. The values of K_m for SC1C2.15, were determined against dialysed sodium hyaluronate, potassium hyaluronate, chondroitin-4-sulphate and chondroitin-6-sulphate in the absence of calcium were 0.17 ± 0.002, 0.3 ± 0.023, 0.48 ± 0.07 and 0.55 ± 0.05 mg ml^{-1}, respectively. Corresponding values of k_{cat} were 55.6, 25.1 ± 2.31, 21.8 ± 1.73, and 2.4 ± 0.24 s^{-1}, respectively. In the presence of calcium the values of K_m for sodium hyaluronate, chondroitin-4-sulphate and chondroitin-6-sulphate were 0.08 ± 0.006, 0.28 ± 0.05, and 0.33 ± 0.04 mg ml^{-1}, respectively. Corresponding

values of k_{cat} were 166.7 ± 1.12, 46.3 ± 8.02 and 6.9 ± 0.28 s^{-1}, respectively, as shown in Table 3.1.

Furthermore, the mode of action of the enzyme was investigated by HPAEC using HA, chondroitin-4-sulphate and chondroitin-6-sulphate as substrates. The enzyme produced only disaccharides; therefore its mode of action is exolytic (Figures 3.14 and 3.15).

The enzyme was crystallized and the diffraction data enabled the determination of crystal parameters (data collection and processing was performed by Dr Edward Taylor, Florence Vincent, Johan P. Turkenburg in Prof. Gideon Davis laboratory at YSBL). Crystals of the native enzyme belong to space group P43212 with unit cell dimensions of a = 141.05, b =141.05 and c=100.87. The three dimensional structure of SC1C2.15 has been solved at a resolution of 2.7 Å.

3.3.1 Protein expression and purification

3.3.1.1 Cloning, expression and purification of SC1C2.15 native recombinant protein

ORF *sc1c2.15* from polysaccharide lyase family 8 encoding a putative lyase from *S. coelicolor* A3(2) was amplified by PCR from the cosmid 1C2, which contains a 42210 bp fragment of *S. coelicolor* A3(2) chromosomal DNA carrying coding sequence (CDS) *sc1c2.15*. Two pairs of primers (section 2.1.3.1) were used to create two PCR products (Stop and No stop; Figure 3.9; section 2.2.2.1.2.1). The forward primer corresponded to nucleotides 97 to 114 (the first 96 nucleotides encodes signal peptide) of the *sc1c2.15* complete gene, and it was designed with the addition of an *Nde* I site at the 5' end of the primer. Reverse and reverse stop primers corresponded to nucleotides 2202-2220 and had an *Xho*I and *Bam*HI site attached at the 5' end of the primers, respectively. PCR

was performed using a DNA polymerase with proof reading activity (*Pfx* polymerase). The amplified DNA was then digested with the appropriate restriction enzymes (section 2.2.2.1.4; Figure 3.1A and B) and ligated into pET-22b or pET-28a previously digested with the same enzymes to generate a plasmid that encoded the protein of interest. These cloned products were then transformed into *E. coli* chemically competent TOP10 cells (section 2.2.1.3). Plasmid DNA was made from one clone and sent for sequencing using the standard sequencing primers T7 promoter and T7 terminator, no mutations were confirmed by sequencing'. The plasmid DNA was then transformed into *E. coli* BL21 (DE3) chemically competent cells (section 2.2.1.3). The recombinant *E. coli* strain was grown at 37 °C until the mid exponential phase, then induced with a final concentration of 1 mM IPTG and the cultures incubated at 20 °C overnight (section 2.2.1.2.2). Cells were harvested by centrifugation and then sonicated until fully broken in 20 mM Na HEPES pH 7.4 containing 10 mM imidazole and 0.5 M of NaCl. Cell debris was removed by centrifugation at 24000 x g for 30 min to obtain cell free extracts (section 2.2.3.2). The protein was purified from cell free extract by immobilized metal affinity chromatography (IMAC) (Figure VC, Appendix V) using a chelating sepharose column and an automated gradient elution technique (section 2.2.3.4). The protein was checked for purity by SDS-PAGE (section 2.2.3.1; Figure 3.2). The concentration of protein was determined by Bradford's assay (section 2.2.3.8; Figure 2.1) and subjected to biochemical analysis (section 2.2.4.1) and crystallisation studies (section 2.2.3.9).

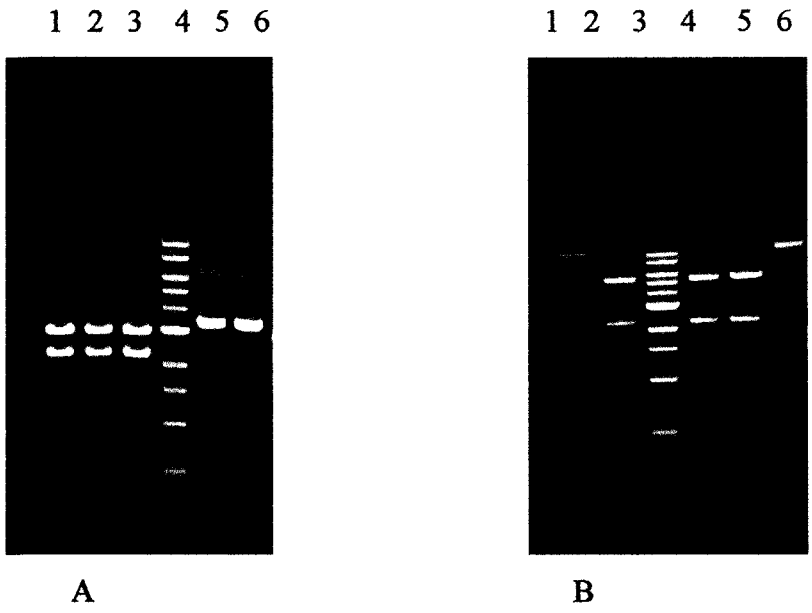

Figure 3. 1: Visualisation of DNA bands following agarose gel electrophoresis. A) DNA fragments generated during a restriction endonuclease digest; Lanes 1 and 2: *sc1c2.15* stop gene digested with *Eco*RI; Lane 3: non-stop gene digested with *Eco*RI; Lane 4: 1 Kb DNA ladder (10, 8, 6, 5, 4, 3, 2, 1.5, 1, 0.5 kb); Lane 5 and 6 plasmid without insert.
B) DNA fragments generated during a restriction endonuclease digest (section 2.2.2.1.4). Lane 2: the plasmid digested with only *Nde*I; Lane 2: sc1c2.15 stop gene digested with *Nde*I and *Bam*HI; Lane 3: 1 Kb DNA ladder (10, 8, 6, 5, 4, 3, 2, 1.5, 1, 0.5 KB); Lane 4: *sc1c2.15* no stop gene restricted with *Nde*I and *Xho*I; Lane 5: *sc1c2.15* stop gene restricted with *Nde*I and *Bam*HI; All DNA samples were subjected to 1 % agarose gel electrophoresis at 100 mA and 200 V for 45 min. Subsequently, gels were immersed in 10 $\mu g \cdot ml^{-1}$ solution of ethidium bromide for 10 min then washed with distilled water and placed on a UV illuminator and a fluorescent image taken (section 2.2.2.1.6).

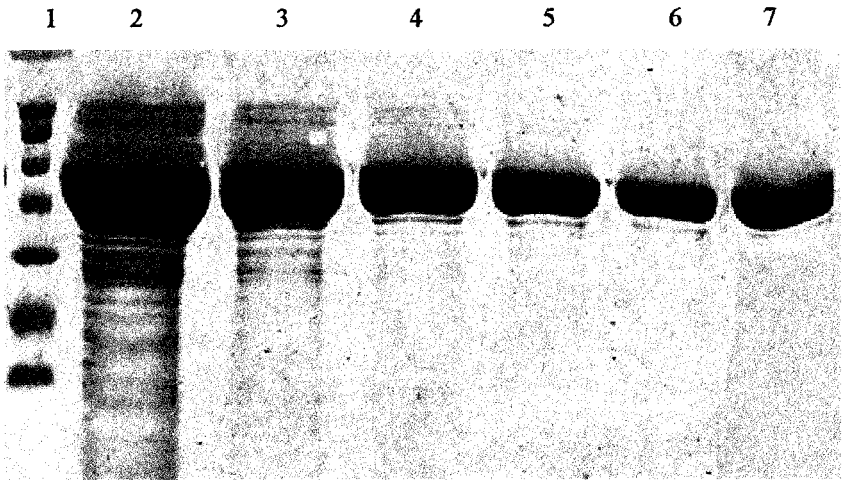

Figure 3.2 12% SDS-PAGE of SC1C2.15 expression.
SC1C2.15 (wild type) was purified from *E. coli* cells by IMAC (section 2.2.3.4). Lane 1: High molecular weight (HMW) markers (205, 116, 97, 84, 66, 55, 45, 36 KDa); Lane 2, 3, 4, 5, 6 and 7 20µl of protein (Fractions 1-6 are shown). Proteins were visualised by staining with Coomassie blue and destained (section 2.2.3.1.1).

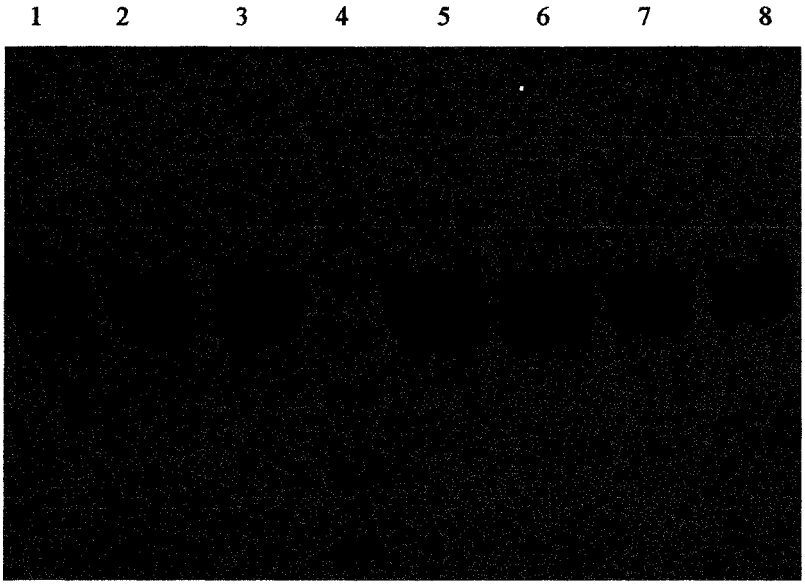

Fig 3.3 12% SDS-PAGE of SC1C2.15 mutant expression.

SC1C2.15 (mutant type) was purified from *E. coli* cells by IMAC (section 2.2.3.4). Lane 4: High molecular weight (HMW) markers (205, 116, 97, 84, 66, 55, 45, 36 KDa); Lanes 1, 2, 3, 5, 6, 7 and 8, 20µl of protein (Fractions 1-7 are shown). Proteins were visualised by staining with Coomassie blue and destained (section 2.2.3.1.1).

3.3.2 Kinetic analysis of SC1C2.15

3.3.2.1 Michaelis-Menten parameters for SC1C2.15

To study the activity of the N-terminally tagged SC1C2.15 against various dialysed substrates (section 2.1.8.2), the enzyme was assayed at 232 nm using different concentrations of substrates. The substrate specificity of the *S. coelicolor* hyaluronate lyase was studied using various GAGs: HA, chondroitin 4-sulphate, chondroitin 6-sulphate, dermatan sulphate, heparin and heparan sulphate.

SC1C2.15 mutants, Y253A and N194A had no activity against HA, chondroitin-4- or 6-sulphate.

Table 3.1: Michaelis-Menten kinetic parameters of SC1C2.15 against various substrates in the absence and presence of calcium. The reactions were performed in triplicate at 37 °C under standard conditions as described in section 2.2.4.1.1. BSA and NaCl were added at a final concentration of 0.1 mg ml^{-1} and 40 mM, respectively. HA: hyaluronan; C4S: chondroitin-4-sulphate; C6S: chondroitin-6-sulphate.

Kinetic parameters	In absence of calcium			In presence of calcium		
	HA	C4S	C6S	HA	C4S	C6S
K_m (mg ml^{-1})	0.17± 0.002	0.48 ± 0.01	0.55 ± 0.24	0.08 ± 0.006	0.28 ±0.05	0.33 ±0.04
k_{cat} (s^{-1})	55.6 ± 0	21.8 ± 1.73	2.4 ± 0.24	166.7 ± 1.12	46.3 ±1.19	6.9 ± 0.28
k_{cat}/K_m (s^{-1} ml mg^{-1})	327.1	45.4	4.4	2083.75	165.4	21.1

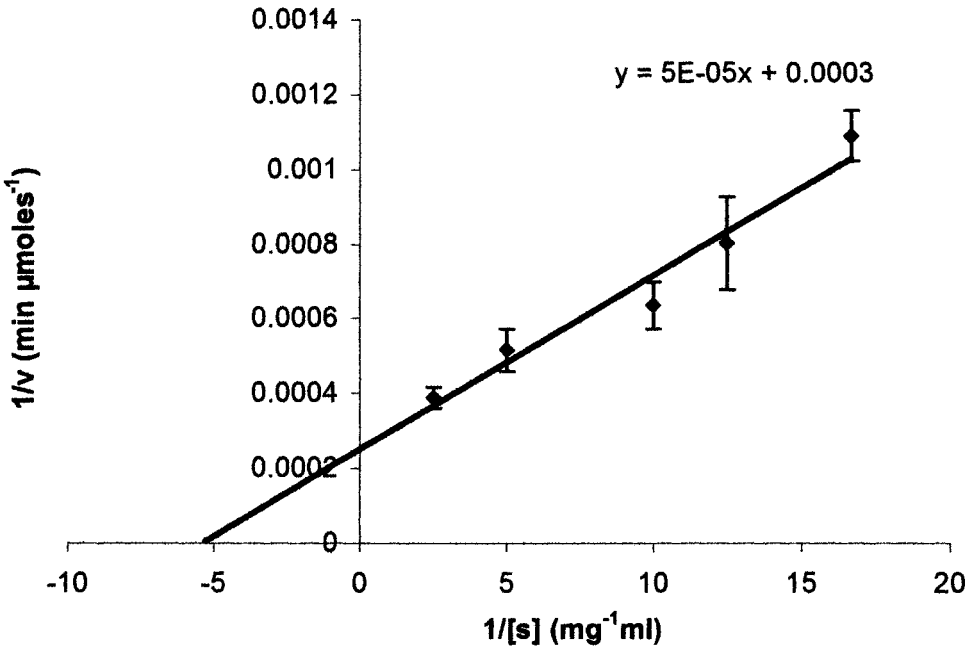

Figure 3.4 Lineweaver-Burke plot for SC1C2.15 against sodium hyaluronate. The data were performed in triplicate with error bars representing the standard deviation from the mean. The reactions were carried out under optimal conditions.

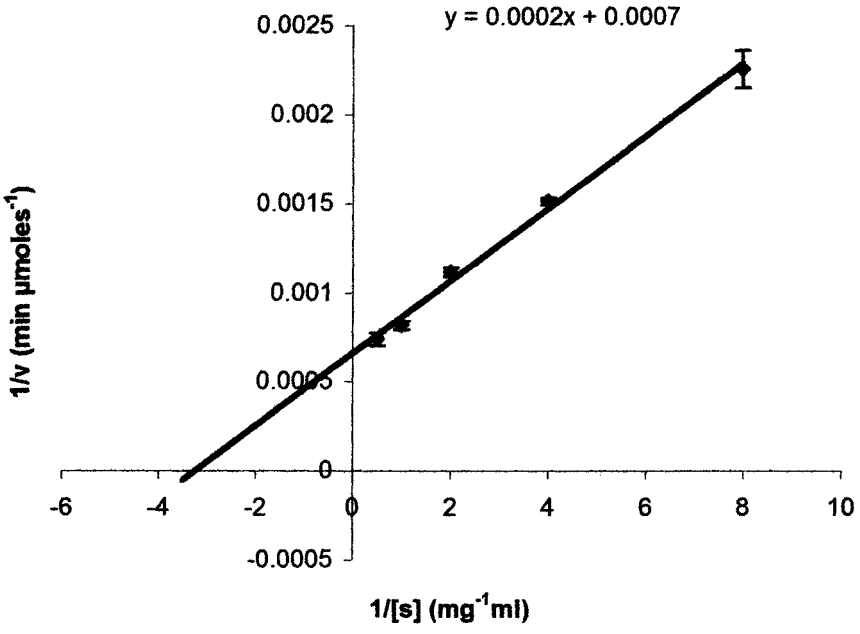

Figure 3.5 Lineweaver-Burke plot for SC1C2.15 against potassium hyaluronate. The data were performed in triplicate with error bars representing the standard deviation from the mean. The reactions were carried out under optimal conditions (Table 2.24).

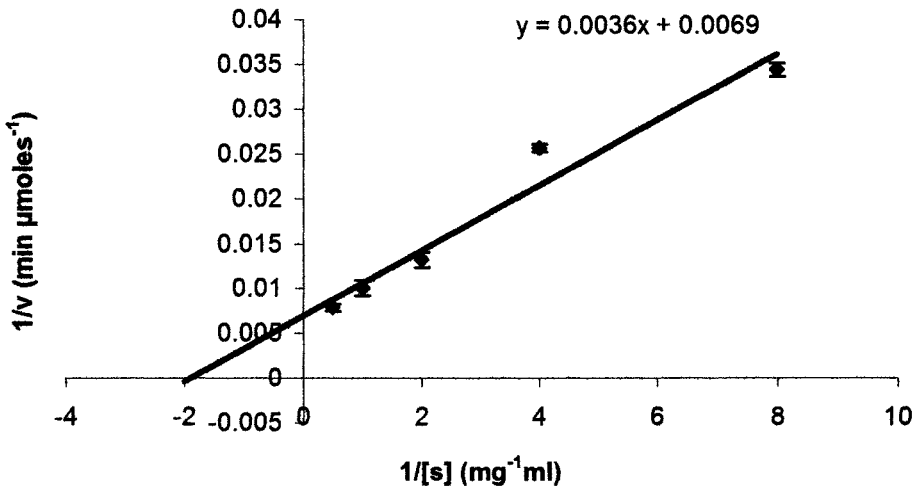

Figure 3.6 Lineweaver-Burke plot for SC1C2.15 against chondroitin-6-sulphate. The data were performed in triplicate with error bars representing the standard deviation from the mean. The reactions were carried out under optimal conditions (Table 2.25).

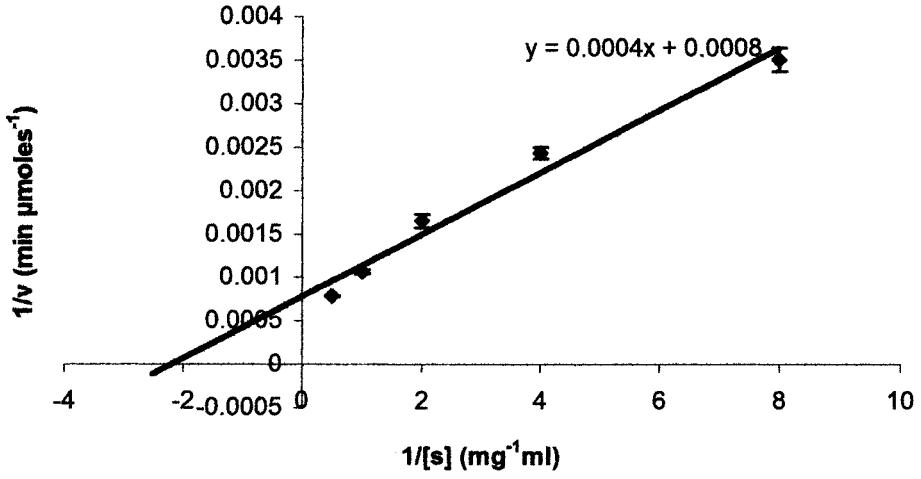

Figure 3.7 Lineweaver-Burke plot for SC1C2.15 against chondroitin-4-sulphate. The data were performed in triplicate with error bars representing the standard deviation from the mean. The reactions were carried out under optimal conditions (Table 2.25).

3.3.3 Biochemical characterisation of *sc1c2.15*

3.3.3.1 Determination of optimum pH

The N-terminally tagged SC1C2.15 protein was shown to have an optimum pH of 5.2 and 4.8 against dialysed potassium hyaluronate and dialysed chondroitin-4 and 6-sulphate, respectively. Sodium acetate buffers that range from 3-7.6 were used to determine optimum pH. Assays were carried out at 37 °C and the rate of absorbance was measured at 232 nm using a spectrophotometer. Figures 3.8 And 3.9 show the effect of pH on enzyme activity against dialysed potassium hyaluronate and chondroitin-4 and 6-sulphate, respectively.

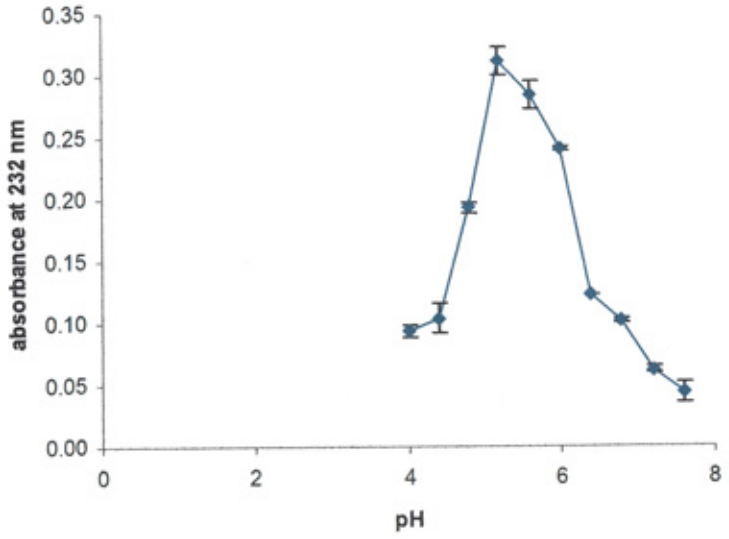

Figure 3.8 Effect of pH on SC1C2.15 activity against potassium hyaluronate. Reactions were performed at 37 °C, with 1 mg ml^{-1} substrate (dialysed potassium hyaluronate), 20 mM sodium acetate buffer in the pH range 4-7.6, 40 mM NaCl final concentration and BSA (0.1mg ml^{-1}). Reactions were performed in triplicate, with initial rate measurements, and error bars represent the standard deviation of the mean.

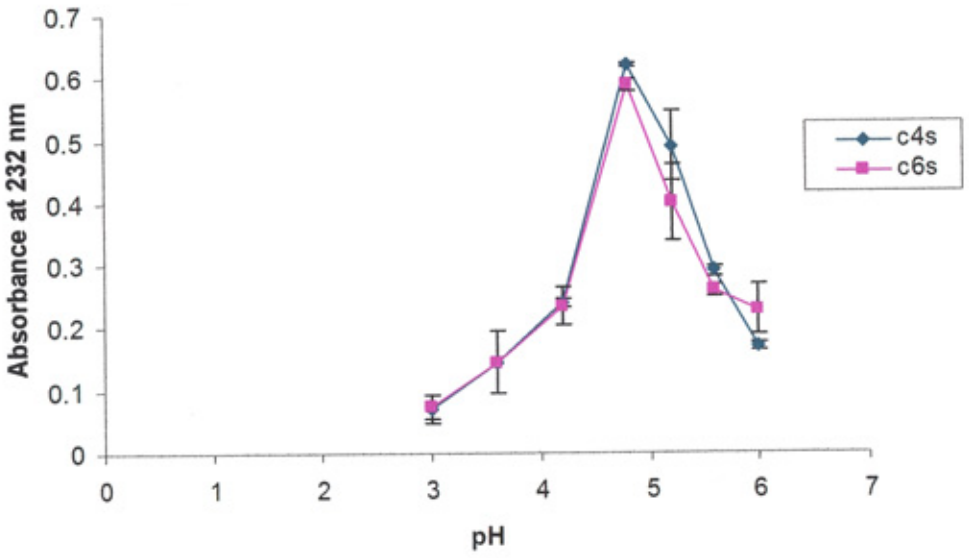

Figure 3.9 Effect of pH on SC1C2.15 activity against chondroitin-4 and 6-sulphate. Reactions were performed at 37 °C, with 1mg ml^{-1} substrate (dialysed chondroitin-4 and 6-sulphate), 20 mM sodium acetate buffer in the pH range 3-6, 40 mM NaCl final concentration and BSA (0.1mg ml^{-1}). Reactions were performed in triplicate, with initial rate measurements, and error bars represent the standard deviation of the mean.

3.3.3.2 Determination of optimum temperature

At 57 °C, SC1C2.15 exhibited the highest amount of activity against the dialysed substrate HA (section 2.1.8.2). When added to a pre-warmed reaction mixture (Figure 3.10), the activity of the enzyme decreased considerably at 77 °C. However, the enzyme was active within a large temperature range of 27–67 °C.

After pre-incubation for 20 min at different temperatures prior to assay (section 2.2.4.1.1.3), the enzyme displayed the highest activity at 27 °C and activity dramatically reduced at temperatures 57 °C and 67 °C, as shown in Figure 3.11.

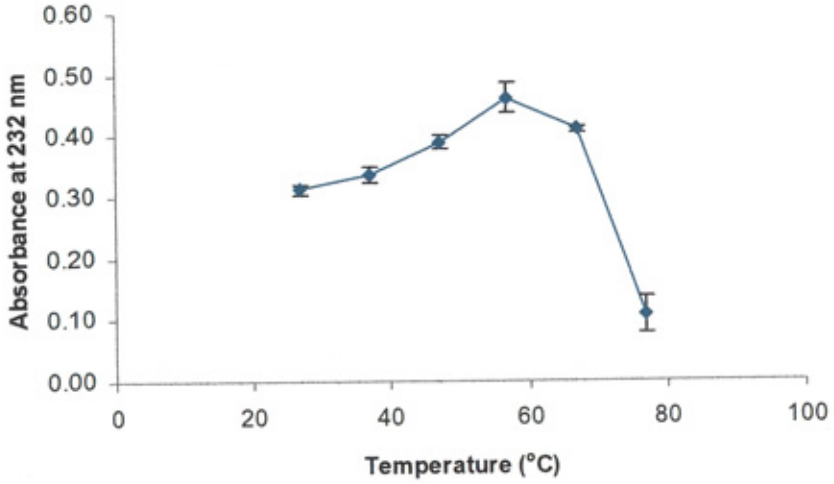

Figure 3.10 Effect of temperature on SC1C2.15 activity
Reactions comprised 1 mg ml^{-1} substrate (dialysed HA), 20 mM sodium acetate buffer pH 5.2, 0.1mg ml^{-1} BSA and 40 mM NaCl. Reactions were performed in triplicate, with initial rate measurements made at 27, 37, 47, 55, 67 and 77 °C (error bars represent the standard deviation of the mean).

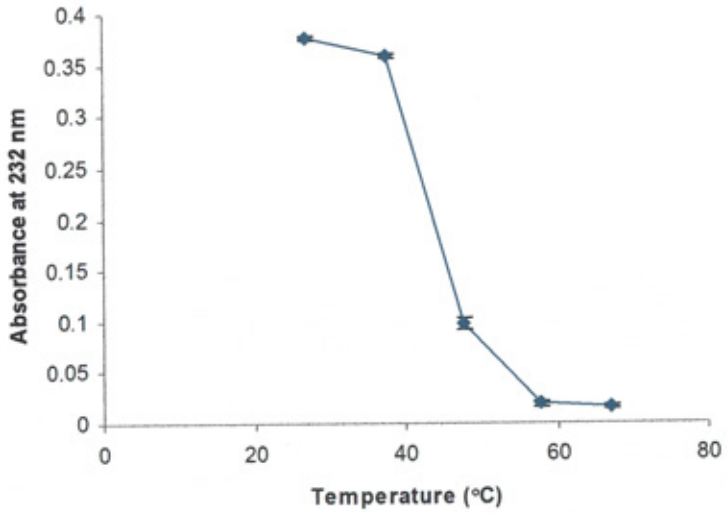

Figure 3.11 Effect of temperature on the stability of SC1C2.15
Reactions were performed at 37°C, with 1 mg ml^{-1} substrate (dialysed HA), 20 mM sodium acetate buffer pH 5.2, 0.1 mg ml^{-1} BSA and 40 mM NaCl. Prior to the reactions, the enzyme was pre-incubated at 27, 37, 47, 57 and 67 °C for 20 minutes. Reactions were performed in triplicate, with initial rate measurements made (error bars represent the standard deviation of the mean).

3.3.3.3 Determination of effect of divalent ion

The effect of various divalent cations at a final concentration of 2 mM (section 2.2.4.1.1.4) was tested against SC1C2.15. It was found that $CaCl_2$ and $MnCl_2$ increased the activity of the enzyme significantly, while $MgCl_2$ and $ZnCl_2$ had no effect on the activity of the enzyme (Figure 3.12). On the other hand, the activity of the enzyme decreased in the presence of $CoCl_2$ and $NiCl_2$.

The activity of the enzyme increased considerably with increasing calcium concentration, reaching optimal activity at concentrations of 2 mM to 4 mM as shown in Figure 3.13. To test the effect of calcium concentration on the kinetic parameters K_m and k_{cat} of the enzyme, these were determined for various substrates in the absence and presence of calcium (Table 3.1).

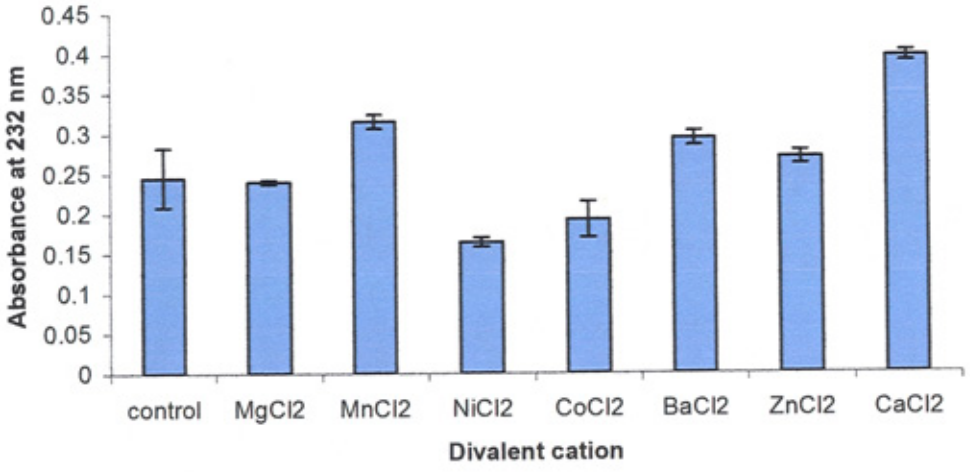

Figure 3.12 Effect of divalent cations on SC1C2.15 activity. Reactions used 1 mg ml^{-1} substrate (dialysed HA), 20 mM sodium acetate buffer pH 5.2, 0.1 mg ml^{-1} BSA and 40 mM NaCl as illustrated in section 2.2.4.1.1. Divalent cation (Mg^{2+}, Mn^{2+}, Ni^{2+}, $C2^{++}$, Ba^{2+}, Zn^{2+} and Ca^{2+}) was added to reactions at a final concentration of 2 mM. Reactions were performed in triplicate, with initial rate measurements made at 37 °C (error bars represent the standard deviation of the mean).

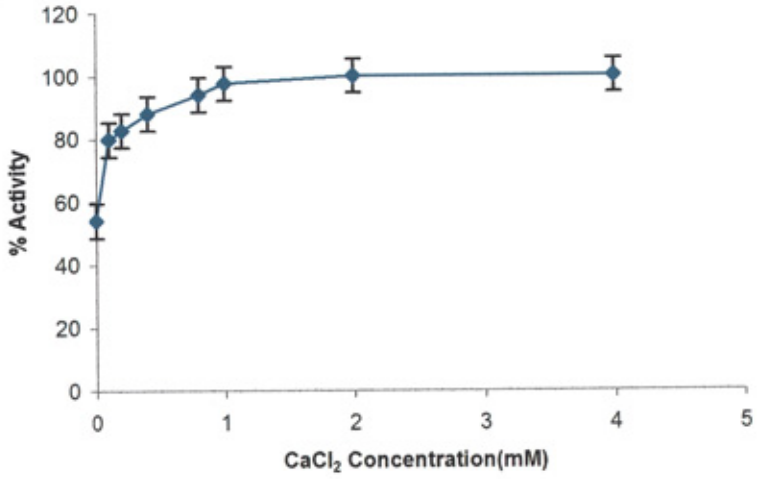

Figure 3.13 Effect of different concentrations of calcium on SC1C2.15 activity. Reactions used 1 mg ml^{-1} substrate (dialysed HA), 20 mM sodium acetate buffer pH 5.2, 40 mM NaCl and 0.1 mg ml^{-1} BSA as illustrated in section 2.2.4.1.1. Calcium was then added (0-4 mM). Reactions were performed in triplicate, with initial rate measurements made at 37 °C (error bars represent the standard deviation of the mean).

3.3.4 Mode of action of SC1C2.15

The mode of action of the *S. coelicolor* enzyme was investigated by the analysis of digestion products by HPAEC using HA, chondroitin-4-sulphate and chondroitin-6-sulphate as substrates.

Upon analysis of the digestion products of SC1C2.15 (section 2.2.4.2) the enzyme appears to display an exolytic mode of cleavage against HA as it produced disaccharides almost exclusively (Figures 3.23). However, it produced oligosaccharides with wide gaps with chondroitin-4-sulphate, which is probably due to the cleavage of only non-sulphated disaccharides (3.24). The method used in this work employs the same elution condition to that reported by Lauder et al., 2000. The method was calibrated using commercial di-, tetra-, hexa- and octa-saccharide. The analysis of digestion by HPAEC revealed the presence of an artefact peak at a retention time between 24 and 26 min, this peak was also observed with other workers, for instance, Lauder et al., 2000 and Smith et al., 2005. The nature of the artefact peak is unknown.

The elution position of HA disaccharide and chondroitin sulphate oligosaccharides was determined and compared to the standards. The elution position was in very close agreement to that of Lauder et al., 2000.

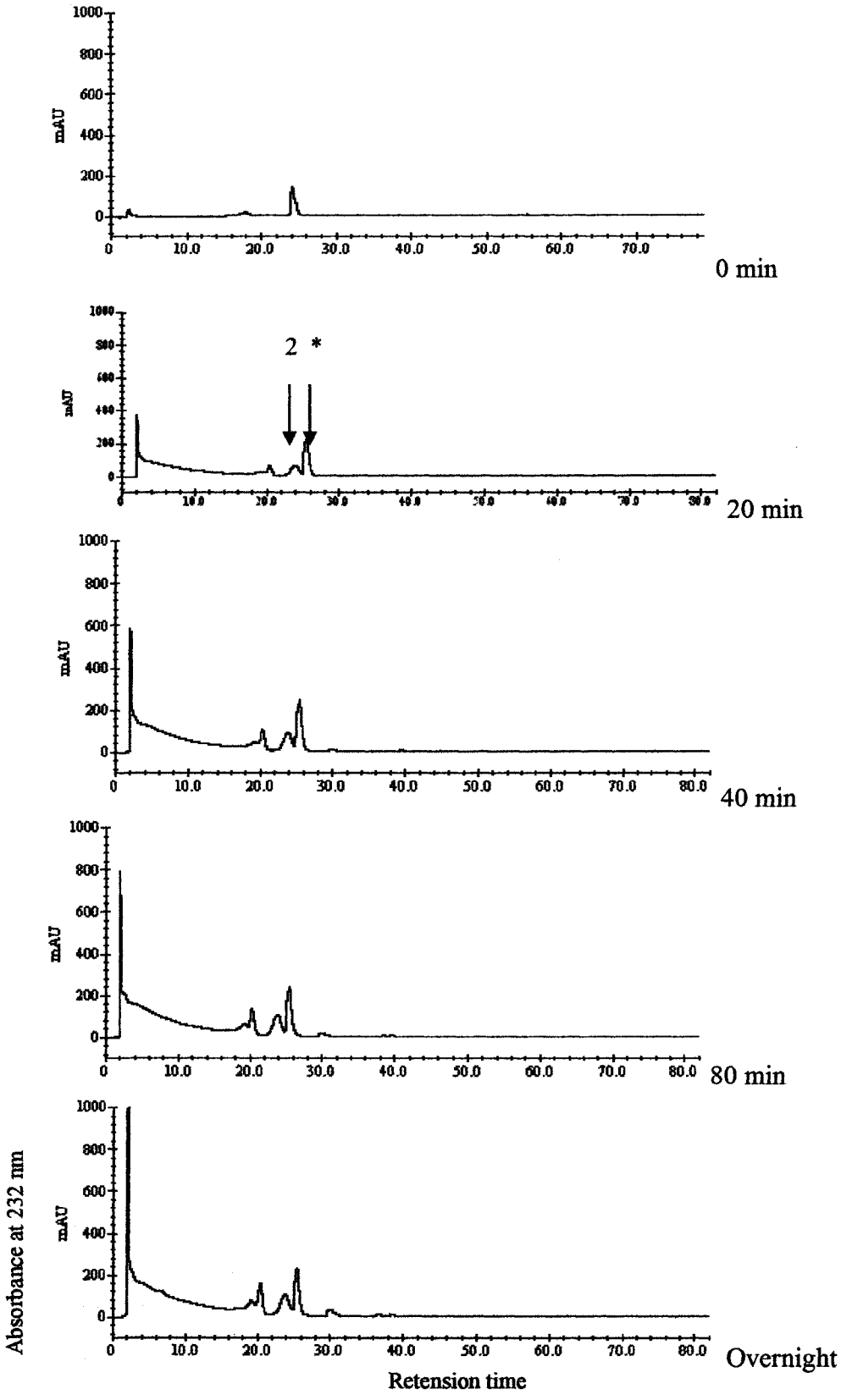

Figure 3. 14: HPAEC of the oligosaccharides derived from hyaluronate lyase digestion of hyaluronan. The oligosaccharides were chromatographed on a CarboPac PA1column (250 mm x 4 mm) maintained at 37 °C. Elution was performed at a flow rate of 1 ml min^{-1} (section 2.2.4.2). The eluent was monitored by absorbance at 232 nm. 2, disaccharide; * artifact.

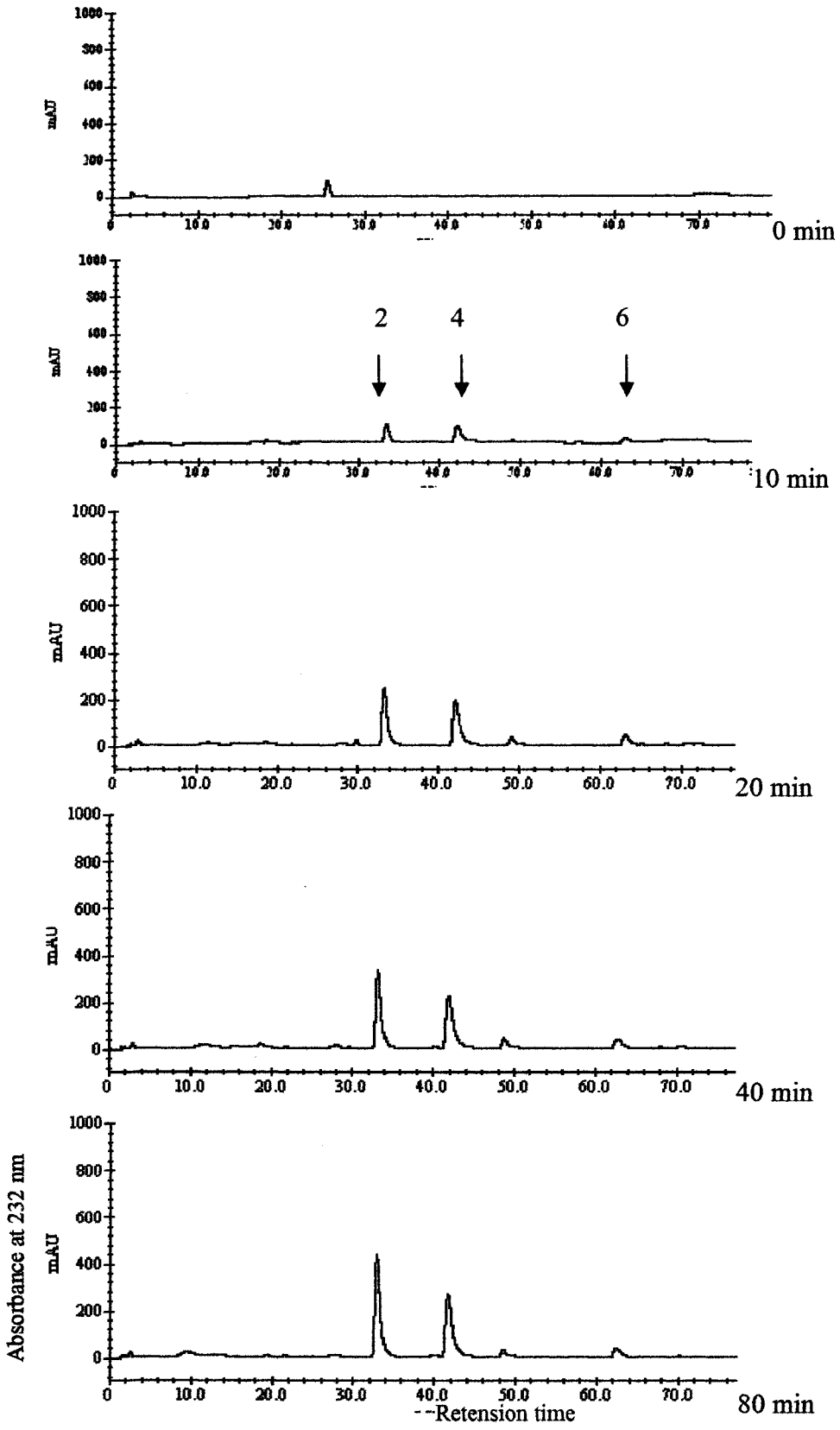

Figure 3.15 HPAEC of the oligosaccharides derived from hyaluronate lyase digestion of chondroitin-4-sulphate. The oligosaccharides were chromatographed on a CarboPac PA 1 column (250 mm x 4 mm) maintained at 37 °C. Elution was at 1 ml min^{-1} (section 2.2.4.2). The eluent was monitored by absorbance at 232 nm. 2, disaccharide; 4, tetrasaccharide; 6, hexasaccharide.

3.3.5 Construction of SC1C2.15 mutants

Through sequence homology with other enzymes in the same family, the conserved amino acids in the binding site were identified and subsequently mutated by site-directed mutagenesis (SDM; section 2.2.2.1.3.1). These residues included Tyr253, Asn194, and His244 and were each substituted with alanine to give Y253A, N194A and H244A. The primers used to generate these mutants by SDM method are shown in section 2.1.3.1.3. PCR conditions are given in section 2.2.2.1.3.1. The PCR products were transformed into *E. coil* TOP10 competent cells (section 2.2.1.3). Plasmid DNA was purified from one colony (section 2.2.2.1.7.3) and was sent for sequencing using the standard sequencing primers T7 promoter and T7 terminator and mutations were confirmed by sequencing. The data showed that the desired single codon mutation was successfully created. Mutant forms were transformed into *E. coli* BL21 (DE3) chemically competent cells (section 2.2.1.3), and the recombinant *E. coli* strain was grown at 37 °C to mid exponential phase. Expression of the SC1C2.15 mutants was induced by the addition of IPTG to a final concentration of 1 mM and the cultures incubated at 20 °C overnight (section 2.2.1.2.2). Cells were harvested by centrifugation and cell free extract was prepared as described in section 2.2.3.2.

The proteins were purified by IMAC under non-denaturing conditions, using a chelating sepharose resin column as illustrated in section 2.2.3.4. The purified mutants are shown in figure 3.3. Proteins were then concentrated using a molecular weight cut off concentrator (section 2.2.3.5) in 10 mM Tris/HCl buffer, pH8 and their concentrations were determined by Bradford's assay (section 2.2.3.8; Figure 2.1).

The kinetic analysis of the mutants showed that the substitution of both mutants Y253A and N194A led to no obvious change in absorbance at 232 nm, indicating that the mutant enzymes were completely inactive against HA, chondroitin-4 and 6-sulphate.

3.3.6 Crystallisation of SC1C2.15

3.3.6.1 Native recombinant crystallisation of SC1C2.15

SC1C2.15 was purified to apparent homogeneity (as judged by SDS-PAGE; section 2.2 3.1.1; Figure 3.2) from a recombinant pET-28a plasmid carrying the *sc1c2.15* gene (N-terminal hexa-histidine tag construct). The protein was concentrated to approximately 12 mg ml^{-1} (section 2.2.3.8). The protein was then screened using the hanging drop vapour diffusion method together with Crystal Screen 1, Crystal Screen 2 and PEG/Ion Screen (Hampton Research, Alison Viejo, USA) and Clear Strategy Screen I and Clear Strategy Screen II (Molecular Dimensions Limited, Cambridgeshire UK) (appendix III; Tables III A, III B, III C, III D and III E respectively). Drops containing 1 µl of protein (at a concentration of 12 mg ml^{-1}) were mixed together with 1 µl and 2 µl of the mother liquor. Also, a drop containing 2 µl of protein was mixed with 1 µl of mother liquor. Crystals were found to grow in condition 33 (4 M sodium formate) of the Crystal Screen 1. Crystals appeared after one week at 22 °C (Figure 3.16). The crystals were smooth and thick with triangular features. A single crystal was removed from the drop using a rayon fibre loop and transferred into a cryo-protectant solution comprising the crystal growth buffer (4 M sodium formate) and 25 % (v/v) glycerol prior to freezing the crystals in liquid nitrogen. A rayon fibre loop was used to raise the crystal and an image collected using a Rigaku x- ray generator and a MAR 30 cm image plate at YSBL. Crystals that diffracted at 2.7 Å were stored in liquid nitrogen for further analysis at the ESRF (Grenoble, France). The structural data is represented in Tables

3.2. All data collection and analysis was performed by Dr Edward Taylor, Dr Florence Vincent, Dr Johan Turkenburg and Prof. Gideon Davis laboratory at YSBL.

3.3.6.2 Crystallisation of SC1C2.15 mutants in complex with substrate

SC1C2.15 mutant proteins were purified to apparent homogeneity (Figure 3.3) and then concentrated in 10 mM Tris/HCl buffer, pH 8 to concentrations ranging between 10-12 mg ml^{-1}. Crystals of SC1C2.15 mutants were grown by the vapour phase diffusion method. Optimisation studies for SC1C2.15 mutants were carried out around the condition of the native protein crystals, which was 4 M sodium formate.

For the enzyme derivative N194A, the concentration was 10 mg ml^{-1} and crystals were attained at 3.8 and 3.9 M sodium formate. For Y253A the concentration was 11.5 mg ml^{-1} and crystals were achieved at 2.9 and 3.5 M sodium formate (Figure 3.17). The ligand complex of HA tetrasaccharide was obtained by soaking mutant Y253A crystals in 2 µl drops of mother liquor; grains of ligand were dissolved adjacent to the crystals and soaked for between 5 and 30 minutes. The other ligands (chondroitin-4-sulphate disaccharide, chondroitin-6-sulphate disaccharide, vitamin C (L-ascorbic acid) were dissolved in water to give a final concentration of 60 mM, whereas L-ascorbic acid-6-hexadecanoate (Vcpal) was dissolved in 5 % DMSO (v/v) and 10 mM Tris-HCl buffer, pH 8 to the final concentration of 60 mM. Then all the ligands were added to the drops of enzyme and mother liquor (1 µl each) at a final concentration of 20 mM, except for the inhibitor, various amounts (1, 1.5 and 2 µl) of which were added, mixed together and equilibrated against 0.5 ml of the mother liquor.

The crystals formed were cryoprotected using 30 % glycerol (v/v) and sodium formate buffer and frozen in liquid nitrogen. Standard fibre loops of suitable size were used to pick up and mount the frozen crystals.

Data were collected by Dr Edward Taylor, Dr Florence Vincent, Dr Johan Turkenburg at the European Synchrotron Radiation Facility (ESRF) from single crystals at 100K with a Dφ of 0.3. Non-complexed data were collected at a wavelength of 0.91680 nm over an oscillation range of 180° on ID29-1 using an ADSC Q210 2D CCD charged-coupled device detector.

3.3.7 Structure solution and refinement

All data were processed with the HKL suit (Otwinowski and Minor, 1997) or Mosflm (Leslie, 1992). All other computing was undertaken using the CCP4 suit unless otherwise stated. The crystals were found to belong to the space group P43212 with the approximate cell dimensions of a =141.05 Å, b = 141.05 Å, c = 100.87 Å (Table 3.2). The SC1C2.15 structure was solved by the molecular replacement program AMORE using pdb 10JM as a search module. An R free of 5% of the total reflections were maintained for cross validation before module.

The refined model of the wild type comprises of 765 residues and 510 water molecules. The final overall *R*-factor for the refined model was 0.18229, with 133324 unique reflections within a resolution range of 36.51-1.50 Å. The free *R*-factor was 0.18229 and the final root-mean square deviations from the standard geometry were 0.012 Å for bond lengths and 1.354 for bond angles (This work were performed by Dr Edward Taylor, Dr Florence Vincent, Dr Johan Turkenburg and Prof. Gideon Davies').

The data in Table 3.2 show the refined structures of the wild type and its mutant with different complexes.

The crystal structures of tetrasaccharide complex, HA disaccharide, C4S disaccharide and Vcpal were solved at 1.7, 1.8, 2.3 and 2.6 Å resolution, respectively. The structure

of these complexes contains residues Ala24 to Ser765, except for the tetrasaccharide complex which contains residues Ala24 to Leu745. The structure of the enzyme with the tetrasaccharide, HA disaccharide, chondroitin-4-sulphate disaccharide and Y253A contained 782, 500, 343 and 1841 water molecules, respectively.

Table 3.2 Crystallographic and refinement statistics of SC1C2.15 wild type ant its complexes

	Wild type	WT complex with C4S disaccharide	N194A mutant complex with HA disaccharide	N194A mutant complex with inhibitor	Y253A mutant (no ligand	WT complex with HA tetrasaccharide
Space group	P43212	P43212	P43212	P43212	H3	P43212
Unit cell						
a (Å)	141.051	140.508	141.051	140.624	317.100	140.389
b (Å)	141.051	140.508	141.051	140.624	317.100	140.389
c (Å)	100.874	100.764	100.874	99.957	82.974	100.114
Low resolution diffraction (outer shell) (Å)	44.72 (2.11)	50.38 (2.42)	30 (1.83)	81.38 (2.74)	59.76 (2.11)	42.84 (1.79)
High resolution diffraction (outer shell) (Å)	2.00 (2.00)	2.30 (2.30)	1.80 (1.80)	2.60 (2.60)	2.00 (2.00)	1.70 (1.70)
Completeness (outer shell) %	100.0 (100.0)	100.0 (100.0)	98.1 (99.2)	99.8 (98.9)	96.6 (78.5)	99.9 (99.8)
Multiplicity (outer shell)	7.5 (7.5)	8.1 (8.2)	5.9 (5.9)	8.4 (8.0)	4.0 (3.2)	6.4 (3.7)
Free R value	0.18229	0.22724	0.18141	0.24707	0.23993	0.21644
Root mean sequare deviation (rms)						
Bond length (Å)	0.012	0.020	0.015	0.009	0.018	0.013
Bond angles (degrees)	1.354	1.838	1.539	1.223	1.601	1.363
Unique reflections	133324	45361	91126	31388	203027	109679
R_{merge} (outer shell)	0.147 (0.429)	0.087 (0.396)	0.071 (0.527)	0.105 (0.800)	0.128 (0.624)	0.105 (0.809)
Mean (I) / sd (I) (outer shell	12.8 (4.7)	18.8 (5.2)	19.67 (4.024)	16.8 (2.0)	9.1 (1.3)	10.4 (1.1)

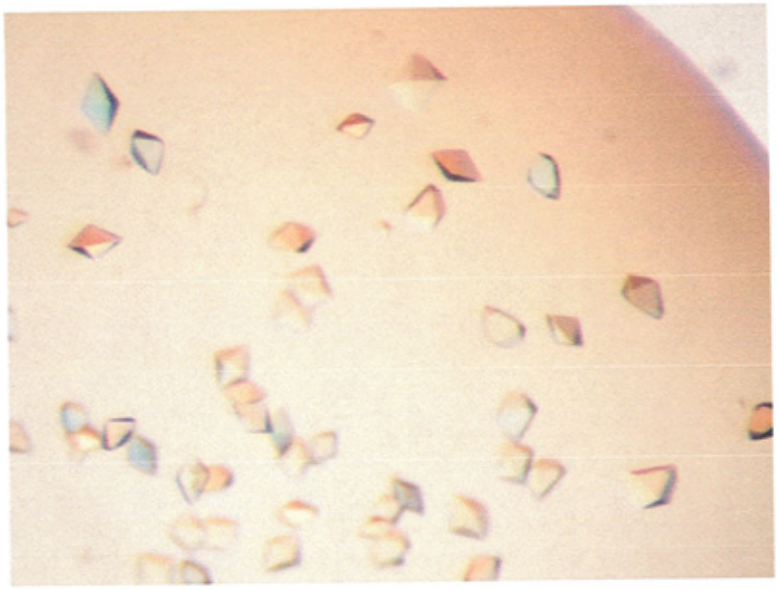

Figure 3.16 Crystals of native recombinant SC1C2.15 from *S. coelicolor*. Crystals were grown by the hanging drop method (Section 2.2.3.9). Equal amounts of protein and reservoir (4 M sodium formate) were mixed and glycerol [25% (v/v) final concentration] was added to the drop. Tetragonal crystals grew after one week at 22 °C.

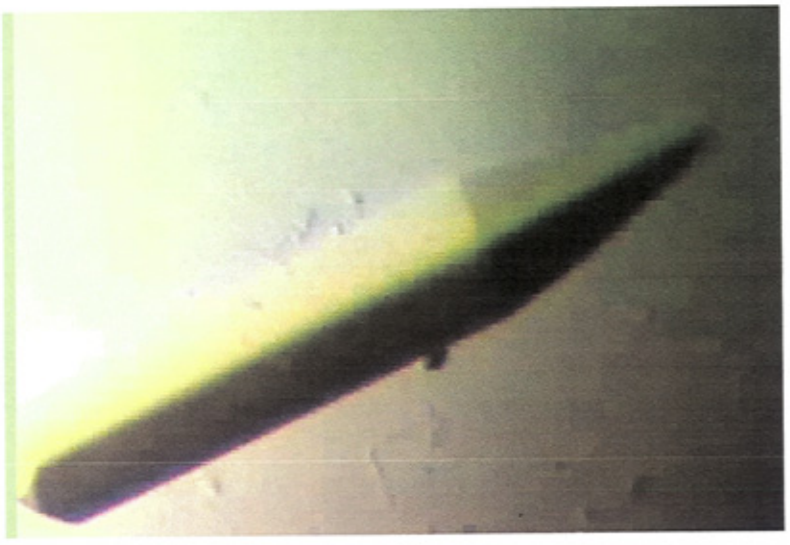

Figure 3.17 Crystal of the mutant Y253A. Crystals were grown by the hanging drop method (Section 2.2.3.9). Equal amounts of protein and reservoir (2.9 M sodium formate) were mixed and glycerol [25% (v/v) final concentration] was added to the drop. Crystals grew after one week at 22 °C.

The structure of N194A has been refined at 1.94 Å resolution with the program REFMAC. The final model is a monomer comprising 5682 non-hydrogen protein atoms with 558 water molecules, a formic acid molecule, glycerol, and a ligand molecule: N-acetylglucosamine bound to a 4-desoxy-glucuronic acid. The crystallographic *R*-factor and *R*-free are respectively 16.9% and 19.4%.

The structure of Y253A has been solved by molecular replacement using AmoRe (Navaza, 1994) with the wild type as a search model at 2.0 Å resolution. The wild type crystallised in a tetragonal space group with one molecule in the asymmetric unit. We used this monomer to solve the structure of Y253A mutant, which crystallised in a trigonal space group with two molecules in the asymmetric unit. The final model of Y253A contains 5624 non-hydrogen protein atoms with 1841 water molecules and a molecule of formic acid per monomer, coming from the crystallisation conditions. The crystallographic *R*-factor and *R*-free values are 18.9% and 22.4 %, respectively

3.3.8 Three dimensional structure of SC1C2.15

The structure of the *S. coelicolor* hyaluronate lyase includes the entire polypeptide chain from residue Ala24 to residue Ser765 (residues from 1-23 represent the signal peptide sequence). The 3D structure of SC1C2.15 was solved at a resolution of 1.8 Å by a combination of the multiple isomorphous replacement (MIR) and multiple-wavelength anomalous diffraction (MAD) approaches conducted at the European Synchrotron Radiation Facility (ESRF, Grenoble, France) on beamline BM14, as illustrated in section 3.3.7. The structure was solved using chondroitin AC lyase from *A. aurescens* (PDB code: 1RW9) (Lunin *et al.*, 2004) as a starting model with

38.9 % identity (Figure 1.6). The structure of the *S. coelicolor* hyaluronate lyase is indeed similar to that of *A. aurescens* AC lyase with a root mean square deviation of 1.35 Å over 704 equivalent C^{α} atoms (calculated with LSQMAN). The *S. coelicolor* hyaluronate lyase has approximate dimensions of 45 x 45 x 72 Å. The 3D structure extends from residues 24Ala to Asp386 for the α–domain, Ala387 to Val396 for the linker and Gly397 to Ser765 for the β-domain (where the numbering corresponds with the full length sequence). The structure of the wild type contains 510 ordered water molecules, in addition to the protein molecule.The structure consists of two different domains of approximately equal sizes: an α-domain and an β-domain (Figure 3.18). The N-terminal α–helical domain composed of 13 α-helices. Ten of them (helix 3–helix 12) form the $(\alpha/\alpha)_5$ toroid common to this polysaccharide lyase family. This domain forms a groove that encloses the active site. These 10 helices are linked by short and long loops. Helix 2 and helix 13 block the opening of the incomplete barrel. The amino acid residues that constitute different α-helices are: α-H1, 24-39; α-H2, 49-67; α-H3, 84-102; α-H4, 112-128; α-H5, 140-162; α-H6, 164-182; α-H7, 193-209; α-H8, 212-226; α-H9, 253-268; α-H10, 278-294; α-H11, 325-342; α-H12, 345-361; and α-H13, 375-386 (Figure 3.19A). Also there is a small α-helix, 307-311, and two short β-strands comprising residues 234-236 and 239-242 (Figure 3.19A).

The inner layer of the toroid is formed by helices α3, α5, α7, α9 and α11. The outer layer consists of helices α4, α6, α8, α10 and α12 all oriented in the direction opposite to the inner helices (Figure 3.19A).

Within the α-domain, there is an elongated cleft, which is narrow at the middle and wider at the two ends. It is located in the vicinity of the interface between the α-domain and the β-domain. The cleft is the position where the substrate can bind and degrade. The substrate binding cleft is situated at the larger end of the barrel. The majority of the residues down the cleft surface are positively charged due to the abundance of basic residues. These residues are Arg53, Arg60, Arg93, Arg120, Arg136, Arg149, Arg166, Arg200, Arg307, Arg311, Lys315, Arg354, Arg361 and Arg410 (Figure 3.18). At one end of the cleft there are four negatively charged residues, Asp233, Thr230, Thr245 and Glu429 forming a negative patch (Figure 3.18). Opposite these residues, two aromatic residues are present, Trp140 and Trp141. Also the catalytic residues, Asn194, His244 and Tyr253 are located in the cleft (Figure 3.18).

The C-terminal domain is a β-domain composed of antiparallel β-strands that form 4 β-sheets. Two sets of β-sheets: the residue 397 to 637 form two 8 stranded β-sheets, and residue 655 to 765 form the second set of sheets, one seven stranded β-sheet and one five stranded. The two sets of β-sheets are separated by a small α-helix (Figure 3.19B). Thus the C-terminal β-domain is comprises 28 strands grouped into 4 β-sheets. These 4 sheets (sheet 1-sheet 4) contain 8, 8, 7 and 5 β-strands, respectively (Figure 3.19B). The number of amino acid residues in these 28 strands , that vary in size, are β-sheet 1 (S1, 397-401; S2, 405-411; S3, 414-419; S4, 444-450; S5, 473-477; S6, 548-559; S7, 589-597; S8, 611-623); β-sheet 2 (S1, 499-503; S2, 508-515; S3, 522-529; S4, 534-539; S5, 566-569; S6, 572-575; S7, 578-582; S8, 631-637); β-sheet 3 (S1, 655-660; S2, 663-668; S3, 693-700; S4, 703-709; S5, 727-732; S6, 758-763; S7, 673-678); and β-sheet 4 (S1, 682-684; S2, 687-689; S3, 718-722; S4, 736-

740). There are 28 loops connecting each strand to the following one in the C-terminal domain. Also, within this domain there are two additional short α-helices. The two domains are connected through a short flexible linker peptide composed of residues Ala387 to Val396 (Figure 3.18).

On the basis of sequence alignment between different members of PL 8 (Figure 1.6), Tyr253, Asn194 and His244 were selected for their possible role in catalysis and they were each mutated to alanine. The mutated residues were then co-crystallised with HA tetrasaccharide, HA disaccharide, chondroitin-4 and 6-sulphate and Vcpal.

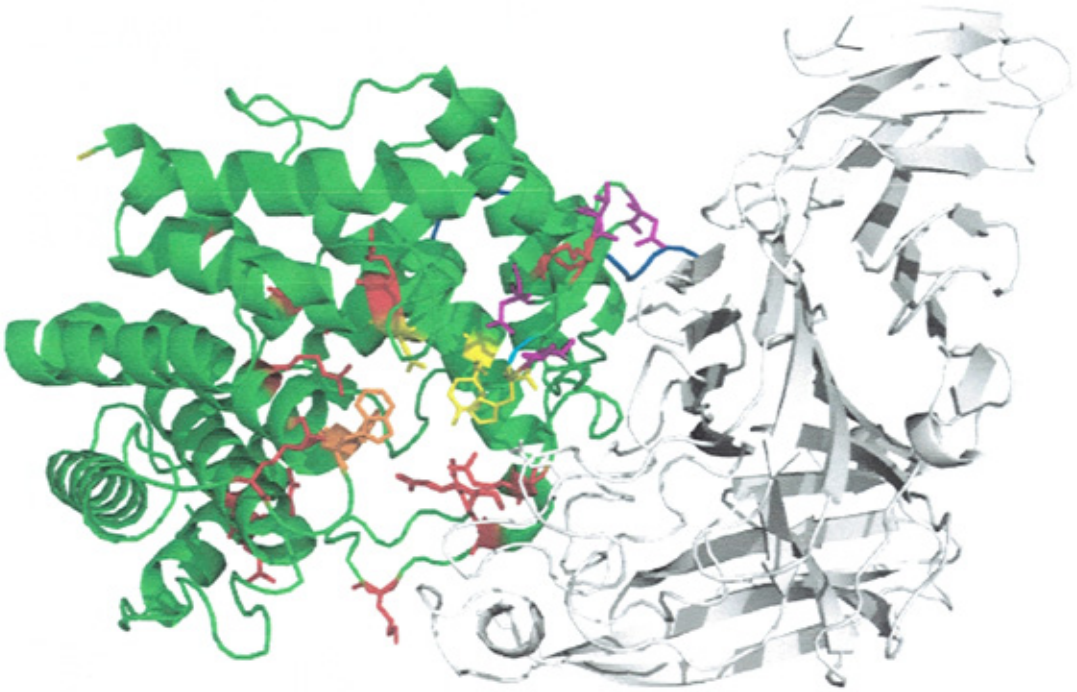

Figure 3.18 Overall structure of hyaluronate lyase. The colours represent elements with a secondary structure (green, α-helices; gray, β-strands; blue, linker). Catalytic residues are coloured in yellow (Tyr253; His244 and Asn194); aromatic patch residues are coloured in orange (Try140 and 141); negative patch residues are coloured in magenta; and positive charged amino acid residues are coloured in red. This figure was prepared using the program PyMol (Delano scientific, pymol.sourceforge.net).

A

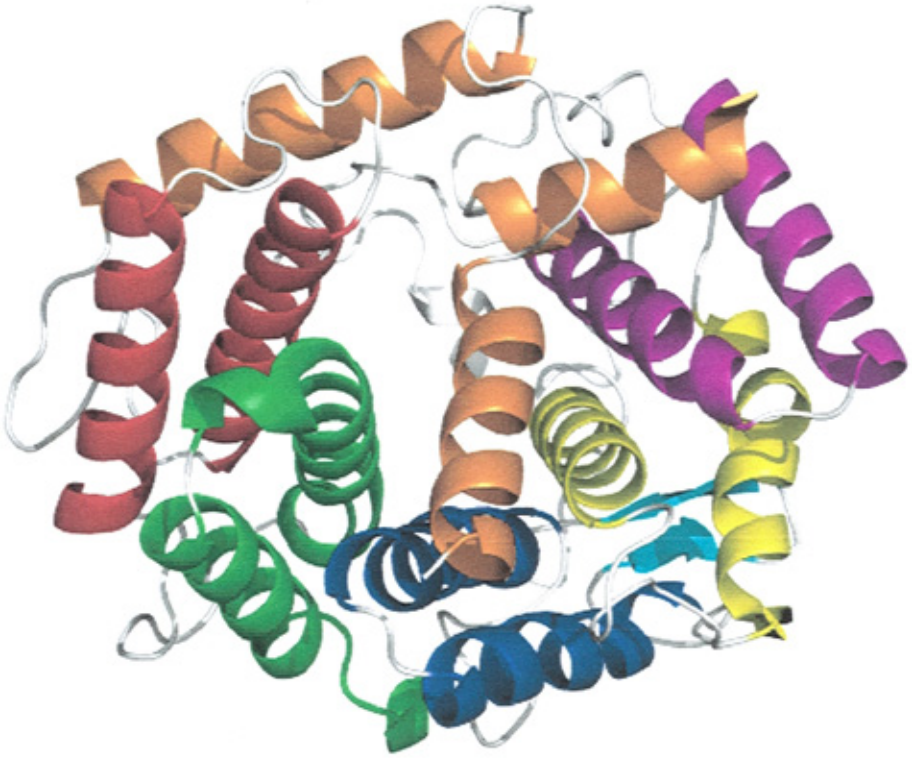

Figure 3.19 A) N-terminal α-helical domain. Five pairs of α -helices [HA3 and HA4 (red), HA5 and HA6 (green), HA7 and HA8 (blue), HA9and HA10 (yellow), and HA11 and HA12 (magenta)] form an incomplete α_5/α_5 barrel structure. The other helices (HA1, HA2 and HA13) are coloured orange.Two short β-strands are coloured cyan. This figure was prepared using the program PyMol (Delano scientific, pymol.sourceforge.net).

B

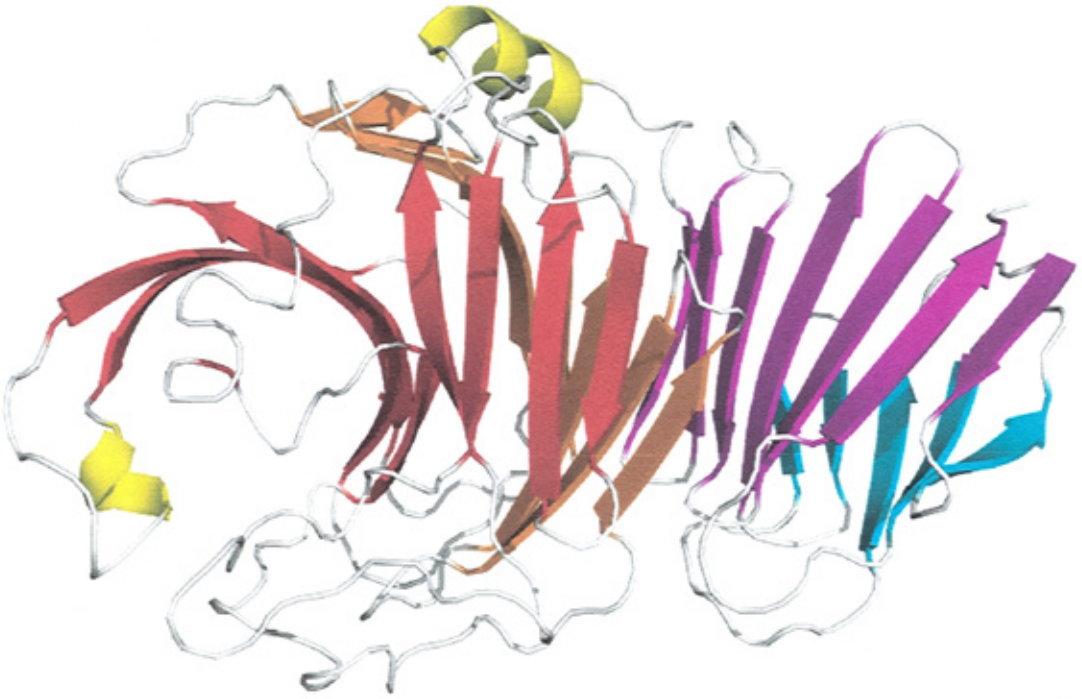

Figure 3.19 B) C-terminal β -sheet domain. The 28 β-strands are arranged in four anti-parallel β–sheets. Sheet 1 (red), sheet 2 (orange), sheet 3 (magenta), and sheet 4 (cyan). Two short α–helices are shown in yellow, and turns and coils are gray. This figure was prepared using the program PyMol (Delano scientific, pymol.sourceforge.net).

3.3.9 Substrate binding and catalysis

The architecture of the catalytic site is formed by the α-domain, the $(\alpha/\alpha)_5$ toroid fold around a groove that encloses the active site. . One feature that is not conserved in this lyase family is the loop before α12, which is bigger than in the other enzymes. This loop functions by closing the non-reducing end of the active site cleft, while not preventing substrate occupation of the -2 subsite. The strictly conserved catalytic residues, that belong mainly to the α-domain, are Asn194, His244, Tyr253, Arg307, Asn432 and Glu429. The latter two residues are the only ones that belong to the β-domain (figures 3.18; 3.20).

In the active site of the N194A complex with HA disaccharide, the electron density in the area of the active site was of sufficient quality to fit a HA disaccharide. Key catalytic site amino acids and the HA disaccharide superimpose with the equivalent residues of *Arthrobacter aurescens* chondroitin AC lyase in complex with tetrasaccharide (PDB code: 1RWF). The disaccharide that can be observed in the *S. coelicolor* hyaluronate lyase is located in the -2 and -1 subsites. A molecule of formic acid is also found in a position close to the C6 O6A O6B of the glucuronic acid moiety, in subsite +1. Most of the residues generally involved in ligand binding are conserved in both enzymes except Gln169, Arg174 and Asn303, that are found only in the *A. aurescens* lyase. Gln169, Arg174 stand on a loop that is longer in *A. aurescens* AC lyase than in the *S. coelicolor* hyaluronate lyase. This loop is situated in-between α7 and α8 of the N-terminal domain. The disaccharide ligand makes contact with Arg311, Tyr253, Trp143, Asn432, and Trp140; all conserved in *S. coelicolor* hyaluronate lyase, *A. aurescens* AC lyase and many other hyaluronate lyases.

Trp141 and 489 provide some stacking interactions in the -1 and +2 subsites in *S. coelicolor* hyaluronate lyase and are conserved in *A. aurescens* AC lyase (Figure 3.20).

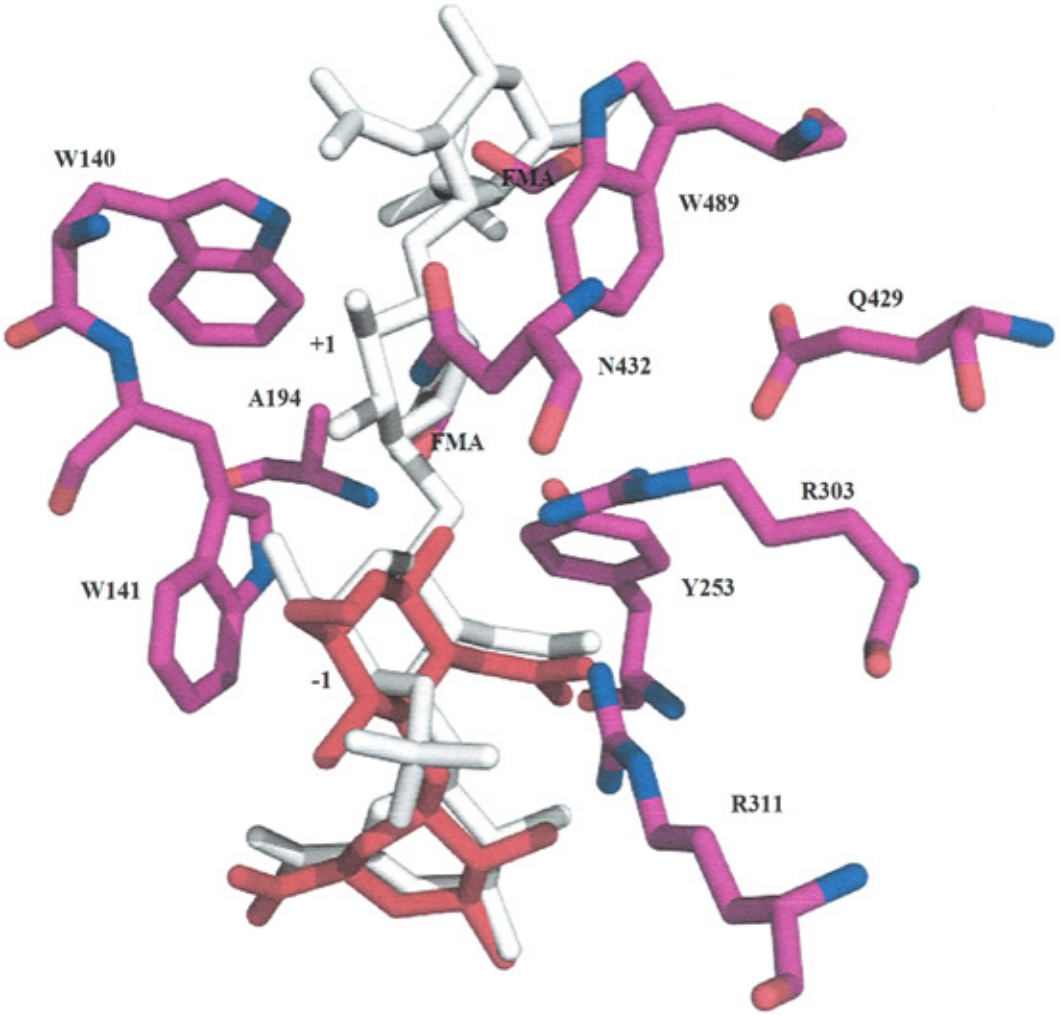

Figure 3.20 Active site of the mutant N194A in complex with HA-disaccharide (red) superimposed with CS-tetrasaccharide (gray). This figure was prepared using the program PyMol (Delano scientific, pymol.sourceforge.net).

Superposition of *S. coelicolor* hyaluronate lyase with the closely related enzymes hyaluronate lyase of *S. pneumoniae* and AC lyase of *A. aurescens* showed that the *S. coelicolor* enzyme superposed onto the two enzymes with a mean root square deviation (RMS) of 2.188Å and 1.128Å, respectively (Figure 3.21). While superposition of *S. coelicolor* hyaluronate lyase with *S. agalactiae* hyaluronate lyase and *P. vulgaris* ABC lyase revealed that the RMS are 3.339 and 8.914, respectively (Figure 3.23A and 3.23B).

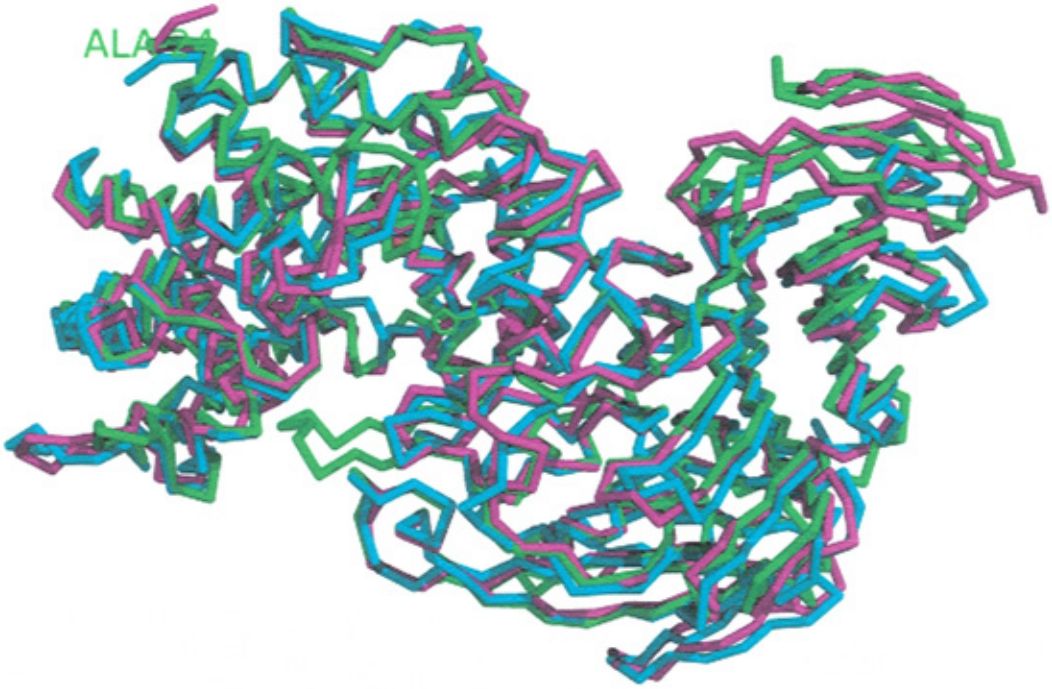

Figure 3.21 Structural alignment of three-dimensional structures of selected lyase enzymes. *S. pneumoniae* (cyan; pdb code:1egu) hyaluronate lyase; *A. auresence* chondroitin AC lyase (magenta; pdb code:1rwh); and *S. coelicolor* hyaluronate lyase (green). This figure was prepared using the program PyMol (Delano scientific, pymol.sourceforge.net).

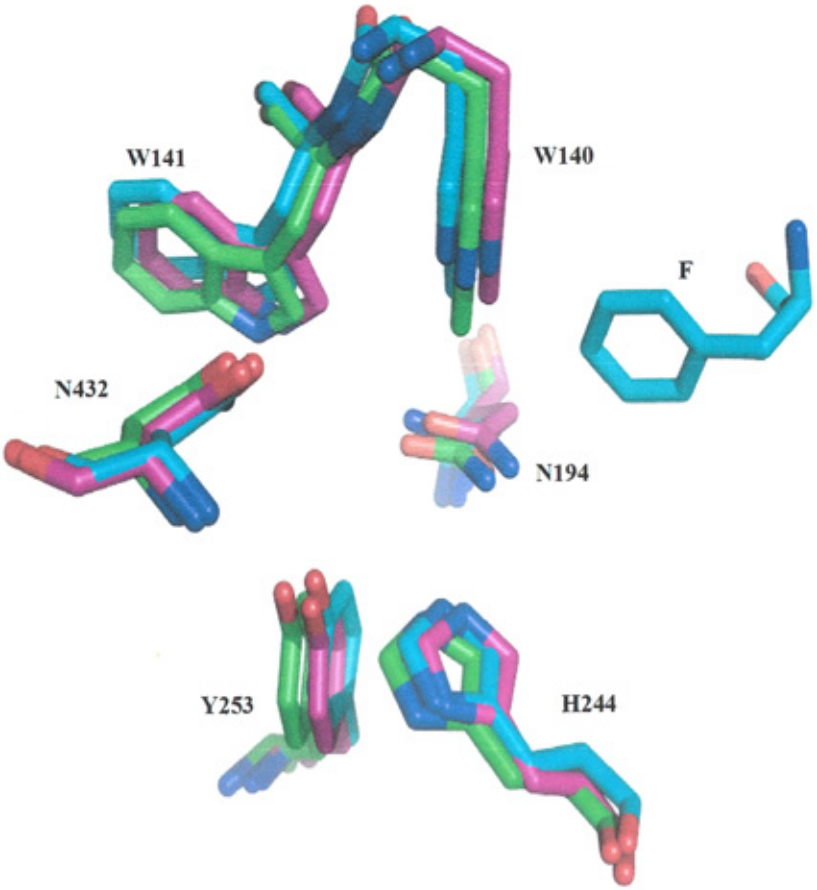

Figure 3.22: Superposition of catalytic site residues. Residues of *S. pneumoniae* lyase (cyan; pdb code:1egu); *S. coelicolor* (green) hyaluronate lyase and *A. auresence* chondroitin AC lyase (magenta; pdb code:1rwh) are shown. Also, the residues responsible for the formation of the hydrophobic patch (Trp and Phe) are shown. This figure was prepared using the program PyMol (Delano scientific, pymol.sourceforge.net).

A

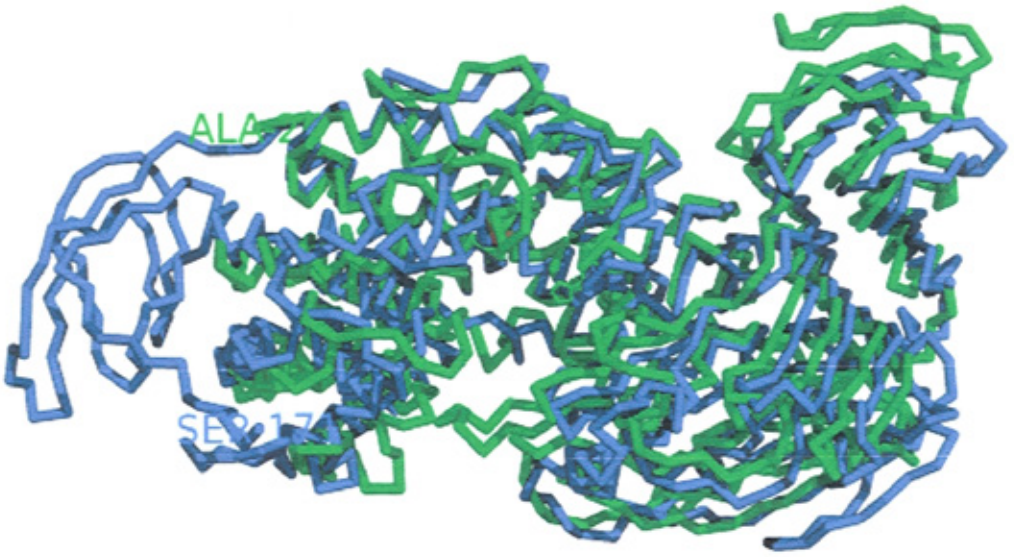

B

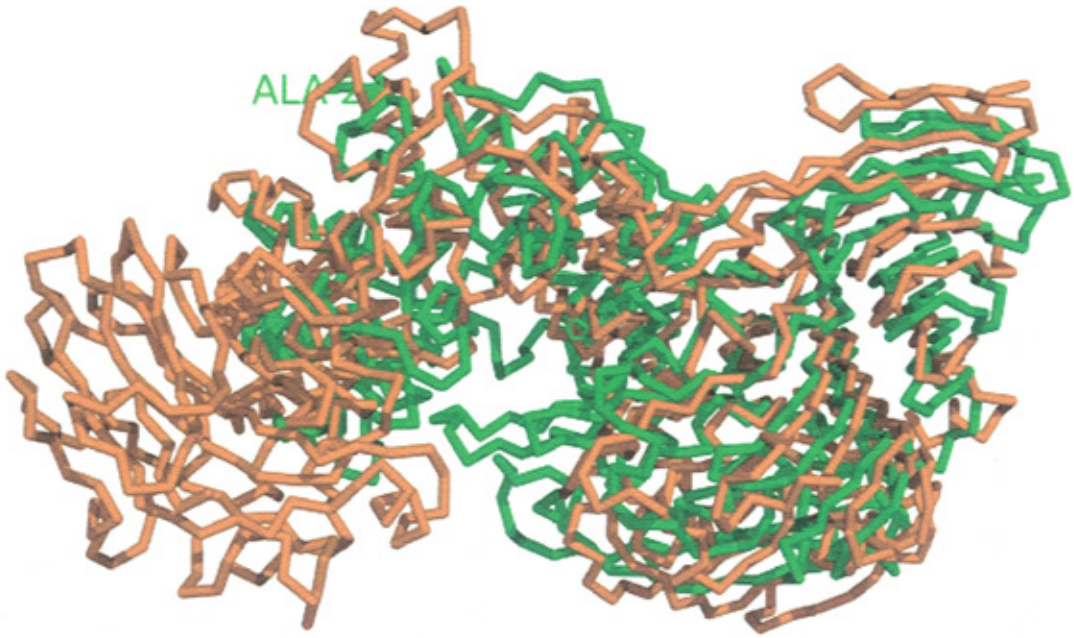

Figure 3.23 Structural alignment of three-dimensional structures of selected lyase enzymes. A) *S. agalactiae* hyaluronate lyase (purple; pdb code:1f1s) and *S. coelicolor* hyaluronate lyase(green). B) *P.* vulgaris ABC lyase (orange; pdb code:1hno); and *S. coelicolor* hyaluronate lyase(green). The figures were prepared using the program PyMol (Delano scientific, pymol.sourceforge.net).

All the crystals of the mutant forms have the same size and shape as those of the wild-type enzyme except for the mutant Y253A (Figure 3.17). The crystals of enzymes with chondroitin-4-sulphate disaccharide and Vcpal complexes diffracted at higher resolutions than the wild-type enzyme crystal. They diffraction were determined at resolutions of 2.3 Å and 2.6 Å, respectively. The X-ray data collection and refinement are summarized in Table (3.2).

The protein structures of all of the complexes are similar to one another and also to the structure of the wild type. The structures of all complexes are analogous in their orientation and position in the cleft of the enzyme. These complexes are bound within the cleft in the N-terminal domain of the enzyme facing the interface between the α- and β-domains demonstrating that the active center (substrate-binding site) is found in the cleft. Chondroitin-4 sulphates bind in exactly the same way as the HA (3.25).

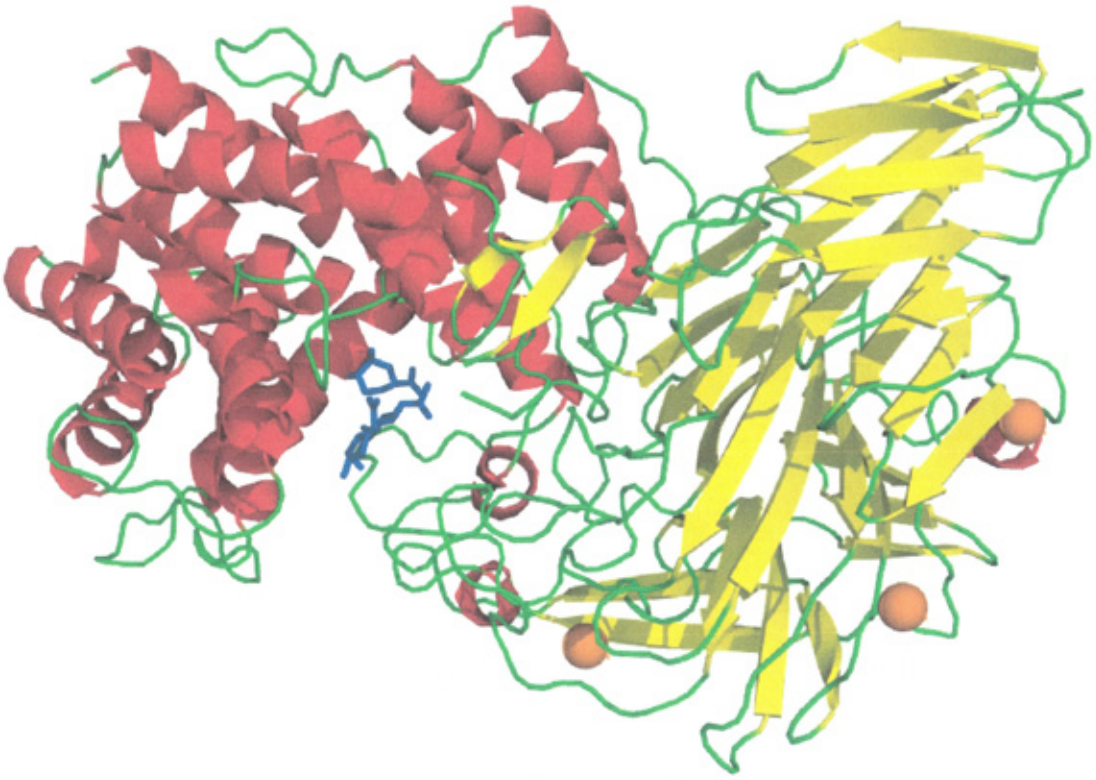

Figure 3.24 3D structure of a mutant (Y253A) complex of SC1C2.15. Red, α-helical domain; yellow, β-sheet domain; green, loops and turns; blue, substrate; orange, calcium ions. This figure was prepared using the program PyMol (Delano scientific, pymol.sourceforge.net).

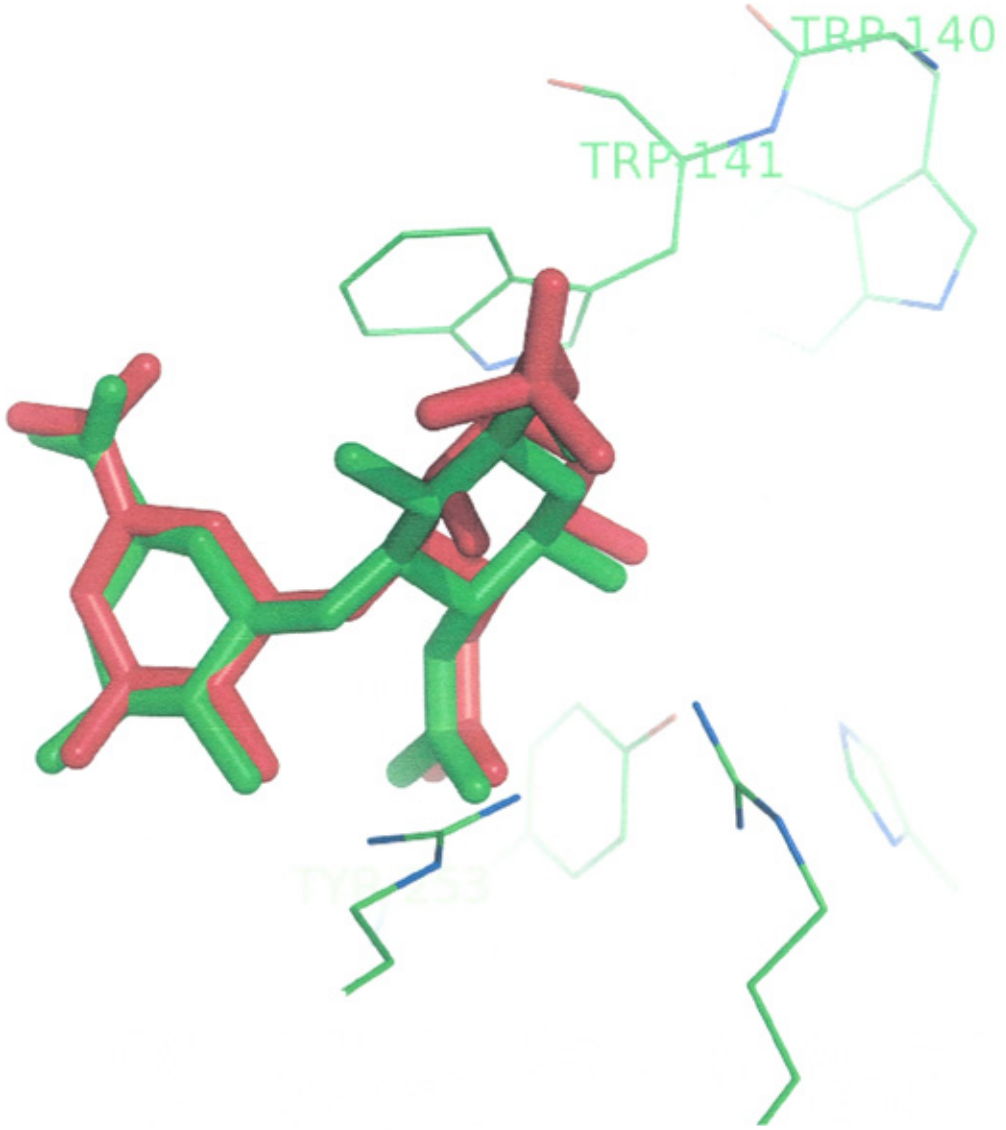

Figure 3.25 comparison of HA-disaccharide (green) and chondroitin-4-sulphate disaccaride (red) interacting with the enzymatic residues of *S. coelicolor*. Enzymatic residues are presented in standard colours corresponding to atom type (red, oxygen; blue, nitrogen; green, carbon). This figure was prepared using the program PyMol (Delano scientific, pymol.sourceforge.net).

The substrates make connections with residues Asn194, His244, Tyr253, Trp140, Trp141, Arg149, Arg307, Arg311 and Asn432. Asn194 makes hydrogen bonds with the carboxyl group of the glucuronic moiety and one salt link with the oxygen atom of the glycosidic bond. Tyr253 is also hydrogen bonded to the β-1,4-linkage oxygen. The side chain of Trp141 interacts through a hydrophobic interaction with the *N*-acetyl-β-D-glucosamine group of the HA2 disaccharide of the substrate, whereas Trp140 interacts via a hydrogen bonding with the *N*-acetyl-β-D-glucosamine group of HA1 (Figures 3.26 and 3.27).

The nitrogen atom of Arg311 forms hydrogen bonds to hydroxyl groups of the glucosyl unit and N-acetyl-β-D-glucosamine, whereas the NH2 of Arg307 is hydrogen bonded only to the hydroxyl group of N-acetyl-β-D- glucosamine (Figure 3.26).

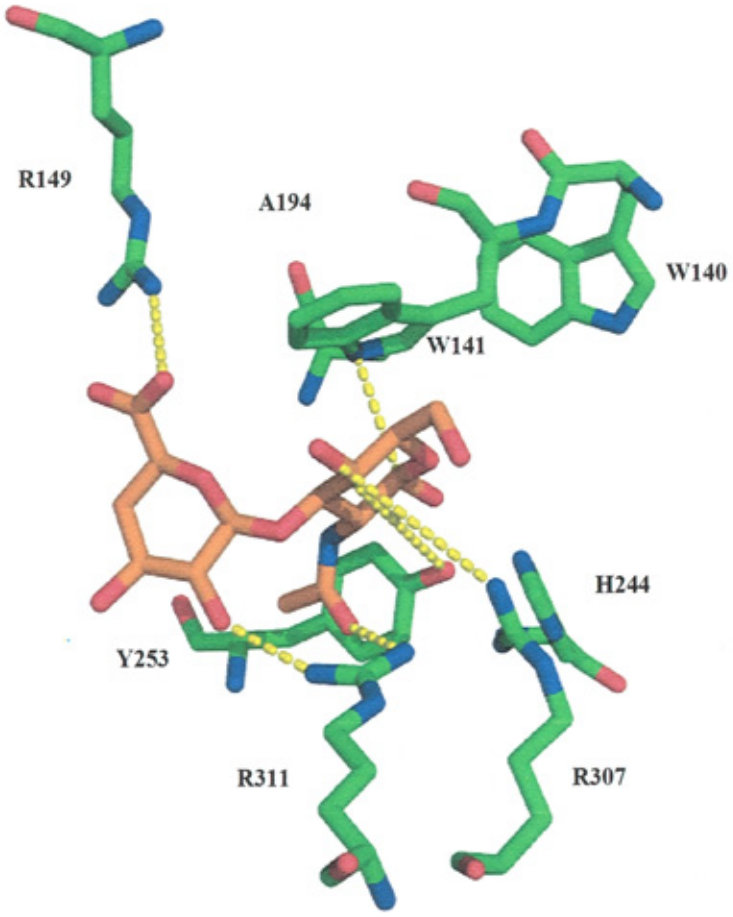

Figure 3.26 Active site of *S. coelicolor* hyaluronate lyase with HA disaccharide. Hydrogen bonds (yellow) between substrate (orange) and active site residues (presented in standard colours corresponding to atom type: red, oxygen; blue, nitrogen; green, carbon) are illustrated in dashed style. This figure was prepared using the program PyMol (Delano scientific, pymol.sourceforge.net).

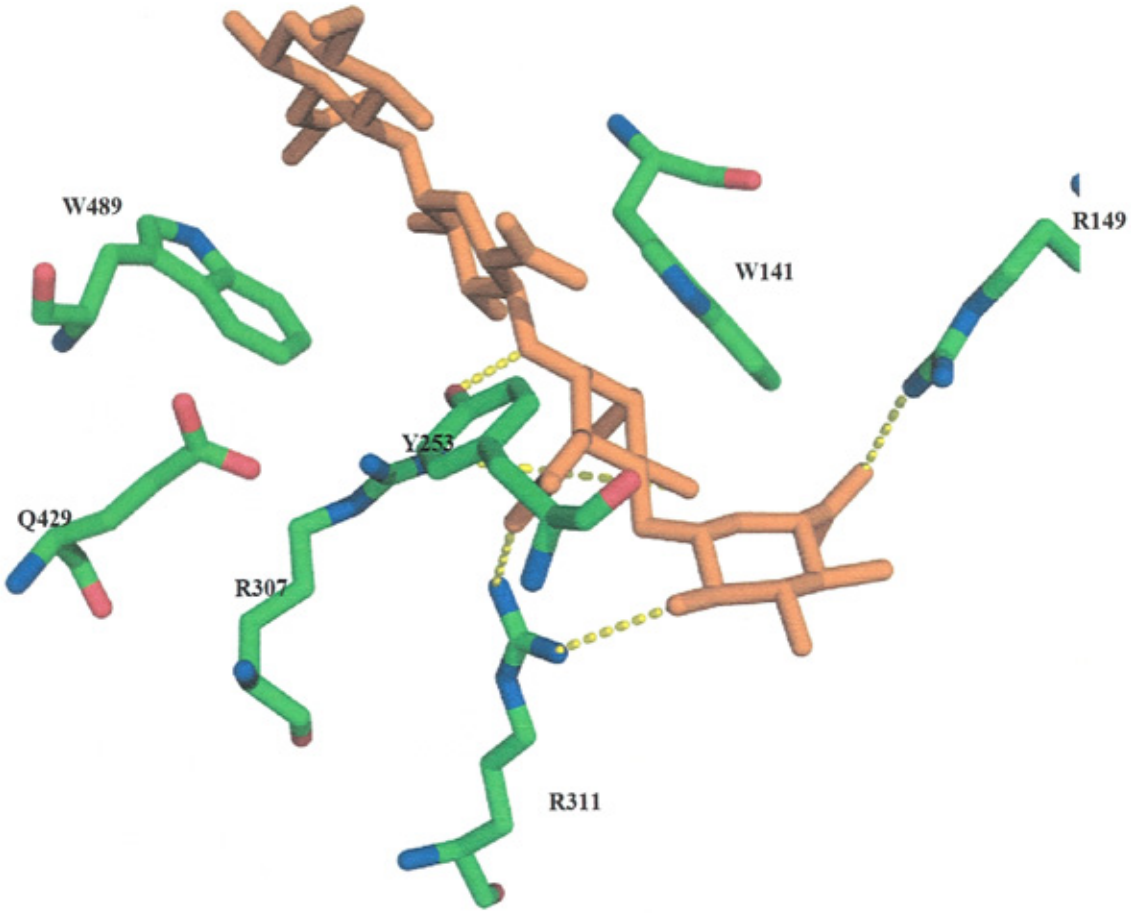

Figure 3.27 Active site of *S. coelicolor* hyaluronate lyase with HA tetrasaccharide. HA tetrasaccharide substrate (orange) and its relative position in the active center. Hydrogen bonds are shown as yellow dots.This figure was prepared using the program PyMol (Delano scientific, pymol.sourceforge.net).

The structure of the wild type enzyme in complex with chondroitin-4-sulphate disaccharide illustrates that introduction of the sulphate group at the 4-position of the N-acetyl-D-galactosamine ring results in no significant change in either the substrate binding mode, as compared to the HA disaccharide or in the protein structure (Figure 3.25). The 4-O-sulpho groups of the substrate form several interactions with protein residues. NH1 of Arg93, NH2 of Arg149 and NH1 of Arg311 form hydrogen bonds with O-6B, O-6A and O2 of the glucuronic acid moiety, respectively (Figure 3.28).

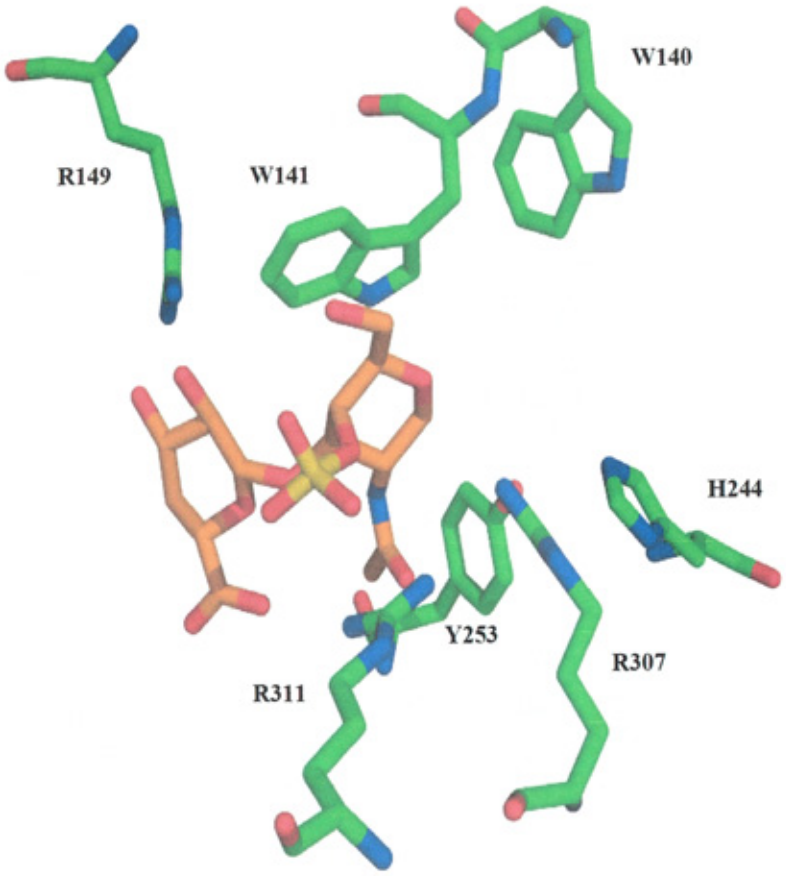

Figure 3.28 Active site of the *S. coelicolor* hyaluronate lyase with chondroitin-4-sulphate disaccharide (orange) and its relative position in the active site. This figure was prepared using the program PyMol (Delano scientific, pymol.sourceforge.net).

As shown in Figure 3.29 there are only two hydrogen bonds that connect the inhibitor with catalytic residues, one between the side chain hydroxyl of Tyr253 and the carboxyl group of the inhibitor. The other bond occurs between the hydroxy group at C5 and Asn194. While the majority of interaction between the enzyme and the inhibitor are hydrophobic which formed with Trp140 and His244.

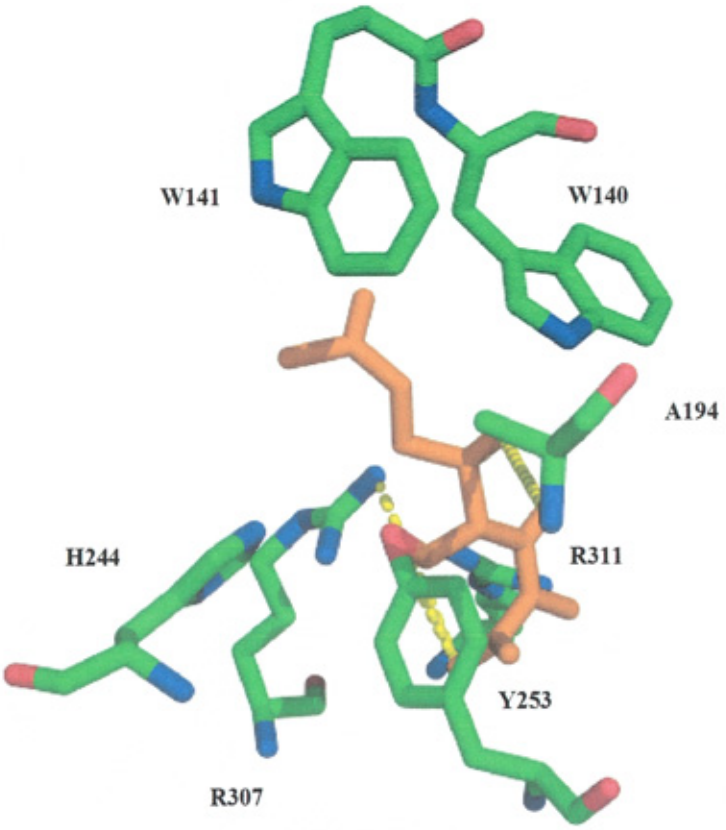

Figure 3.29 The binding site with L-ascorbic acid-6-hexadecanoate (Vcpal). The relative position of Vcpal (orange) to the active center residues. Hydrogen bonds are shown as dotted lines; Vcpal (orange). This figure was prepared using the program PyMol (Delano scientific, pymol.sourceforge.net).

3.3.10 Cloning, expression and purification of α- and β- domains

The genes encoding the α- and β- domains were amplified by PCR from recombinant plasmid pET-28a harbouring the *sc1c2.15* gene. Different pairs of primers were used to generate two PCR products for each domain: one pair with a *Nde*I site at the 5' end of the forward primer and a *Bam*HI site and stop codon at the 5' end of the reverse primer (named Stop) (section 2.2.2.1.2.2); and another pair with a *Nde*I site at the 5' end of the forward primer and a *Xho*I site at the 5' end of the reverse primer (named No stop). The PCR products (Figure 3.30A) of ~1103 bp were A tailed (section 2.2.2.1.11). The A-tailed product was then ligated into the pGEM-T® Easy vector (section 2.2.2.1.12) and transformed into *E. coli* TOP10 (section 2.2.1.4) with very high transformation efficiency. One white colony containing a putative recombinant plasmid was picked from each agar plate (Stop and No stop for each domain) and incubated overnight for the subsequent purification of plasmid DNA (section 2.2.2.1.7.2). pStop and pNostop for each domain were then cut with the restriction enzyme *EcoR*I to confirm the presence of an insert (Figure 3.30B). Once inserts had been identified, pStop and pNostop were digested with *Nde*I to identify the orientation of the fragment within the vector. Also pStop and pNostop for each domain were digested with *Bam*HI and *Xho*I respectively to check linearity. An aliquot (5 μg) of pNostop and pStop of both domains was then digested sequentially with *Xho*I or *BamH*I followed by *Nde*I (Figure 3.30C), with 0.25 μg of DNA run on a gel after completion of the first digestion to confirm that the recombinant molecule was linear. After the second digestion, the insert from each plasmid for both domains was purified by gel purification (section 2.2.2.1.8). The purified inserts were then ligated into the appropriate pET vectors, which had been pre-digested with the appropriate restriction enzymes (section 2.2.2.1.4).

The ligations were then transformed into *E. coli* TOP10 (section 2.2.1.4). A transformed colony from each new pET construct was then grown overnight and plasmid DNA was prepared from the culture (section 2.2.2.1.7.2). Prepared pAlpha and pBeta domain were then digested with the appropriate restriction enzymes to confirm the presence of the insert, then each construct was transformed into *E. coli* BL21 (DE3) (section 2.2.1.4). All constructs were expressed in insoluble form in BL21 (DE3) as judged by SDS-PAGE.

Unfortunately, all attempts proved unsuccessful to derive soluble products by altering expression conditions (temperature, induction time, IPTG concentration), using different types of expression vectors for *E. coli* such as pET-32c (which has thioredoxin reductase) or using different strains of *E. coli* such as Tuner, Rosseta PlysS and Orgami B (DE3). Therefore, the insoluble proteins were denatured and refolded (section 2.2.3.7) in order to obtain soluble truncated proteins.

For expression and purification, transformed BL21 (DE3) colonies containing the constructs were grown overnight as 5 ml starter cultures and used to inoculate 2 x 500 ml of LB. The cultures were then incubated overnight at 20 °C after induction as described in section 2.2.1.2.3. Cells were harvested by centrifugation and then resuspended in starting buffer (section 2.1.4.3.6.1). The suspensions were sonicated to disrupt the cells and then centrifuged for 40 min at 4°C at 24,000 x g. The cell free extracts were discarded and the pellet for each domain was re-suspended in the starting buffer containing 8 M urea to denature the protein. The proteins were purified under denaturing conditions by IMAC using a chelating sepharose column and an automated gradient elution technique (section 2.2.3.4). An aliquot (20 µl) of

each fraction was analysed by SDS-PAGE (sections 2.2.3.1; 2.2.3.1.1; Figure 3.31 and 3.32) to check purity. Fractions containing the protein were dialysed against 50 mM Tris- HCl buffer, pH 8, containing a decreasing concentration of urea as described in section 2.1.9.3 and 2.2.3.7. Dialysis of the α-domain against different concentrations of urea was successful, but the β-protein was aggregated upon dialysis in low concentrations of urea. Many trials were attempted to refold the β-protein, but these met with little success.

After concentration the α-protein (section 2.2.3.8) was tested against different dialysed substrates (section 2.1.9.2). It was found that the α-protein was active toward all substrates for only a few minutes and then degraded and lost its activity. Different strategies for preventing the degradation of the α-protein were tried. These included using different pHs, adding different cations, and high concentrations of BSA; nevertheless no improvement in enzyme stability was achieved.

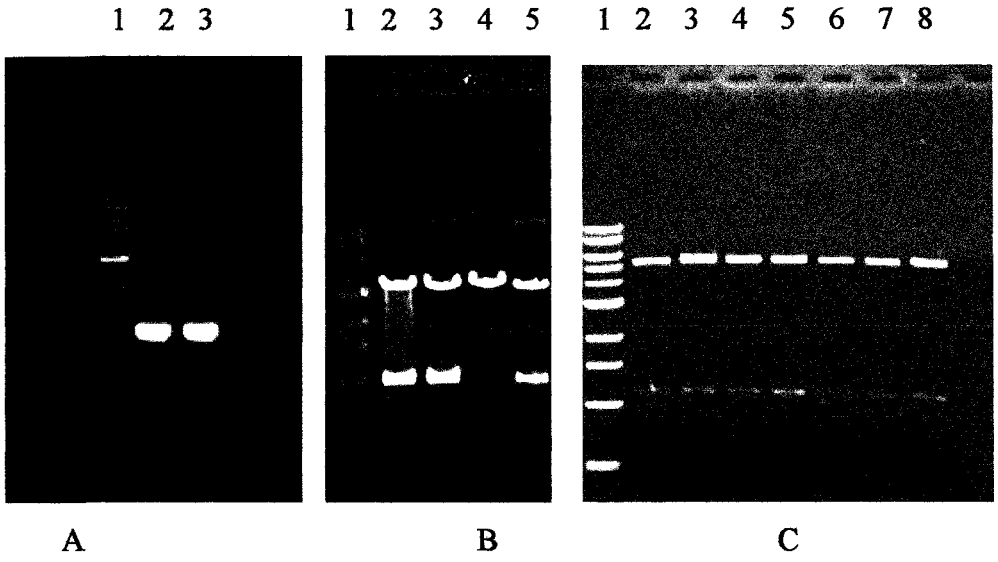

Figure 3.30: Visualisation of DNA bands following agarose gel electrophoresis.
A) DNA products generated during a typical PCR reaction. Lane 1: 1 kb DNA ladder (10, 8, 6, 5, 4, 3, 2, 1.5, 1, 0.5 kb); Lane 2: alpha subunit stop gene (1.113 kb); Lane 3: beta subunit stop gene (1.113 kb).
B) DNA fragments generated during a restriction endonuclease digest. Lane 1: 1 kb DNA ladder (10, 8, 6, 5, 4, 3, 2, 1.5, 1, 0.5 kb); Lane 2 and 3: alpha subunit digested with *Eco*RI; Lane 5: beta subunit digested with *Eco*RI.
C) DNA fragments generated during a restriction endonuclease digest (section 2.2.2.1.4). Lane 1: 1 kb DNA ladder (10, 8, 6, 5, 4, 3, 2, 1.5, 1, 0.5 Kb); Lane 2: alpha subunit stop gene restricted with *Nde*I and *Bam*HI; Lane 3: alpha subunit no stop gene restricted with *Nde*I and *Xho*I; Lane 4: beta subunit stop gene restricted with *Nde*I and Bam I; Lane 5: beta subunit no stop gene restricted with *Nde*I and *Xho* I. All DNA samples were subjected to 1 % agarose gel electrophoresis at 100 mA and 200 V for 45 min. Subsequently, gels were immersed in 10 μg ml^{-1} solution of ethidium bromide for 10 min then washed with distilled water and placed on a UV illuminator and a fluorescent image was taken (section 2.2.2.1.6).

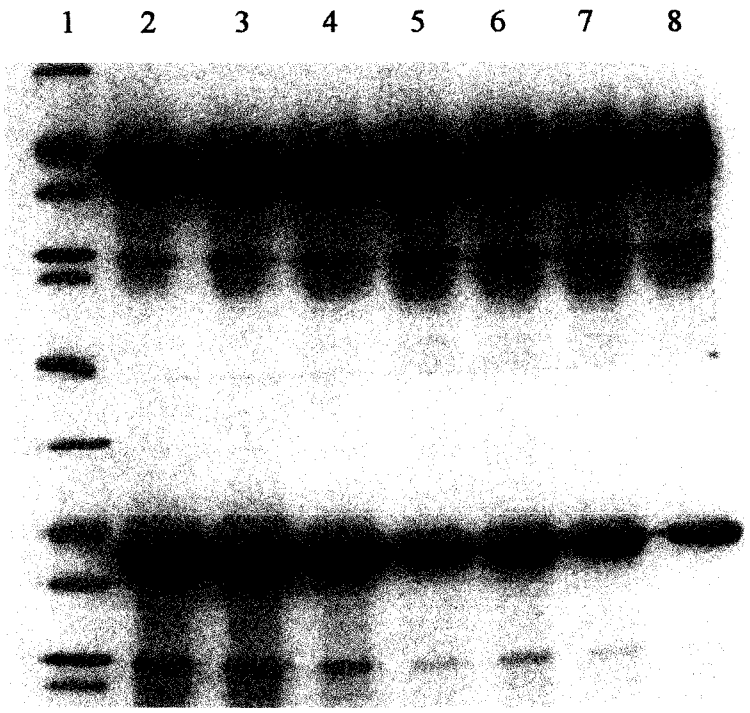

Figure 3.31: 12% SDS-PAGE of α- subunit protein of *S. coelicolor.* Purified from *E. coli* cells by IMAC under denaturing conditions (insoluble protein was denatured in 8 M urea). Lane 1: Low molecular weight (LMW) markers (66, 45, 36, 29, 24 and 20 kDa); Lane 2, 3, 4, 5, 6, 7 and 8 20 µl of protein (fractions 1-14 are shown). Proteins were visualised by staining with coomassie blue and destained (section 2.2.3.1.1).

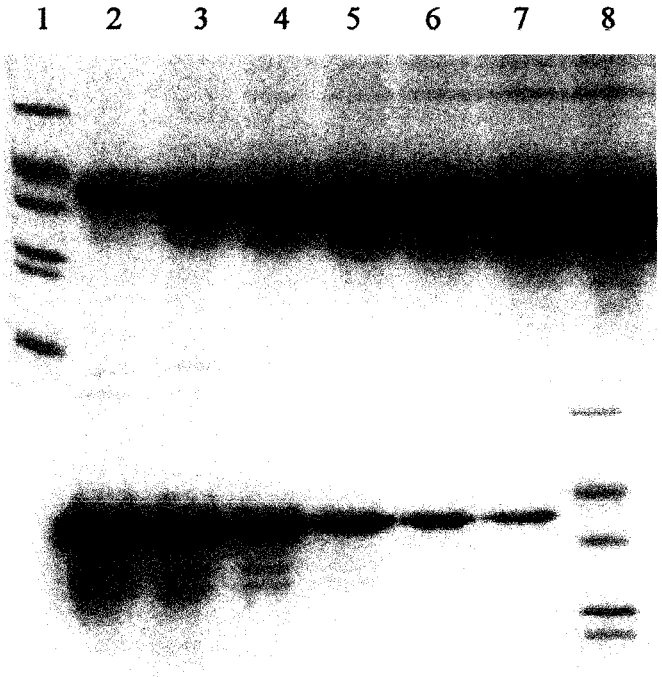

Figure 3.32: 12% SDS-PAGE of β subunit protein of *S. coelicolor*. Purified from *E. coli* cells by IMAC under denaturing conditions (insoluble protein was denatured in 8 M urea). Lane 1: Low molecular weight (LMW) markers (66, 45, 36, 29, 24 and 20 kDa); Lane 2 to 13; 20 µl of protein (fractions 1-13 are shown). Proteins were visualised by staining with Coomassie blue and destained (section 2.2.3.1.1).

Chapter 4 Discussion: biochemical characterisation and x-ray crystallographic studies of a *Streptomyces coelicolor* A3(2) hyaluronate lyase

4.1 Introduction

The aim of the work undertaken in this chapter was to biochemical characterise the putative hyaluronate lyase of *Streptomyces coelicolor* A3(2). The biochemical characterization was achieved through the measurement of the formation of a double bond at 232 nm using a spectrophotometer (Appendix V, figure VA). The mode of action of this enzyme was determined by HPAEC. In addition, the 3D structures of the native enzyme and its mutant forms in complex with different substrates were determined.

4.1.1 Glycosaminglycan lyases

Various microorganisms secrete GAG lyases, which are enzymes that degrade GAGs. Soil bacteria use these lyases to degrade connective tissues of dead animals, and then use the products as a source of carbon from their natural environments (Ernst *et al.*, 1995; Sutherland, 1995). Most of these enzymes are apparently non-specific, acting on different GAGs with different affinities. These enzymes have gained increased attention due to their importance in characterising the proteoglycans and GAGs that are essential in the regulation of different cellular activities (Hong *et al.*, 2002).

These enzymes (section 1.3.2.2.2; 1.3.2.2.3) act through a β-elimination mechanism producing unsaturated disaccharides (Menzel and Farr, 1998; Hynes and Walton, 2000; Li *et al.*, 2000; Jedrezejas and Li, 2002). This mechanism involves the elimination of a

C5 proton from the uronic acid residue, followed by the exclusion of a C4-linked hexosamine resulting in the production of a Δ4,5-unsaturated uronic acid residue at the non-reducing end of the oligosaccharide or polysaccharide product (Baker *et al.*, 2002).

Hyaluronate lyases constitute a special group of polysaccharide degrading enzymes that are capable of breaking down the long chains of alternating units of N-acetyl glucosamine and D-glucuronic acid present in HA, the main component of animal connective tissues (Li *et al.*, 2000; Jedrezejas and Li, 2002; Akhtar and Bhakuni, 2003). Also some hyaluronate lyases can cleave the alternating units of N-acetyl-D-galactosamine and D-glucuronic acid of chondroitin sulphate (Baker *et al.*, 1997; Baker and Pritchard, 2000; Baker *et al.*, 2002).

4.2 Discussion

4.2.1 Biochemical characterization of SC1C2.15

Successful cloning and expression of ORF *sc1c2.15* of *Streptomyces coelicolor* A3(2) has shown that this protein has hyaluronate lyase activity. This is the first time that SC1C2.15 has been cloned, expressed, characterized and crystallised using both the native enzyme and its mutants with different substrates.

S. coelicolor hyaluronate lyase has the ability to degrade HA, chondroitin 4 and 6-sulphate, but exhibits no activity against heparin, heparan sulphate and dermatan sulphate. This specificity is similar to some hyaluronate lyases of *S. pneumoniae, S. agalactiae* and *Peptostrecoccus* sp. which have the capability to degrade HA, chondroitin 4 and 6-sulphate, although the latter two are degraded at comparatively slower rates compared to HA (Tam and Chan, 1985; Baker *et al.*, 1997; Baker and Pritchard, 2000). It has been suggested that these enzymes degrade chondoritin 4-sulphate chains only at unsulphated regions (Pritchard *et al.*, 1994; Baker *et al.*, 1997;

Baker and Pritchard, 2000, Pritchard *et al.*, 2000). This is because Phe423 in *S. agalactiae* and its equivalent in *S. pneumoniae* is in steric conflict with this sulphate group of the substrate, and consequently cannot degrade sulphated units of chondroitin-4-sulphate (Li and Jedrzejas, 2001). For this reason, these enzymes have less affinity toward chondroitin sulphate. It is likely that the absence of this residue in *S. coelicolor* hyaluronate lyase results in the observed activity of this enzyme on chondroitin-4-sulphate, in contrast to the other hylauronate lyases.

The kinetic parameters of SC1C2.15 showed that this enzyme has different kinetics with different substrates. The enzyme displayed higher values of k_{cat} and more affinity against sodium hyaluronate than other substrates. The values of K_m and k_{cat} against sodium hyaluronate, potassium hyaluronate, chondroitin-4-sulphate and chondroitin-6-sulphate were 0.17 ± 0.002, 0.3 ± 0.023, 0.48 ± 0.07 and 0.55 ± 0.05 mg ml^{-1} and 55.6, 25.1 ± 2.31, 21.8 ± 1.73, and 2.4 ± 0.24 s^{-1}, respectively. In the presence of calcium the values of K_m for sodium hyaluronate, chondroitin-4-sulphate and chondroitin-6-sulphate were 0.08 ± 0.006, 0.28 ± 0.05, and 0.33 ± 0.04 mg ml^{-1}, respectively. Values of k_{cat} were 166.7 ± 1.12, 46.3 ± 8.02 and 6.9 ± 0.28 s^{-1}, respectively. Addition of the calcium thus increased k_{cat} about three fold, while reducing the K_m two fold. Consequently the catalytic efficiency (as k_{cat} / K_m) of the SC1C2.15 enzyme increased significantly. Michel and his colleagues have documented that calcium may have a role in substrate binding and catalysis, probably via the stabilisation of the negative charge on the C5 carboxylate moiety (Michel *et al.*, 2004).

In contrast to the previously described hyaluronate lyases obtained from *S. agalactiae* (Pritchard *et al.*, 1994; Baker *et al.*, 1997; Baker and Pritchard, 2000, Pritchard *et al.*, 2000) and *Peptosreptococcus* sp. (Tam and Chan, 1985), which all showed very low

activity against chondroitin-4-sulphate, *S. coelicolor* hyaluronate lyase displayed more activity against chondroitin–4-sulphate. When the activity of SC1C2.15 for HA was taken as 100%, the values of activity of the enzyme for chondroitin-4-sulphate and chondroitin-6-sulphate were 40 % and 10 %, respectively.

The enzyme displayed a lower K_m and higher k_{cat} against sodium hyaluronate from streptococcal fermentation, as compared to umbilical cord potassium hyaluronate. This preference for sodium hyaluronate may be attributed to the difference in molecular weight between these two substrates as the molecular weight of HA varies from 10^5 to10^7 Da (Tammi et al., 2002; Kakehi *et al.*, 2003), or due to the presence of large impurities such as other forms of GAGs. It has been demonstrated that the purified HA oligosaccharides prepared from human umbilical cord contained significant amounts of CS (Mahoney *et al.*, 2001).

In comparison, the values of K_m and V_{max} of *S. dysgalactiae* hyaluronate lyase varied with different molecular weight HA substrates; values of K_m decreased and those of V_{max} increased with the increasing molecular weight of HA (Hamai *et al.*, 1989). Moreover Cramer and his colleagues found that the K_m of testicular hyaluronidase also decreased with an increase in the size of hyaluronan (Cramer *et al.*, 1994). Indeed, this characteristic has also been found in *Bacteriodes stercoris* heparinase, which is an enzyme that is unrelated in sequence and specificity to *S. coelicolor* hyaluronate lyase and which displayed very high activity toward heparan sulphate from bovine intestine, whereas it exhibits little activity toward the same substrate from porcine intestine (Kim *et al.*, 2000).

The K_m values of *S. pneumoniae, S. agalactia* and *Peptostreptococcus* sp. hyaluronate lyases are 0.12 ± 0.02 (Kelly *et al.*, 2001), 0.0817 (Ozegowski *et al.*, 1994) and 0.14 mg ml^{-1} (Tam and Chan, 1985), respectively. These K_m values are similar to that of *S.*

coelicolor (0.08 ± 0.006 mg ml^{-1}). On the other hand, the turnover number of *S. coelicolor* hyaluronate lyase is considerably less than that of other hyaluronate lyases, such as those from group B streptococcus.

The activity of some polysaccharide lyases shows an absolute requirement for calcium. This is true of the pectate lyases of *Erwinia chrysanthemi* (Tardy *et al.*, 1997) and *P. cellulosa* (Brown *et al.*, 2001), and the chondroitinase B of *F. heparinium* (Michel *et al.*, 2004) and *S. pneumoniae* (Jedrzejas *et al.*, 1998; Ponnuraj and Jedrzejas, 2000; Kelley *et al.*, 2001; Li *et al.*, 2001). However, this study has demonstrated that SC1C2.15 does not absolutely require calcium for its activity. However, increasing the calcium concentration resulted in a considerable increase in the activity of the enzyme, with a maximal activity at 2 - 4 mM (Figure 3.13).

The optimum pH of SC1C2.15 is slightly different for HA (5.2) and chondroitin-4 and 6-sulphate (4.8). This phenomenon has also been seen in other enzymes such as with the hyaluronate lyase of *Peptostreptococcus* sp. (Tam and Chan, 1985) and ABC lyase of *P. vulgaris* (Yamagata *et al.*, 1968, Thurston et al., 1975). *Peptostreptococcus* sp. exhibited an optimum pH of 7.2 against hyaluronan, 7.6 against chondroitin-4-sulphate and 8 against chondroitin-6-sulphate. Similarly, ABC lyase displays different optimum pHs against HA, chondroitin and chondroitin sulphate of 6.2, 6.8 and 8, respectively (Yamagata *et al.*, 1968, Thurston *et al.*, 1975). It is currently unclear why these enzymes exhibit different optimum pHs with different substrates. Interestingly the *S. coelicolor* hyaluronate lyase exhibited an acidic optimum pH almost similar to the hyaluronidases of human serum and placenta, which have an optimum pH range of 3.4 - 4.5 (Csoka *et al.*, 1997).

Gorham and his colleagues reported that the optimum pH of testicular hyaluronidase is decreased in the presence of NaCl, and Joy and co-workers documented that the optimum pH of pig liver hyaluronidase against potassium hyaluronate decreases with an increasing concentration of NaCl (Gorham *et al.*, 1975; Joy *et al.*, 1985). Conversely, in this study the optimum pH of *S. coelicolor* hyaluronate lyase is the same irrespective of the presence or absence of 0.2 M NaCl. On the other hand, it has been found that the optimum pH of urinary hyaluronidase increases in the presence of NaCl, from 3.4 in the absence of NaCl to 3.8 in its presence (Csoka *et al.*, 1997).

It has been found that the addition of NaCl is important to a number of enzymes for stability and sometimes for activity. These include the hyaluronidase of Indian copra (Girish et al., 2004), testicular hyaluronidase (Gorham *et al.*, 1975), urinary hyaluronidase (Csoka *et al.*, 1997), the hyaluronate lyase of *S. coelicolor* (this study), alginate lyase of *Pseudomonas aeruginosa* (Linker and Evans, 1984) and the ABC I lyase of *P. vulgaris* (Prabhakar *et al.*, 2005a; Prabhakar *et al.*, 2005b).

An interesting observation is the importance of the presence of NaCl in the buffer system for the stability of *S. coelicolor* hyaluronate lyase. Therefore, NaCl was added to all assay buffers at a final concentration of 40 mM. This result is in agreement with those of Linker and Evans, (1984), who found that the alginate lyase of *Pseudomonas aeruginosa* was stable only at high concentrations of NaCl, while it degraded most efficiently in low concentrations of NaCl. Also, it is in clear agreement with the findings of the investigation by Gorham and co-workers that testicular hyaluronidase is stable and highly active in the presence of NaCl and to those of Girish *et al.*, who reported that the activity of Indian copra hyaluronidase is more active in the presence of 0.15 M NaCl (Gorham *et al.*, 1975; Linker and Evans, 1984; Girish *et al.*, 2004).

Moreover, it was found that the presence of NaCl is very important for the activity of ABC I lyase of *P. vulgaris*, especially with DS which showed only 5 % of activity in the absence of any salt, while for chondroitin-6-sulphate as substrate the enzyme was active even in the absence of NaCl. The reason for this, as suggested by Prabhakar and colleagues, is that the salt is important for DS in eliminating non-specific interactions of this substrate with the enzyme. This is because DS has significant intrinsic flexibility as a result of the presence of iduronic acid in its structure. Consequently it can exhibit a broad range of possible interactions than can chondroitin-6-sulphate, and may perhaps bind to the positively charged patch present on the surface of the enzyme, rather than that in the active site (Prabhakar *et al.*, 2005b).

It is difficult to explain why a soil bacterium such as *S. coelicolor*, which is unlikely to be exposed to temperatures higher than 20 °C in nature, produces enzyme display optimum catalytic activity at a temperature of 57 °C (Figure 3.17). Indeed, many enzymes produced by soil bacteria display high temperature optima between 40-75 °C. These include the AC lyase of *A. auresence* (Hiyama and Okada, 1975), the hyaluronate lyase of *S. hyaluronolyticus* (Ohya and Kaneko, 1970), and the pectate lyase of *P. cellulosa* (Brown *et al.*, 2001) and *Bacillus* sp. (Bellamy, 1990; Ernst *et al.*, 1995). These enzymes showed optimum temperatures of 40 °C, 60 °C, 62 °C and 75 °C, respectively.

The activity of SC1C2.15 after pre-incubation for 20 min at temperatures ranging from 27 °C to 77 °C illustrate that the maximum activity was displayed at 27 °C indicating that the enzyme is not very thermostable. However, the enzyme lost about 18 % of its activity compared to its activity when tested at 37 °C without pre-incubation. Pre-incubating the enzyme at temperatures higher than 37° C results in a significant reduction of activity and it becomes virtually inactive at 57 °C and 67 °C.

To determine the effects of divalent ions at 2 mM, different divalent ions were tested against SC1C2.15 activity. A concentration of 2 mM was chosen to ensure that any increase in activity could be detected. Also, because the effect of calcium concentration upon SC1C2.15 reached a maximum at 2 mM, the same concentration for all divalent cations was therefore selected. Although *S. coelicolor* hyaluronate lyase was active without adding any divalent cations, its activity nevertheless increased in the presence of calcium. This ion perhaps increases the affinity of the enzyme for its substrate, and it appears that this enzyme is able to utilize a broad range of divalent ions, working optimally with Ca^{2+} followed by Mn^{2+} and Ba^{2+}. A major issue that arises from this study is whether divalent ions interact with the enzyme or with the substrate. It is possible that these ions complex with the substrate, thus increasing its enzymatic susceptibility.

4.2.2 Mode of action of SC1C2.15

Several techniques are used to differentiate between the mode of action of enzymes such as thin layer chromatography, high performance liquid chromatography and reversed-phase ion-pair chromatography (Cramer and Bailey, 1991). In this project, high performance anion exchange chromatography was used to explore the mode of action of the enzymes.

The size of the products of different enzymes of PL 8 show some differences. Some only produce disaccharides whilst others produce a wide range of oligosaccharides. The *S. coelicolor* hyaluronate lyase exhibited an exolytic mode of action as it produced only disaccharides as the end product. Similar studies of the *S. pneumoniae* hyaluronate lyase (Jedrzejas *et al.*, 1998a, b; Jedrzejas, 2000; Li *et al.*, 2000; Kelly *et al.*, 2001; Nukui *et al.*, 2003) and that of *S. agalactiae* (Pritchard *et al.*, 1994; Pritchard *et al.*,

2000) have shown that the mode of action of both bacterial lyases is also exolytic with the end products being disaccharides. Moreover, the hyaluronate lyase of *S. dysgalactiae* (Hamai *et al.*, 1989) and *Peptostreptococcus* sps (Tam and Chan, 1985) also produce disaccharides as the main end product. This pattern of degradation has been found in other enzymes of this family, such as the AC lyase of *A. aurescens* (Hyiama and Okada, 1976; Lunin *et al.*, 2004) and the xanthan lyase of *Bacillus* sp. (Hashimoto *et al.*, 2001; Hashimoto *et al.*, 2003). However, this is different from the pattern shown by the non-pathogenic bacteria *S. hyalurolyticus* (Park *et al.*, 1997; Price *et al.*, 1997; Maccari *et al.*, 2004) and testicular hyaluronidase (Cramer *et al.*, 1994; Oettl *et al.*, 2003), which produce tetrasaccharides and hexasaccharides as their final product.

On the other hand, the partial digestion of chondroitin-4-sulphate with the SC1C2.15 enzyme resulted in the presence of several oligosaccharides with very different characteristics. This may indicate that the enzyme cleaves chains randomly and then the presence of sulphate groups probably interferes with its processive movement along the chain due to the conflict between these groups and residues Trp141 and Asn194. Pritchard and his collaborators reported that polyacrylamide gel electrophoresis analysis of chondroitin sulphate digested with group B hyaluronate lyases indicated the presence of a series of oligosaccharide products (Pritchard *et al.*, 1994). A suggestion which has been put forward is that group B hyaluronate lyases cleave only non-sulphated disaccharide regions (Pritchard *et al.*, 1994; Baker *et al.*, 1997; Baker and Pritchard, 2000; Pritchard *et al.*, 2000) as a result of sulphate groups preventing the interaction of the carboxylate group with Asn349 (of *S. pneumoniae*), so that the C5 proton cannot be acidic (Baker *et al.*, 1997). Therefore, the endolytic cleavage will predominate until the whole molecule is degraded (Rigden *et al.*, 2003; Akhtar and Bhakun, 2004).

It has been emphasised that the mode of action of exolytic enzymes is processive, in which the enzyme makes a random cut and then progresses through the length of the hyaluronan chain, cleaving off disaccharide fragments as it passes (Pritchard *et al.*, 1994). However, the incapability of hyaluronate lyases to processively cleave the CS chain is almost certainly due to the presence of sulphate groups. Consequently, the processive cleavage of CS by hyaluronate lyases is not possible.

4.2.3 Difference in overall structure between the wild type enzyme and its mutant (Y253A)

The structure of Y253A mutant shows a significant difference with the wild type. The superposition of Y253A onto wild type shows a root mean square deviation of 2.07Å for 742 equivalent C^{α} atoms. The superimposition shows that the β-domain superimpose perfectly with the one in wild type but the top of the α-domain is rotated of around 40° around an axis that would go along the bottom of the groove in-between the two domains, so that the helices at the top of the α-domain are moving a lot and the helices at the bottom of the α-domain namely α13, α12 and α11, don't move. The movement of the helices (α1 to α10) lead to the opening of the groove, and as a consequence the catalytic residues are moving away from the ligand binding site.

In the Y253A mutant the shape of the binding site change drastically. In this mutant the Tyr253 has been mutated into an Ala. Tyr253 is known to be involved in crucial contacts with the substrate. The hydroxyl group of Tyr253 makes a hydrogen bond with the bridging oxygen between the +1 and -1 sugars. This hydroxyl group is also within H-bonding distance with other atoms (O5 of the +1 sugar, C5 of the glucuronic acid). This mutation produces an extreme change in the shape of the binding site. The groove formed by the α-domain gets wider, and the residues involved in the ligand binding as

well as the catalysis are moving away from their original position. Only the key residues standing at the bottom of the groove and the ones coming from the β-domain don't move. Trp140, Trp141 are moving of about 7Å away and Asn194 is moving away of about 5 Å (Figure 4.1).

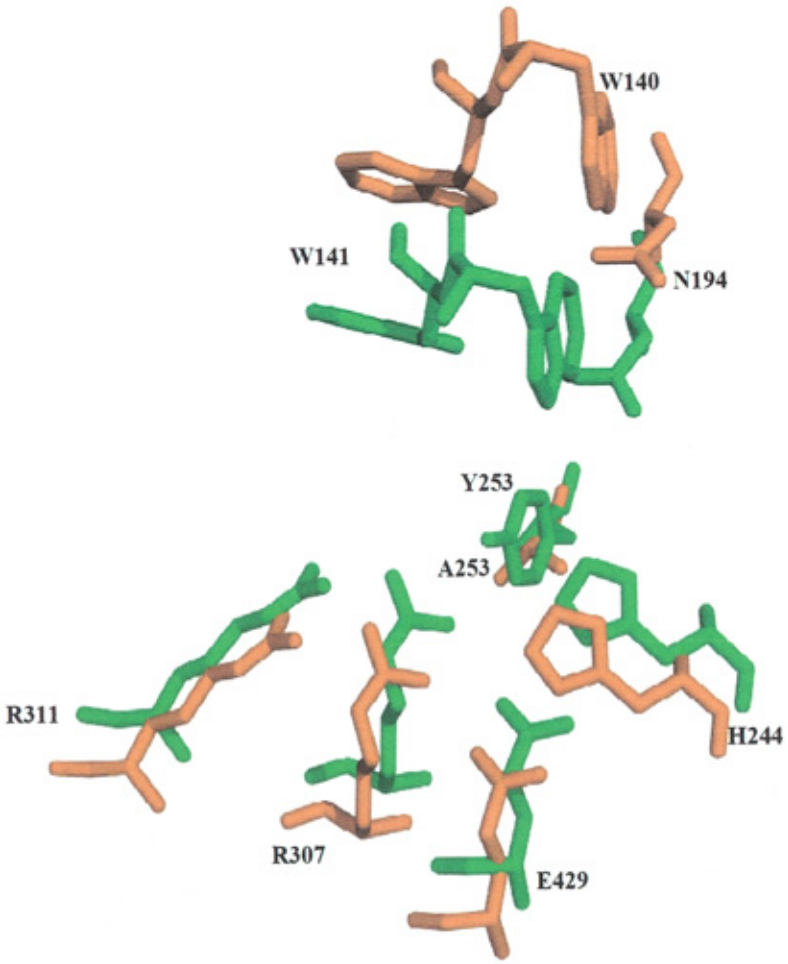

Figure 4.1 alignment of the active centre residues of the wild type (green) and mutant Y253A (orange). This figure was prepared using the program PyMol (Delano scientific, pymol.sourceforge.net).

4.2.4 Structural comparison of polysaccharide lyases

The 3D structures of polysaccharide lyases from families 1-10 and 16 have been determined. The α/α -barrel structure which is found in families 5 and 8, is also found in enzymes from glycoside hydrolase families that are completely unrelated in sequence, such as the endoglucanases of family 8 of glycoside hydrolase, which exhibit an $(\alpha/\alpha)_6$ barrel comprising six inner and six outer α-helices (Alzari *et al.*, 1996).

The structure of SC1C2.15 was solved at a resolution of 2.7 Å. A comparison of the structure of *S. coelicolor* hyaluronate lyase with the known structures of PL 8 lyases shows that the structures are quite similar but there are some differences. The overall structures consist of a catalytic α-helical domain at the N-terminus and a β-sheet domain at the C-terminus (Figure 3.18). The architecture of the active site and its immediate surroundings are conserved between these proteins and, based on sequence homology, are likely to be common to all PL 8 enzymes. Nevertheless, some structural differences were detected between *S. coelicolor* hyaluronate lyase, the ABC lyase of *P. vulgaris* and *S. agalactiae* hyaluronate lyase (Figures 3.23A and 3.23 B). Both of the latter enzymes have a small N-terminal β-domain prior to the α-helical domain (Li and Jedrzejas, 2001; Huang *et al.*, 2003). Also the cleft of both enzymes is considerably wider than in the *S. coelicolor* hyaluronate lyase. Comparison between ABC lyase and the hyaluronate lyase of *S. coelicolor* highlights another difference which is that the chondroitin ABC lyase has 15 α-helices (Huang *et al.*, 2003), whilst the hyaluronate lyase of *S. coelicolor* has only13.

In addition, the C-terminal β-sheet domain of the hyaluronate lyase of *S. coelicolor* is slightly smaller than that of xanthan lyase which is composed of 30 strands (Hashimoto *et al.*, 2003).

A comparison of the structure of the *S. coelicolor* hyaluronate lyase with the *F. heparinium* AC lyase reveals that in the case of the *S. coelicolor* enzyme there are two

insertions in the α-domain; residues 43-58 (α2); 363-386 (α13+loop) and residues 313-322 close a great region of the cleft resulting in a deep cavity (Figure 4.2). This deep cavity enables the enzyme to bind only two or three units of polymeric substrate, which is consistent with its exolytic mode of action. On the contrary this region is missing from the AC lyase of *F. heparinium*, which makes its active-site cleft more open, and therefore it can bind to the middle of an extended polysaccharide chains. This observation is consistent with the observed endolytic mode of action for this enzyme (Figure 4.2).

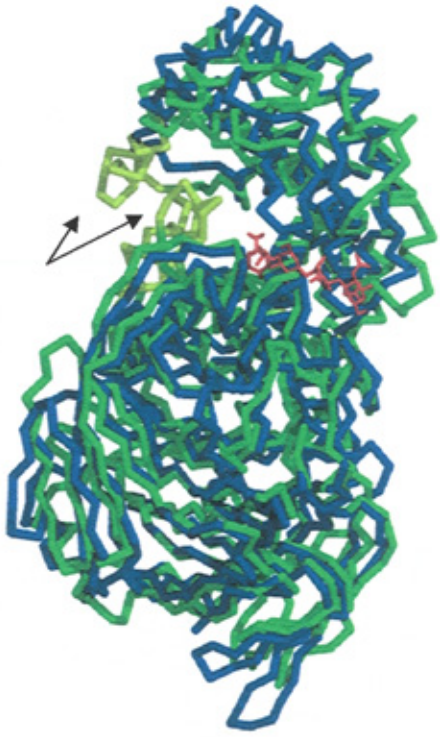

Figure 4.2 Comparison between the structure of *S. coelicolor* hyaluronate lyase (green) and *F. heparinium* AC lyase (blue). The two insertions (lime) are shown by arrows; the substrate (red) is shown in stick. This figure was prepared using the program PyMol (Delano scientific, pymol.sourceforge.net).

Superposition of the *S. coelicolor* hyaluronate lyase with the closely related hyaluronate lyase of *S. pneumoniae* and AC lyase of *A. aurescens* showed that the *S. coelicolor* enzyme superposed onto the two enzymes with a mean root square deviation (RMS) of 2.188Å and 1.128Å respectively. They have two domains, the N-terminal domain that contains 13 α-helices for each lyase. The other domain is the β-sheet domain at the C-terminus. However, superpositions of these enzymes showed small differences between them which mainly occur in the β–strands. Both the *S. coelicolor* hyaluronate lyase and the *A. aurescens* AC lyase have four β-sheets in the β-domain with 28 and 30 strands respectively. Whereas the β- domain of *S. pneumoniae* hyaluronate lyase has five β-sheets arranged in 24 strands. Strand 5 (S5) and S6 of β-sheet 4, and S4 of β-sheet 5 of the SC1C2.15 molecule (residues Gly727 - Ala 732; His758-The763; Val736-Ala740, respectively) are more extended than those in the *S. pneumoniae* enzyme. A dissimilarity was also found due to an insertion of 10 residues that is located in the loop before α-H12 which are more extended in the SC1C2.15 molecule than that in the *S. pneumoniae* hyaluronate lyase and the *A. aurescens* AC lyase. Also, the three enzymes are similar with respect to the arrangement of the active site residues (Figure 3.22).

Within the α-domain of the *S. coelicolor* enzyme there is a cleft region where the substrate binds and is cleaved, that is positively charged. Since the substrate is negatively charged, the charge complementarities between the substrate and cleft facilitate substrate binding. All the positive residues in the cleft of *S. coelicolor* enzyme are arginines, except one which is a lysine. This is unlike other hyaluronate lyases which are composed of about equal numbers of arginines and lysines. The presence of these positive residues in the cleft holds the substrate chain in position during catalysis (Li *et al.*, 2000; Li and Jedrzejas, 2001). This characteristic is common to all characterized family 8 polysaccharide lyases which degrade acidic polysaccharides.

In addition, it has been suggested that part of the interaction between the substrate and the enzyme is due to the match between the aromatic patch in the enzyme cleft and the hydrophobic patch in the substrate molecule (Li *et al.*, 2000; Li and Jedrzejas, 2001; Nuku *et al.*, 2003).

Sequence comparison of the *S. coelicolor* hyaluronate lyase with other hyaluronate lyases of PL 8 shows that only 19 residues are conserved in the *S. coelicolor* lyase along the cleft out of the 25 residues that are conserved among all other hyaluronate lyases of this family. The majority of these residues are located along the middle narrow part of the cleft.

There was no conformational change between the protein structures with and without substrate. The substrate, either HA or chondroitin-4-sulphate, was bound in the cleft located on the N-terminal domain of the enzyme in front of the interface between the N- and C-terminal domains (Figure. 3.24; 3.25), revealing that the active centre (substrate-binding site) is found in the cleft.

Three groups of residues are accumulated on one site of the cleft. These include the catalytic group Asn194, His244 and Tyr253, the hydrophobic patch Trp140, Trp141 and the negative patch Thr245, Asp233, Thr230 and Glu429 (Figure. 3.18). It was suggested that the function of hydrophobic patch is to select the cleavage site on the substrate chain and place it precisely for catalysis and cleavage by the catalytic residues (Li *et al.*, 2000; Kelly *et al.*, 2001; Jedrzejas *et al.*, 2002; Nukui *et al.*, 2003). Also, the suggestion has been made that the hydrophobic residues are essential for the determination of the size of the product (Jedrzejas, 2000; Nukui *et al.*, 2003).

Superposition of the catalytic domain of the *S. coelicolor* enzyme with the related *S. pneumoniae* and *A. aurescense* catalytic domains illustrates the presence of residues

Asn194, His244 and Tyr253 of the *S. coelicolor* enzyme in positions equivalent to the proposed catalytic residues Asn349, His399 and Try408 of the *S. pneumoniae* enzyme, and to Asn183, His233 and Tyr244 of the *A. aurescens* enzyme (Figure 3.22). Also that the aromatic patch of the *S. pneumoniae* enzyme comprises Trp291, Trp292 and Phe343, but the latter residue is absent from both the *S. coelicolor* and the *A. aurescens* enzymes (Figure 3.22). It has been suggested that the presence of phenylalanine (one of the aromatic patch residues) in the *S. pneumoniae* and the *S. agalactiae* hyaluronate lyases makes them act exolytically, producing only disaccharides. While the absence of this residue in some enzymes of PL 8 make them act endolytically, producing mixtures of oligosaccharides of different sizes (Li and Jedrzejas, 2001). However, despite the absence of this residue in the *S. coelicolor* and *A. aurescens* enzymes, the mode of action is exolytic. On the other hand, this residue is present in the *S. pyogenes* hyaluronate lyase which acts endolytically. Therefore, its presence or absence seems unlikely to contribute to the mode of action as has been proposed.

X-ray crystallographic analysis of the wild type enzyme showed that the hydroxyl group of Tyr253 interacts in the active cleft with the oxygen atom of the glycosidic bond of the substrate involved in the creation of the double bond. Removing the Tyr253 side chain affects the conformation of this loop and results that the active cleft becomes more open. This is consistent with the biochemical data showing that the substitution of alanine at this position abolishes the activity of the enzyme completely. The finding of this study illustrates that Tyr253 is important for the catalytic reaction of *S. coelicolor* enzyme. This is in agreement with many structural studies that have been reported on the importance of this catalytic residue for the xanthan, chondroitin AC and hyaluronate lyases of *S. pneumoniae* and *S. agalactiae* (Jedrzejas, 2000; Li *et al.*, 2000; Ponnuraj and Jedrzejas, 2000; Huang *et al.*, 2001; Li *et al.*, 2001; Capila *et al.*, 2002; Jedrzejas *et al.*, 2002; Li and Jedrzejas, 2002; Hashimoto *et al.*, 2003).

Asn194 directly interacts with the carboxylate group of the glucuronate unit of HA1. This interaction permits Asn194 to attract the charge of the carboxyl group of HA1 away from the C-5 of glucuronate. Therefore, substituting the Asn194 and His244 with alanine would result in loss of these interactions and causes the *S. coelicolor* hyaluronate lyase to be inactive. These findings suggest that these residues are centrally involved in the β-elimination mechanism of the hyaluronate lyase of *S. coelicolor*. These three residues are conserved in all PL 8 lyases except for Asn194, which is replaced by Arg in the cases of chondroitin AC of *F. heparinium* and ABC lyases of *P. vulgaris*.

Comparably, the Asn349 and His399 residues of the hyaluronate lyase from *S. pneumoniae* have been proven to contribute to the catalytic reaction, because it has been found that the substitution of these two amino acids by alanine in *S. pneumoniae* (Li *et al.*, 2000; Kelly *et al.*, 2001; Jedrzejas *et al.*, 2002; Nuku *et al.*, 2003) and its equivalent in *S. agalacitiae* (Li and Jedrezajas, 2001; Mello *et al.*, 2002), strongly decreases the activity of the enzyme to about 6 % and 12 %, respectively.

In the same way, it has been shown that the Asn194, His246, and Tyr255 residues of the xanthan lyase (Hashimoto *et al.*, 2003) and the His225 and Tyr234 residues of the *F. heparinium* AC lyase (Huang *et al.*, 2001), which are equivalent to the Asp349, His399 and Tyr408 residues of the *S. pneumoniae* hyaluronate lyase, are critical for the catalytic mechanism in these enzymes as well (Li *et al.*, 2000; Jedrzejas *et al.*, 2002; Li and Jedrzejas, 2001; Hashimoto *et al.*, 2003).

As shown in Figure 3.29, Vpal binds inside the catalytic site of the enzyme in the same way as the substrate. Figure 3.29 shows that the greater part of the interactions between

the enzyme and the inhibitor are hydrophobic. The exceptions are the interaction between Tyr253 and the inhibitor which occurs via the hydrogen bond between the hydroxyl group of Tyr253 and the carboxylic group of the inhibitor, and that between the hydroxyl group at C5 and Asn194.

Many possible mechanisms have been postulated for the action of PL 8. The nature of the amino acid residue that is responsible for neutralizing the charge of the carboxylic group of glucuronic acid is still a point of controversy among researchers. Li *et al.* in 2000 suggested that His399 of the *S. pneumoniae* enzyme, and its equivalent in other lyases of PL 8, acts as a general base abstracting a proton from the C-5 carbon of the glucuronic acid. On the other hand, it has been proposed that a tyrosine residue performs both functions, firstly acting as a general base and then as a general acid (Huang *et al.*, 2001). Likewise, in alginate lyases which are structurally homologous to family 8 lyases, it was found that Tyr246 plays a vital role in the abstraction and donation of a proton during catalysis (Yoon *et al.*, 2001). Moreover, Lunin *et al.* (2004) suggested that His233 is unlikely to perform the abstraction of a proton, and therefore the Tyr residue functions as a general base, whereas the neutralization of the charge on the glucuronate acidic group is achieved by Asn183 and His233.

From the enzyme complexes with their various substrates in this study, the closeness of Tyr253 to the glycosidic oxygen of the substrate at the site of cleavage demonstrates that this residue is well placed to play role in protonating the leaving group as suggested by Li *et al.* (2000) and Li and Jedrzejas (2001). Also, His244 is located 3.2 Å from the substrate suitably positioned to serve as the general base, and the proximity of Asn194 to the uronic acid C-5 proton confirms its possible function in the stabilisation of the carbanion intermediate formed during catalysis.

In this study, each domain has been amplified and cloned separately in order to identify their roles. However, the hyperexpression of the α and β domains in soluble form unfortunately failed, because neither protein would fold correctly when expressed in pET-22b or -28a in *E. coli* BL21 as the expression host. The conditions were also varied to include different temperatures with and without induction. The molecules were also cloned into pET 32c and hyperexpressed in *E. coli* Origami (DE3) and plysS variant of this host, but the proteins were still insoluble. Therefore, both proteins were purified after being denatured and refolded by dialysis at 4 °C. When the activity of the α-domain was tested against HA and chondroitin-4 and 6-sulphate at 232nm, it was found that the activity against the different substrates persisted only for few minutes and then the increase of absorbance stopped, possibly as a result of the absence of the β-domain. This suggests that the N-terminal α-domain requires the C-terminal β-domain for its stability. At the same time the presence of small amounts of activity, representing approximately 10% of activity compared with the wild type enzyme, reveals that the N-terminal α-domain is the functional domain of *S. coelicolor* hyaluronate lyase. On the other hand, the failure to refold the β-domain makes it impossible to characterise this domain. However, no amino acid residues from this domain were found to be directly involved in catalysis from the structural studies. Therefore, one possibility that could be proposed for the function of the β C-terminal is that this domain might have a role in holding the substrate chain during glycosidic bond cleavage. It has been suggested that the β-sheet might modulate the access of substrate to the catalytic cleft of the α-domain (Li *et al.*, 2000; Jedrzejas, 2000; Li and Jedrzejas, 2001; Nukui *et al.*, 2003). Therefore, the role played by the β-domain in substrate degradation is still not fully understood, and definitive answers to questions regarding its role in PL 8 demand additional studies.

4.3 Summary

To recapitulate the main points arising from this work, the study of SC1C2.15 from the soil bacterium *Streptomyces coelicolor* A3(2) has demonstrated that this ORF codes for hyaluronate lyase that was active against HA and chondroitin-4 and 6-sulphate. Characterisation of the N-terminal tagged *S. coelicolor* hyaluronate lyase demonstrated that this enzyme displayed an optimum pH of 5.2 against HA and 4.8 against chondroitin-4 and 6-sulphate with an optimum temperature at 57 °C. Moreover, analysis of the digestion of HA and chondroitin-4-sulphate by HPAEC revealed that the enzyme exhibits an exolytic mode of action with HA, producing exclusively disaccharide products. However, with chondroitin sulphate, several larger and highly variable oligosaccharides were produced as a result of the presence of sulphate groups in the substrate which prevent the enzyme from cleaving the substrate processively. The three-dimensional structure of the *S. coelicolor* hyaluronate lyase was determined and it has a similar topology to other PL 8 lyases. It is comprises of two domains. The α-helix domain at the N-terminal and the β-sheet domain at the C-terminal are connected via a short peptide linker and there is a deep cleft in the N-terminal domain facing the interface between the N- and C-terminal domains. The cleft contains four different groups, which are the catalytic group, aromatic group, positive patch and negative patch. Based on the crystal structure of the enzyme complexes with different ligands the deep cleft in the enzyme was revealed to be responsible for the recognition of the substrate and the catalytic reaction. Aromatic and positively charged amino acid residues in the active cleft directly interact with the carboxyl group of the polymeric substrate through the formation of hydrogen bonds. In this thesis, it has been shown that Tyr253, His244 and Asn194 are important residues for catalysis, as mutations of these residues resulted in the abolition of the activity of the enzyme. The crystal structure of a complex of the *S. coelicolor* hyaluronate lyase with the inhibitor L-ascorbic acid-6-hexa

deconate illustrates the interaction of the inhibitor with the amino acids in the active site.

4.4 Future work

Even though SC1C2.15 of *Streptomyces coelicolor* A3(2) has been widely characterised both biochemically and structurally, there is still work to be done. For example, further biochemical characterisation of the wild type with different sizes of oligosaccharides can be achieved. Also, the inhibitory effect of Vcpal on the activity of the wild type enzyme could be investigated. An interesting observation that needs further study is why the *S. coelicolor* hyaluronate lyase is active against chondroitin-4-sulphate to nearly the same extent as that observed for potassium hyaluronate. This is unlike other hyaluronate lyases belonging to the same family which have very little activity toward chondroitin-4-sulphate. Moreover, the development of a successful hyperexpression system enabling the α and β-subunits to be expressed in soluble form would allow further conclusions to be drawn regarding the function and likely interplay of these domains.

Chapter 5 Results: biochemical characterisation of the *Streptococcus pyogenes* SF370 hyaluronate lyase

5.1 Introduction

Streptococci are Gram-positive bacteria classified into six groups (A, B, C, D, E and F) according to the group specific carbohydrate identified serologically on the bacterial cell surface. The group A carbohydrate antigen is composed of N-acetyl-β-D-glucosamine linked to a polymeric rhamnose backbone (Cunningham, 2000). Also, group A streptococcus (GAS, *Streptococcus pyogenes*) can be further subdivided into specific serological types according to the presence of type specific M protein antigens. More than 70 types of different M proteins have been identified, indicating antigenic variation of this family of proteins even though they all share pathogenic features (Hollingshead *et al.*, 1986). *S. pyogenes* strains are commonly classified on the basis of serologic differences in the M protein. The clinically important strains are the β-haemolytic group *S. pyogenes.* As pathogens, group A streptococci have developed complex virulence mechanisms to avoid host defences (Cunningham, 2000; Bisno *et al.*, 2003).

GAS is the main cause of morbidity and mortality throughout the world (Wessels *et al.*, 1991). This is due to its serious effects in humans, so it is considered one of the most important human pathogens. *S. pyogenes* causes several diseases ranging from uncomplicated infections such as pharyngitis,the infection of the mucous membranes lining the pharynx and impetigo which affects exposed areas on children's faces, arms and leg. Also, GAS can cause sever infections, including erysipelas which mainly affects superficial layers of the skin and involves the lymphatics.

Necrotizing fasciitis is a type of wound infection, which is caused by the entry of GAS into the soft tissues through the skin. Patients with Necrotizing fasciitis may develop streptococcal toxic shock syndrom which is caused by streptococcal toxins released by GAS in the blood flow. Acute rheumatic fever and glomerulonephritis may also develop following acute infection caused by GAS (Stevens, 1992; Molinari and Chatwal, 1998; Cunningham, 2000; Fontaine *et al.*, 2003). Acute rheumatic fever arises only after pharyngeal infections. In poor countries, streptococcal infections are a serious health problem due to the weak health care services. Rheumatic fever is the leading case of heart disease among children in poor countries (Bisno, 1991; Bisno, 1993).

5.1.1 Virulence factors of GAS

The distribution of GAGs on the surface of host tissues makes them principal targets for the attachment of pathogens. Therefore pathogenic bacteria have developed mechanisms to interact specifically with these compounds, and this is directly related to the potential virulence of a number of microorganisms (Menozzi *et al.*, 2002).

Several different virulence factors of GAS have been characterised that may play a role in the survival and growth of streptococci in the host or contribute to streptococcal mediated disease (Kehoe, 1991). These include the antiphagocytic HA capsule and the fibrillar M protein located on the cell surface. Moreover, virulence factors also include hyaluronate lyase and streptokinase enzymes, which might contribute to invasive infections. GAS also secrete the membrane damaging toxins streptolysin S and O (Kehoe 1991). *S. pyogenes* can invade the human host via mucosal membranes and skin and then secrete several surface proteins that facilitate its attachment to various host tissue sites (Frick *et al.*, 2003). The major virulence factors are discussed as follows.

5.1.1.1 M protein

It has been reported that M proteins exist on the streptococcal cell surface as extended dimeric fibrillar proteins. The amino terminal protrudes from the cell while the carboxy terminus is associated with the cell wall (Hollingshead *et al.*, 1986; Bison *et al.*, 2003). Numerous studies have established that streptococcal M proteins are members of a large family of bacterial cell wall-associated proteins called M-like proteins (Kehoe, 1991). Among virulence factors, M proteins have received particular interest as they are thought to be vital for streptococcal survival in the human host. This is probably due to the multiple binding properties exhibited to a variety of mammalian proteins like fibrinogen, fibronectin and plasminogen. These interactions are possibly implicated in the capability of streptococci to resist non-immune phagocytosis (Fischetti, 1989; Perez-casal *et al.*, 1993; Eyal *et al.*, 2003). It has also been reported that M proteins are involved in the adherence of streptococci to human tissues, a step that is essential for the initiation of infection (Eyal *et al.*, 2003).

5.1.1.2 Capsule

The capsules of GAS are made up of the polysaccharide HA which is comprises of repeating units of glucuronic acid and N-acetyl glucosamine. It completely surrounds the cell wall of the bacteria (Wessels *et al.*, 1991; Moses *et al.*, 1997; Cunningham, 2000).

Despite the fact that most capsular polysaccharides can induce an immune response, GAS capsular HA is only slightly immunogenic as a result of the structural similarity between these capsules and the HA of host connective tissues (Cunningham, 2000; Bisno *et al.*, 2003). This allows the bacterium to conceal its own antigens and go unrecognised by the host. Therefore the HA capsule is considered one of the main

virulence factors in *S. pyogenes*. Moreover, the HA capsule is involved in the opening of tight junctions in cells, allowing streptococci to invade into deeper tissues (Eyal *et al.*, 2003).

Streptococcal strains differ significantly in their degree of encapsulation and those with large capsules have a mucoid appearance. Also, streptococcal strains that are rich in M proteins and contain a capsule are extremely dangerous to humans (Stollerman, 1996; Wessels *et al.*, 1991). Wessels and his colleagues have demonstrated that loss of the capsule reduces the virulence of the organisms in mice by about 100-fold compared to those microbes with capsules (Wessels *et al.*, 1991).

During invasion, the capsule is an essential determinant of virulence in conjunction with the M protein, conferring antiphagocytic properties upon the streptococcal cell (Moses *et al.*, 1997). Furthermore the capsule might be an essential adherence factor in the pharynx as it binds to CD44 receptors on epithelial cells.

5.1.1.3 Hyaluronate lyase

Groups A, B, C and G streptococci can produce hyaluronate lyase which breaks down HA, a main component of the connective tissue of the host. This in turn facilitates the access of the pathogen and its secreted toxins at the site of infection. The production of unsaturated disaccharide is thought to be a source of carbon allowing enhanced growth at the site of hyaluronate lyase production (Baker *et al.*, 2002; Allen *et al.*, 2004).

In addition to chromosomal hyaluronate lyase, GAS carry hyaluronate lyases encoded by the prophage derived from a temperate bacteriophage. These enzymes lack similarity with their chromosomally encoded counterparts (Gase *et al.*, 1998). *S. pyogenes* SF370

produces three bacteriophage hyaluronate lyases (Smith *et al.*, 2005). Interestingly, these enzymes have different biochemical properties.

5.1.1.4 Streptolysins

S. pyogenes produces two different haemolysins, namely Streptomycin O (oxygen-labile) and Streptolysin S (serum-soluble). Both Streptolysins lyse erythrocytes and polymorphonuclear leucocytes by creating pores in their cell membranes (Bisno *et al.*, 2003).

Streptolysin O is one of the important virulence factors; it is highly immunogenic, secreted by the majority of GAS, and is a potent cytolytic toxin (Fontaine *et al.*, 2003). A strong immune response to streptolysin O is used as an indicator of the onset of acute rheumatic fever and acute poststreptococcal glomerulonephritis (Velazquez *et al.*, 2005). Intravenous injection of Streptolysin O into experimental animals causes death within two to three minutes due to the severe toxic effect on the heart (Fontaine *et al.*, 2003).

Streptolysin S also has a very potent cytolytic activity against a variety of cells. It is a non-immunogenic peptide, which loses its activity upon separation from various carrier proteins (Bisno *et al.*, 2003; Fontaine *et al.*, 2003). Streptolysin S is responsible for β-haemolysis around colonies on blood agar plates (Bisno *et al.*, 2003).

The focus of the study undertaken in this chapter was to clone and express the *hylA* gene from *S. pyogenes* SF370, which encodes a hyaluronate lyase from family 8 of the polysaccharide lyases. Biochemical properties such as optimum pH, optimum temperature stability and activity, the effect of divalent cations, substrate specificity and

kinetic parameters were determined for the wild type enzyme. Also, mutant forms of the enzyme were expressed and their kinetic parameters were determined.

5.2 Results

The results revealed that ORF *hylA* of *S. pyogenes* was successfully cloned and expressed in *E. coli* BL21 (DE3). This enzyme was shown to be active only on the HA substrate and it was inactive against other types of GAGs: chondroitin-4-sulphate, chondroitin-6-sulphate, dermatan sulphate, sodium heparin and heparan sulphate. The N-terminal His tagged protein has an optimum pH of 6 and an optimum temperature of 47 °C. The kinetic parameters K_m and k_{cat} of the wild type and its mutant H307A were determined and were found to be 0.206 ± 0.012 mg ml^{-1}; 17.3 ± 1.04 s^{-1} and 0.91 ± 0.35 mg ml^{-1}; 0.86 ± 0.29 s^{-1}, respectively. Also, the enzyme has been crystallised and the diffraction data facilitated the determination of crystal parameters. The crystal of the wild type enzyme belongs to space group P212121 and has unit cell dimensions of a = 51.111, b = 88.497, c = 159.089. However the structure was shown to only contain the β-domain.

5.2.1 Protein expression and purification

5.2.1.1 Cloning, expression and purification of hylA native recombinant protein

The *hylA* gene encoding hyaluronate lyase was amplified by PCR (section 2.2.2.2.1.2.3) from *S. pyogenes* SF370 genomic DNA template using primers that contained ligation independent cloning specific 5' ends (section 2.1.3.2). The amplified PCR product was prepared for vector insertion by purification (section 2.2.2.1.9) and treatment with T4 DNA polymerase in the presence of dATP. The prepared insert was annealed into BseR1-cut pET-YSBLIC treatment with T4 DNA polymerase in the presence of dTTP (Bonsor *et al.*, 2006) and directly transformed into *E. coli* TOP10 competent cells

(section 2.2.1.3) for plasmid identification and recovery. The recovered plasmids were subsequently transformed into high-efficiency competent expression host *E. coli* BL21 (DE3) (section 2.2.1.3) for protein production upon IPTG induction. After incubation overnight at 30 °C, the cells were collected by centrifugation and then cells were resuspended in starting buffer (section 2.1.4.3.6.1) containing one tablet of protease inhibitor mixture. The cells were then disrupted by sonication and cell free extract (section 2.2.3.2) was obtained by centrifugation. The protein was then purified using IMAC (section 2.2.3.4) and gel filtration (section 2.2.3.6).

SDS-PAGE analysis indicated that HylA was expressed in a soluble form and showed satisfactory purity with only weak contaminant bands (Figure 5.2), and the highest expression levels were reached at 30 °C. The protein was purified to high purity and 30 mg of pure protein was obtained with 1 L culture. The purified protein was subjected to biochemical analysis (section 2.2.4.1). The protein was stable for up to 4 weeks at 0 °C after which it tended to precipitate.

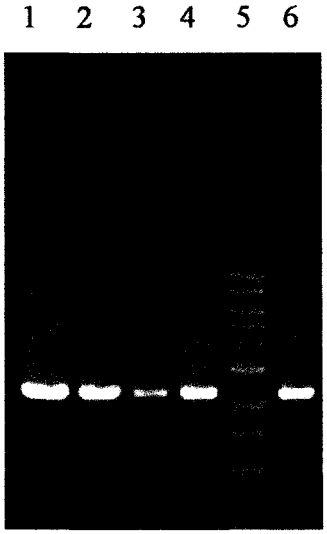

Figure 5.1 Visualisation of DNA bands following agarose gel electrophoresis
DNA products created during a PCR. Lanes 1, 2, 3, 4, and 6: 5 µl of *hylA* (2418 bp) from *S. pyogenes* SF370, using different annealing temperatures; Lane 5: 1 Kb DNA ladder (10, 8, 6, 5, 4, 3, 2, 1.5, 1, 0.5 Kb). DNA samples were subjected to 1 % agarose gel electrophoresis at 100 mA and 200 V for 45 min (section 2.2.2.1.5). Subsequently, gels were immersed in a10 µg ml^{-1} solution of ethidium bromide for 10 min then washed with distilled water and placed on a UV illuminator and a fluorescent image was taken (section 2.2.2.1.6).

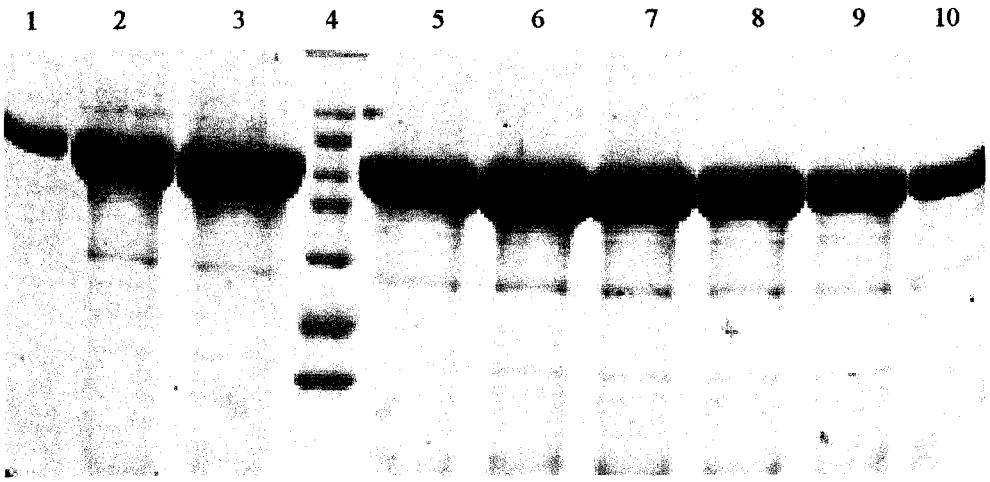

Figure 5.2 12% SDS-PAGE of HylA expression.
HylA (wild type) was purified from *E. coli* cells harbouring plasmid pET-YSBLIC containing the *hylA* fragment by IMAC (section 2.2.3.4). Lane 4: High molecular weight (HMW) markers (205, 116, 97, 84, 66, 55, 45, 36 kDa); Lanes 1, 2, 3, 5, 6, 7, 8, 9 and 10. 20 µl of protein (fractions 1-3, 5-10 are shown). Proteins were visualised by staining with Coomassie blue and destained (section 2.2.3.1.1).

5.2.2 Biochemical characterisation of HylA

5.2.2.1 Determination of optimum pH

The optimal pH value of the N-terminally tagged HylA protein was determined to be 6 at 37 °C in 20 mM sodium acetate buffer. While the enzyme showed high activity between pH 5.5 and 6, very little activity was observed at pH 4.0.

5.2.2.2 Determination of optimum temperature

As shown in Figure 5.4, the activity of the enzyme increased gradually with increasing temperature, and activity reached a maximum at 47 °C, while there was a rapid decrease in its activity after 47 °C.

The thermostability of HylA was assayed by pre-incubating the enzyme at different temperatures, which ranged from 27 °C to 77 °C for 20 min (section 2.2.4.1.1.3), followed by an assay for residual enzyme activity. This enzyme was found to be very stable at 27°C - 37 °C but the activity was significantly reduced at temperatures 47°C, 57°C and 67 °C as illustrated in Figure 5.5.

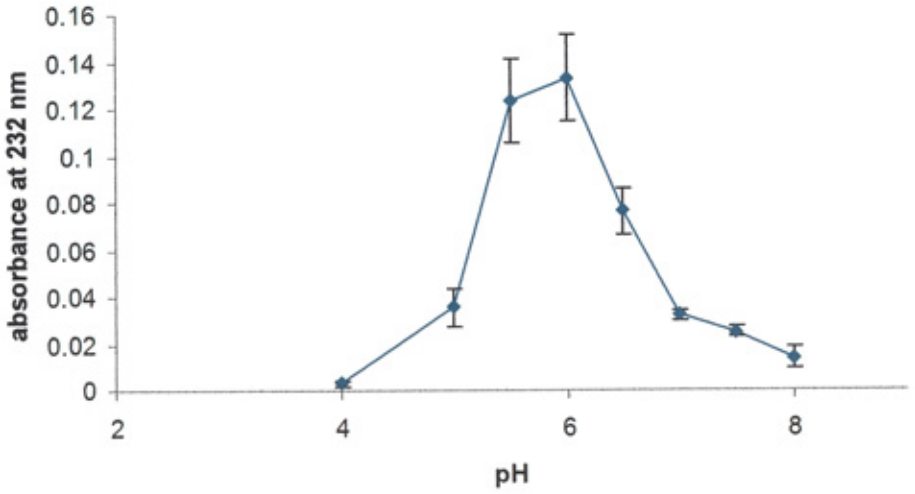

Figure 5.3 Influence of pH on activity of HylA against sodium-hyaluronate. Reactions mixtures containing enzyme, 1 mg ml^{-1} substrate (dialysed sodium hyaluronate), 0.1 mg ml^{-1} BSA, and 20 mM sodium acetate buffer at various pH values (4-8). Reactions were performed at 37 °C in triplicate, with initial rate measurements, and error bars represent the standard deviation of the mean.

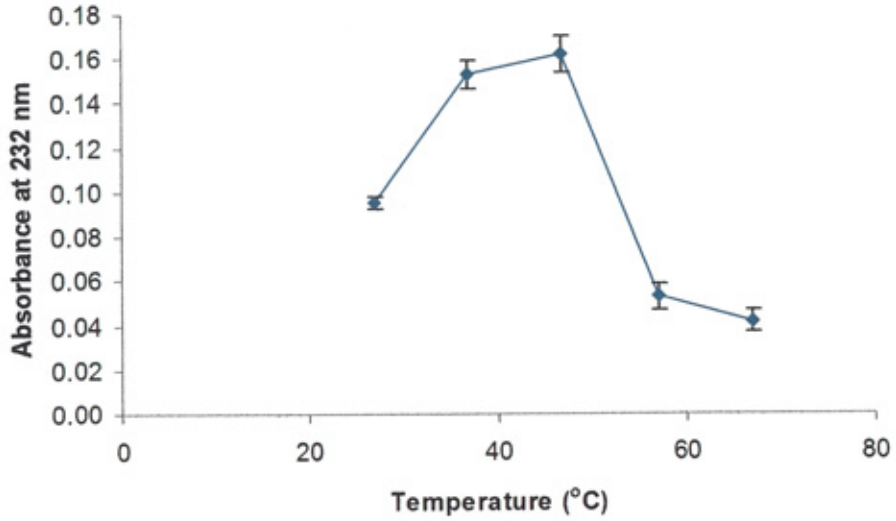

Figure 5.4 Influence of temperature on HylA activity.
Reaction mixtures containing enzyme, 1 mg ml^{-1} substrate (dialysed sodium hyaluronate), 20 mM sodium acetate buffer pH 6, and 0.1 mg ml^{-1} BSA. Reactions were performed in triplicate, with initial rate measurements made at 27, 37, 47, 55 and 67 °C (error bars represent the standard deviation of the mean).

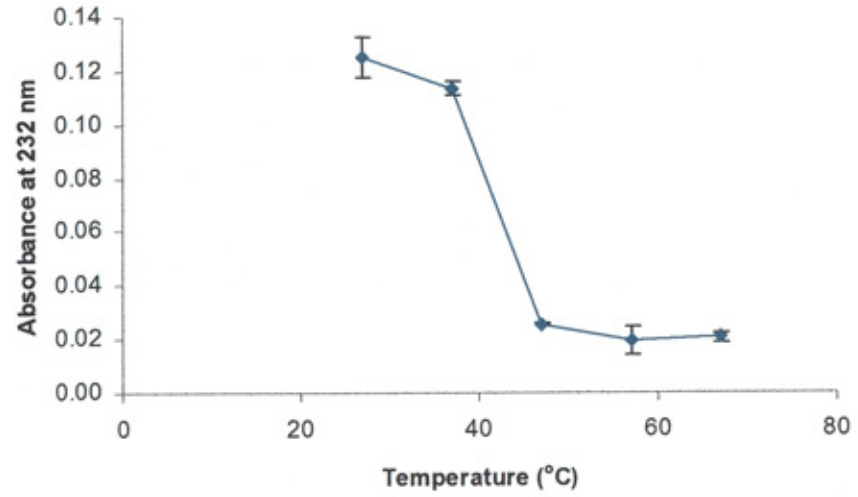

Figure 5.5 Influence of temperature on the stability of HylA.
Reactions were performed at 37 °C, with 1 mg ml^{-1} substrate (dialysed sodium hyaluronate), 20 mM sodium acetate buffer pH 6, and 0.1 mg ml^{-1} BSA. Prior to addition to the reactions, the enzyme was pre-incubated at 27, 37, 47 57 and 67 °C for

20 min. Reactions were performed in triplicate, with initial rate measurements made (error bars represent the standard deviation of the mean).

5.2.2.3 Determination of the effect of divalent ions

The effects of various divalent cations at a final concentration of 2 mM (section 2.2.4.1.1.4) were tested against HylA. The activity was slightly reduced in the presence of 2 mM $ZnCl_2$, whereas $MnCl_2$, $MgCl_2$ and $CaCl_2$ increased the activity by 200 %, 168.8 % and 162.5 %, respectively, when the control was taken as 100 %. At the same concentration, $CoCl_2$ and $NiCl_2$ showed no significant effect on the enzyme (Figure 5.6).

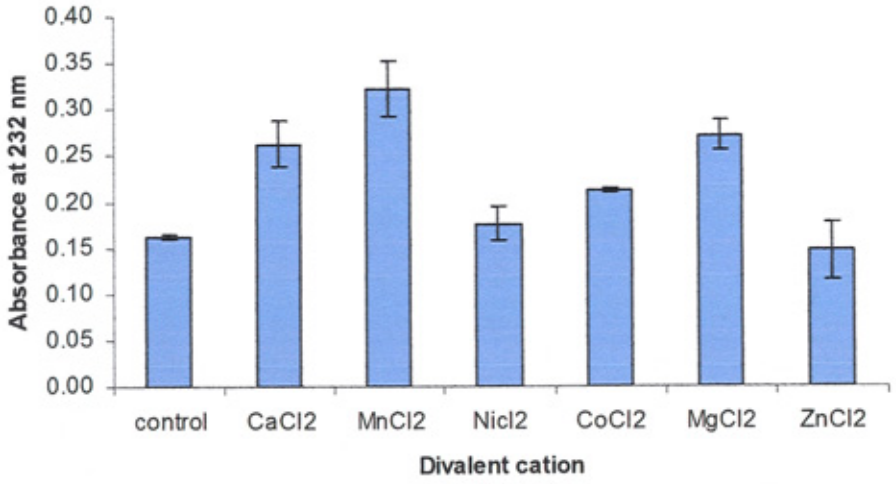

Figure 5.6 Influence of various divalent cations on HylA activity. Reactions were 1 mg ml^{-1} substrate (dialysed sodium hyaluronate), and 20 mM sodium acetate buffer pH 6. Divalent cations (Ca^{2+}, Mn^{2+}, Ni^{2+}, Co^{2+}, Mg^{2+} and Zn^{2+}) were added to the reactions at a final concentration of 2 mM. Reactions were performed in triplicate, with initial rate measurements made at 37 °C (error bars represent the standard deviation of the mean).

5.2.3 Kinetic analysis of HylA

5.2.3.1 Substrate specificity

In order to investigate the substrate specificity of HylA, the polysaccharides HA, chondroitin-4-sulphate, chondroitin-6-sulphate, dermatan sulphate and sodium heparin

were digested with the enzyme. The enzyme was found to be highly specific; it degrades HA, but it does not degrade either chondroitin-4-sulphate, chondroitin-6-sulphate or any other type of GAGs. The values of K_m and k_{cat} of the wild type for the degradation of sodium hyaluronate were estimated at 0.206 ± 0.012 mg ml^{-1}; and 17.3 ± 1.04 s^{-1}, respectively.

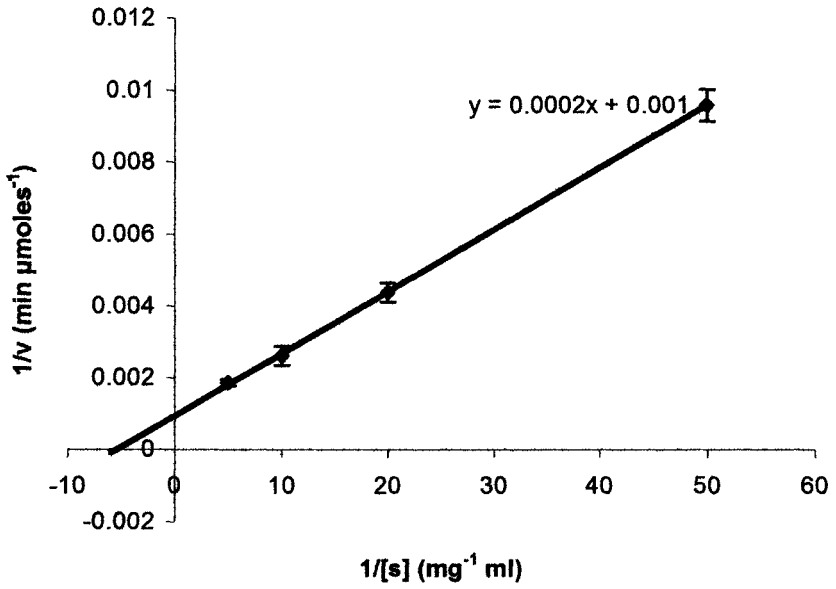

Figure 5.7 Lineweaver-Burke plot for HylA against sodium hyaluronate. The data were performed in triplicate with error bars representing the standard deviation from the mean. The reactions were carried out under optimal conditions.

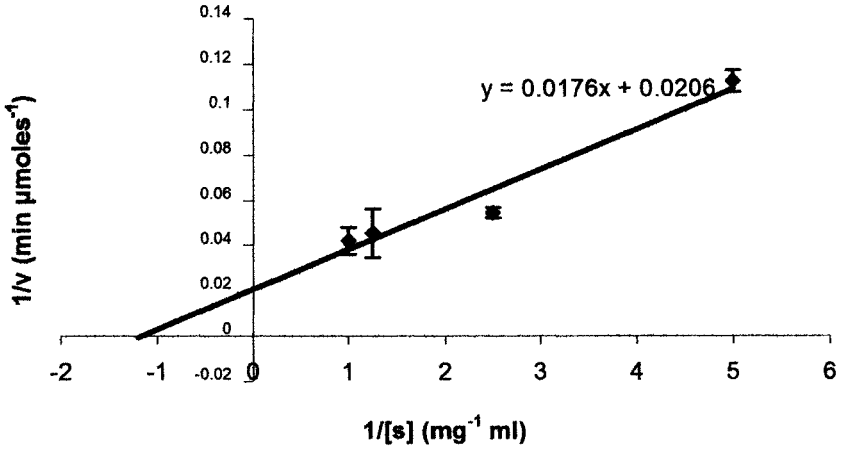

Figure 5.8 Lineweaver-Burke plot for HylA mutant H307A against sodium hyaluronate. The data were performed in duplicate with error bars representing the standard deviation from the mean. The reactions were carried out under optimal conditions.

5.2.4 Effect of vitamin C on the activity of HylA

The effect of various concentrations of vitamin C (Vc) on the enzymatic activity of *S. pyogenes* hyaluronate lyase was examined in order to discover whether or not Vc can inhibit the enzyme.

The effect of Vc from 0 mM to 24 mM at different time points was investigated using a DNSA reducing sugar assay, and the absorbance was measured at 570 nm in a 96-well plastic microtitre plate. The results show that the compound had a weak inhibitory effect on the activity of *S. pyogenes* hyaluronate lyase as shown in Figure 5.10.

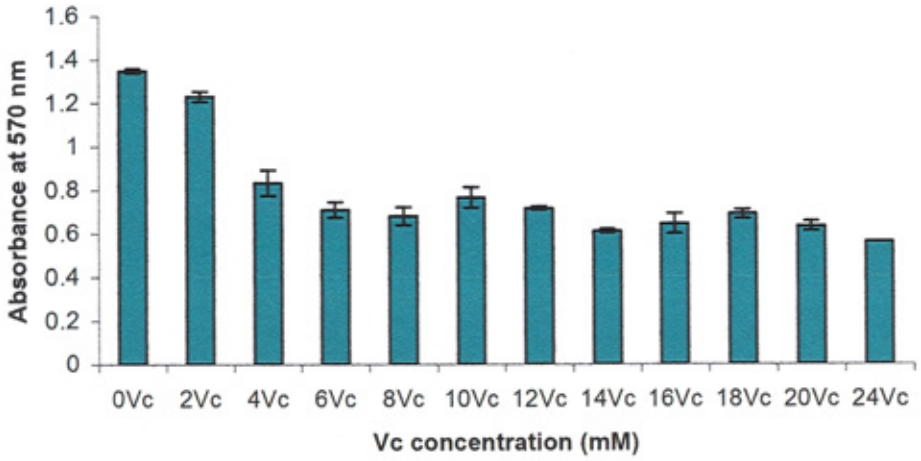

Figure 5.9 The effect of various concentrations of Vc on the activity of *S. pyogenes* hyaluronate lyase. The final enzyme concentration was 2.3 mg ml^{-1}. The final Vc concentrations were 2-24 mM. Each column represents the mean value of three independent measurments with error bars representing the standard deviation from the mean.

5.2.5 Mode of action

The mode of action of *S. pyogenes* Hyla was investigated by the analysis of digestion products by HPAEC using HA as substrate. Sodium hyaluronate was incubated with Hyla for a range of times, and the resulting digests were analysed by HPAEC. A digest of 5 min produced a range of different sizes of oligosaccharides ranging from tetrasaccharides to greater than 20-mers. As the time of digest was increased, the average size of the oligosaccharides was progressively reduced, demonstrating that the enzyme has an endolytic mode of action (Figure 5.9). After digestion for 160 min, two end products corresponding in size to tetrasaccharide and disaccharide were detected. The elution position of different size of HA oligosaccharides was determined and confirmed by compared to the standards (di-, tetra-, hexa- and octa-saccharide). The elution time of HA oligosaccharides obtained in this work is consistent to that of Lauder et al., 2000 and Smith et al., 2005.

Size exclusion chromatography on Bio-gel P-6 was used as the initial step in the large-scale purification of 20 min of digestion (Figure VE, appendix V). The purification of these products resulted in single absorbance peaks being detected at 232 nm. Sample purity was confirmed by the presence of a single peak, each corresponding to a definitive size of oligosaccharide monitored by absorbance at 232 nm using HPAEC.

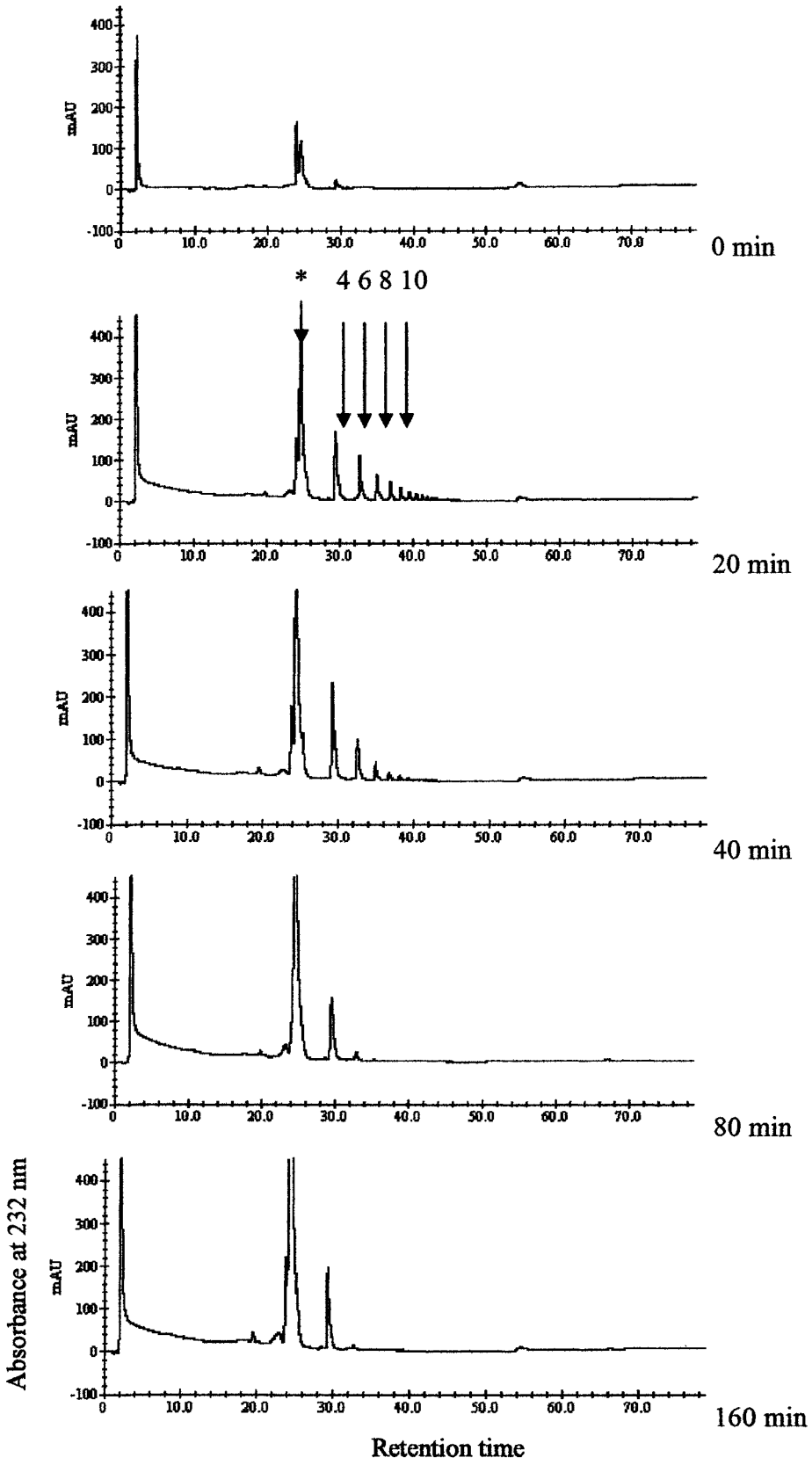

Figure 5.10 HPAEC of the oligosaccharides derived from hyaluronate lyase digestion of hyaluronan. The oligosaccharides were chromatographed on a CarboPac PA 1 column (250 mm x 4 mm) maintained at 37 °C. Elution was at 1 ml min^{-1} (section 2.2.4.2). The eluent was monitored by absorbance at 232 nm. Degradation products are indicated with arrows, 4: tetrasaccharide; 6: hexasaccharide; 8: octasaccharide; 10: decasaccharide;
*: artifact. The duration of the digest is shown on the right of each chromatogram.

5.2.6 Construction of the mutant forms of HylA

plasmid (pET-YSBLIC) containing the *hylA* gene was used as the template to generate four single mutations using site-directed mutagenesis as described in materials and methods. Briefly, the mutants were produced by plasmid denaturation and the annealing of complementary oligonucleotide primers (section 2.1.3.2.1) containing the desired mutation. This was followed by extension of the primers with a thermocycler (under the conditions described in section 2.2.2.1.3.2) and *PfuTurbo* DNA polymerase, resulting in a mutated plasmid with staggered nicks. The digestion of the hemimethylated DNA of the parental template with *Dpn*I endonuclease selected for the mutation-containing synthesized DNA. The mutated plasmids (pAsn257Ala, pHis307Ala, pTyr327Ala and pTyr327Phe) were transformed into *E. coli* TOP10 competent cells (section 2.2.1.3). The plasmids were prepared using a miniprep kit (Qiagen) (section 2.2.2.1.7.3). Each clone was sent for sequencing to MWG Biotech, mutations were confirmed by sequencing. The data illustrated that the desired single mutation had been successfully created. Plasmid DNA was then transformed into *E. coli* BL21(DE3) competent cells.

5.2.6.1 Over-expression and purification of mutant enzymes

The mutant forms of the enzyme, N257A, H307A, Y327A and Y327F were overexpressed and purified following the same method as that for the native enzyme. In brief, the over-expression of mutants was performed by growing *E. coli* BL21 (DE3) (section 2.2.1.3), harbouring the appropriate clone in LB media (section 2.1.4.1.1.1) with kanamycin selection at 37 °C until the OD reached approximately 0.6, after which the culture was induced with 1 mM IPTG and incubated at 30 °C overnight (section 2.2.1.2.2). Cells were harvested by centrifugation. The proteins were then purified by immobilised metal affinity chromatography under non-denaturing conditions, using a chelating Sepharose nickel column (section 2.2.3.4; Figure 5.11) followed by gel

filtration. The concentrations of the proteins were determined by Bradford's assay (section 2.2.3.8).

The kinetic parameters of the mutants demonstrated that substituting tyrosine327 with either alanine (Y327A) or phenylalanine (Y327F) resulted in the enzyme becoming completely inactive. Also, substituting asparagine257 with alanine (N257A) led to no apparent change in absorbance at 232 nm. The H307A mutant displayed very little activity against HA of about 5 % relative to the activity of the wild type. On the other hand the K_m of the H307A mutant was approximately 5 times greater than that of the wild type enzyme.

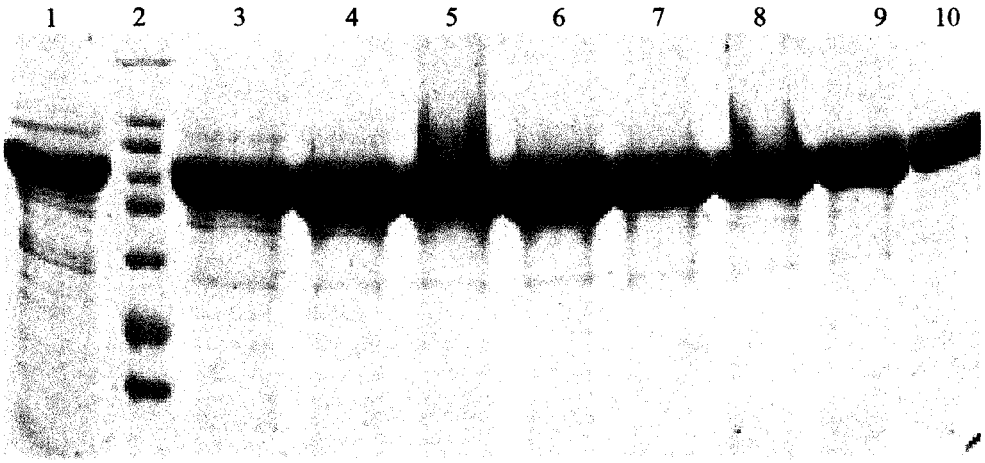

Figure 5.11 12% SDS-PAGE of HylA mutant expression (YF).

HylA (mutant) was purified from *E. coli* cells harbouring plasmid pET-YSBLIC containing hylA fragment by IMAC (section 2.2.3.4). Lane 2: High molecular weight (HMW) markers (205, 116, 97, 84, 66, 55, 45, 36 KDa); Lane 1, 3, 4, 5, 6, 7, 8, 9 and 10. 20 µl of protein (Fractions 1-9 are shown). Proteins were visualised by staining with Coomassie blue and destained (section 2.2.3.1.1)

5.2.7 Crystallisation of HylA

HylA was purified to apparent homogeneity (as judged by SDS-PAGE; section 2.2 .3.1.1; Figure 5.2) from pET-YSBLIC to generate a N-terminal tagged recombinant enzyme. The protein was concentrated to approximately 30 mg ml^{-1}

(section 2.2.3.8) and then diluted in water to give a final concentration of 15 mg ml^{-1}. The protein was then screened using the hanging drop vapour diffusion method together with the Crystal Screen 1, Crystal Screen 2 and PEG/Ion Screen (Hampton Research, Alison Viejo, USA) and Clear Strategy Screen I and Clear Strategy Screen II (Molecular Dimensions Limited, Cambridgeshire UK) (Appendix III; Tables III A, III B, III C, III D and III E respectively). Drops containing 1 µl of protein (at a concentration of 15 mg ml^{-1}) were mixed together with 1 µl and 2 µl of the mother liquor. Feather-shaped crystals appeared in drops containing 20% (w/v) PEG 3350 + 0.2M of di-ammonium tartrate (condition 38 of the PEG/Ion Screen 1). Further optimisation was carried out around the preliminary conditions with varying parameters until good diffracting crystals were obtained. Good crystals were grown after four weeks at 22 °C in 220 mM of di-ammonium tartrate + 20% PEG 3350 (Figure 5.44). The crystals were smooth and thick with feathered characteristics growing to a size of approximately 0.2 x 0.1 x 0.2 mm. A single crystal was removed from the drop using a rayon fibre loop and transferred into a cryo-protectant solution comprising the crystal growth buffer (0.22 M of di-ammonium tartrate + 20 % (w/v) PEG 3350) and 30 % (v/v) glycerol prior to freezing the crystals in liquid nitrogen. A rayon fibre loop was used to raise the crystal and an image collected using a Rigaku X- ray generator and a MAR 30 cm image plate at YSBL. Crystals diffracting to 2.5 were stored in liquid nitrogen for further analysis at the ESRF (Grenoble, France). The structural data are shown in Table 5.1.

5.2.7.1 Diffraction analysis of HylA

Initial X-ray diffraction analysis revealed that the crystals of HylA belong to space group P212121 with unit cell dimensions a = 51.111, b = 88.497 and c = 159.089 and diffracted beyond 2.5.X-ray diffraction data were processed using the molecular

replacement programme. The data that were collected at the ESRF on beam line ID-14.2, are presented in Table 5.1.

Table 5.1 Crystal parameters of HylA

Crystal parameter	HylA
Space group	P212121
Cell-dimension a (°A)	51.111
Cell-dimension b (°A)	88.497
Cell-dimension c (°A)	159.089

5.2.7.2 Crystallisation of HylA mutants in complex with substrate

HylA mutant proteins were purified to apparent homogeneity (Figure 5.11) and concentrated in H_2O to a concentration of about 15 mg ml^{-1}. Crystals of HylA mutants were grown by the vapour phase diffusion method, using the same conditions as for the native protein crystals of 220 mM of di-ammonium tartrate + 20% PEG3350. The mutant proteins were co-crystallised with di, tetra and hexasaccharides of HA which were dissolved in water to give a final concentration of 60 mM. The ligands were added to the drops of enzyme and reservoir buffer (1 µl each) at a final concentration of 20 mM, mixed together and equilibrated against 0.5 ml of reservoir buffer. The crystals (Figure 5.13) formed were cryoprotected using 30 % glycerol (v/v) and 220 mM of di-ammonium tartrate + 20% PEG3350 and frozen in liquid nitrogen. Standard fibre loops of suitable size were used to pick up and mount the crystals.

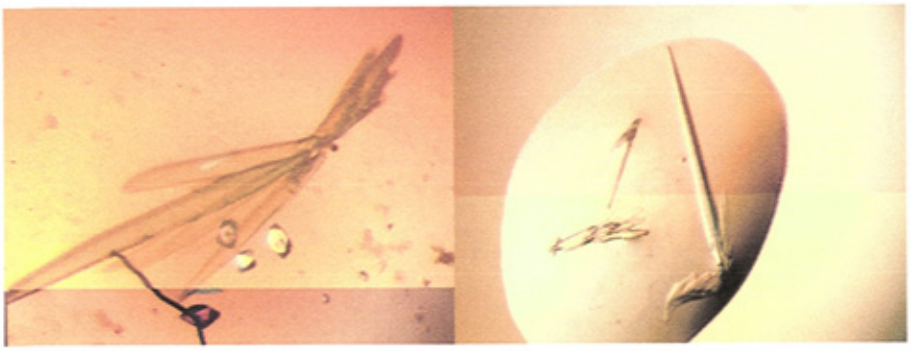

Figure 5.12 Crystals of native recombinant HylA from *Streptococcus pyogenes* SF370. Crystals were grown by the hanging drop method (section 2.2.3.9). Equal amounts of protein and reservoir (0.22 M of di-ammonium tartrate + 20% PEG 3350) were mixed and glycerol [30 % (v/v) final concentration] was added to the drop. Feather crystals grew after four weeks at 22 °C.

Figure 5.13 Crystals of the mutant Y327F. Crystals were grown by the hanging drop method (section 2.2.3.9). Equal amounts of protein and reservoir (0.22 M of di-ammonium tartrate + 20% PEG 3350) were mixed and glycerol [30 % (v/v) final concentration] was added to the drop. Crystals grew after four weeks at 22 °C.

Chapter 6 Discussion: biochemical characterisation of the *Streptococcus pyogenes* SF370 hyaluronate lyase

6.1 Introduction

The objectives of this study were to biochemically characterise a hyaluronate lyase of *S. pyogenes* SF370 through the determination of optimum pH, optimum temperature, the effect of divalent cations and the substrate specificity of the enzyme. Also the mode of action of this enzyme and the purification of its products were achieved through the use of HPAEC and P-6 gel filtration, respectively.

6.1.1 Hyaluronate lyases

Hyaluronidases are enzymes responsible for most of the degradation of HA as they catalyse the random hydrolysis of 1,4-linkages between N-acetyl-β-D-glucosamine and D-glucuronate residues in HA (Kreil, 1995). From biochemical analysis and reaction products, it has been demonstrated that hyaluronidases can be classified into three groups which cleave HA by different mechanisms: hyaluronate-4-glycanohydrolases, hyaluronate-3-glycanohydrolases and hyaluronate lyases (Menzel and Farr, 1998; Hynes and Walton, 2000; Akhtar and Bhakun, 2004; Girish *et al.*, 2004).

Bacterial hyaluronate lyases (EC 4.2.2.1) differ from other hyaluronidases in their mode of action. They cleave the glycosidic bond using a β-elimination reaction, leaving a C4-C5 unsaturated bond containing product which is identified easily by ultraviolet (UV) absorbance (Li *et al.*, 2000; Li *et al.*, 2001; Li and Jedrzejas, 2001).

A number of investigators have noted the existence of HA-degrading enzymes in many microorganisms such as strains of *Micrococcus*, *Streptococcus*, *Peptococcus*, *Propionibacterium*, *Bacteroides* and *Streptomyces* (Akhtar and Bhakun, 2004).

Hyaluronate lyases have been identified in several genera and species of streptococci. These include *Peptostreptococcus* (Tam and Chan, 1985), *Propionibacterium* (Ingham *et al.*, 1979), *S. pneumoniae* (Jedrzejas *et al.*, 1998; Li *et al.*, 2000), *S. agalactiae* (Baker *et al.*, 1997; Li and Jedrzejas, 2001), *S. suis* (Allen *et al.*, 2004), *S. dygalactiae* (Hamai *et al.*, 1989), *S. intermedius* and *S. consellatus subsp. constellatus* (Takao *et al.*, 1997; Takao, 2003) and *S. pyogenes* (this thesis). The degradation of HA by the hyaluronate lyases of pathogenic bacteria decreases the viscoelasticity of the ECM resulting in increased spreading of the bacteria and the toxins in the tissues (Baker *et al.*, 2002; Allen *et al.*, 2004; Botzuki *et al.*, 2004). Many streptococcal hyaluronate lyases can degrade chondroitin and chondroitin sulphates as well. They cleave them at every unsulphated disaccharide repeat, resulting in unsaturated hexuronic acid residues at their non-reducing ends (Akhtar and Bhakun, 2004).

6.2 Discussion

6.2.1 Biochemical characterization of HylA

The gene encoding a hyaluronate lyase has been cloned from *S. pyogenes* SF370 into pET-YSBLIC and expressed with a N-terminal Histidine tag at high levels in *E. coli* BL21 (DE3).

Interestingly, the hyaluronate lyases of PL 8 which have been characterised, differ in many aspects from the hyaluronate lyase of *S. pyogenes*. For instance, one of the most notable features of this enzyme is its activity solely against HA. This is in contrast to most hyaluronate lyases of this family, which degrade chondroitin-4 and 6-sulphate besides degrading HA. The only pathogenic bacterial hyaluronate lyases that may exhibit substrate specificities analogous to HylA are *S. constellatus subsp. constellatus* hyaluronate lyases which exhibit absolute specificity for HA (Takao, 2003).

Furthermore, *S. dysgalactiae* lyases degrade chondroitin at very low rates of less than 5 % of rate of its degradation of HA (100 %) while it is unable to degrade other GAGs which contain sulphate groups (Hamai *et al.*, 1989). The specificity of the *S. pyogenes* HylA therefore differs from that of *S. pneumoniae*, *S. agalactiae* and *S. intermedius* which have all been reported to be specific for both HA and chondroitin-4 and 6-sulphate (Baker *et al.*, 1997; Takao *et al.*, 1997; Baker *et al.*, 2002; Takao, 2003). Moreover, the hyaluronidases (which are a group of hydrolases) of Indian copra (Girish *et al.*, 2004) and Southern copperhead (Kudo and Tu, 2001) display the same properties regarding their specificity. By contrast, this study has shown that *S. coelicolor* hyaluronate lyase degrades both chondroitin-4 and 6-sulphate in addition to HA, and it shows a high level of activity on chondroitin-4-sulphate almost similar to that observed toward potassium hyaluronate.

Another significance properties of the *S. pyogenes* hyaluronate lyase characterised during this study is its ability to work with a wide range of divalent cations, since its activity is noticeably increased in the presence of 2 mM $MnCl_2$, $MgCl_2$ or $CaCl_2$.

The optimum pH for the activity of the *S. pyogenes* hyaluronate lyase enzyme is within the range of 5.5-6. Similar pH optima have been reported for *S. pneumoniae* (Jedrzejas *et al.*, 1998; Li *et al.*, 2000), *S. agalactiae* (Ozegowski *et al.*, 1994) and *S. constellatus subsp. constellatus* (Takao, 2003) of 5.5-6, 6 and 6.2, respectively.

Since *S. pyogenes* is a human pathogen and is thus unlikely to be exposed to higher temperatures than those found in man it is therefore consistent for it to display optimum catalytic performance at 37 °C to 47 °C (Figure 5.37). At temperatures higher than 47 °C, the enzyme activity decreased markedly. Similar temperature optima were reported

by Tam and Chan (1985) for similar enzymes from *Peptostreptococus* sp., and by Ozegowski *et al* (1994) for *S. agalactiae*.

Heating the enzyme for 20 min at various temperatures from 27 to 77 °C prior to assay showed that HylA is very sensitive to thermal denaturation. This temperature stability study indicates that there was a general decrease in the stability of the enzyme with increasing temperature as indicated by a decrease in enzyme activity. This decrease in stability is shown in Figure 5.5, where the highest stability is at 27 °C and the lowest stability is at 67 °C. This inactivation of the enzyme by temperature could be attributed to the general thermal denaturation.

The turnover numbers of most lyases are approximately 15-2005 s^{-1} (Ernst *et al.*, 1995). It is, however, relatively difficult to compare the kinetic results obtained in this work with previously published results of other enzymes from the same family due to the different experimental conditions used. The values of k_{cat} previously reported for hyaluronate lyases of group B streptococcus are 120 times higher than that obtained for the corresponding enzyme of *S. pyogenes*, which was 17.3 s^{-1}.

The K_m and k_{cat} of HylA were 0.2 mg ml^{-1} and 17.3 s^{-1}, respectively. The K_m of *Peptostreptococcus* sp. (0.14 mg ml^{-1}) is slightly lower than that reported for HylA of *S. pyogenes*, while the K_m of *S. pneumoniae* (0.09 mg ml^{-1}) is considerably lower than of *S. pyogenes* (Kelly *et al.*, 2001). The k_{cat} of HylA is significantly lower compared to those determined for other hyaluronate lyases of this family. Likewise, the values of k_{cat} of structurally unrelated Hylp1 (PL16) from the same strain also displayed a very low turnover number, of 7.2 s^{-1} (Smith *et al.*, 2005).

The k_{cat} value with sodium hyaluronate is 20 times higher in the case of wild type HylA compared to the H307A mutant, whereas the value of K_m is nearly 5 times higher in the mutant form than in the wild type. This suggests that decreased substrate binding affinity and turnover number of the H307A mutant is responsible for reducing its

catalytic efficiency and demonstrated that this amino acid plays an essential role in catalysis. These results are nearly identical to those of *S. pneumonia* mutant H399A, the activity of which was only12 % compared to that of the native enzyme (Kelly *et al.*, 2001; Nukui *et al.*, 2003).

This study provides insights into the effects of the mutations on the catalytic mechanism of *S. pyogenes* hyaluronate lyase. TheY327A and Y327F mutants were basically inactive, thus indicating that this amino acid has a critical role in catalysis.
Also, kinetic data of another putative catalytic residues Asn257, provides direct evidence for the catalytic functions of this residue.

The results showed that vitamin C had only a weak influence on the activity of *S. pyogenes* hyaluronate lyase against HA. On the other hand, vitamin C inhibited the *S pneumoniae* hyaluronate lyase activity with an IC50 of about 5.8 mM (Li *et al.*, 2001), while it had no effect on bovine testicular hyaluronidase up to 100 mM (Li *et al.*, 2001). The structure of vitamin C resembles the structure of one of the sugar units of HA, the glucuronic acid residue, which is also the precursor of the biosynthesis of vitamin C. Therefore, due to this similarity, vitamin C is considered a substrate analogue of hyaluronate lyase. This structural similarity gives vitamin C the ability to protect hyaluronan, which is the major constituent of connective tissues, from degradation by bacterial hyaluronate lyases. Additionally, this inhibitor may possibly be used as drug, i.e. as antibacterial compound. It was recently discovered that the derivative of vitamin C, L-ascorbic acid-6-hexadecanoate has a much greater inhibitory effect on the hyaluronate lyases of *S. pneumoniae* and *S. agalactiae* strain 4755 with values of IC50 of 100 and 4 μM, respectively (Botzuki *et al.*, 2004). However, the inhibitory effect of L-ascorbic acid-6-hexadecanoate was not tried against *S. pyogenes*, due to the precipitation of the enzyme in the presence of this compound.

6.2.2 Mode of action

Studies on the mode of action of *S. pyogenes* Hyla have shown that this enzyme cleaves HA in a random endolytic manner producing a mixture of different sizes of oligosaccharides. This mode of action is another interesting characteristic of the *S. pyogenes* hyaluronate lyase presented in this study, as all other hyaluronate lyases of PL 8 possess an exolytic mode of action; for example enzymes from *S. pneumonia, S. agalactiae* and *S. suis* (Li *et al.*, 2000; Kelly *et al.*, 2001; Li *et al.*, 2001; Mello *et al.*, 2002; Nukui *et al.*, 2003; Allen *et al.*, 2004). The random endolytic cleavage of HylA was a surprising observation and suggests that this enzyme has the capacity to accept a wide range of substrate binding modes, resulting in the gradual cleavage of longer oligomers into shorter products without the accumulation of these products early in the reaction.

Other PL 8 enzymes that display an endolytic cleavage are the ABC lyase I of *P. vulgaris* and the AC lyase of *F. heparinium* (Thurston *et al.*, 1975; Huang *et al.*, 2003; Prabhakar *et al.*, 2005) and (Huang *et al.*, 2001; Capila *et al.*, 2002), respectively. However, these enzymes are not specific only to HA.

Bacterial hyaluronate lyases have therefore been divided into two groups (Li and Jedrezaj, 2001). Group I enzymes yield only diasaccharides from the beginning of the reaction, such as those of *S. coelicolor* (this study), *S. pneumoniae* (Li *et al.*, 2000; Kelly *et al.*, 2001, Li *et al.*, 2001; Nukui *et al.*, 2003) and *S. agalactiae* (Mello *et al.*, 2002); while group II enzymes produce a mixture of oligosaccharides such as *F. heparinum* AC lyase (Huang *et al.*, 2001; Capila *et al.*, 2002). Consequently, the *S. pyogenes* hyaluronate lyase belongs to group II. In group II, the enzymes leaves the substrate chain after the first degradation, before re-attaching randomly to another site on the same or different substrate chain. On the other hand, exolytic cleavage involves

binding of the enzyme to a cleavage site of the substrate chain, degrading it and progressing along the substrate chain continually until the whole chain is degraded (Li and Jedrezejas, 2001).

Interestingly, analysis of the mutant enzymes of HylA by SDS-PAGE showed that these proteins degraded after about two weeks of purification. This probably resulted from a residual protease activity that co-purified with the mutants, which was able to function in spite of the existence of a protease inhibitor. This means that the native enzyme and its mutants are sensitive to proteolytic degradation. Accordingly, when the crystals of the native enzyme were subjected to X-ray crystallographic analysis, it was found that only the β-domain was present whilst the α-domain had degraded. Therefore it is apparently impossible to obtain ligand complexes with the native enzyme or its mutants due to this degradation.

More crystallization trials were set up with the various protein in an attempt to obtain crystals of the whole enzyme. Also, crystallization trials were set up with HA disaccharide with both native enzyme as well as mutant forms, and different concentrations of the various proteins were added. But even after many trials and trying various conditions, the structure of the entire protein could not be obtained.

Sequence comparisons between chromosomal hyaluronate lyase and bacteriophage hyaluronate lyases produced from the same organism showed that no homology was found between these enzymes. It seems that *S. pyogenes* uses hyaluronate lyases of bacteriophage origin in the degradation of its capsule (Smith *et al.*, 2005), while using the chromosomal hyaluronate lyase in degrading the connective tissues of the host. Also, these enzymes differ from each other in their structure and biochemical characteristics.

6.3 Summary

A non-sulphated GAG, HA is the main constituent of human connective tissue. It is targeted by different virulence factors of pathogenic bacteria such as *S. pneumoniae*, *S. agalacatiae* and *S. pyogenes*. Therefore the development of hyaluronate inhibitors is required in order to prevent the effects of such virulence factors. This aim will be achieved through the study of the biochemical and three-dimensional properties of these enzymes, in order to achieve a comprehensive understanding of their mechanism of action.

The ORF *hylA* of 2418 bp from pathogenic bacterium *S. pyogenes* strain SF370 which encodes a hyaluronate lyase was cloned and expressed at a high levels in a soluble form in *E. coli* BL21 (DE3). The biochemical characterization of the enzyme has been determined, and it was found that the optimum activity of *S. pyogenes* hyaluronate lyase is at pH 6 and 47 °C. The kinetic parameters, K_m and k_{cat}, of the wild type against HA were 0.206 ± 0.012 mg $ml^{-1}$and 17.3 ± 1.04 s^{-1}, respectively. Furthermore, HPAEC analysis revealed that the enzyme exhibits endolytic action producing various oligosaccharides. The endolytic cleavage of HA will allow the use of this enzyme as an effective reagent in preparing different sizes of oligasaccharides for studies of structure and function. *S. pyogenes* hyaluronate lyase HylA was crystallized and sufficient quality diffraction data obtained for structure solution. The crystals belong to space group P212121 and have unit cell dimensions of a = 51.111 Å, b = 88.497 Å and c = 159.089 Å. In addition, mutant proteins were generated of highly conserved amino acids within the active site of HylA. These mutant forms were expressed solubly in high levels in *E. coli* BL21 (DE3) and were purified in the same manner as the wild type enzyme. The mutants Y327A, Y327F and N257A were completely inactive toward HA, while the

mutant H307A showed very little activity against HA which was approximately 5 % of the level of activity of the wild type.

6.4 Future work

The biochemical characterisation of hyaluronate lyase HylA from *S. pyogenes* SF370 has been determined in this work. However, due to insufficient time several areas of analysis were not covered in this study that would be very useful in helping to understand the enzyme. For instance, determining the effect of different concentrations of $MnCl_2$ and $CaCl_2$ on the activity and on the kinetic parameters of the enzyme would be illuminating. Additionally, the purification of sufficient quantities of oligosaccharides of varying d.p. to enable their subsequent use to further study the kinetic parameters of the enzyme would enable further insight. Furthermore, this project has initiated the structural study of the enzyme; therefore optimisation of enzyme expression in order to prevent its degradation will facilitate in determining the structure of the full length the wild type as well as mutant forms, and also in complex with different oilgosaccharides, vitamin C and L-ascorbic acid-6-hexadecanoate. Designing high affinity inhibitors may result in reducing the virulence of pathogenic bacteria that produce hyaluronate lyases.

Chapter 7 Results and discussion: cloning, expression and characterisation of Spy0628 encoding a putative heparin lyase from *Streptococcus pyogenes* SF370

7.1 Introduction

The genome of *S. pyogenes* a Gram-positive pathogen, was sequenced in 2001, and was found to be composed of 1,852,442-bp and to contain 1,752 predicted protein-encoding genes. Roughly one-third of these genes have unknown functions, while the remainder are categorised as of known function. More than 40 putative virulence-associated genes have been recognized. It is well known that *S. pyogenes* is accountable for a wide diversity of human diseases than any other bacterial species (Ferretti et al., 2001). Among these virulence genes is Spy0628, which encodes putative heparin lyase.

Heparin lyases are a general class of enzymes which are able to cleave the glycosidic bonds in heparin and heparan sulphate. A number of heparin lyases of bacterial origin have been purified and characterized from different species such as *Flavobacterium heparinum* (Yang et al., 1985; Lohse and Linhardt, 1992), *Bacteroides heparinolyticus* (Watanabe et al., 1998), and *Bacteroides stercoris* HJ-15 (Kim et al., 2000; Kim et al., 2004). Heparinases from *F. heparinum*, have been extensively studied and three heparin lyases have been cloned, expressed, purified and characterized (Lohse and Linhardt, 1992; Sasisekharan et al., 1993; Ernst *et al.*, 1996;). These enzymes vary in their ability to cleave heparin and heparan sulfate, which are major components of the extracellular matrix and are also found at the cell surface as part of proteoglycan-cell surface receptors. Recently, the structure of Heparinase II from *F. heparinum*

(*Pedobacter heparinum*) has been solved and it has been found that the overall structure of this protein is similar to the enzymes of PL 8 and PL 5 (Shaya et al., 2006). However, while PL 8 enzymes which form monomers, Heparinase II forms dimers, with two active sites formed separately within each monomer (Shaya et al., 2006).

PL 12 comprises 44 bacteria producing heparin lyases, 41% of these organisms in this family are streptococci species, 39% are streptococci group B and 61% are streptococci group A. As it can be seen from Figure 7.1 that the aligment between these enzymes revealed that there are 23 conserved amino acids. The number of conserved amino acids in PL 12 are higher than that between the members of PL 8 indicating that the enzymes of this family are more similar.

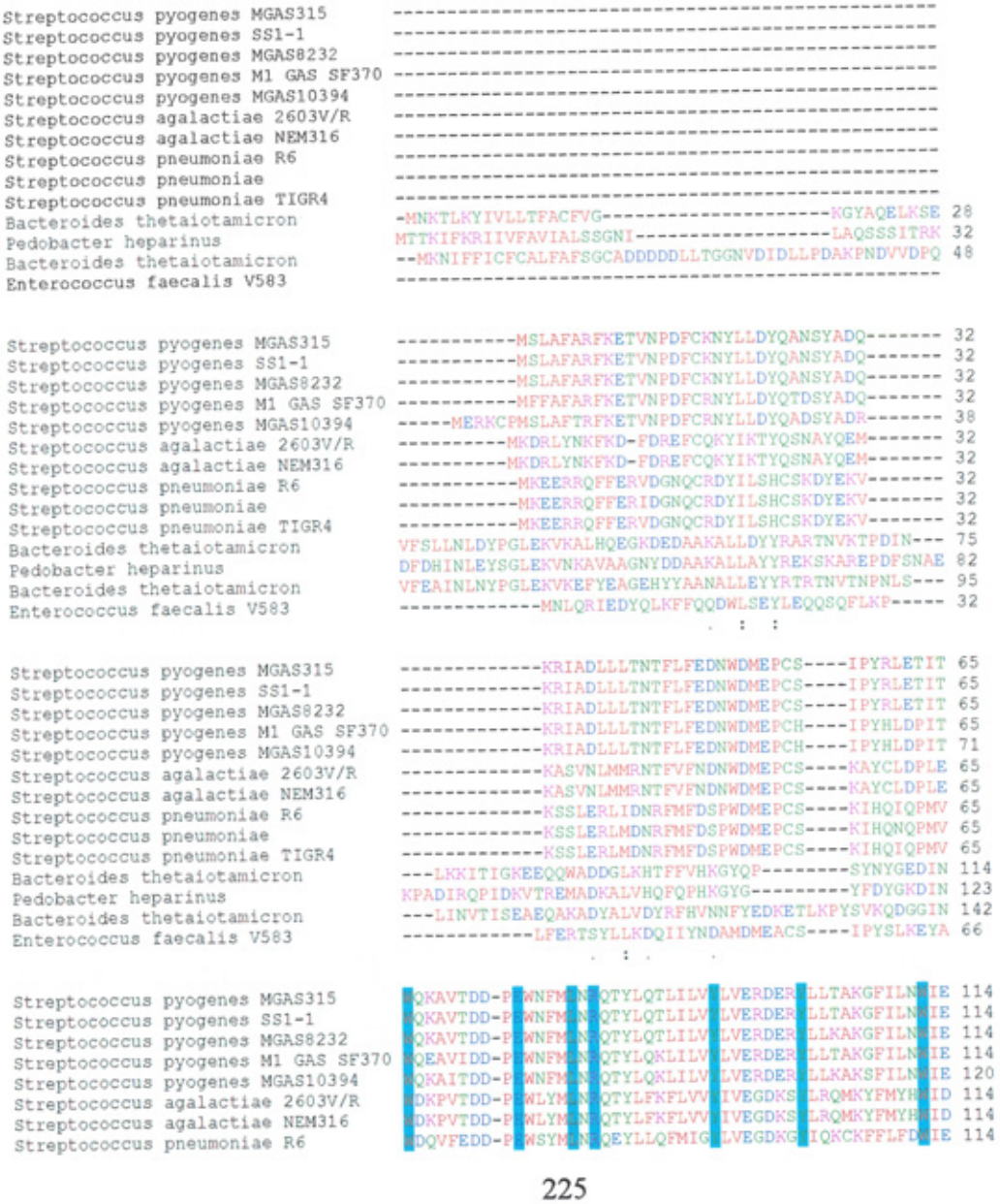

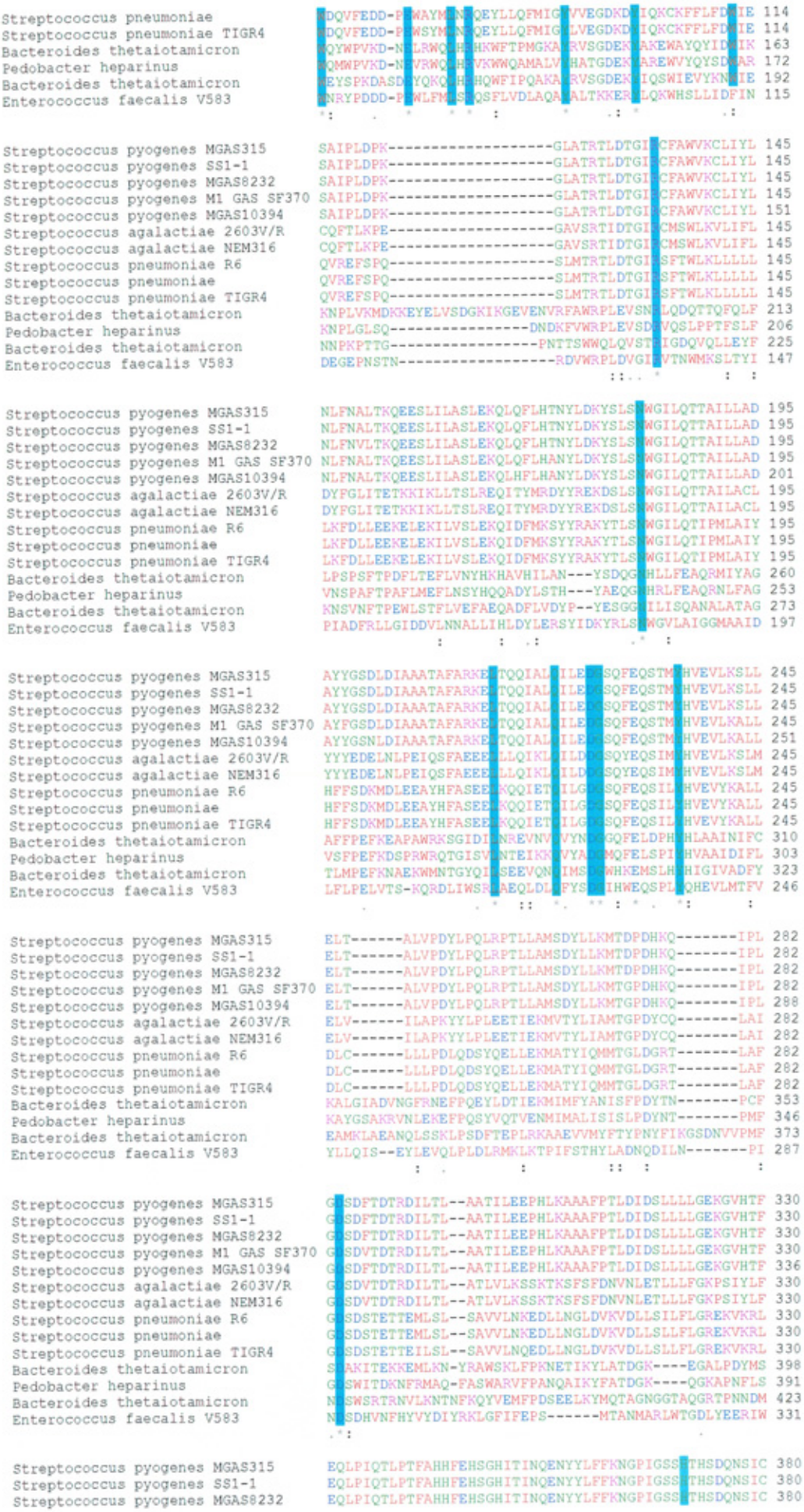
Streptococcus pneumoniae
Streptococcus pneumoniae TIGR4
Bacteroides thetaiotamicron
Pedobacter heparinus
Bacteroides thetaiotamicron
Enterococcus faecalis V583
Streptococcus pyogenes MGAS315
Streptococcus pyogenes SS1-1
Streptococcus pyogenes MGAS8232
Streptococcus pyogenes M1 GAS SF370
Streptococcus pyogenes MGAS10394
Streptococcus agalactiae 2603V/R
Streptococcus agalactiae NEM316
Streptococcus pneumoniae R6
Streptococcus pneumoniae
Streptococcus pneumoniae TIGR4
Bacteroides thetaiotamicron
Pedobacter heparinus
Bacteroides thetaiotamicron
Enterococcus faecalis V583

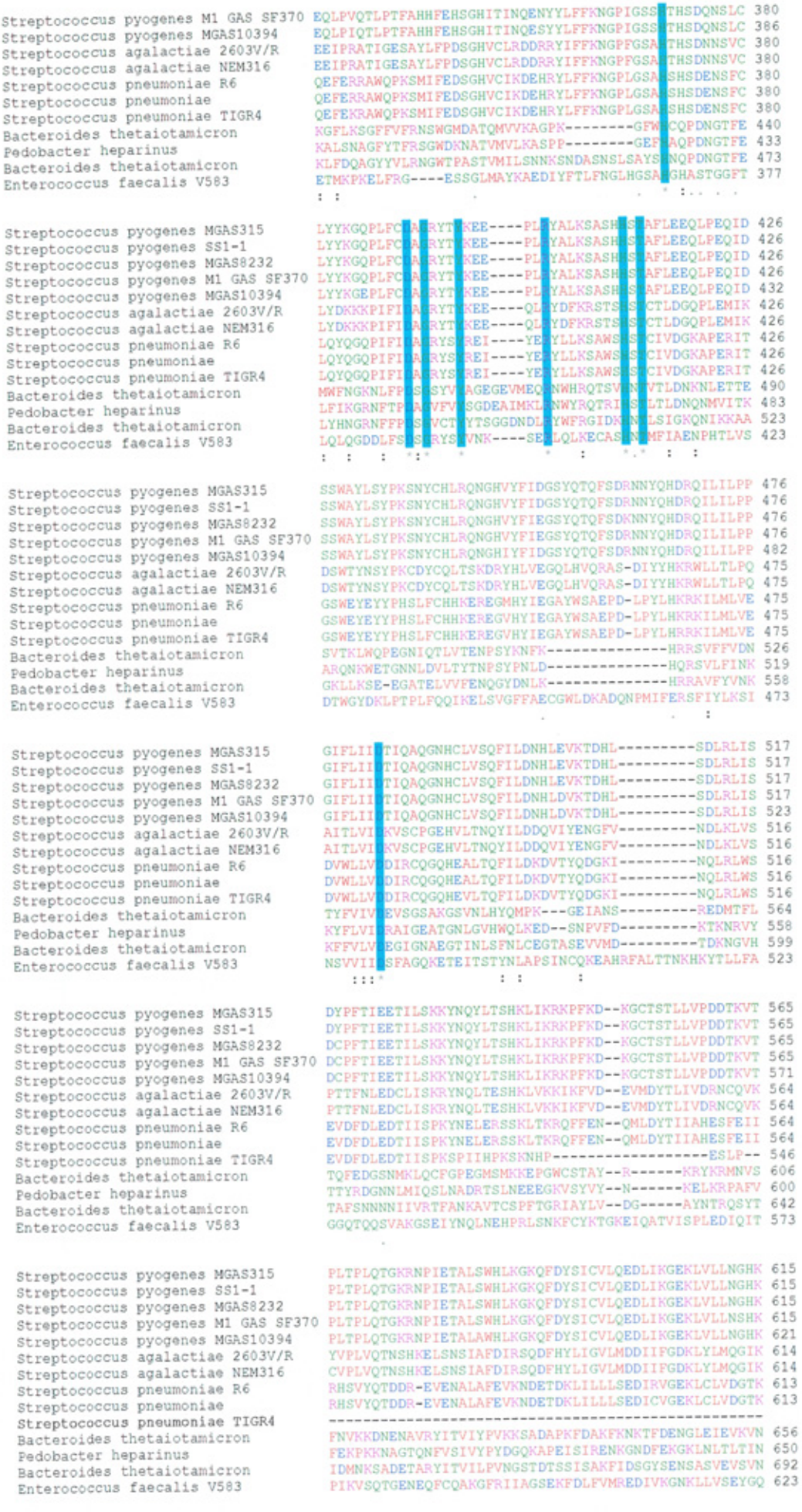
Streptococcus pyogenes M1 GAS SF370
Streptococcus pyogenes MGAS10394
Streptococcus agalactiae 2603V/R
Streptococcus agalactiae NEM316
Streptococcus pneumoniae R6
Streptococcus pneumoniae
Streptococcus pneumoniae TIGR4
Bacteroides thetaiotamicron
Pedobacter heparinus
Bacteroides thetaiotamicron
Enterococcus faecalis V583
Streptococcus pyogenes MGAS315
Streptococcus pyogenes SS1-1
Streptococcus pyogenes MGAS8232
Streptococcus pyogenes M1 GAS SF370
Streptococcus pyogenes MGAS10394
Streptococcus agalactiae 2603V/R
Streptococcus agalactiae NEM316
Streptococcus pneumoniae R6
Streptococcus pneumoniae
Streptococcus pneumoniae TIGR4
Bacteroides thetaiotamicron
Pedobacter heparinus
Bacteroides thetaiotamicron
Enterococcus faecalis V583

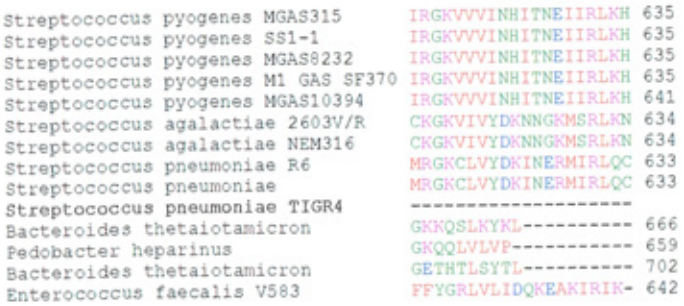

Figure 7.1 Sequence aligment of Spy0628 with heparine lyases of different organisms of PL 12. Sequence was colored according to residue properties: red, hydrophobic; magenta, Basic positively charged; blue, Acidic negatively charged; green, hydroxyl + Amine + basic-Q.

The purpose of the part of the research described in this thesis was to clone, express, purify and characterise the ORF Spy0628 from *S. pyogenes* SF370 which encodes the heparin sulphate lyase of polysaccharide lyase family 12. No structural information was previously available for this family.

7.2 Cloning, expression and purification of Spy0628 recombinant protein

The gene *Spy0628* of 1901 bp from *S. pyogenes* SF370 encodes heparin sulphate lyase which belongs to polysaccharide lyase family 12. It was directly amplified by PCR from *S. pyogenes* SF370 genomic DNA. To facilitate cloning into pET-28a and -22b *Nde I* restriction site was engineered at the 5 end and a *BamH I* and *xho I* site at the 3 end of the gene. Subsequently, PCR products of 1901 bp were ligated into expression vectors pET-28a and pET-22b and the ligation product was transformed into *E. coli* cells and screened for positive clones. The plasmid DNA was isolated and transformed into BL21 (DE3) for expression. Spy0628 was expressed solubly in *E. coli* in two forms, one with an N-terminal histidine tag and the other without tag in pET-28a and -22b respectively.

The histidine tag enabled quick purification of the enzyme on a charged nickel-charged chelating resin column.

E. coli cells harbouring pSpy0628 were grown at 20 °C in LB media supplemented with kanamycinin, the presence of IPTG at 1 mM for the induction of gene expression. Induced cultures were allowed to grow overnight. Cultured cells were harvested by centrifugation at 5500 x g for 10 min at 4 °C. The resulting cell pellets were suspended in starting buffer. The suspension was disrupted by a period of sonication for 2 min, then cell debris was removed by centrifugation at 24000 x *g* for 30 min at 4 °C. Unless otherwise specified, all operations were conducted at 4 °C. 20 ml of the supernatant was purified through affinity chromatography using nickel-charged Sepharose chelating fast flow resin that had been pre-equilibrated with 50 mM sodium phosphate, followed by gel filtration chromatography. It has an apparent molecular weight of 75 kDa as estimated by SDS-PAGE, according to the procedure previously described by Laemmli (1970). Then the purified protein was concentrated and exchanged into 10mMHepes buffer, pH 7.4.

A check of absorbance at 232 nm was performed using a spectrophotometer, which was adjusted to different temperatures, including 30, 37 and 40 °C, with different concentrations of recombinant enzyme in order to check the formation of the double bond in the degradation reaction. The reaction used heparin and heparan sulphate as substrates. The enzyme showed negligible activity against both heparin and heparan sulphate substrates.

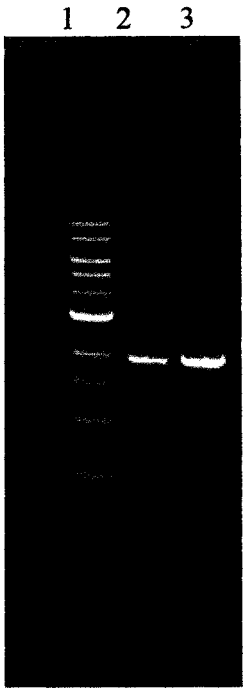

Figure 7.2 Visualisation of DNA bands following agarose gel electrophoresis
DNA products created during a PCR. Lane 1: 1 Kb DNA ladder (10, 8, 6, 5, 4, 3, 2, 1.5, 1, 0.5 Kb). Lane 2: 5 µl of *Spy0628* stop (1901bp); Lane 3: 5 µl of *Spy0628* no-stop from *S. pyogenes* SF370; DNA samples were subjected to 1 % agarose gel electrophoresis at 100 mA and 200 V for 45 min (section 2.2.2.1.5). Subsequently, gels were immersed in 10 $\mu g \cdot ml^{-1}$ solution of ethidium bromide for 10 min then washed with distilled water and placed on a UV illuminator and a fluorescent image was taken (section 2.2.2.1.6).

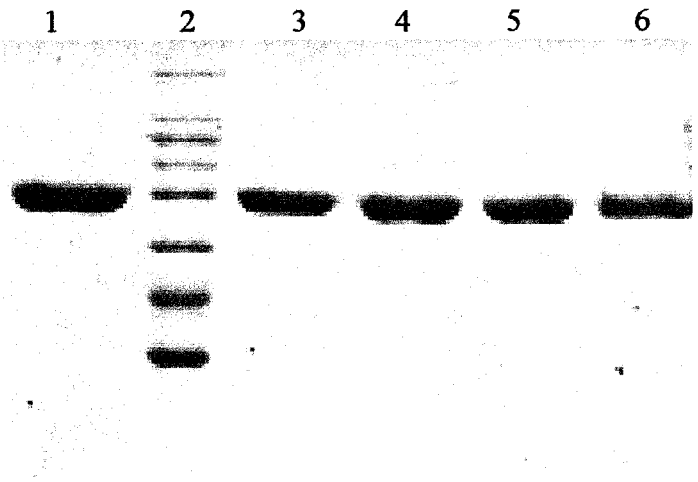

Figure 7.3 12% SDS-PAGE of Spy0628 expression.

Spy0628 was purified from *E. coli* cells harbouring plasmid 28a containing Spy0628 fragment by IMAC (section 2.2.3.4). Lane 2: High molecular weight (HMW) markers (205, 116, 97, 84, 66, 55, 45, 36 kDa); Lanes 1, 3, 5 and 6. 20 µl of protein (fractions 1-5 are shown). Proteins were visualised by staining with Coomassie blue and destained (section 2.2.3.1.1).

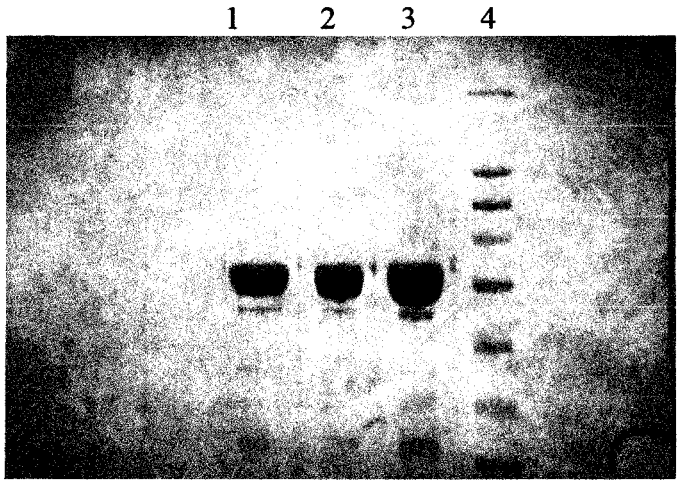

Figure 7.4 12% SDS-PAGE of Spy0628 purification through gel filtration column (section 2.2.3.6). Lane 1, 2 and 3. 20 µl of protein (fractions 1-3) Lane 4: high molecular weight (HMW) markers (205, 116, 97, 84, 66, 55, 45, 36 kDa). Proteins were visualised by staining with Coomassie blue and destained (section 2.2.3.1.1).

7.3 Crystallisation of Spy0628

Spy0628 encoded heparin sulphate lyase from *S. pyogenes* SF370 was purified to apparent homogeneity (as judged by SDS-PAGE; section 2.2 3.1.1; Figure7.2) from the plasmid 28a to produce the protein of N-terminal histadine tag.

Purified proteins were divided into two parts. One part was concentrated in water and the other part was concentrated in 10 mM Tris-HCl, pH 8 to a concentration of between 8 to 10 mg ml^{-1} (section 2.2.3.8) using membranes with appropriate molecular weight cutoffs. The protein was then screened for crystallization conditions using all the available screens Crystal Screen 1, Crystal Screen 2 and PEG/Ion Screen and Clear Strategy Screen I and II (appendix III; Tables III A, III B, III C, III D and III E respectively). Drops containing 1 µl of protein (at a concentration of 9 mg ml^{-1}) were mixed together with 1 µl and 2 µl of the reservoir. More crystallization trials were set up with the protein in an attempt to make crystals. But even after many trials and trying various conditions, crystals could not be achieved. A possible reason is that the protein tends to aggregate with all types of reservoir solutions.

7.4 Discussion

Many pathogenic and non-pathogenic bacteria produce heparine lyases, including *S. pyogenes* of different strains, *S. pneumoniae, Bacteriodes stercoris, Bacteroides heparinolyticus* and *F. heparimum* (CAZy database, http://afmb.cnrs-mrs.fr/CAZY/PL.html). The majority of bacteria that produce heparinases are found in soil (Ernst *et al.*, 1995). These enzymes cut glucosamine-uronate linkages by an elimination mechanism resulting in the formation of products containing unsaturated double bonds that can be simply identified by ultraviolet absorbance at 232 nm (Yang *et al.*, 1985; Lohse and Linhardt, 1992; Sasisekharan *et al.*, 1993; and Shaya *et al.*, 2006).

The gene coding for heparin sulphate lyase was expressed in *E. coli* BL21 (DE3). This enzyme consists of 635 amino acid and has a molecular weight of 75 kDa. The enzyme was found to be inactive against heparin and heparan sulphate as well as all other GAGs. The only enzymes that have been purified and characterised from family 12 are three different enzymes from *F. heparinium*. These enzymes are heparinase I which acts mainly on heparin, heparinase II which degrades both heparin and heparan sulphate and heparinase III which merely cleaves heparan sulphate. These enzymes have molecular weights of 42.5, 85.9 and 73.9 kDa respectively (Yang *et al.*, 1985;). The molecular weight of Spy0628 is similar to that of heparinase III. According to the clustalW alignment of Spy0628 with other lyases of family 12 (Figure 8.1), the enzyme has 16 % identity with the heparinase III of *F. heparinum*, which degrades only heparane sulphate.

Chapter 8 General discussion

Hyaluronidases are a group of very different enzymes, which degrade HA, the main compound of the ECM (Kreil, 1995; Frost et al., 1996; Csoka et al., 1997). Some of these enzymes have the ability to degrade other GAGs such as chondroitin, chondroitin-4-sulphate and chondroitin-6-sulphate but at a slower rate. The majority of eukaryotic hyaluronidases have both hydrolytic and transglycosidase activities, while bacterial hyaluronidases perform β-elimination mechanism (Morey et al., 2006), which results in unsaturated oligosaccharides of various lengths or disaccharides on the terminal glucuronyl group with a double bond in 4,5-position (Hertel et al., 2006). hyaluronate lyases of pathogenic bacteria have been implicated as virulence factors contribute to the spreading of microorganisms in tissues. They catalyze the cleavage of glycosidic bonds between the uronic acid and hexosamine residues of the HA (Rigden et al., 2006).

On the basis of the results for both enzymes, *S. coelicolor* hyaluronate lyase differs from *S. pyogenes* hyaluronate lyase in several respects, but the active sites and catalytic residues of the two enzymes were found to be nearly similar. Sequence alignment between *S. coelicolor* hyaluronate lyase and *S. pyogenes* revealed that the catalytic residues and some of the aromatic patch are conserved between these two enzymes. In *S. pyogenes* and *S. coelicolor* hyaluronate lyases the catalytic residues are His307, Tyr327, Asn257 and His244, Tyr253, Asn194; respectively. Site-directed mutagenesis and enzymatic activity measurement on the catalytic residues of these two enzymes had shown that mutations of these residues eliminate the activity of both enzymes.

The hyaluronate lyase of *S. coelicolor* shows low level of homology to *S. pyogenes* (21% identity) extending over the entire length of the enzymes. Since the N-terminal domain of *S. coelicolor* hyaluronate lyase is responsible for substrate binding and catalysis, the low level of homology between their N-terminal domains result in the difference in the substrate specificity and mode of action between these two enzymes. In view of the fact that both enzymes have some sequence similarity and belong to the same family, this implies that they come from the same ancestor.

The optimum pH values were also not significantly different, 5.2 in the case of the *S. coelicolor* hyaluronate lyase and 6 in the *S. pyogenes* hyaluronate lyase. Interestingly, the *S. coelicolor* hyaluronate lyase was more active at acidic pH especially within the range of 4.8 to 5.6 compared to the *S. pyogenes* hyaluronate lyase which was more active at pH values higher than 5.6. This may indicate that the *S. coelicolor* hyaluronate lyase has a mechanistic feature allowing it to function at a lower pH. However, the two differed in terms of specificity, kinetic constants, optimum temperatures of activity, the effect of divalent cations on activity and the mode of action. *S. pyogenes* hyaluronate lyase exhibited absolute specificity for HA than that of the *S. coelicolor* enzyme which degraded a relatively broad spectrum of substrates including HA, chondroitin-4-sulphate and chondroitin- 6-sulphate and the *S. coelicolor* enzyme was remarkably more active at high temperatures than the *S. pyogenes* enzyme. The specificity of *S. pyogenes* hyaluronate lyase toward only HA could be useful tool for degrading HA without affecting chondroitin sulphate. Therefore it may possibly used instead of bovine testicular hyaluronidase which degrades both HA and chondroitin sulphate.

Additionally, in contrast to the *S. pyogenes* hyaluronate lyase, which is endo-acting releasing a series of different sizes of unsaturated oligosaccharides from HA, the *S.*

coelicolor hyaluronate lyase was exo-acting releasing disaccharides throughout the digestion time. Degradation of HA by hyaluronate lyase has two possible roles in the biology of *S. pyogenes,* increase invasion and spread of the bacteria during infection by the degradation of HA polymer to provide smaller molecules that can then be used as carbon sources in the metabolism of the bacteria. These roles may be essential during pathogenesis of the different diseases caused by *S. pyogenes*.

Moreover, the catalytic efficiency of *S. coelicolor* hyaluronate lyase was significantly lower than *S. pyogenes* hyaluronate lyase, possibly because in the case of *S. coelicolor* hyaluronate lyase, the enzyme binds to a cleavage site of the polymeric substrate chain, degrades it and moves along the substrate chain continually until the whole chain is degraded (processive pattern). Consequently it is faster than *S. pyogenes* hyaluronate lyase which leaves the substrate chain after the first degradation, then binds randomly to another cleavage site on the same or different substrate chain (non processive).
In the activity inhibition test, the results showed that vitamin C (L-ascorbic Acid) has certain inhibitory effects on the enzyme activity of *S. pyogenes* hyaluronate lyase. It can be considered as a substrate analogue of hyaluronate lyase since it competitively inhibits the HA degradation. Large concentration of Vc in human tissues give a low level of natural resistance to such bacterial invasion. On the other hand this compound had no significant influence on the activity of *S. coelicolor* hyaluronate lyase

Study of hyaluronidases and their inhibitors is essential as these enzymes are implicated in several physiological and pathological processes. It is known that hyaluronidases are able to enhance the tissue membrane permeability and cause reduction in viscosity of the injected fluids. Therefore they have been widely used in therapeutics. They improve the distribution of the intramuscularly or subcutaneously administered compounds in

the tissue and enhance their absorption, extravasated blood in the tissues and increase the efficiency of local anesthetics. Consequently, they have an extensive application in orthopaedics, dermatology, surgery, ophthalmology, oncology, internal medicine and gynecology. (Manzel and Farr, 1998; Frost et al. 1996). Furthermore, it was reported, that treatment with hyaluronate lyases block lymph node invasion by tumour cells in an animal model of T cell lymphoma.

Moreover hyaluronidase inhibitors could be valuable as pharmacological tools to clarify the specific roles of hyaluronidases or as drugs combined with antibiotics, in antibacterial therapy of hyaluronate lyase producing bacteria (Botzki et al., 2004).

Additionally these enzymes have numerous applications in studies of the chemical structure and biological functions of GAGs and could be suitable for commercial development. Also, they are useful for the preparation of low molecular weight fragments of GAGs which have potential commercial value.

Chapter 9 References

Abramson, C. and Friedman, H. (1969). Electrophoretic characteristics of Staphylococcal hyaluronate lyase. *Journal of Bacteriology*. **97** (2), 715-718.

Adams, J.C., and Watt, F.M. (1993). Regulation of development and differentiation by the extracellular matrix. *Development*. **117**, 1183-1189.

Akhtar, S., and Bhakun, V. (2003). Streptococcus pneumoniae hyaluronate lyase contains two non-cooperative independent folding/unfolding structural domains. *The Journal Of Biological Chemistry*. **278** (28), 25509-25516.

Akhtar, S., and Bhakun, V. (2004) *Streptococcus pneumoniae* hyaluronate lyase: An overview. *Current Science*. **86** (2), 285-295.

Alberti, S; Ashbaugh, C.D; and Wessels, M.R. (1998). Structure of the has operon promoter and regulation of hyaluronic acid capsule expression in group A Sreptococcus. *Molecular Microbiology*. **28** (2), 343- 353.

Allen, A.G., Lindsay, H., Seilly, D., Bolitho, S., Peters, S.E., and Maskell, D.J. (2004). Identification and characterisation of hyaluronate lyase from Streptococcus suis. *Microbial Pathogenesis*. **36**, 327-335.

Ashbaugh, C.D., Alberti, S., and Wessels, M.R. (1998). Molecular analysis of the capsule gene region of group A Streptococci: the hasAB genes are sufficient for capsule expression. *Journal of Bacteriology*. **180** (18), 4955-4959.

Bajorath, J; Greenfield, B; Munro, S.B; Day, A.J; and Aruffo, A. (1998). Identification of CD44 residues important for hyaluronan binding and delineation of the binding site. *The Journal of Biological Chemistry*. **273** (1), 338-343.

Baker, J.R., Yu, H., Morrison, K., Averett, W. F., and Pritchard. D.G. (1997). Specificity of the hyaluronate lyase of group-B streptococcus toward unsulphated regions of chondroitin sulphate. *Biochemical Journal*. **327** (1). 65-71.

Baker, J.R., and Pritchard. D.G. (2000). Action pattern and substrate specificity of hyaluronan lyase from group B Streptococci. *Biochemical Journal*. 348. 465-471.

Baker, J.R., Dong, S. and Pritchard. D.G. (2002). The hyaluronan lyase of Streptococcus pyogenes bacteriophage H4489A. Biochimical Journal. **365**, 317-322.
Baltz, R.H. (1998). Genetic manipulation of antibiotic-producing Streptomyces. Trends in Microbiology. 6 (2), 76-82.

Bame, K.J. (2001). Heparanases: endoglycosidases that degrade heparan sulphate proteoglycans. *Glycobiology*. **11** (6), 91-98.

Bellamy, W.R. (1990). A novel Bacillus sp. Capable of degrading sulphated glycosaminoglycans. In: Superbugs, Microorganisms in Extreme Enviroments. Pp. 143-157. Horikoshi, K. and Grant, W.D., Eds., Japan Scientific Societies Press, Tokyo.

Bentley, S.D., Chater, K.F., Cerdeno-Tarraga, A.-M., Challis, G.L., Thompson, N.R., James, K.D., *et al.* (2002) Complete genome sequence of the model actinomycete *Streptomyces coelicolor* A3(2). *Nature* **417,** 141–147.

Bentley, S.D., Brown, S., Murphy, L.D., Harris, D.E., Quail, M.A., Parkhill, J., Barrell, B.G., McCormick, J.R. Losick, S.R., Yamasaki, M., Kinashi, H., Chen, C. W., Chandra, G., Jakimowicz, D., Kieser, H. M., Kieser, T., and Chater, K. F. (2004). SCP1, a 356 023 bp linear plasmid adapted to the ecology and developmental biology of its host, Streptomyces coelicolor A3(2). *Molecular Microbiology*. **51**, 1615–1628.

Bisno, A.L. (1979). Alternate complment pathway activation by group A streptococci: role of M-protein. *Infection and Immunity*. **26** (3), 1172-1176.

Bisno, A.L. (1991). Group-A streptococcal infection and acute Rheumatic-fever. *New England Journal of Medicine*. **325** (11): 783-793.

Bisno, A.L. (1993). Acute Rheumatic-fever: A present-day perspective. *Medicine*. **72**, 278-283.

Bisno, A.L., Brito, M.O., and Collins, C.M. (2003). Molecular basis of group A streptococcus virulence. *The Lancet: Infections Diseases*. **3,** 191-200.

Bonsor, D., Butz, S.F., Solomons, J., Grant, S., Fairlamb, I.J.S., Fogg, M.J., and Grogan, G. (2006). Ligation independent cloning (LIC) as a rapid route to families of recombinant biocatalysts from sequenced prokaryotic genomes. *Organic and Biomolecular Chemistry*. **4** (7), 1252-1260.

Bosman, F.T., and Stamenkovic, I. (2003). Functional structure and composition of the extracellular matrix. *Journal of Pathology*. **200**, 423-428.

Botzki, A., Rigden, D.J., Braun, S., Nukui, M., Salmen, S., Hoechstetter, J., Bernhardt, G., Dove, S., Jedrzejas, M.J., and Buschauer, A. (2004). L-Ascorbic acid 6-hexadecanoate, a potent hyaluronidase inhibitor. X-ray structure and molecular modelling of enzyme-inhibitor complexes. *The Journal of Biological Biochemistry*. **279** (44), 45990-45997.

Bradford, M. M. (1976). A refined sensitive method for the quantitation of microgram quantities of protein utilizing the principal of protein-dye binding. *Analytical Biochemistry*. **72**, 248-254.

Brecht, M., Mayer, U., Schlosser, E., and Prehm, P. (1986). Increased hyaluronate synthesis is required for fibroblast detachment and mitosis. *Biochemical Journal*. **239**, 445-450.

Brown, I.E., Mallen, M.H., Charnock, S.J., Davies, G.J., and Black., G.W. (2001). Pectate lyase 10A from Pseudomonas cellulose is a modular enzyme containing a family 2a caebohydrate-binding module. *Biochemical journal*. **355**, 155-165.

Buckwalter, J.A., and Mankin, H.J. (1997). Articular cartilage: Tissue Design and Chondrocyte-Matrix Interactions. *Journal of Bone and Joint Surgery*. **79** (4), 60-64.

Calabro, A., Midura, R., Wang, A., West, L., Plass, A., and Hascall, V.C. (2001). Flurophore-assisted carbohydrate electrophoresis (FACE) of glycosaminoglycans. *Osteoarthritis and Cartilage*. **9**, Supplement A, S16-S22.

Campbell, J.A., Davies, G.J., Bulone, V., and Henrissat, B. (1997). A classification of nucleotide-diphospho-sugar glycosyltransferases based on amino acid sequence similarities. *Biochemical Journal*. **326**, 929-942.

Capila, I., Wu, Y., Rethwisch, D.W., Matte, A., Cygler, M., Linhardt, R.J. (2002). Role of arginine 292 in the catalytic activity of chondroitin AC lyase from Flavobacterium heparinum. *Biochimica et Biophysica Acta*. **1597**, 260-270.

Caplan, A.I., and Bruder, S.P. (2001). Mesenchymal stem cells: Building blocks for molecular medicine in the 21st century. *Trends in Molecular Medicine*. 7, 259-264.

CCP4 (Collaborative Computational Project Number 4; 1994). *Acta Crystallographica Section D Biological Crystallography*. **50**, 760-763.

Charnock, S.J., Brown, I.E., Turkenburg, J.P., Black, G.E. and Davies, G.J. (2002a) Convergent evolution sheds light on the anti β-elimination mechanism common to family 1 and 10 polysaccharide lyases. *Proceedings of the National Academy of Sciences, USA*. **99**, (19), 12067-12072.

Chiquet-Ehrismann, R., and Tucker, R.P. (2004). Connective tissues. *The International Journal of Biochemistry and Cell Biology*. **36**, 1085-1089.

Cohen, S.N., Chang, A.C.Y., and Hsu, L. (1972). Nonchromosomal antibiotic resistance in bacteria: Genetic transformation of E. coli by R-factor DNA. *Proceedings of the National Academy of Sciences, USA.* ***69***, 2110-2114

Coleman, P.J. (2002). Evidence for a role of hyaluronan in the spacing of fibrils within collagen bundles in rabbit synovium. *Biochemicia et Biophysica Acta.* **1571**, 173-182.

Coutinho, P.M., and Henrissat, B. (1999). Carbohydrate-active enzymes server at URL: http://afmb.cnrs-mrs.fr/~cazy/CAZY/index.html

Cramer, J.A., Bailey, L.C., Bailey, C.A., Miller, R.T. (1994). Kinetic and mechanistic studies with bovine testicular hyaluronidase. *Biochimica et Biophysica Acta.* **1200**, 315-321.

Crater, D.L., and Van de Rijn, I. (1995). Hyaluronic acid synthesis operon (has) expression in group A Streptococci. *The journal of Biological chemistry.* **270** (31). 18452-18458.

Csoka, T.B., Frost, G.I., Wong, T., Stern, R. (1997). Purification and microsequencing of hyaluronidase isozymes from urine. *FEBS Letters.* **417**, 307-310.

Csoka, T.B., Frost, G.I., Heng, H.H., Schener, S.W., Mohapatra, G., and Stern, R. (1998). The hyaluronidase gene HYAL1 maps to chromosome 3p21.2-p21.3 in human and 9F1-F2 in mouse, a conserved candidate tumor suppressor locus. *Genomics.* **48** (1), 63-70.

Csoka, T.B., Frost, G.I., and Stern, R. (2001). The six hyaluronidase-like genes in the human and mouse genomes. *Matrix Biology.* **20**, 499-508.

Culty, M., Nguyen, H.A., and Underhill, C. B. (1992). The hyaluronan receptor (CD44) participates in the uptake and degradation of hyaluronan. *Journal of Cell Biology* **116**, 1055-1062.

Cunningham, M.W. (2000). Pathogenesis of group A Streptococcal infections. *Clinical Microbiology Reviews.* **13** (3), 470-511.

Davies, G. J. (1998). Structural studies on cellulases. *Biochemical Society Transactions.* **26**, 167-173.

Davies, G.J., and Henrissat, B. (1995). Structures and mechanisms of glycosyl hydrolases. *Structure.* **3**, 853-859.

Davies, G.J., Wilson, K.S. and Henrissat, B. (1997). Nomenclature for sugar-binding subsites in glycosyl hydrolases. *Biochemical Journal.* **321**, 557-559.

Davies, G.J., Gloster,T.M., and Henrissat, B. (2005). Recent structural insights into the expanding world of carbohydrate-active enzymes. *Current Opinion in Structural Biology* **15**:637–645

Day, A.J., and Sheehan, J.K. (2001). Hylauronan: polysaccharide chaos to protein organisation. *Current Opinion in Structural Biology.* **11**. 617-622.

Day, A.J., and Prestwich, G.D. (2002). Hyaluronan-binding proteins: Tying up the giant. *The journal of Biological chemistry.* **277** (7), 4585-4588.

Dougherty, B.A. and Van de Rijng, I. (1994). Molecular characterization of hasA from an operon required for hyaluronic Acid synthesis in group A Streptococci. *The journal of Biological chemistry.* **269** (1), 169-175.

Ernst, S., Langer, R., Cooney, C.L., and Sasisekharan, R. (1995). Enzymatic degradation of glycosaminoglycans. *Critical Reviews in Biochemistry and Molecular Biology.* **30** (5), 387-444.

Ernst, S., Venkataraman, G., Winkler, S., Godavarti, R., Langer, R., Cooney, C.L., and Sasisekharan, R. (1996). Expression in Escherichia coli, purification and characterization of heparinase I from Flavobacterium heparinum. *Biochemical Journal.* **315**, 589-597.

Esko, J.D., and Lindahl, U. (2001). Molecular diversity of heparan sulphate. *The Journal of Clinical Investigation.* **108** (2), 169-173.

Eyal, O., Jadoun, J., Bitler, A., Skutelski, E, and Shlomo, S. (2003). Role of M3 protein in the adherence and internalisation of an invasive *Streptococcus pyogenes* strain by epithelial cells. *FEMS Immunology and Medical Microbiology.* **38**, 205-213.

Fethiere, J., Eggimann, B. and Cygler, M. (1999). Crystal structure of chondroitin AC lyase, a representative of a family of glycosaminoglycan degrading enzymes. *Journal of Molecular Biology.* **288**, 635-647.

Fischetti, V.A. (1989). Streptococcal M protein: molecular design and biological behavior. *Clinical Microbiology Review.* **2**, 285-314.

Fontaine, M.C, Lee, J.J, and Kehoe, M.A. (2003). Combined contributions of streptolysin O and streptolysin S tovirulence of serotype M5 streptococcus pyogenes strain Manfredo. *Infection and Immunity.* **71** (7). 3857-3865.

Franco, C.R.C., Rocha, H.A.O., Trindade, E.S., Santos, I.A.N., Leite, E.L., Veiga, S.S., Nader, H.B., and Dietrich, C.P. (2001). Heparan sulphate and control of cell division: adhesion and prolifiration of mutant CHO-745 cells lacking xylosyl transferase. *Brazilian Journal of Medical and Biological Research.* **34** (8) 971-975.

Fraser, J. R. E., Kimpton, W. G., Laurent, T. C., Cahill, R. P., and Vakakis, N. (1988). Uptake and degradation of hyaluronan in lymphatic tissue. *Biochemical Journal.* **256**, 153-158.

Fraser, J.R.E., and Laurent, T.C. (1997). Hyaluronan. Minisymposium. *Journal of Internal Medicine.* **242**, 25-26.

Fraser, J.R.E., Laurent, T.C. and Laurent, U.B.G (1997). Hyaluronan: its nature, distribution, functions and turnover. *Journal of Internal Medicine*. **242,** 27-33.

Frick, I., Schmidtchen, A., and Sjobring, U. (2003). Interactions between M proteins of *streptococcus pyogenes* and glycosaminoglycans promote bacterial adhesion to host cells. *European Journal of Biochemistry*. **270**, 2303-2311.

Frost, G.I., Cso´ka, T.B., and Stern, R. (1996). The hyaluronidases: A chemical, biological and clinical overview. Trends In Glycoscience and Glycotechnology. 8 (44): 419-434.

Frost, G.I., Cso´ka, T.B., Wong, T., and Stern, R. (1997). Purification, Cloning, and Expression of Human Plasma Hyaluronidase. *Biochemical and Biophysical Research Communication.* **236,** 10–15.

Funderburg, J.L. (2000). Keratan sulphate: Structure, Biosynthesis and function. *Glycobiology*. **10** (10), 951-958.

Gacesa, P. (1987). Alginate-modifying enzymes. A prpposed unified mechanism of action for the lyases and epimerises. *FEBS*. **212** (2), 199-202.

Gase, K., Ozegowski, J., and Malke, H. (1998). The *Streptococcus agalactiae* hylB gene encoding hyaluronate lyase: completion of the sequence and expression analysis. *Biochimica et Biophysica Acta.* **1398** (1), 86-98.

Gerdin, B., and Hallgren, R. (1997). Dynamic role of hyaluronan (HYA) in connective tissue activation and inflammation. *Journal of Internal Medicine*. **242**, 49-55.

Girish, K.S., Shashidharamurthy, R., Nagaraju, S., Gowda, T.V., Kemparaju, K. (2004). Isolation and characterization of hyaluronidase a "spreading factor" from Indian cobra (Naja naja) venom. *Biochimie*. **86**, 193-202.

Gorham, S.D., Olavesen, H., and Dodgson, K.S. (1975). Effect of ionic strength and pH on the properties of purified bovine testicular hyaluronidase. *Connective Tissue Research*. **3**, 17-25.

Greiling, H., Stuhlsatz, H.W., and Eberhard, A. (1975). Studies on the mechanism of hyaluronate lyase action. *Connective Tissues Research*. **3**, 135-139.

Hamai, A., Morikawa, K., Horie, K., and Tokuyasu, K. (1989). Purification and characterisation of hyaluronidase from Streptococcus dysgalactiae. *Agriculture of Biological Chemistry*. **53**. 2163-2168.

Hamai, A., Hashimoto, N., Mochizuki, H., Kato, F., Makiguchi, Y., Horie, K., and Suzuki, S. (1997). Two distinct chondroitin sulphate ABC lyases. An endoeliminase yielding tetrasaccharides and an exoeliminase preferentially acting on oligosaccharides. *The Journal of Biological Biochemistry*. **272** (14), 9123-9130.

Hanahan D. (1983). Studies on transformation of Escherichia coli with plasmids. *Journal of Molecular Biology*. **166**, 557-580.

Hardingham, T.E. (1979). The role of link-protein in the structure of cartilage proteoglycan aggregates. *Biochemical Journal*. 177,237-247.

Hardingham, T.E., and Fosang, A.J. (1992). Proteoglycans: many forms and many functions. *The FASEB Journal*. **6**, 861-870

Hashimoto, W., Miki, H., Tsuchiya, N., Nankai, H., and Murata, K. (2001). Polysaccharide Lyase: Molecular cloning, sequencing, and overexpression of the Xanthan Lyase Gene of *Bacillus* sp. Strain GL1. *Applied and Environmental Microbioogyl.* **67**, 713–720

Hashimoto, W., Nankai, H., Mikami, B. and Murata, K. (2003). Crystal structure of Bacillus sp GL1 xanthan lyase, which acts on the side chains of xanthan. *The Journal of Biological Chemistry*. **278**, 7663-7673.

Haug, I., Weissenborn, A., Brolle, D., Bentley,S., Kieser, T., and Altenbuchner, J. (2003). Streptomyces coelicolor A3(2) plasmid SCP2*:deductions from the complete sequence. *Microbiology*. **149**, 505–513

Hedlund, H., Hedbom, E., Henegard, D., Mengarelli-Widholm, S., Reinhalt, F.P., and Svenssay, O. (1999). Association of the aggrecan keratan sulphate-rich region with collagen in bovine articular cartilage. *The Journal of Biological Chemistry*. **279** (9), 9777-9781.

Henrissat, B. (1991). A classification of glycosyl hydrolases based on amino acid sequence similarities. *Biochemical Journal*. **280**, 309-316.

Henrissat, B., and Bairoch, A. (1996). Updating the sequence-based classification of glycosyl hydrolases. *Biochemical Journal*. **316**, 695-696.

Henrissat, B., and Davies, G.J. (1997). Structural and sequence-based classification of glycoside hydrolases. *Current Opinion in Structural Biology*. 7, 637-644.

Henrissat, B. and Coutinho, P.M. (2000). CAZY website: http:// afmb.cnrsmrs.fr/CAZY/.

Henrissat, B., Coutinho, P.M., and Davies, G.J. (2001).A census of carbohydrate-active enzymes in the genome of Arabidopsis thaliana. *Plant Molecular Biology*. **47** (1-2), 55-72.

Hertel, W., Peschel, G., Ozegowski, H., J_rgen Muller, P. (2006). Inhibitory Effects of Triterpenes and Flavonoids on the Enzymatic Activity of Hyaluronic Acid-Splitting Enzymes. *Archieve of Pharmacology and Chemistry Life Science*. **339**, 313-318

Hiyama, K. (1976). Action of chondroitinases. *Journal of Biochemistry*. **80**, 1209-1214.

Hiyama, K. and Okada, S. (1975). Crystallization and some properties of chondroitinase from Arthrobacter aurescens. *Journal of Biological Chemistry*. **250** (5), 1824-1828.

Hollingshead, S.K; Fischettit, V.A; and Scott, J.R. (1986). Complete nucleotide sequence of type 6 M protein of the group A Streptococcus. *The Journal of Biological Chemistry*. **261**, (4). 1677-1686.

Hong, S., Kim, B., Shin, H., Kim, W., Lee, K., Kim, Y., and Kim, D. (2002). Purification and characterization of novel chondroitin ABC and AC lyases from Bacteroides stercoris HJ-15, a human intestinal anaerobic bacterium. European *Journal of Biochemisrey*. **269**, 2934-2940.

Hsu, C.H., Chu, Y.F., Argin-Soysal, S., Hahm, T.S., and LO, Y.M. (2004). Effects of surface characteristics and xanthan polymers on the immobilization of *Xanthomonas campestris* to fibrous matrices. *Journal of Food Science*. **69** (9), E441-E448.

Huang, W; Matte, A; Li, Y; Kim, Y. S; Linhardt, R. J; Su, H; and Cygler, M. (1999). Crystal Structure of Chondroitinase B fromFlavobacterium heparinum and its Complex

with aDisaccharide Product at 1.7 A Resolution. *Journal of Molecular Biology.* **294**, 1257-1269.

Huang, W., Boju, L., Tkalec, L., Su, H., Yang, H.O., Gunay, N.S., Linhardt, R.J., Kim, Y.S., Matte, A., and Cygler, M. (2001). Active site of chondroitin AC lyase revealed by the structure of enzyme oligosaccharide complexes and mutagenesis. *Biochemistry.* **40** (8), 2359-2372.

Huang, W., Lunin, V.V., Li, Y., Suzuki, S., Sugiura, N., Miyazono, H., and Cygler, M. (2003). Crystal structure of Proteus vulgaris chondroitin sulphate ABC lyase I at 1.9A resolution. *Journal of Molecular Biology.* **328** (3), 623-634.

Huber, M., Trattnig, S., and Lintner, F. (2000). Anatomy, biochemistry and physiology of articular cartilage. *Investigative Radiology.* **35** (10), 573-580.

Hynes, W.L., Hancock, L., and Ferreti, J.J. (1995). Analysis of a Second Bacteriophage Hyaluronidase Gene from *Streptococcus pyogenes*: Evidence for a Third Hyaluronidase Involved in Extracellular Enzymatic Activity. *Infection and Immunity.* **63**, 3015–3020

Hynes, W.L., and Walton, S.L. (2000). Hyaluronidases of Gram positive bacteria. *FEMS Microbiology Letters.* **183**, 201-207.

Ingham, E., Holland, K.T., Gowland, G. and Cunliffe, W.J. (1979). Purification and partial characterization of hyaluronate lyase (EC 4.2.2.1) from Propionbacterium acnes. *Journal of General Microbiology.* **115**, 411-418.

Itano, N., Atsumi, F., Sawai, T., Yamada., Y., Miyaishi., O., Senga, T., Hamaguchi, M., and Kimata, K. (2002). Abnormal accumulation of hyaluronan matrix diminishes contact inhibition of cell growth and promotes cell migration. *Proceedings of the National Academy of Sciences.* **99** (6). 3609-3614.

Itano, N., and Kimata, K. (1996). Expression cloning and molecular characterisation of Has protein, a Eukaryotic hyaluronan synthase. *The Journal of Biological Chemistry.* **271** (17). 9875-9878.

Iozzo. R.V. (1998). Matrix proteoglycans: from molecular design to cellular function. *Annual Review of Biochemistry.* **67**, 609-652.

Jandik, K.A., Gu, K., and Linharlt, R.J. (1994). Action pattern of polysaccharide lyases on glycosaminoglycans. *Glycobiology.* **4**, 289-296.

Jedrzejas, M.J., Mewbourne, R.B., Chantalat, L. and McPherson, D.T. (1998a). Expression and purification of *Streptococcus pneumoniae* hyaluronate lyase from *Escherchia coli. Protein Expression and Purification.* **13**, 83-89.

Jedrzejas, M.J., Chantalat, L. and Mewbourne, R.B. (1998b). Crystallization and preliminary X-ray analysis of *Streptococcus pneumoniae* hyaluronate lyase. *Journal of Structural Biology*. **121**, 71-73.

Jedrzejas, M.J. (2000). Structural and functional comparison of polysaccharide-degrading enzymes. *Critical Reviews in Biochemistry and Molecular Biology*. **35** (3), 221-251.

Jedrzejas, M.J., and Chantalat, L. (2000). Structural studies of Streptococcus agalactiae hyaluronate lyase. Acta Crystallogrphica. Section D *Biological Crystallography*. **56,** 460-463.

Jedrzejas, M. J. (2002). Three-dimensional structures of hyaluronate lyases from Streptococcus species and their mechanism of hyaluronan degradation. *Science of Hayluronan Today*; Glycoforum www.glycoforum.gr.jp/science/hyaluronan.

Jedrzejas, M.J., Mello, L.V., De Groot, B.L., and Li, S. (2002). Mechanism of hyaluronan degradation by Streptococcus pneumoniae hyaluronate lyase: structures of complexes with the substrate. *The Journal of Biological Chemistry*. **277**, 28287-28297.

Joy, M.B., Dodgson, K.S., Olavesen, A.H., and Gacesa, P. (1985). The purification and some properties of pig liver hyaluronidase. *Biochimica et Biophysica Acta.* **838**, 25263.

Junqueira, L.C., Carneiro, J., and Kelley, R.O. (1998). Basic Histology. 9th edi. Appleton and Lange Stamford. pp

Kakehi, K; Kinoshita, M; and Yasueda, S. (2003). Hyaluronic acid: separation and biological implications. *Journal of Chromatography B*, **797**, 347-355.

Karagouni, A.D., Vionis, A.P., Baker, P.W., Wellington, EMH. (1993). The effect of soil moisture content on spore germination, mycelium development and survival of a seeded streptomycete in soil. *Microbiology Release*. **2**, 47-51.

Kehoe, M.A. (1991). Group A streptococcal antigens and vaccine potential. *Vaccine*. **9** (11): 797-806

Kelly, S.J., Taylor, K.B., Li, S. and Jedrzejas, M.J. (2001). Kinetic properties of Streptococcus pneumoniae hyaluronate lyase. *Glycobiology.* **11**(4), 297-304.

Kiani, C., Chen, L., Wu, Y.J., Yee, A.J., and Yang, B.B. (2002). Structure and function of aggrecan. Cell Research. 12, 19-23.

Kim,, B., Kim, W., Kim, Y., Linhardt, R.J., and Kim, D. (2000). Purification and Characterization of a novel heparinase from *Bacteroides stercoris* HJ15. *Journal of Biochemistry.* **128**, 323-328.

Kim, W., Kim, B., Kim, D., and Kim, Y. (2004). Purification and Characterization of Heparin Lyase I from *Bacteroides stercoris* HJ15. *Journal of Biochemistry and Molecular Biology.* **37**, 684-690.

Kinashi, H and Shimaji-Murayama, M. (1991). Physical Characterization of SCP1, a Giant Linear Plasmid from Streptomyces coelicolor. *Journal of Bacteriology.* **173** (4). 1523-1529.

Knudson, W., Bartnik, E., and Knudson, C.B. (1993). Assembly of pericellular matrices by COS-7 cells transfected with CD44 lymphocyte-homing receptor genes. *Proceedings of the National Academy of Sciences, USA.* **90**, 4003-4007.

Knudson, W., Casey, B., Nishida, Y., Eger, W., Kuettner, K.E., and Knudson, C.B. (2000). Hyaluronan oligosaccharides perturb cartilage matrix homeostasis and induced chondrocytic chondrolysis. **43** (5). 1165-1174.

Knudson, C.B., and Knudson, W. (2001). Cartilage proteoglycans. *Cell and Development biology.* **12**. 69-78.

Kreil, G. (1995). Hyaluronidases- A group of neglected enzymes. *Protein Science.* **4**, 1666-1669.

Kuberan, B., Lech, M., Zhang, L., Wu, Z.L., Beeler, D.L., and Rosenberg, R.D. (2002). Analysis of heparan sulphate oligosaccharides with ion reverse phase capillary performance liquid chromatography- microelectrospray ionisation time of flight mass spectrometry. *Journal of American Chemical Society.*

Kudo, K., and Tu, A. T. (2001). Characterization of Hyaluronidase Isolated from *Agkistrodon contortrix contortrix* (Southern Copperhead) Venom. *Archives of Biochemistry and Biophysics.* **386** (2), 154–162

Kuettner, K.E. (1992). Biochemistry of articular cartilage in health and disease. *Clinical Biochemistry*. **25** (3), 155-163.

Kuhn, A.V., Raith, K., Sauerland,V., Neubert, R.H.H. (2003).Quantification of hyaluronic acid fragments in pharmaceutical formulations using LC-ESI-MS. *Journal of Pharmaceutical and Biomedical Analysis*, **30**, 1531-1537.

Lauder, R.M., Huckerby, T.N., and Nieduszynski, I.A. (2000). A fingerprinting method for chondroitin/dermatan sulphate and hyaluronan oligosaccharides. Glycobiology. 10 (4), 393-401.

Laurent, T.C. and Fraser, R.E. (1992). Hyaluronan. *FASEB.J.* **6**, 2397-2404

Laurent, U.B., Fraser, J.R., Engstrom-Laurent, A., Reed, R.K., Dahl, L.B., and Laurent, T.C. (1992). Catabolism of hyaluronan in the knee joint of the rabbit. *Matrix*. **12** (2), 130-136.

Laurent, T.C. Laurent, U.B., and Fraser, R.E. (1996). The structure and function of hyaluronan: an overview. *Immunology and Cell Biology*. **74**, AA7.

Leslie, A. G. W. 1992. Recent changes to the MOSFLM package for processing film and image plate data, Joint CCP4 and ESF-EACMB newsletter on protein crystallography, vol. **26**. Daresbury Laboratory, Warrington, UK.

Li, S., Kelly, S.J., Lamani, E., Ferraroni, M., and Jedrzejas, M.J. (2000). Structural basis of hyaluronan degradation by *Streptococcus pneumoniae* hyaluronate lyase. *EMBO Journal.* **19**:1228-1240.

Li, S. and Jedrzejas, M.J. (2001). Hyaluronan binding and degradation by Streptococcus agalactiae hyaluronate lyase. *The Journal of Biological chemistry.* **276**, 41407-41416.

Lin, B., Hollingshead, S.K., Coligan, J.E., Egan, M.L., Baker, J.R., and Pritchard, D.G. (1994). Cloning and expression of the gene for groip B streptococcal hyaluronate lyase. *The Journal of Biological chemistry.* **269** (48), 30113-30116.

Linhardt, R. J., Galliher, P. M. & Cooney, C. L. (1986).Polysaccharide lyases. *Applied Biochemistry and Biotechnology* **12**,135-176.

Linker, A., and Evans, L.R. (1984). Isolation and characterization of an alginase from mucoid strains of Pseudomonas aeruginosa. *Journal of Bacteriology*. **159**, 958-964.

Lohse, D.L., and Linhardt, R.J. (1992). Purification and characterisation of heparin lyases from Flavobacterium heparinum. *The Journal of Biological Chemistry*. **267**, 24347-24355.

Lunin, V.V., Li, Y., Linhardt, R.J., Miyazono, H., Kyogashima, M., Kaneko, T., Bell, A.W. and Cygler, M. (2004). High-resolution crystal structure of *Arthrobacter aurescens* chondroitin AC lyase: an enzyme-substrate complex defines the catalytic mechanism. *Journal of Molecular Biology*. **337**, 367-386.

Maccari, F., Tripodi, F., and Volpi, N. (2004). High-performance capillary electrophoresis separation of hyaluronan oligosaccharides produced by *Strptomyces hyalurolyticus* hyaluronate lyase. *Carbohydrate Polymers*. **56**, 55-63.

Mahoney, D.J., Aplin, R.T., Calabro, A., Hascall, V.C., and Day, A.J. (2001). Novel methods for the preparation and characterisation of hyaluronan oligosaccharides of defined length. *Glycobiology*. **11** (12), 1025-1031.
Malmstrom, A., Aberg, L. (1982). Biosynthesis of dermatan sulphate Assay and properties of the uronosyl C-5 epimerase. *Biochemical Journal*. **201**, 489-493.

Mao, W., Thanawiroon, C., and Linhardt, R. J. (2002). Capillary electrophoresis for the analysis of glycosaminoglycans and glycosaminglycan-derived oligosaccharides. *Biomedical chromatography*. **16** (2), 77-94.

Mello, L.V., De Groot,B.L., Li, S. and Jedrzejas, M.J. (2002). Structure and flexibility of Streptococcus agalactiae hyaluronate lyase with its substrate. Insight into the mechanism of processive degradation of hyaluronan. *The Journal of Biological Chemistry*. **277**, 36678-36688.

Menozzi, F.D., Pethe, K., Bifani, P., Soncin, F., Bernnan, M.J., and Locht, C. (2002). Enhanced bacterial virulence through exploitation of host glycosaminoglycans. *Molecular Microbiology*. **43** (6), 1379-1386.

Menzel, E.J., and Farr., C. (1998). Hyaluronidase and its substrate hyaluronan: biochemistry, biological activities and therapeutic uses. *Cancer Letters*. **131**, 3-11.

Meyer, K. (1971). Hyaluronidases. In: *The Enzymes*. Vol. 5. P.D. Boyer (Ed.). Third Edition, pp 307-319. Academic Press, London.

Michelacci, Y.M., Horton, D.S. and Poblacion, C.A. (1987). Isolation and characterization of an induced chonroitinase ABC from Flavobacterium heparinum. *Biochimical et Biophysical Acta*. **923**, 291-301.

Michel, G., Pojasek, K., Li, Y., Sulea, T., Linhardt, R.J., Raman, R., Prabhakar, V., Sasisekharan, R., and Cygler, M. (2004). The structure of chondroitin B lyase complexed with glycosaminglycan oligosaccharides unravels a calcium dependent catalytic machinery. *The Journal of Biological Chemistry*. **279** (31), 32882-32896.

Midura, R.J., Salustri, A., Calabro, A., Yanagishita, M., and Hascall, V.C. (1994). High-resolution separation of disaccharide and oligosaccharide alditols from chondrotin sulphate, dermatan sulphate and hyaluronan using CarboPac PA1 chromatography. *Glycobiology*. **4** (3), 333-342.

Mishra, P., Akhtar, S., and Bhakuni, V. (2006). Unusual structural features of the bacteriophage-associated hyaluronate lyase (hylp2). *The Journal of Biological Chemistry*. **281** (11), 7143-7150.

Misra S., Ghatak S., Zoltan-Jones A., and Toole, B.P (2003). Regulation of multidrug resistance in cancer cells by hyaluronan. *The Journal of Biological Chemistry*. **278** (28), 25285-25288.

Molinari, G. and Chhatwal, G. S. (1998). Invasion and survival of Streptococcus pyogenes in Eukaryotic cells correlates with the source of the clinical isolates. *Journal of Infectious Diseases*. **177**, 1600-1607.

Morey, S.S., Kiran,K.M., Gadag, J.R. (2006). Purification and properties of hyaluronidase from Palamneus gravimanus (Indian black scorpion) venom. Toxicon. **47**, 188–195

Moses, A.E., Wessels, M.R., Zalcman, K., Alberti, S., Natanson-Yaron, S., Menes, T., and Hanski, E. (1997). Relative contributions of hyaluronic acid capsule and M protein to virulence in a mucoid strain of the group A streptococcus. *Infection and Immunity*. **65**, 64-71.

Mourao, P.A., Rozenfeld, S., Laredo, J., and Dietrich, C.P. (1976). The distribution of chondroitin sulphates in articular and growth cartilages of human bones. *Biochimica et Biophysica Acta*. **428**, 19-26.

Nadanaka, S., Clement, A., Masayama, K., Faissner, A., and Sugahara, K. (1998). Characteristic hexasaccharide sequence in octasaccharides derived from shark cartilage chondroitin sulphate D with a neurite outgrowth promoting activity. *The Journal of Biological Chemistry*. **237** (6), 3296-3307.

Nadanaka, S., Kitagawa, H., Goto, F., Tamura, J., Neumann, K.W., Ogawa, T., and Sugahara, K. (1999). Involvement of the core protein in the first β-N-acetylgalactosamine transfer to the glycosaminoglycan-protein linkage-region tetrasaccharide and in the subsequent polymerisation: the critical determining step for chondroitin sulphate biosynthesis. *Biochemical Journal*. **340,** 353-357.

Navaza, J. (1994). Amore - an automated package for molecular replacement. *Acta Crystallographic. section. A.* **50**, 157-163

Nukui, M., Taylor, K.B., McPherson, D.T., Shigenaga, M.K., and Jedrzejas, M.J. (2003). The function of hydrophobic residues in the catalytic cleft of Streptococcus pneumoniae hyaluronate lyase. *The Journal of Biological Chemistry.* **278** (5), 3079-3088.

Ohya, T., and Kaneko, Y. (1970). Novel hyaluronidase from Streptomyces. *Biochimica et Biophysica Acta.* **198**, 607-609.

Oetti, M., Hoechstetter, J., Asen, I., Bernhardt, G., and Buschauer, A. (2003). Comparative characterization of bovine testicular hyaluronidase and a hyaluronate lyase from Streptococcus agalactiae in pharmaceutical preparations. *European Journal of Pharmaceutical Sciences.* **18**, 267-277.

Okorukwu, O.N., and Vercruysse, K.P. (2003). Effects of ascorbic acid and analogs on the activity of testicular hyaluronidase and hyaluronan lyase on hyaluronan. *Journal of Enzyme Inhibition and Medical Chemistry.* **18** (4), 377-382

Otwinowski, Z., and W. Minor. 1997. Processing of X-ray diffraction data collected in oscillation mode, p. 307-326, Macromolecular Crystallography, Pt A, **276**. ACADEMIC PRESS INC, San Diego.

Ozegowski, J.H., Gunther, E. and Reichardt, W. (1994). Purification and characterization of hyaluronidase from Streptococcus agalactiae. *Zentralbl. Bakteriology.* **280**, 497-506.

Park, Y., Cho, S. and Linhardt, R.J. (1997). Exploration of the action pattern of Streptomyces hyaluronate lyase using high-resolution capillary electrophoresis. *Biochimica et Biophysica Acta.* **1337**, 217-226.

Perez-Casal, J., Price, J.A., Maguin, E., and Scott, J.R. (1993). An M protein with a single C repeat prevents phagocytosis of *Streptococcus pyogenes*: use of a temperature-sensitive shuttle vector to deliver homologus sequences to the chromosome of S. pyogenes. *Molecular Microbiology.* **8** (5), 809-819.

Perrimon, N., and Bernfield, M. (2001). Cellular functions of proteoglycans-an overview. *Seminars in Cell and Developmented Biology.* **12** (2): 65-67

Piepersberg, W. (1993). Streptomyces and Corynebacteria. In: Biotechnolgy, Rehm H, Reed G, Piihler A, Stadler P (ed). VCH, Weinheim, 434-468.

Pojasek, K., Shriver, Z., Kiley, P., Venkataraman, G., and Sasisekharan, R. (2001). Recombinant expression, purification and kinetic characterization of chondroitinase AC and chondroitinase B from Flavobacterium heparinium. *Biochemical and Biophysical Research Communications*. **286**, 343-351.

Pojasek, K., Raman, R., Kiley, P., Venkataraman, G., and Sasisekharan, R. (2002). Biochemical characterization of the chondroitinase B active site. *The Journal of Biological Chemistry*. **277** (34), 31179-31186.

Ponnuraj, K. and Jedrzejas, M. (2000). Mechanism of Hyaluronan Binding and Degradation:Structure of Streptococcus pneumoniae Hyaluronate Acid Disaccharide at 1.7 A Resolution. *Journal of Molecular Biology*. **299**, 885-895.

Pope, R.M., Raska, C.S., Thorp, S.C., and Liu, J. (2001). Analysis of heparan sulphate oligosaccharides by nano-electrospray ionisation mass spectrometry. *Glycobiology*. **11** (6), 505-513.

Prabhakar, V., Capila, I., Bosques, C.J., Pojasek, K., ., and Sasisekharan, R. (2005 a). Chondrotinase ABC I from Proteus vulgaris: cloning, recombinant expression, and active site identification. *Biochemical Journal*. **386**, 103-112.

Prabhakar, V., Raman, R., Capila, I., Bosques, C.J., Pojasek, K., and Sasisekharan, R. (2005 b). Biochemical characterization of the chondroitinase ABC I active site. *Biochemical Journal*. **390**, 395-405.

Prathiba, V., and Gupta, P.D. (2000). Cutaneous wound healing: Significance of proteoglycans in scar formation. *Current Science*. **78** (6): 697.

Price, K.N., Tuinman, A., Baker, D.C., Chisena, C., and Cysyk, R.L. (1997). Isolation and characterization by electrospray-ionization mass spectrometry and high-performance anion-exchange chromatography of oligosaccharides derived from hyaluronic acid by hyaluronate lyase digestion: observation of some heretofore unobserved oligosaccharides that contain an odd number of units. *Carbohydrate Research*. **303**, 303-311.

Prinz, W.A., Åslund, F., Holmgren, A., and Beckwith, J. (1997). The Role of the Thioredoxin and Glutaredoxin Pathways in Reducing Protein Disulfide Bonds in the *Escherichia coli* Cytoplasm. *The Journal of Biological Chemistry*. **272**, 15661 - 15667

Pritchard, D.G., Lin, Bo., Willingham, T.R., and Baker, R. (1994). Characterization of the group B Streptococcal hyaluronate lyase. *Archives of Biochemistry and Biophysics.* **315** (2), 431-437.

Pritchard, D.G., Trent, J.O., Zhang, P., Egan, M.L., and Baker, J.R. (2000). Characterization of the active site of group B Streptococcal hyaluronate lyase. *Proteins: Structure, Function, and Genetics.* **40**, 12134-12139.

Rautela, G.S. and Abramson, C. (1973). Crystallization and partial characterization of Staphylococcus aureus hyaluronate lyase. *Archives of Biochemistry and Biophysics.* **158**, 687-694.

Rigden, D.J., and Jedrzejas, M.J. (2003). Genome based identification of a carbohydrate binding module in Streptococcus pneumoniae hyaluronate lyase. *Proteins, Structure, Function, and Genetics.* **52**, 203-211.

Rigden, D.J., Littlejohn, J.E., Joshi, H.V., de Groot, B.L., Jedrzejas, M. (2006). Alternate Structural Conformations of Streptococcus pneumoniae Hyaluronan Lyase: Insights into Enzyme Flexibility and Underlying Molecular Mechanism of Action. *Journal of Molecular Biology* **358**, 1165–1178

Rodrigues, E.D., Pimentel, E.R., Mourão, P.A.S., and Gomes, L. (2005). Distribution of small proteoglycans and glycosaminoglycans in humerus-related articular cartilage of chickens. *Brazilian Journal of Medical and Biological Research.* **38** (3) 381-390.

Rosenberg, R.D., Shworak, N.W., Liu, J., Schwart, J.J., and Zhang, L. (1997). Heparan sulfate proteoglycans of the cardiovascular system. Specific structures emerge but how is synthesis regulated ? *Journal of Clinical Investigation.* **99**, 2062-2070.

Ross, M.H., Kaye, G.I., and Pawlina, W. (2003). Histology: a text and atlas. 4th ed. Philadelphia Lippincott Williams and Wilkins. Baltimore. New York. London. 875p

Rosso, F., Giordano, A., Barbarisi, M., and Barbarisi, A. (2004). From cell-ECM intersctions to tissue engineering. *Journal of cell physiology.* **199** (2), 174-180.

Roughley, P.J. and Lee, E.R. (1994). Cartilage proteoglycans: structure and potential functions. *Microscopy Research and Technique.* **28**, 385-397.

Ruijssenaars, H. J., S. Hartmans, and J. C. Verdoes. 2000. A novel gene encoding xanthan lyase of *Paenibacillus alginolyticus* strain XL-1. *Applied and Environmental Microbiology* **66**:3945–3950.

Ruoslahtie, (1989). Proteoglycans in cell regulation. The Journal of Biological Chemistry. 264 (23), 13369-13372.

Rye, C. and Withers, S.G. (2000). Glycosidase mechanism. Current Opinion in chemical Biology. 4, 573-580.

Rye, C. and Withers, S.G. (2004). The synthesis of a novel thio-linked disaccharide of chondroitin as a potential inhibitor of polysaccharide lyases. *Carbohydrate Research.* **339**, 699-703.

Salmivirta, M., Lidholt, K., U. (1996). Heparan sulphate: a piece of information. *FASEB J.* **10**. 1270-1279.

Sanderson, P.N., Huckerby, T.N., and Nieduszynski, I.A. (1989) Chondroitinase ABC digestion of dermatan sulphate. N.m.r. spectroscopic characterization of the oligo- and poly-saccharides. *Biochememical Journal.* **257**, 347–354

Scott, J.E. (1992). Supramolecular organisation of extracellular matrix glycosaminoglycans, in vitro and in the tissues. *FASEB. J.* **6**, 2639-2645.

Shaya, D., Tocilj, A., Li, Y., Myette, J., Venkataraman, G., Sasisekharan, R., and Cygler M. (2006). Crystal structure of Heparinase II from Pedobacter heparinus and its complex with disaccharide product. *The Journal of Biological Chemestry.* **281,** 15525-15535.

Shuhei, Y., and Kazuyuki, S. (1998). Structure of oligosaccharides isolated from heparan sulphate/heparin and substrate specificities of the degrading enzymes of bacterial origin. *Trends in Glycoscience and Glycotechnology.* **10** (52), 95-123.

Shyjan, A.M., Heldin, P., Butcher, E.C., Yoshino, T. (1996). Functional cloning of the cDNA for a human hyaluronan synthase. *The Journal of Biological Chemistry.* **271**. (38), 23395-23399.

Smith, N.L., Taylor, D.J., Lindsay, A. M., Charnock, S.J., Turkenburg, J.P., Dodson, E.J., Davies, G.J., and Black, G.W. (2005). Structure of a group A streptococcal phage-encoded virulence factor reveals a catalytically active triple-stranded β-helix. *Proceedings of the National Academy of Sciences, USA.* **102** (49), 17652-17657.

Stern, R; Shuster, S; Wiley, T.S; and Formby, B. (2001). Hyaluronidase can modulate expression of CD44. *Experimental Cell Research.* **266**, 167-176.

Steven, D.L. (1992). Invasive group A streptococcus infection. Clinical Infectious Disease. 14 (1), 2-11.

Stollerman, G.H. (1996). The nature of rheumatogenic streptococci. *Mount Sinai Journal of Medicine*. **63**, 144-158.

Stringer, S.E., Kandola, B.S., Pye, D.A., and Gallagher, J.T. (2003). Heparin sequencing. *Glycobiology*. **13** (2), 97-107.

Sugumarans, G., and Silbert, J.E. (1990). Relationship of Sulfation to Ongoing Chondroitin Polymerizationduring Biosynthesis of Chondroitin 4-Sulfate by Microsoma Preparations from Cultured Mouse Mastocytoma Cells. *The Journal of Biological Chemistry*. **265** (30), 18284-18288.

Sutherland, I.W. (1995). Polysaccharide lyases. *FEMS Microbiology Reviews*. **16**, 323-347.

Su, H., Blain, F., Musil, R.A., Zimmermann, J.J.F., Gu, K., and Bennett, C. (1996). Isolation and expression in Escherichia coli of hepB and hepC, genes coding for the glycosaminoglycan-degrading enzymes heparinase II and Heparinase III, respectively, from Flavobacterium heparinum. *Applied and Environmental Microbiology*. **62** (8), 2723-2734.

Takao, A., Nagashima, H., Usui, H., Sasaki, F., Maeda, N., Ishibashi, K., and Fujita, H. (1997). Hyaluronidase activity in human pus from which *Streptococcus intermedius* was isolated. *Microbiology and Immnuology*. **41** (10), 795-798.

Takao, A. (2003). Cloning and expression of hyaluronate lyase genes of Streptococcus intermedius and Streptococcus constellatus subsp. Constellatus. *FEMS Microbiology Letters*. **219,** 143-150.

Takegawa, K., Iwahara, K., and Iwahara, S. (1991). Purification and properties of chondroitinase produced by a bacterium isolated from soil. *Journal of Fermintation and Bioengineering*. **72** (2), 128-131.

Tam, T.C. and Chan, E.C.S. (1985). Purification and characterization of hyaluronidase from oral Peptostreptococcus species. *Infection and Immunity*. **47**, 508-513.

Tammi,M.L., Day, A.J., and Turley, E.A. (2002). Hyaluronan and homeostasis: a balancing act. *The journal of Biological chemistry*. **277** (7), 4581-4584.

Tardy, F., Nasser, W., Robert-Baudouy, J., and Cotte-Pattat, N.H. (1997). Comparative analysis of the five major Erwinia chrysanthemi pectate lyases: enzyme characteristics and potential inhibitors. *Journal of Bacteriology*. **179** (8), 2503-2511.

Termeer, C.C., Hennies, J., Vaith, V., Ahrens, T., Weiss, J.M., Prehm, P. and Simon, J.C. (2000). Oligosaccharides of Hyaluronan are potent activators of Dendritic cells. *The journal of Immunology*. **165**, 1863-1870.

Thurston CF. (1975). The kinetic of degradation of chondroitin of sulphates and hyaluronic acid by chondroitinase form Proteus vulgaris. *Biochemical Journal*.**145**, 397-400

Tkalec, A., Fink, D., Blain, F.O., Zhang-Sun, G., Laliberte, M.D., Bennett, C., Gu, K., Zimmermann, J. F., and Su, H. (2000). Isolation and Expression in *Escherichia coli* of *cslA* and *cslB*, Genes Coding for the Chondroitin Sulfate-Degrading Enzymes Chondroitinase AC and Chondroitinase B, Respectively, from *Flavobacterium heparinum. Applied and Environmental Microbiology*.**66**, 29-35.

Turley, E.V., Noble, P.W., and Bouryuignon, L.Y.W. (2001). Signaling properties of hyaluronan receptors. *The journal of Biological chemistry*. **277** (7), 4589-4592.

Underhill, C. (1992). CD44: The hyaluronan receptor. Journal of Cell Science. 103, 293-298.

Van den Hoogen, B.M., Van Weeren, P.R., Cardozo, M.L. (1998). A microtiter plate assay for the determination of uronic acids. *Analytical Biochemistry*. **257,** 107-111.

Varki, A., Cumming, R., Esko, J., Freeze, H., Hart, G., and Marth, J. (2003). Essentials of Glycobiology. Cold Spring Harbor Laboratory Press, Cold Spring Harbor, New York.

Velazquez, B; Massaldi, H; Battistoni, J; and Chabalgoity, J.A. (2005). Construction and expression of recombinant streptolysin-O and preevaluation of its use in immunoassays. *Clincal and diagnostic laboratory immunology*. **12** (5), 683-684.

Vynios, D.H., Karamanos, N.K., Tsiganos, C.P. (2002). assessment of physiological and pathological states of connective tissues. *Journal of Chromatography B*, **781**, 21–38.

Watanabe, H., Cheung, S.C., Itano, N., Kimata, K., and Yamada, Y. (1997). Identification of hyaluronan-binding domains of Aggregan. *The Journal of Biological Chemistry*. **272**. (44), 28057-28065.

Watanabe, K., and Yamaguchi, Y. (1996). Molecular identification of a putative human hyaluronan synthase. *The Journal of Biological Chemistry*. **271** (38), 22945-22948.

Watanabe, M., Tsuda, H., Yamada, S., Shibata, Y., Nakamura, T., and Sugahara, K. (1998). Characterization of heparinase from an oral bacterium *Prevotella heparinolytica*. *Journal of Biochemistry*. **123**, 283-288.

Weigel, P.H, Hascall, V.C., and Tammi, M. (1997). Hyaluronan synthases. *The Journal of Biological Chemistry*.**272**, 13997-14000.

Wessels, M.R; Moses, A.E; Goldberg, J.B; and Dicesare, T.J. (1991). Hyaluronic acid capsule is a virulence factor for mucoid group A streptococci. . *Proceedings of the National Academy of Sciences. USA*. **88**, 8317-8321.

Xu, H., Ito, T., Tawada, A., Maeda, H., Yamanokuchi, H., Isahara, K., Yoshida, K., Uchiyama, Y., and Asari A. (2002). Effect of hyaluronan oligosaccharides on the expression of heat shock protein 72. *The Journal of Biological Chemistry*. **277** (19), 17308–17314.

Yamada, S., and Sugahara, K. (1998). Structure of oligosaccharides isolated from heparan sulphate/heparin and substrate specificities of the degrading enzymes of bacterial origin. *Trends in Glycoscience and Glycotechnology*. **10** (52), 95-123.

Yamagat, T; Saito, H; Habuchi, O; and Suzuki, A.S. (1969). Purification and Properties of Bacterial Chondroitinasesand Chondrosulfatases. *The Journal of Biological Chemistry*. **243** (7). 1523-1535.

Yang, V.C., Linhardt, R.J., Berstein, H., Cooney, C.L., Langer, R. (1985). Purification and characterisation of heparinase from Flavobacterium heparinum. *The Journal of Biological Chemistry*. **260**, 1849-1857.

Yoon, H. J., Hashimoto, W., Miyake, O., Murata, K. and Mikami, B. (2001). Crystal structure of alginate lyase A1-III complexed with trisaccharide product at 2.0 A° resolution. *Journal of* Molecular *Biology*. **307**, 9–16.

Zhang L, Underhill CB and Chen L (1995) Hyaluronan on the surface of tumor cells is correlated with metastatic behavior. *Cancer Research*. **55**, 428-433.

Appendix I

Chemicals, media and enzymes used in this study

IA: Chemicals

Acros
- Imidazole
- Lithium acetate
- Sodium phosphate (dibasic)
- Sodium phosphate (monobasic)

BDH Laboratory Supplier
- Nitric acid
- Propan-2- ol

Bio-Gene
- %-bromo-4-chloro-3-indoyl-β-D-galactoside (X-GAL)

Fisher BioReagents
- Acrylamide/Bisacrylamide 37,5:1, 40% solution
- Coomassie blue R-250
- Lysozyme, egg white
- Methanol
- Phenol

Fisher Chemicals
- Acetic acid, glacial
- Ammonium acetate
- Ammonium citrate
- Ammonium dihydrogen phosphate
- Ammonium nitrate
- Di-Ammonium hydrogen phosphate
- Tert-Butyl alcohol
- Cadmium chloride
- Cadmium sulphate
- Caesium chloride
- Cobalt chloride
- Calcium acetate
- Dimethyl sulphoxide (DMSO)
- 1,4-Dioxane
- Ethyleneglycol
- Formaldehyde
- Iron (II) chloride
- Lithium chloride
- Lithium nitrate
- Lithium sulphate
- Magnesium acetate
- Magnesium nitrate
- PEG 200
- PEG 400

PEG 600
PEG 1000
PEG1500
PEG 4000
PEG 6000
PEG 8000
Polypropyleneglycol 2000
Potassium bromide
Tri-Potassium acetate
Potassium fluoride
Potassium formate
Potassium iodide
Potassium nitrate
Potassium sodium tartrate
Potassium sulphate
Potassium thiocyanate
Sodium cacodylate
Sodium citrate
Sodium iodide
Sodium fluoride
Sodium formate
Sodium nitrate
Sodium sulphate
Sodium tartrate
Sodium thiocyanate
Zinc acetate
Zinc sulphate

Fluka

Tri-lithium citrate
PEG 550mme
PEG 2000mme
PEG 5000mme
PEG 10000
PEG 20000

Hampton Research

Aqua Sil

Hayman Ltd

Absolute alcohol (ethanol)

Melford Laboratories Ltd

Agarose (High gel strength)
Glycine
Isopropyl-β-D-Thiogalactopyranoside (IPTG)
Kanamycin monosulphate
Tris [Hydroxymethyl] aminomethane (Tris-HCl)

Riedel-deHaen

- Hydrochloric acid
- Sulphuric acid

Sigma

- Ammonium chloride
- Ammonium fluoride
- Ammonium formate
- Ammonium persulphate (APS)
- Ammonium sulphate
- Ammonium tartrate
- Ampicillin (D[-]α-Aminobenzylpencillin)
- Barium chloride dihydrate
- Boric acid
- Bradford reagent
- Bovine serum albumin, Fraction V (BSA)
- Bromophenol Blue
- Calcium chloride, dihydrate
- Chloramphenicol
- Citric acid, trisodium salt dihydrate
- Cobalt chloride, hexahydrate
- Ethidium bromide
- Ethylene diamine tetraacetic acid, disodium salt (EDTA)
- Ferrous sulphate, heptahydrate
- Glycerol
- N-(2-Hydroxyethyl) piperazine-N-[2-ethanesulphonic acid] (HEPES)
- Hexaamminecobalt (III) chloride
- Isopropanol
- Lauryl sulphate, sodium salt (SDS)
- Magnesium chloride, hexahydrate
- Magnesium sulphate, heptahydrate
- Magnesium chloride, tetrahydrate
- 2-Mercaptoethanol
- Methyl mercury (II) chloride
- Nickel sulphate
- PEG 3350
- Platinium (II) 2,2,6,2-terpyridine, dihydrate
- Polyethyleneimine, (50% w/v)
- Potassium acetate
- Potassium chloride
- Potassium dichromate
- Potassium phosphate, dibasic
- Potassium phosphate monobasic
- Silver nitrate
- Sodium acetate anhydrous
- Sodium carbonate
- Sodium chloride
- Sodium hydroxide
- Sodium sulphite, anhydrous

N,N,N,N-tetramethylethylene diamine (TEMED)
Tetracycline
Triton X-100
Urea

IB: Media
Oxoid

Agar (Bacteriological agar N° 1)
N Z Amine (Casein hydrolysate)
Tryptone
Yeast Extract

IC: Enzymes

The enzymes and reaction buffers used in this study are shown in the Tables ICa, ICb and ICc.

Invitrogen Corp

Table ICa: Enzyme and reaction buffer (1x)

Enzyme	Buffer composition 1x
Pfx (DNA polymerase)	Patented

New England Biolabs:

Table ICb: Enzymes and reaction buffers (1x)

Enzyme	Buffer composition (1x)
*Dpn*I	Buffer 4 (20 mM Tris-acetate, 10 mM Magnesium acetate, 50 mM Potassium acetate, 1mM DTT pH 7.9)
*Hind*III	Buffer 2 (10 mM Tris-HCl, 10mM $MgCl_2$, 50mM NaCl, 1mM DTT, pH 7.9
*Nde*I	Buffer 4 (20 mM Tris-acetate, 10 mM Magnesium acetate, 50 mM Potassium acetate, 1mM DTT pH 7.9)
*Xho*I	Buffer 2 (10 mM Tris-HCl, 10 mM $MgCl_2$, 50mM NaCl, 1 mM DTT, pH 7.9
Lysozyme (Hen egg white)	un-buffered
T4 DNA ligase	50 m MTris-HCl pH7.5, 10 mM $MgCl_2$, 10 mM DTT, 1mM ATP, 25μg.ml acetylated BSA.

Promega

Table ICc Enzymes and reaction buffers (1x)

Enzyme	Buffer composition
*Bam*HI	Buffer E (60 mM Tris-HCl, 6 mM $MgCl_2$, 100 mM NaCl, 1 mM DTT, pH 7.5
*Eco*RI	Buffer H (90 mM Tris-HCl, 10 mM $MgCl_2$ 50 mM NaCl, pH7.5
*Eco*RV	Buffer D (6 mM Tris-HCl, 6 mM $MgCl_2$ 150 mM NaCl, 1mM DTT, pH 7.9
*Sal*I	Buffer D (6 mM Tris-HCl, 6 mM $MgCl_2$ 150 mM NaCl, 1mM DTT, pH 7.9
T4 DNA ligase	30 mM Tris-HCl pH 7.8, 10 mM $MgCl_2$, 10 mM DTT, 1 mM ATP, 5% PEG
Pfu (DNA polymerase)	10 mM KCl, 10 mM NH_4SO_4, 20 mM Tris-HCl pH 8.8, 2 mM $MgSO_4$, 0.1% Triton X-100, 0.1mg.ml^{-1} BSA (nuclease free)
Taq (DNA polymerase)	10 mM Tris-HCl pH 9.0, 1.5 mM $MgCl_2$, 50 mM KCl, 0.1%Triton X-100

Id: Size standards

DNA

New England Biolabs:

1kb DNA ladder (10, 8, 6, 5, 4, 3, 2, 1.5, 1, 0.5 kb)

Promega

100bp DNA (1500, 1000, 900, 800, 700, 600, 500, 400, 300, 200, 100 bp)

Protein
Sigma

Table ID: Molecular weight distribution in sigma Markers

Protein	MW (Da)	High	Low
Myosin rabbit muscle	205000	X	
B-Galactosidase, E.coli	116000	X	
Phosphorylase b, rabbit muscle	97000	X	
Fructose-6-phospho kinase, rabbit muscle	84000	X	
Albumin, Bovine serum	66000	X	X
Glutamic dehydrogenase, Bovine liver	55000	X	X
Ovalbumine, chicken egg	45000	X	X
Glyceraldehyde-3-phosphate dehydrogenase, rabbit muscle	36000	X	X
Carbonic Anhydrase, bovine erythrocytes	29000		X
Trypsinogen, bovine pancrease	24000		X
Trypsin inhibitor, soybean	20000		X
A-Lactalbumin, bovine milk	14200		X
Aprotinin, bovine lung	6500		X

IE: Kits
Macherey-Nagel GmbH (Germany)

NucleoSpin Extract
NucleoSpin plasmid

Table IEa: Components of NucleoSpin

Buffer components /	Function
Buffer A1	Resuspension buffer contains RNAase
Buffer A2	Lysis buffer
Buffer A3	Binding buffer contains guanidinium Hydrochloride
Buffer A4	Wash buffer contains ethanol
Buffer AE	Elution buffer 5mM Tris-HCl pH 8.5
Buffer AW	Wash buffer contains guanidinium Hydrochloride
Buffer NT1	Binding buffer
Buffer NT2	
Buffer NT3	contains ethanol
Buffer NE	Elution buffer 5mM Tris-HCl pH 8.5

Stratagene:

Quik Change™ Site-Directed Mutagenesis kit.

Table IEb: Components provided with Quik change™Site-Directed Mutagenesis kit

Materials provided
Pfu turbo DNA polymerase (2.5 U μ^{-1}) reaction buffer 10x
*Dpn*I restriction enzyme (10 U μ^{-1})
dNTP mix

IF: Resins

Amersham Pharmacia Biotech AB

Chelating Sepharose™ fast flow resin

Sephadex™ G-25 medium resin

Appendix II

Vectors used in this study and their expanded polylinker region.
IIA: pGEM-T® Easy (Promega)

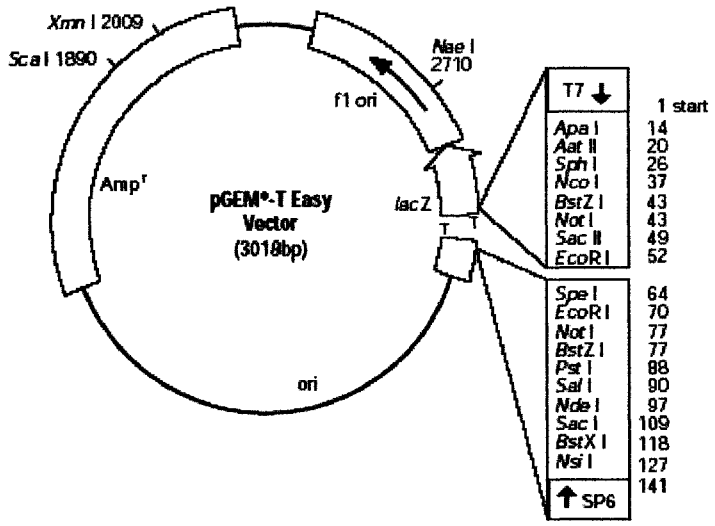

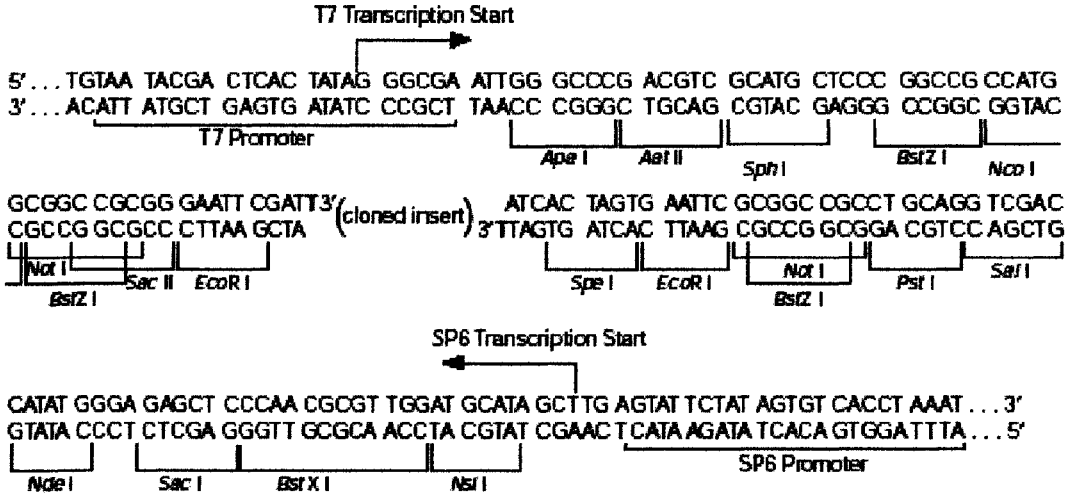

Figure IIA: pGEM-T® Easy vector. Plasmid DNA prepared by digestion with EcoR V and 3' terminal thymidines added.

IIB: pCR®-Blunt (Invitrogene Corp)

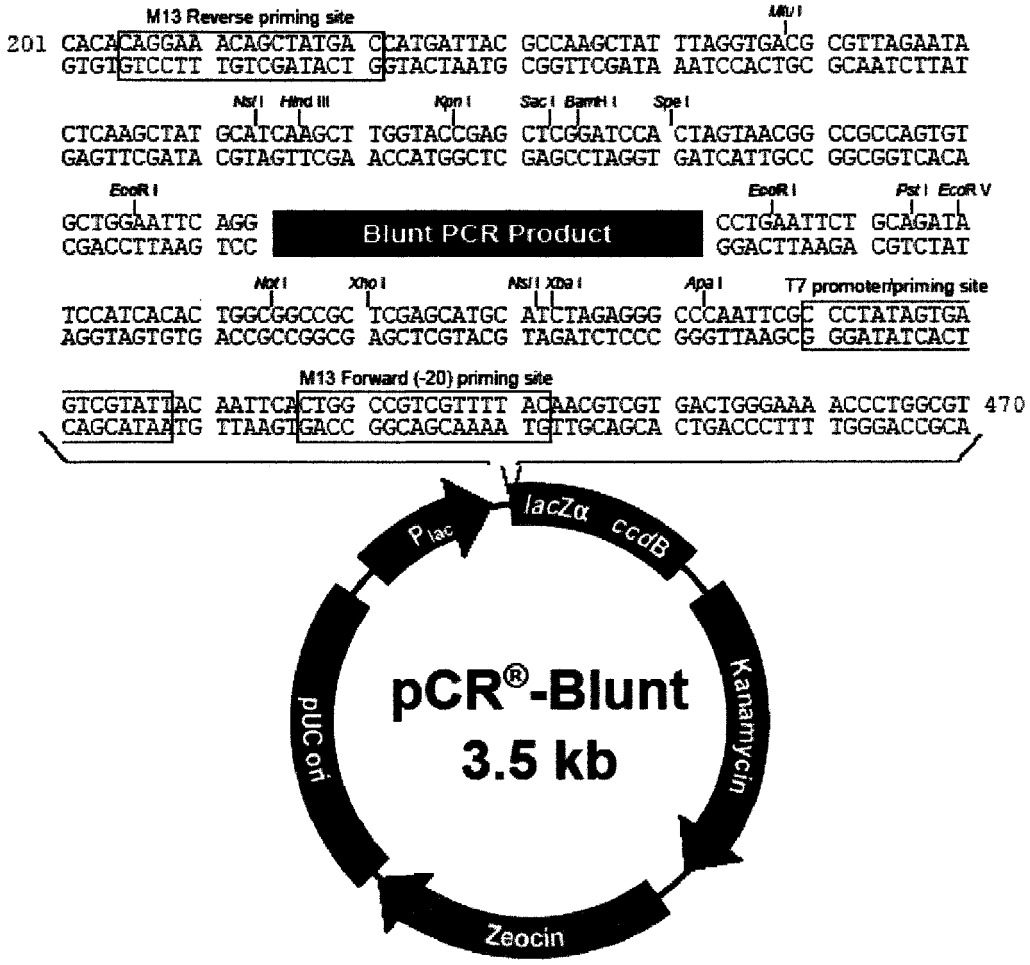

Figure IIB: pCR® –Blunt vector

IIC: pET-22b (Novagen)

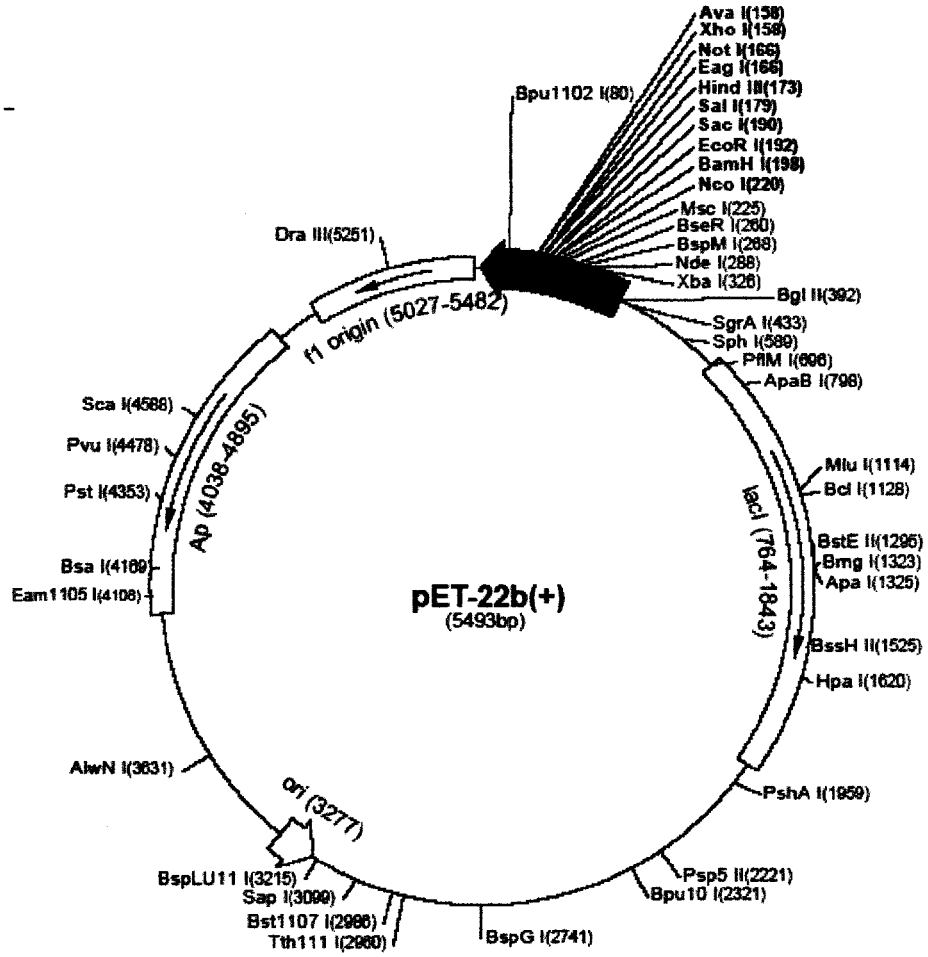

Figure IIC: pET-22b vector

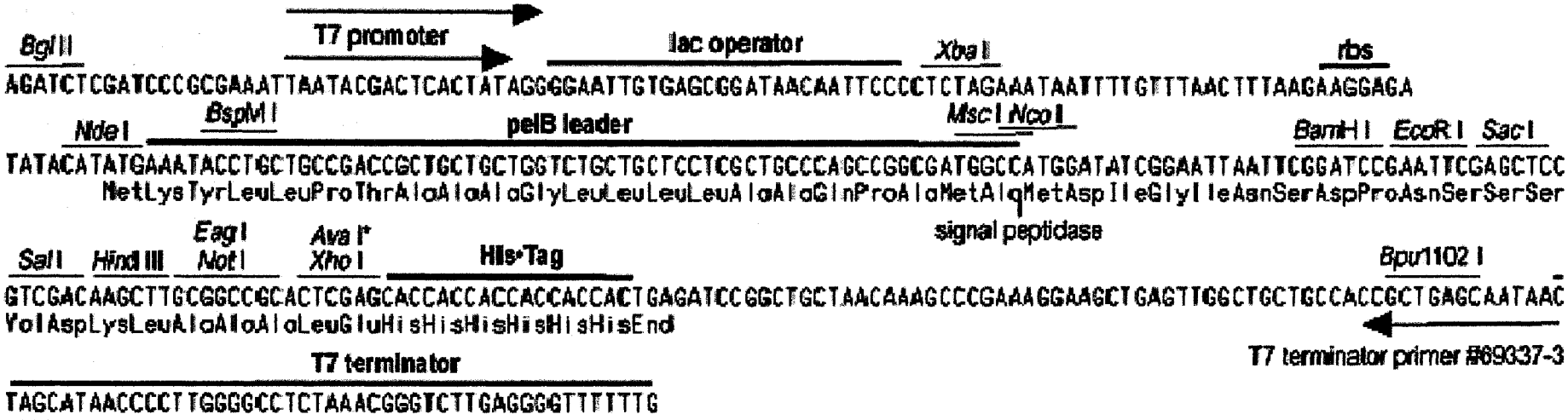

pET-22b(+) cloning/expression region

IID: pET-28a (Novagen)

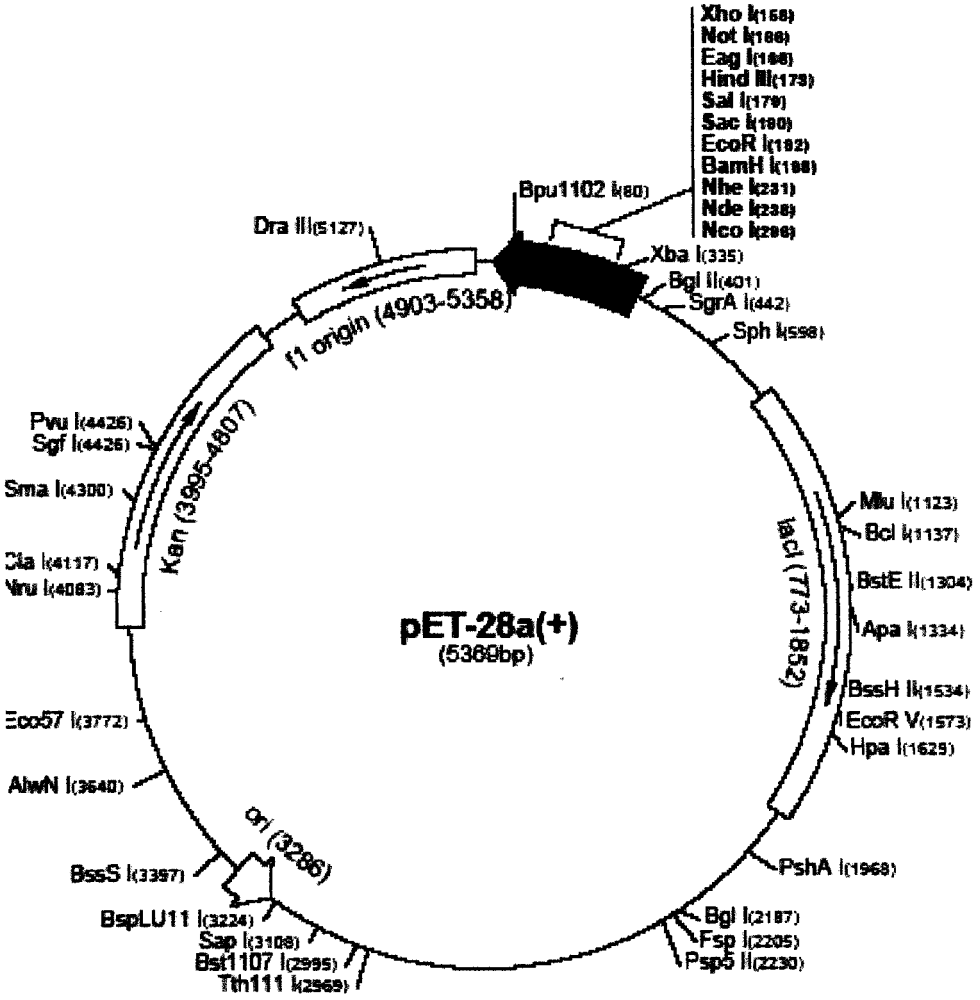

Figure IID: pET-28a vector

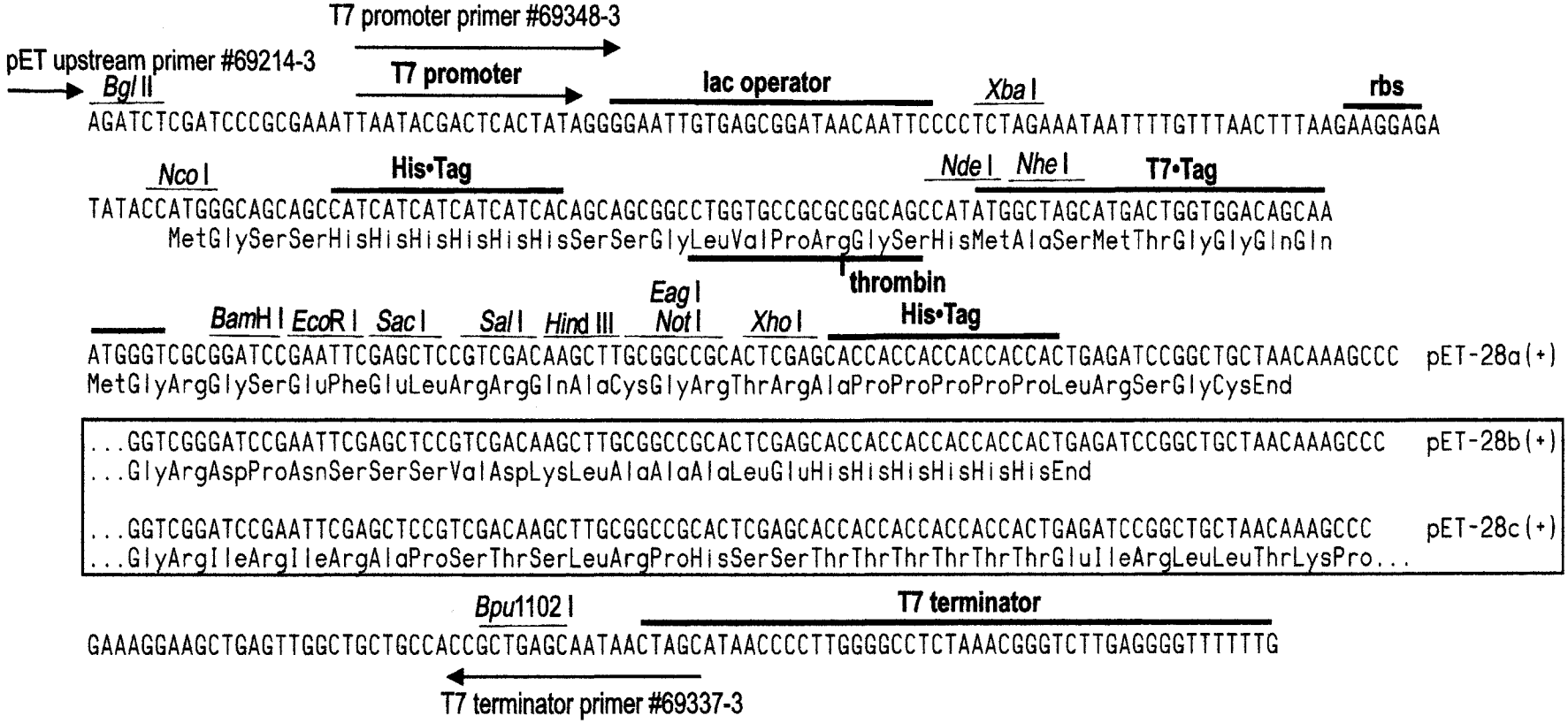

pET-28a-c(+) cloning/expression region

IIE: pET-32C (Novagen)

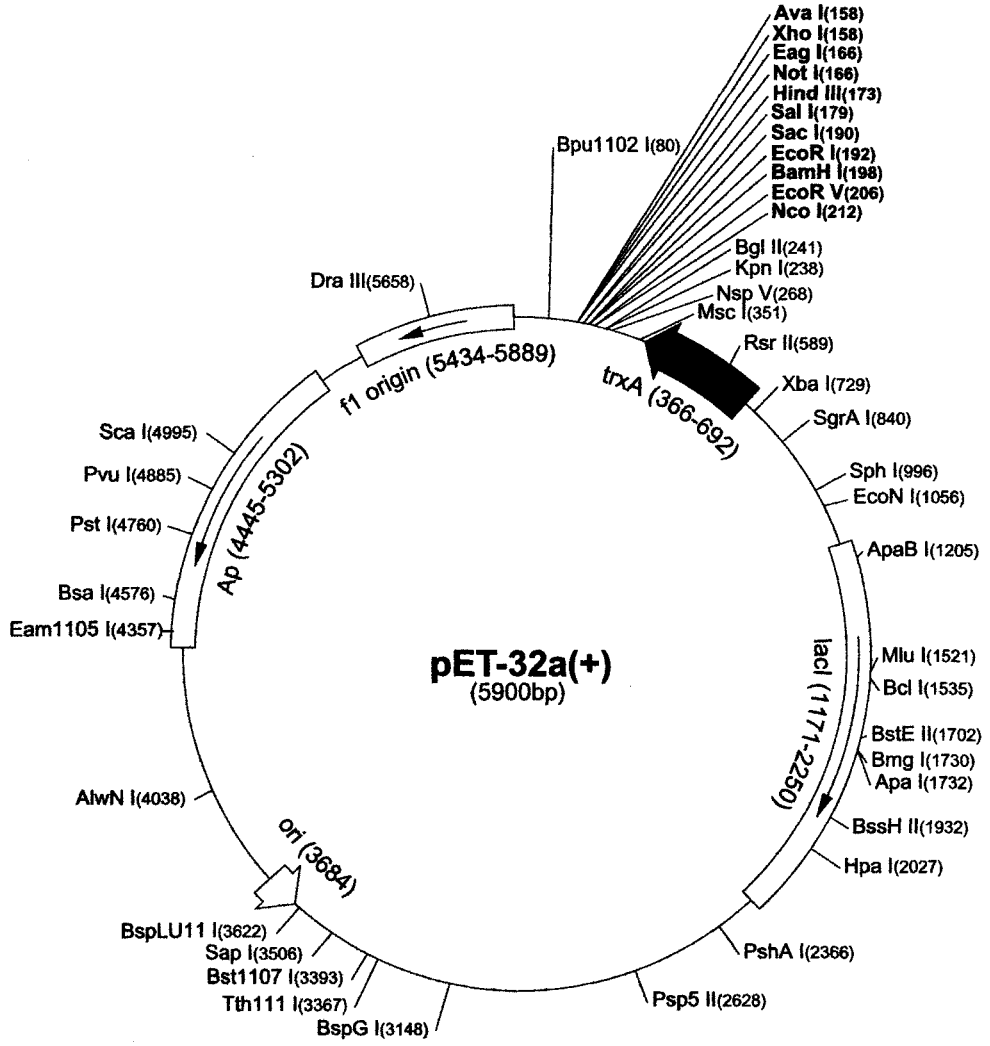

Figure IIE: pET-32C vector

pET32 cloning/expression region

IIF: pET28a-LIC

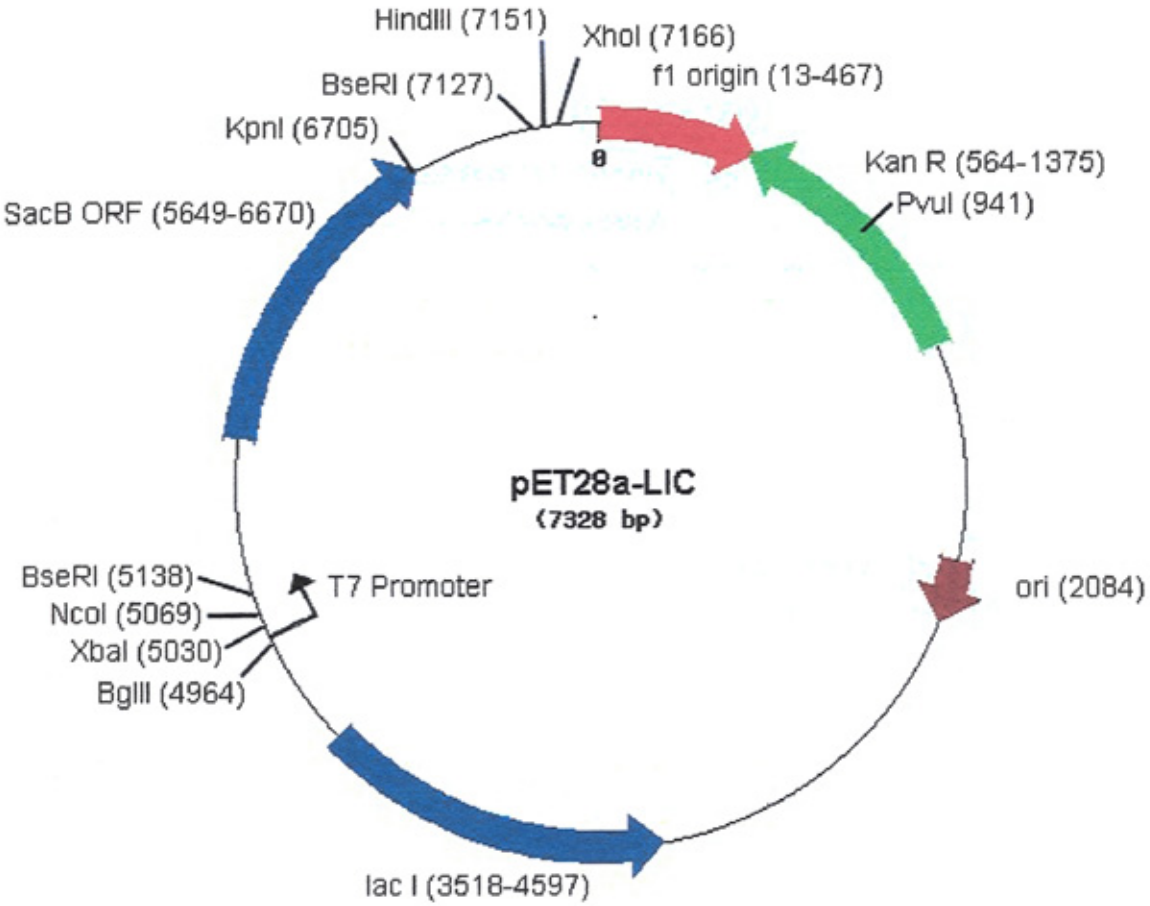

Polylinker Region

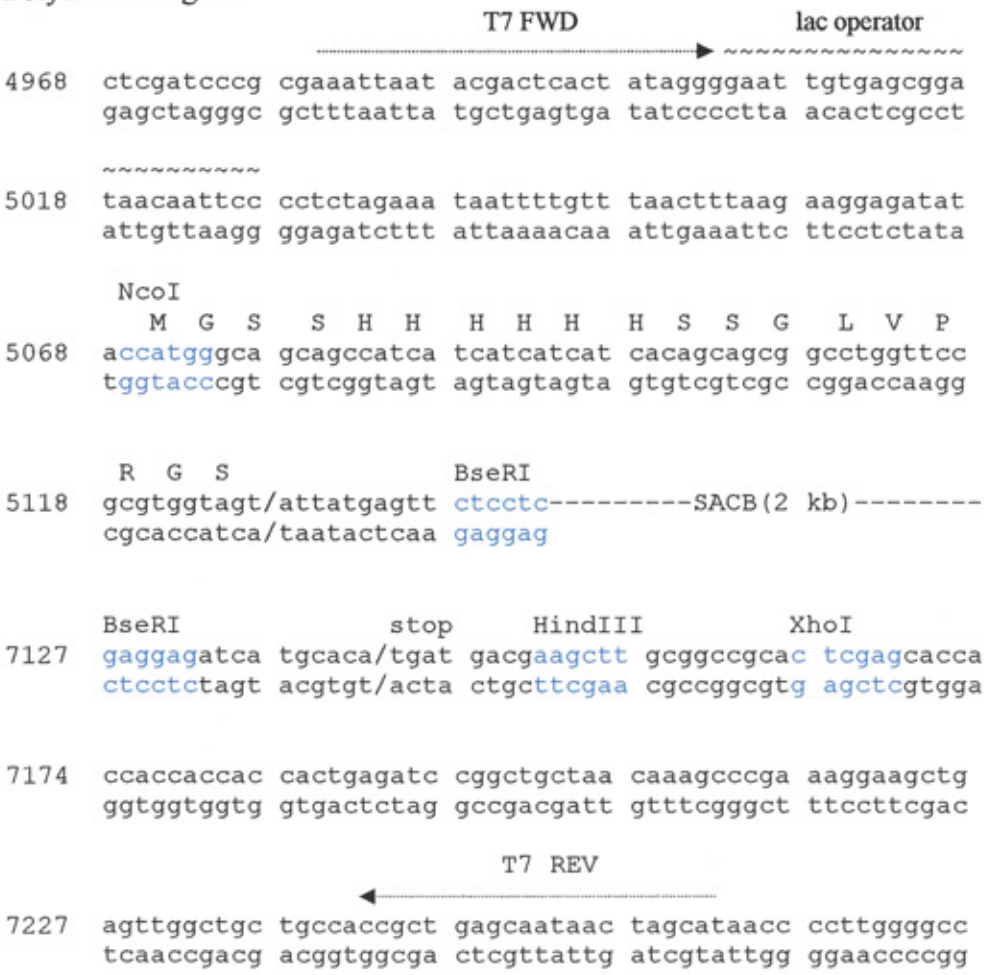

Figure IIF: pET-28aLIC

Construct = pET-YSBLIC

GAGGAG BseRI
GGCGCGCC AscI
CATATG NdeI

PreScission (3C) Protease
CTGGAAGTTCTGTTCCAGGGGCCC

Parent vector, Pet-28a containing 3C protease site

5′-AGATATACCATGGGCAGCAGCCATCATCATCATCATCACAGCAGCGGCCTGGAAGTTCTGTTCCAGGGGCCC**CATATG**GCTAGCATGACTGGTGGACAGCAAATG-3′
3′-TCTATATGGTACCCGTCGTCGGTAGTAGTAGTAGTAGTGTCGTCGCCGGACCTTCAAGACAAGGTCCCCGGG**GTATAC**CGATCGTACTGACCACCTGTCGTTTAC-5′
ArgArgTyrMetGlySerSerHisHisHisHisHisSerSerGly**LeuGluValLeuPheGlnGlyPro**HisMetAlaSerMetThrGlyGlyGlnGlnMet

YSBL pET-28a LIC

5′-AGATATACCATGGGCAGCAGCCATCATCACCACCACCACA**G**GCGCGCCTTCTCCTCACTGTTCCAGGGGCCCCATATGGCTAGCATGACTGGTGGACAGCAAATG-3′
3′-TCTATATGGTACCCGTCGTCGGTAGTAGTAGTAGTAGTGT**C**CGCGCGGAAGAGGAGTGACAAGGTCCCCGGGGTATACCGATCGTACTGACCACCTGTCGTTTAC-5′
ArgArgTyrMetGlySerSerHisHisHisHisHisHis

Non Cleavable Tag
LIC site
9/10 additional N-terminal amino acids

BseRI digest

5′-GCAGCAGCCATCATCACCACCACCACA**G**G-3′
3′-CGTCGTCGGTAGTAGTGGTGGTGGTG**T**-5′

5′-CGCGCCTTCTCCTCACTGTTCCAGGGGCCC**CATATG**G-3′
3′-CCGCGCGGAAGAGGAGTGACAAGGTCCCCGGG**GTATAC**C-5′

T4 pol/dTTP Treatment

GCAGCAGCAGCCATCAT-3′
CGTCGTCGTCGGTAGTAGTGGTGGTGGTG**T** -5′

5′-CGCGCCTTCTCCTCACTGTTCCAGGGGCCC**C**
3′-TGAC GGTCCCCGGG**G**

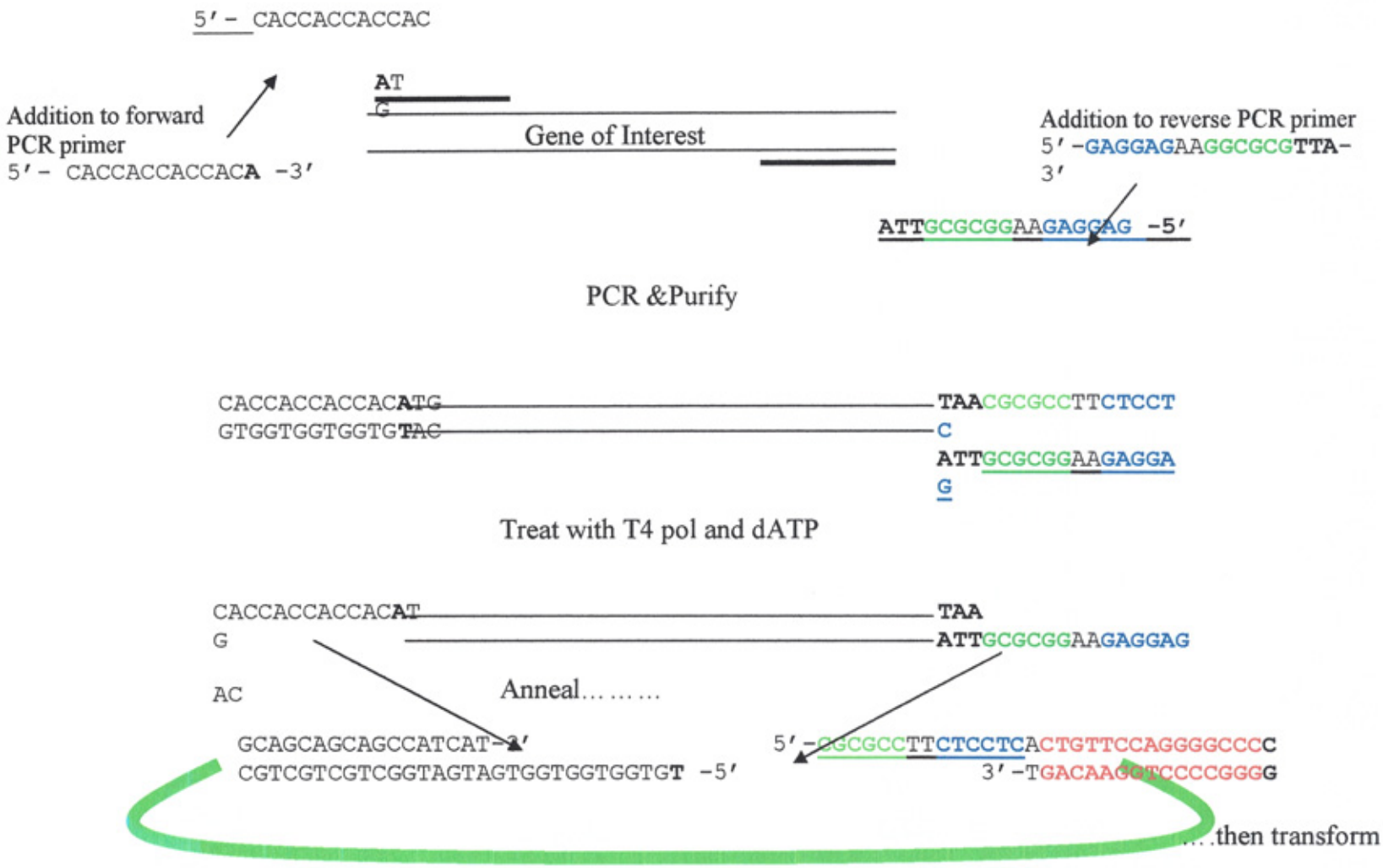

Figure IIG Annealing the LIC vector with the insert

Appendix III

Protein crystallisation screens
Solutions used to screen for crystal development are shown in Tables IIIA, IIIB, IIIC, IIID andIIIE.
IIIA and IIIB are called Clear Strategy Screen (CSS) I and II respectively from Molecular Dimensions

CSS I
Table IIIA: CSS I components

Tube Number	Salt	Precipitant
1	0.3M Sodium acetate	25% (w/v)PEG 2Kmme
2	0.2M Lithium Sulphate	25% (w/v)PEG 2Kmme
3	0.2M Magnesium Chloride	25% (w/v)PEG 2Kmme
4	0.2M Potassium Bromide	25% (w/v) PEG 2Kmme
5	0.2M Potassium Thiocyanate	25% (w/v) PEG 2Kmme
6	0.8M Sodium Formate	25% (w/v) PEG 2Kmme
7	0.3M Sodium Acetate	15% (w/v) PEG 4K
8	0.2M Lithium Sulphate	15% (w/v) PEG 4K
9	0.2Mmagnesium Chloride	15% (w/v) PEG 4K
10	0.2M Potassium Bromide	15% (w/v) PEG 4K
11	0.2M Potassium Thiocyanate	15% (w/v) PEG 4K
12	0.8M Sodium Formate	15% (w/v) PEG 4K
13	0.3M Sodium Acetate	10% (w/v) PEG 8K, 10%(w/v) PEG 1K
14	0.2M Lithium Sulphate	10% (w/v) PEG 8K, 10%(w/v) PEG 1K
15	0.2Mmagnesium Chloride	10% (w/v) PEG 8K, 10%(w/v) PEG 1K
16	0.2M Potassium Bromide	10% (w/v) PEG 8K, 10%(w/v) PEG 1K
17	0.2M Potassium Thiocyanate	10% (w/v) PEG 8K, 10%(w/v) PEG 1K
18	0.8M Sodium Formate	10% (w/v) PEG 8K, 10%(w/v) PEG 1K
19	0.3M Sodium Acetate	8% (w/v)PEG 20K, 8% (w/v) PEG 550mme
20	0.2M Lithium Sulphate	8% (w/v)PEG 20K, 8% (w/v) PEG 550mme
21	0.2Mmagnesium Chloride	8% (w/v)PEG 20K, 8% (w/v) PEG 550mme
22	0.2M Potassium Bromide	8% (w/v)PEG 20K, 8% (w/v) PEG 550mme
23	0.2M Potassium Thiocyanate	8% (w/v)PEG 20K, 8% (w/v) PEG 550mme
24	0.8M Sodium Formate	8% (w/v)PEG 20K, 8% (w/v) PEG 550mme

CSS II

Table IIIB: CSS II components.

Tube Number	Salt	Precipitant
1	1.5M Ammonium Sulphate	
2	0.8M Lithium Sulphate	
3	2M Sodium Formate	
4	0.5M Potassium dihydrogen Phosphate	
5	0.2M Calcium Acetate	25% (w/v) PEG 2Kmme
6	0.2M Calcium Acetate	15% (w/v) PEG 4Kmme
7	2.7M Ammonium Sulphate	
8	1.8M Lithium Sulphate	
9	4M Sodium Formate	
10	1M Potassium dihydrogen Phosphate	
11	0.2M Calcium Acetate	10% (w/v) PEG 8K, 10%(w/v) PEG 1K
12	0.2M Calcium Acetate	8% (w/v) PEG 20K, 8% (w/v) PEG550mme
13		40% (v/v) MPD
14		40% (v/v) 2,3-Butane-diol
15	5mM Calcium Chloride	20% (w/v) PEG 4K
16	0.15M Potassium Thiocynate	20% (w/v) PEG 550mme
17	0.15M Potassium Thiocynate	20% (w/v) PEG 600
18	0.15M Potassium Thiocynate	20% (w/v) PEG 1500
19		35% (v/v) Isopropanol
20		30% (v/v) Jeffamine 600M pH 6.5
21	5mM Nickel Chloride	20% (w/v) PEG 4K
22	0.15M Potassium Thiocynate	18% (w/v) PEG 3350
23	0.15M Potassium Thiocynate	18% (w/v) PEG 5mme
24	0.15M Potassium Thiocynate	15% (w/v) PEG 6K

Hampton screen I

Table IIIC: Hampton screen I components

Tube number	Salt	Buffer	Precipitant
1	0.02M Cacium chloride dihydrate	0.1M Sodium Acetate trihydrate pH 4.6	30% (v/v) 2-Methyl-2,4-pentanediol
2			0.4M Potassium Sodium Tartrate tetrahydrate
3			0.4M Ammonium dihydrogen Phosphate
4		0.1M Tris Hydrochloride pH 8.5	2M Ammonium Sulphate
5	0.2M tri-Sodium Citrate dihydrate	0.1M HEPES Sodium pH7.5	30% (v/v) 2-Methyl-2,4-pentanediol
6	0.2M Magnesium Chloride hexahydrate	0.1M Tris Hydrochloride pH 8.5	30% (w/v) PEG 4000
7		0.1M Sodium Cacodylate pH 6.5	1.4M Sodium Acetate trihydrate
8	0.2M tri-Sodium Citrate dihydrate	0.1M Sodium Cacodylate pH 6.5	30% (v/v) Isopropanol
9	0.2M Ammonium Acetate	0.1M tri-Sodium Citrate dihydrate pH5.6	30% (w/v) PEG 4000
10	0.2M Ammonium Acetate	0.1M Sodium Acetate trihydrate pH 4.6	30% (w/v) PEG 4000
11		0.1M tri-Sodium Citrate dihydrate pH5.6	1M Ammonium dihydrogen Phosphate
12	0.2M Magnesium Chloride hexahydrate	0.1M HEPES Sodium pH7.5	30% (v/v) Isopropanol
13	0.2M tri-Sodium Citrate dihydrate	0.1M Tris Hydrochloride pH 8.5	30% (w/v) PEG 400
14	0.02M Cacium chloride dihydrate	0.1M HEPES Sodium pH7.5	28% (w/v) PEG 400
15	0.2M Ammonium Sulphate	0.1M Sodium Cacodylate pH 6.5	30% (w/v) PEG 8000
16		0.1M HEPES Sodium pH7.5	1.5M Lithium Sulphate monohydrate
17	0.2M Lithium Sulphate monohydrate	0.1M Tris Hydrochloride pH 8.5	30% (w/v) PEG 4000
18	0.2M Magnesium Acetate tetrahydrate	0.1M Sodium Cacodylate pH 6.5	20% (w/v) PEG 8000
19	0.2M Ammonium	0.1M Tris	30% (v/v)

	Acetate	Hydrochloride pH 8.5	Isopropanol
20	0.2M Ammonium Sulphate	0.1M Sodium Acetate trihydrate pH 4.6	25% (w/v) PEG 4000
21	0.2M Magnesium Acetate tetrahydrate	0.1M Sodium Cacodylate pH 6.5	30% (v/v) 2-Methyl-2,4-pentanediol
22	0.2M Sodium Acetate trihydrate	0.1M Tris Hydrochloride pH 8.5	30% (w/v) PEG 4000
23	0.2M Magnesium Chloride hexahydrate	0.1M HEPES Sodium pH7.5	30% (w/v) PEG 400
24	0.02M Cacium chloride dihydrate	0.1M Sodium Acetate trihydrate pH 4.6	20% (v/v) Isopropanol
25		0.1M Imidazole pH 6.5	1M Sodium Acetate trihydrate
26	0.2M Ammonium Acetate	0.1M tri-Sodium Citrate dihydrate pH5.6	30% (v/v) 2-Methyl-2,4-pentanediol
27	0.2M tri-Sodium Citrate dihydrate	0.1M HEPES Sodium pH7.5	20% (v/v) Isopropanol
28	0.2M Sodium Acetate trihydrate	0.1M Sodium Cacodylate pH 6.5	30% (w/v) PEG 8000
29		0.1M HEPES Sodium pH7.5	0.8M Potassium Sodium Tartrate tetrahydrate
30	0.2M Ammonium Sulphate		30% (w/v) PEG 8000
31	0.2M Ammonium Sulphate		30% (w/v) PEG 4000
32			2M Ammonium Sulphate
33			4M Sodium Formate
34		0.1M Sodium Acetate trihydrate pH 4.6	2M Sodium Formate
35		0.1M HEPES Sodium pH7.5	0.8M Sodium dihydrogen Phosphate, 0.8M Potassium dihydrogen Phosphate
36		0.1M Tris Hydrochloride pH 8.5	8% (w/v) PEG 8000
37		0.1M Sodium Acetate trihydrate pH 4.6	8% (w/v) PEG 4000
38		0.1M HEPES Sodium pH7.5	1.4M tri-Sodium Citrate dihydrate
39		0.1M HEPES Sodium pH7.5	2% (v/v) PEG 400, 2M Ammonium Sulphate
40		0.1M tri-Sodium Citrate dihydratpH5.6	20% (v/vIsopropanol, 20% (w/v) PEG 4000
41		0.1M HEPES Sodium	10% (v/v)

		pH7.5	Isopropanol, 20% (w/v) PEG 4000
42	0.05M Potassium dihydrogen Phosphate		20% (w/v) PEG 8000
43			30% (w/v) PEG 1500
44			0.2M Magnesium Formate
45	0.2M Zinc Acetate dihydrate	0.1M Sodium Cacodylate pH 6.5	18% (w/v) PEG 8000
46	0.2M Cacium Acetate hydrate	0.1M Sodium Cacodylate pH 6.5	18% (w/v) PEG 8000
47		0.1M Sodium Acetate trihydrate pH 4.6	2M Ammonium Sulphate
48		0.1M Tris Hydrochloride pH 8.5	2M Ammonium dihydrogen Phosphate

Hampton screen II

Table IIID: Hampton screen II components.

Tube Number	Salt	Buffer	Precipitant
1	2M Sodium Chloride		10% (w/v) PEG 6000
2	0.5M Sodium Chloride; 0.1M Magnesium Chloride hexahydrate		0.01M Hexadecyltrimethylammonium Bromide
3			25% (v/v) Ethylene Glycol
4			35% (v/v) Dioxane
5	2M Ammonium Sulphate		5% (v/v) Isopropanol
6			1M Imidazole pH 7.0
7			10% (w/v) PEG 1000; 10% (w/v) PEG 8000
8	1.5M Sodium Chloride		10% (v/v) Ethanol
9		0.1M Sodium Acetate trihydrate pH 4.6	2M Sodium Chloride
10	0.2M Sodium Chloride	0.1M Sodium Acetate trihydrate pH 4.6	30% (v/v) MPD
11	0.01M Cobaltous Chloride hexahydrate	0.1M Sodium Acetate trihydrate pH 4.6	1M 1,6 Hexanediol
12	0.1M Cadmium Chloride dihydrate	0.1M Sodium Acetate trihydrate pH 4.6	30% (v/v) PEG 400
13	0.2M Ammonium Sulphate	0.1M Sodium Acetate trihydrate pH 4.6	
14	0.2M Potassium Sodium Tartrate tetrahydrate	0.1M tri Sodium Citrate dihydrate pH 5.6	2M Ammonium Sulphate
15	0.5M Ammonium Sulphate	0.1M tri Sodium Citrate dihydrate pH	1M Lithium Sulphate monohydrate

		5.6	
16	0.5M Sodium Chloride	0.1M tri Sodium Citrate dihydrate pH 5.6	2% (w/v) Ethylene Imine Polymer
17		0.1M tri Sodium Citrate dihydrate pH 5.6	35% (v/v) tert-Butanol
18	0.01M Ferric Chloride hexahydrate	0.1M tri Sodium Citrate dihydrate pH 5.6	10% (v/v) Jeffamine M-600
19		0.1M tri Sodium Citrate dihydrate pH 5.6	2.5M 1,6 Hexanediol
20		0.1M MES pH 6.5	1.6M Magnesium Sulphate heptahydrate
21	0.1M Sodium dihydrogen Phosphate; 0.1M Potassium dihydrogen Phosphate	0.1M MES pH 6.5	2M Sodium Chloride
22		0.1M MES pH 6.5	12% (w/v) PEG 20000
23	1.6M Ammonium Sulphate	0.1M MES pH 6.5	10% (v/v) Dioxane
24	0.05M Caesium Chloride	0.1M MES pH 6.5	30% (v/v) Jeffamine M-600
25	0.01M Cobaltous Chloride hexahydrate	0.1M MES pH 6.5	1.8M Ammonium Sulphate
26	0.2M Ammonium Sulphate	0.1M MES pH 6.5	30% (w/v) PEG 5000mme
27	0.01M Zinc Sulphate heptahydrate	0.1M MES pH 6.5	25% (w/v) PEG 550mme
28			1.6M tri-Sidium Citrate dihydrate pH 6.5
29	0.5M Ammonium Sulphate	0.1M HEPES pH7.5	30% (v/v) MPD
30		0.1M HEPES pH7.5	10% (w/v) PEG 6000; 5% (v/v) MPD
31		0.1M HEPES pH7.5	20% (v/v) Jeffamine M-600
32	0.1M Sodium Chloride	0.1M HEPES pH7.5	1.6M Ammonium Sulphate

33		0.1M HEPES pH7.5	2M Ammonium Formate
34	0.05M Cadmium Chloride hydrate	0.1M HEPES pH7.5	1?M Sodium Acetate trihydrate
35		0.1M HEPES pH7.5	70% (v/v) MPD
36		0.1M HEPES pH7.5	4.3M Sodium Chloride
37		0.1M HEPES pH7.5	10% (w/v) PEG 8000; 8% (v/v) Ethylene Glycol
38		0.1M HEPES pH7.5	20% (w/v) PEG 10000
39	0.2M Magnesium Chloride hexahydrate	0.1M Tis pH 8.5	3.4M 1,6 Hexanediol
40		0.1M Tis pH 8.5	25% (v/v) tetra- Butanol
41	0.01M Nickle (II) Chloride hexahydrate	0.1M Tis pH 8.5	1M Lithium Sulphate monohydrate
42	1.5M Ammonium Sulphate	0.1M Tis pH 8.5	12% (v/v) Glycerol anhydrous
43	0.2M Ammonium dihydrogen Phosphate	0.1M Tis pH 8.5	50% (v/v) MPD
44		0.1M Tis pH 8.5	20% (v/v) Ethanol
45	0.01M Nickle (II) Chloride hexahydrate	0.1M Tis pH 8.5	20% (w/v) PEG 20000mme
46	0.1M Sodium Chloride	0.1M Bicine pH 9.0	20% (w/v) PEG 550mme
47		0.1M Bicine pH 9.0	2M Magnesium Chloride hexahydrate
48		0.1M Bicine pH 9.0	2% (v/v) Dioxane; 20% (w/v) PEG 20000mme 10% (w/v) PEG 20000

PEG ion screen

Table IIIE: PEG ion screen components.

Tube number	Salt	Precipitant
1	0.2M Sodium Fluoride	20% (w/v) PEG 3350
2	0.2M Potassium Fluoride	20% (w/v) PEG 3350
3	0.2M Ammonium Fluoride	20% (w/v) PEG 3350
4	0.2M Lithium Chloride anhydrous	20% (w/v) PEG 3350
5	0.2M Magnesium Chloride hexahydrate	20% (w/v) PEG 3350
6	0.2M Sodium Chloride	20% (w/v) PEG 3350
7	0.2M Calcium Chloride dihydrate	20% (w/v) PEG 3350
8	0.2M Potassium Chloride	20% (w/v) PEG 3350
9	0.2M Ammonium Chloride	20% (w/v) PEG 3350
10	0.2M Sodium Iodide	20% (w/v) PEG 3350
11	0.2M Potassium Iodide	20% (w/v) PEG 3350
12	0.2M Ammonium Iodide	20% (w/v) PEG 3350
13	0.2M Sodium Thiocyanate	20% (w/v) PEG 3350
14	0.2M PotassiumThiocyanate	20% (w/v) PEG 3350
15	0.2M Lithium Nitrate	20% (w/v) PEG 3350
16	0.2M Magnesium Nitrate hexahydrate	20% (w/v) PEG 3350
17	0.2M Sodium Nitrate	20% (w/v) PEG 3350
18	0.2M Potassium Nitrate	20% (w/v) PEG 3350
19	0.2M Ammonium Nitrate	20% (w/v) PEG 3350
20	0.2M Magnesium Formate	20% (w/v) PEG 3350
21	0.2MSodium Formate	20% (w/v) PEG 3350
22	0.2M Potassium Formate	20% (w/v) PEG 3350
23	0.2M Ammonium Formate	20% (w/v) PEG 3350
24	0.2M Lithium Acetate dihydrate	20% (w/v) PEG 3350
25	0.2M Magnesium Acetate tetrahydrate	20% (w/v) PEG 3350
26	0.2M ZincAcetate dihydrate	20% (w/v) PEG 3350
27	0.2M Sodium Acetate trihydrate	20% (w/v) PEG 3350
28	0.2M Calcium Acetate hydrate	20% (w/v) PEG 3350
29	0.2M Potassium Acetate	20% (w/v) PEG 3350
30	0.2M Ammonium Acetate	20% (w/v) PEG 3350
31	0.2M Lithium Sulphate monohydrate	20% (w/v) PEG 3350
32	0.2M Magnesium Sulphate heptahydrate	20% (w/v) PEG 3350
33	0.2M Sodium Sulphate decahydrate	20% (w/v) PEG 3350
34	0.2M Potassium Sulphate	20% (w/v) PEG 3350
35	0.2M Ammonium Sulphate	20% (w/v) PEG 3350

36	0.2M di-Sodium tartrate dihydrate	20% (w/v) PEG 3350
37	0.2M PotassiumSodium tartrate tetrahydrate	20% (w/v) PEG 3350
38	0.2M di-Ammonium Tartrate	20% (w/v) PEG 3350
39	0.2M Sodium dihydrogen Phosphate monohydrate	20% (w/v) PEG 3350
40	0.2M di-Sodium hydrogen Phosphate dihydrate	20% (w/v) PEG 3350
41	0.2M Potassium dihydrogen Phosphate	20% (w/v) PEG 3350
42	0.2M di-Potassium hydrogen Phosphate	20% (w/v) PEG 3350
43	0.2M Ammonium dihydrogen Phosphate	20% (w/v) PEG 3350
44	0.2M di-Ammonium hydrogen Phosphate	20% (w/v) PEG 3350
45	0.2M tri Lithium Citrate tetrahydrate	20% (w/v) PEG 3350
46	0.2M tri-Sodium Citrate dihydrate	20% (w/v) PEG 3350
47	Tri-Potassium Citrate monohydrate	20% (w/v) PEG 3350
48	0.2M di-Ammonium hydrogen Citrate	20% (w/v) PEG 3350

Appendix IV

Equipment

IVA: Autoclaving
Autoclave sterilization was achieved using a benchtop Prestige® Medical 2100 Classic autoclave at 121 C, 32 lb/inch pressure for 20 min.

IVB: Incubators
For the growth of bacteria in liquid culture a GallenKamp orbital shaker was used. Growth of bacteria on solid media was performed in a static GallenKamp incubator. Crystal growth was carried out in a LMS cooled incubator.

IVC: Centrifugation
Centrifugation of volumes below 1.5 ml was achieved using small Sigma* 1-15 bench top micro-centrifuge. Volumes above 1.5 ml were centrifuged in a large Sigma* 3K18C refrigerated bench top centrifuge, using the rotors and inserts suitable to the application (Table IVC).

Table IVC: Centrifuge rotors, vessels and applications.

Rotor	Vessel containing solution	Insert	RCF	Application
11133	25ml plastic universal	Clay universal holder (part N 17049)	2700	Concentration of cells in preparation for compotent cells
11133	30KDa cut-off protein concentrator (Amicon)	Clay universal holder (part N 17049)	3000	Concentration of protein
11133	200ml plastic centrifuge vessel (part N 15202)	None	5500	Concentration of cells
12158	30ml plastic centrifuge tube CEN9534(part N 3119-0030)	None	24000	Separation of soluble cell extract, from lysed cells
12131	1.5 ml microcentrifuge tube	None	24000	Isolation of pellet on crude plasmid extraction

IVD: Reaction vessels
Volums up to 0.2 ml were contained in 0.2 ml micro-centrifuge tubes (Starstedt), 0.2-1.5 ml volumes in 1.5 ml micro-centrifuge tubes (Starstedt) and for volumes .1.5 ml, 28 ml sterile plastic universal containers were used (Fisherbrand®).

IVE: Freeze drier
Proteins and substrates were lyophilised using the Christ® Alpha 1-2 freeze drier.

IVF: pH meter
All adjustments to the pH of solutions and media were attained using a Jenway Ion Meter 3340 calibrated with buffers at pH 4, 7 and 9.2.

IVG: Agarose gel kits
Electrophoresis of DNA was achieved using an Owl Scientific EASY-cast™ electrophoresis system powered by an E-C 570-90 E-C Apparatus Corporation power pack.

IVH: SDS-PAGE gel kit
Electrophoresis of proteins was achieved using a Bio-Rad Mini-PROTEAN® 3 Cell kit powered by an E-C 570-90 E-C Apparatus Corporation power pack.

IVI: Gel documentation
Visualisation of agarose and SDS-PAGE gels was achieved using a Bio-Rad gel Doc 2000 system and Quantity One ™ software. Hard copies of the gel picture were produced using a Mitsubishi Video Copy Processor Processor (Model P91), with Mitsubishi thermal paper (K65HM-$_{CE}$/High density type, 110 mm x 21 m).

IVJ: Sonication
Cell lysis was achieved using a MES Soniprep 150 ultra-sonication machine.

IVK: Large scale protein purification
For the large scale purification of proteins a FPLC® (Applied Biosystems) system was used equipped with the hardware shown in Table IVK, together with a EYELA Pump MP-3 peristaltic pump.

IVL: High performance anion exchange chromatography (HPAEC)
HPAEC analysis was performed on a Dionex DX 500 ion chromatography system (hardware detailed in Table IVL) equipped with PA-1column (4mm x 250mm).

IVM: Spectrophotometer
Spectrophotometric measurements were made using a UV visible Heλios α Spectronic Unicam spectrophotometer.

IVN: PCR machine
All PCR reactions were performed in an Eppendorf MasterCycler ™ PCR.

IVO: Microtitre plate reader
DNSA assays were measured A_{570} using a FL600 FAK microtiter plate reader (Bio-Tek Kontron Instruments Inc.) using Micro Tek OS software (MTK version 2.5).

Table: IVK Hardware used for large-scale protein purification

Hardware (AB)	Part number or code
Pumps x2	P-500
Conductivity meter	Conductivity monitor code N° 18-1500
UV visible Spectrophotometer	LKB- Uvicord VW 2251
Fraction collector	FRAC - 100

Table: IVL Hardware used in HPAEC analysis

Hardware (Dionex)	Part number or code
Auto-sampler	AS40
Gradient pump	GP50
UV detector	

Appendix V

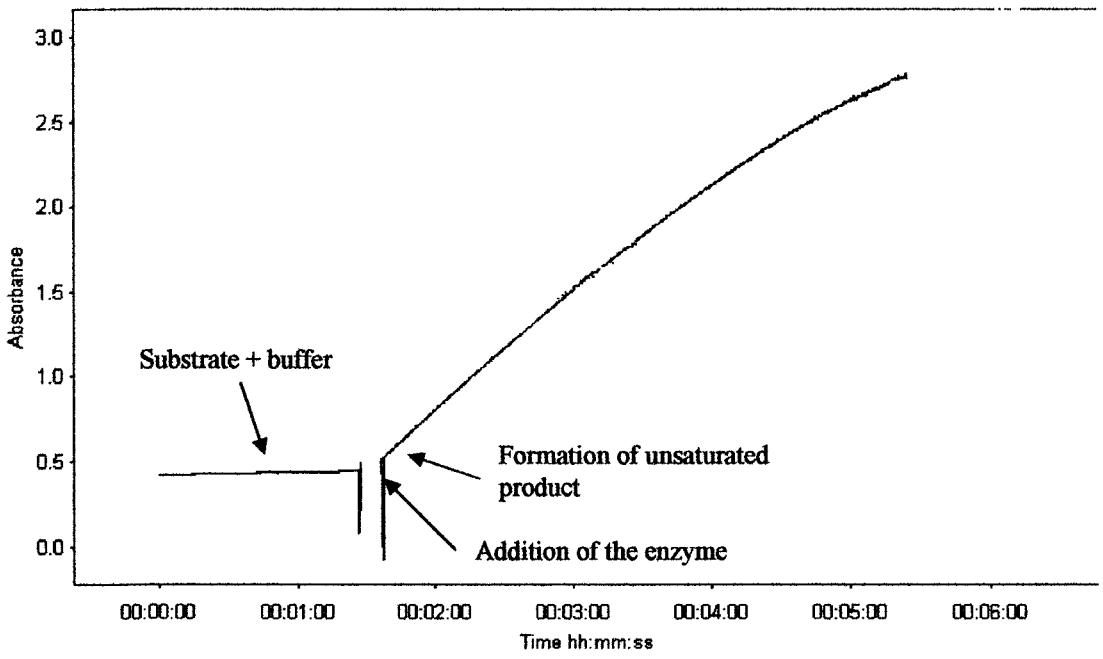

Figure VA The increase in the absorbance at 232 nm by SC1C2.15 against HA due to the formation of double bond. Reactions were performed in a total volume of 500 µl, and all components except the enzyme were pre-warmed to 37 °C in a heated holder within a spectrophotometer pre-zeroed against water at 232 nm. The reaction was started by the addition of the enzyme. Data were then collected by observing an increase in absorbance at 232 nm due to the formation of a double bond by β-elimination and analysed using Vision 2000 software.

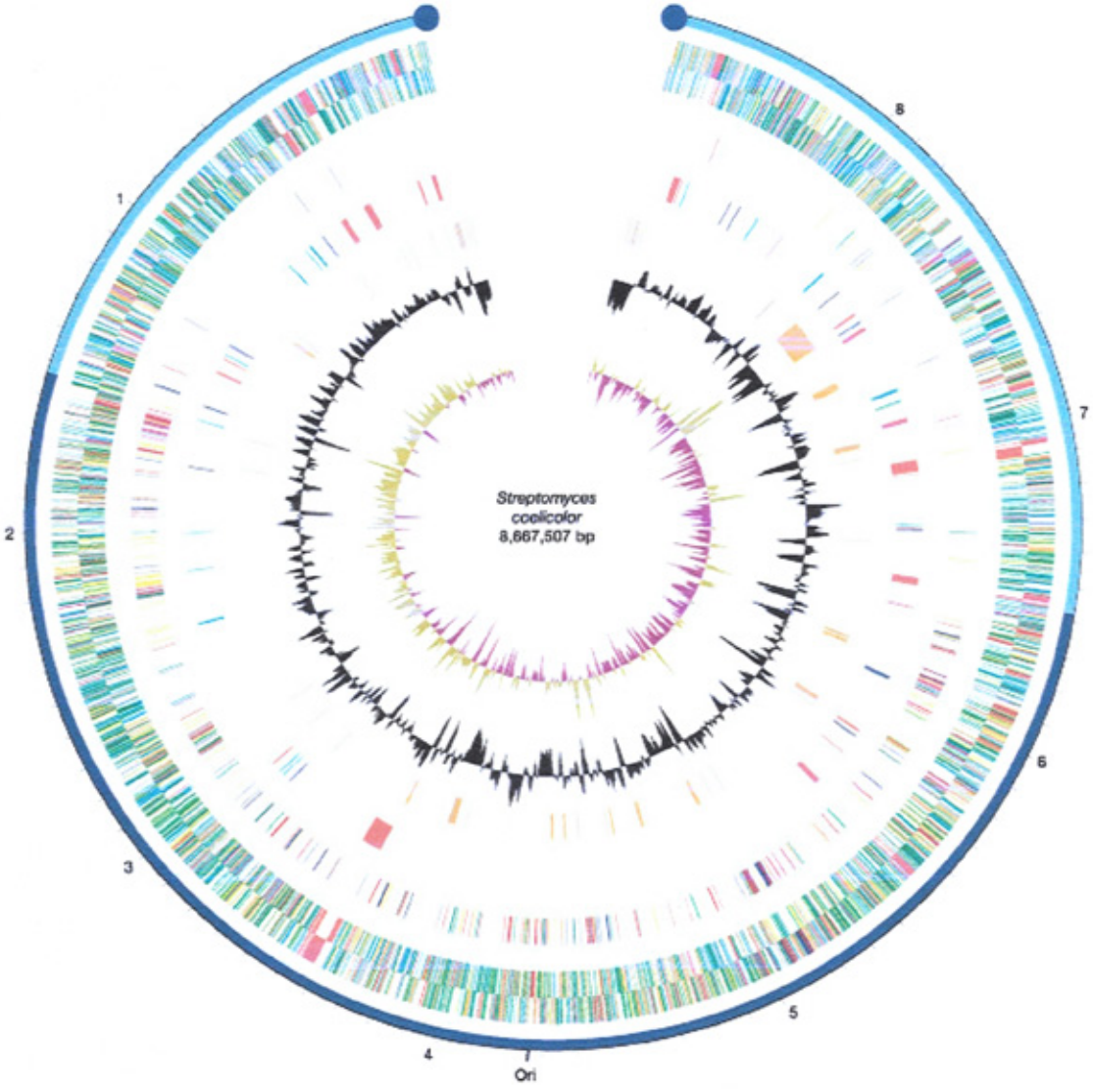

Figure VB *Streptomyces coelicolor* chromosome. The central part of the chromosome, shown in blue, has been reported to carry mainly 'house-keeping' genes, whereas both arms, in cyan, encode mostly adaptive functions. The size scale (in Mbp) and position of the *oriC* origin of replication are indicated.

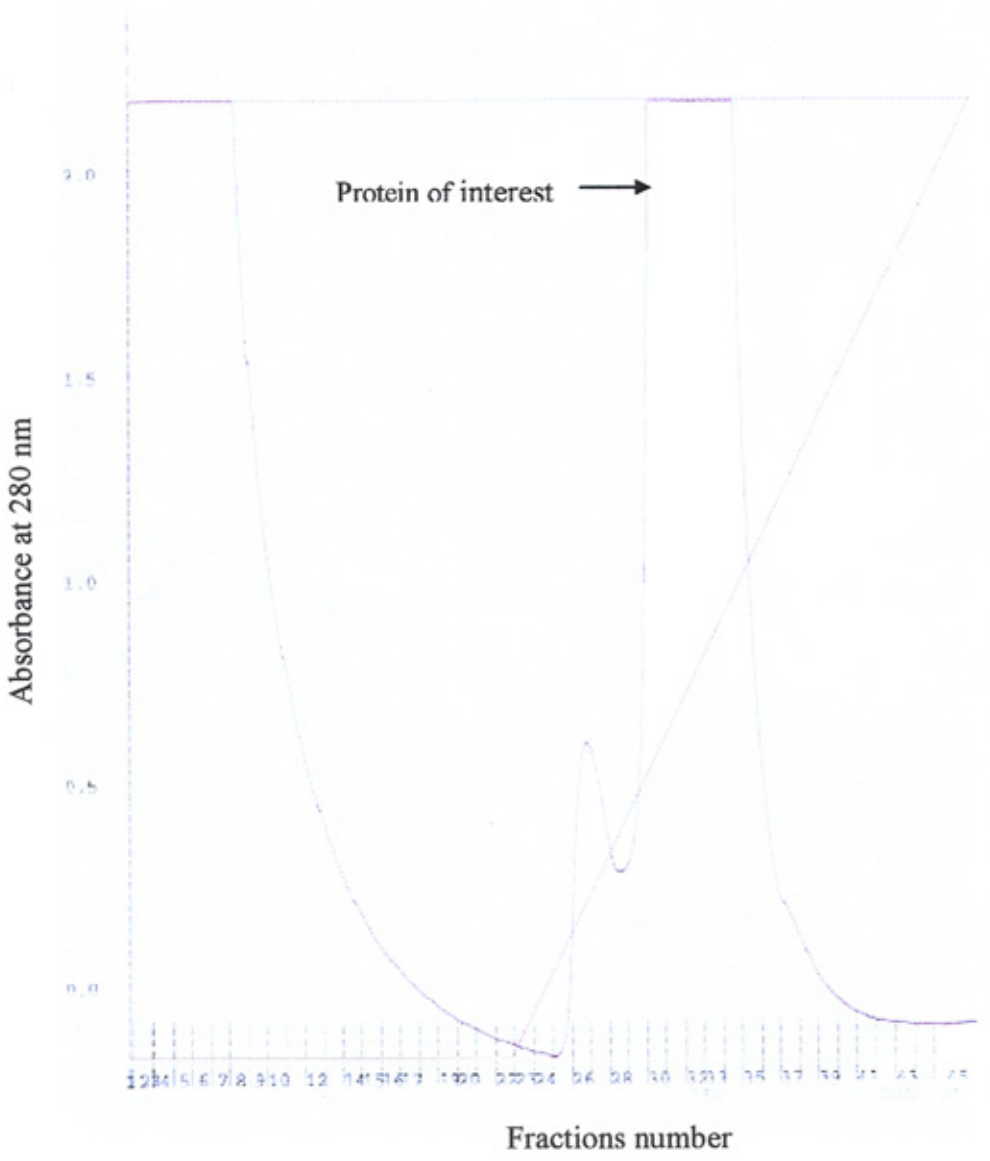

Figure VC: purification of hyluronate lyase of *S. coelicolor* by IMAC.

Cell free extract was loaded onto the column and then washed with 100 ml of starting buffer at a flow rate of 5 ml min^{-1}. Finally the protein was eluted at a flow rate of 5 ml min^{-1} using a linear gradient of imidazole extending from 10 mM to 500 mM. The position of the target protein was determined by monitoring absorbance at 280 nm using an inline UV spectrometer connected to the FPLC, and samples were collected in 5 ml volumes on a fraction collector. The fractions numbers are shown on the x-axis.

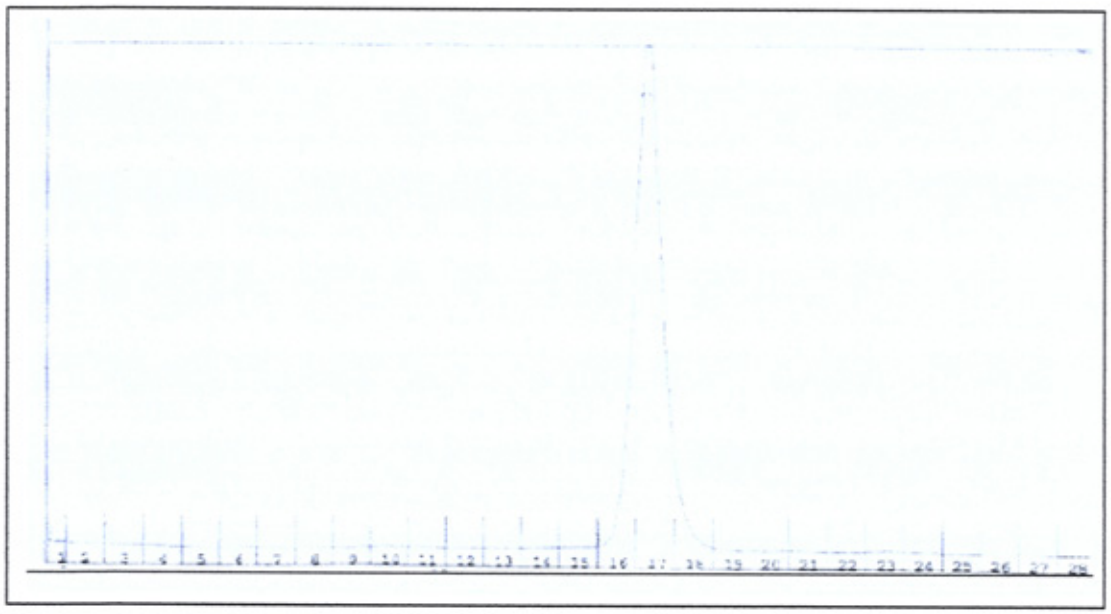

Figure VD: purification of hyluronate lyase of *S. coelicolor* by gel filtration chromatography. A sample of 0.5 ml of concentrated protein was loaded onto the column pre – equilibrated with 10 mM Tris-HCl buffer (pH 8) containing 0.2 M NaCl. The column was eluted with the same buffer and fractions of 5 ml were collected at a flow rate of 1 ml min^{-1}. The elution point of the target protein (the peak) was identified by monitoring the absorbance at 280 nm using the inline UV spectrophotometer. The fractions numbers are shown on the x-axis.

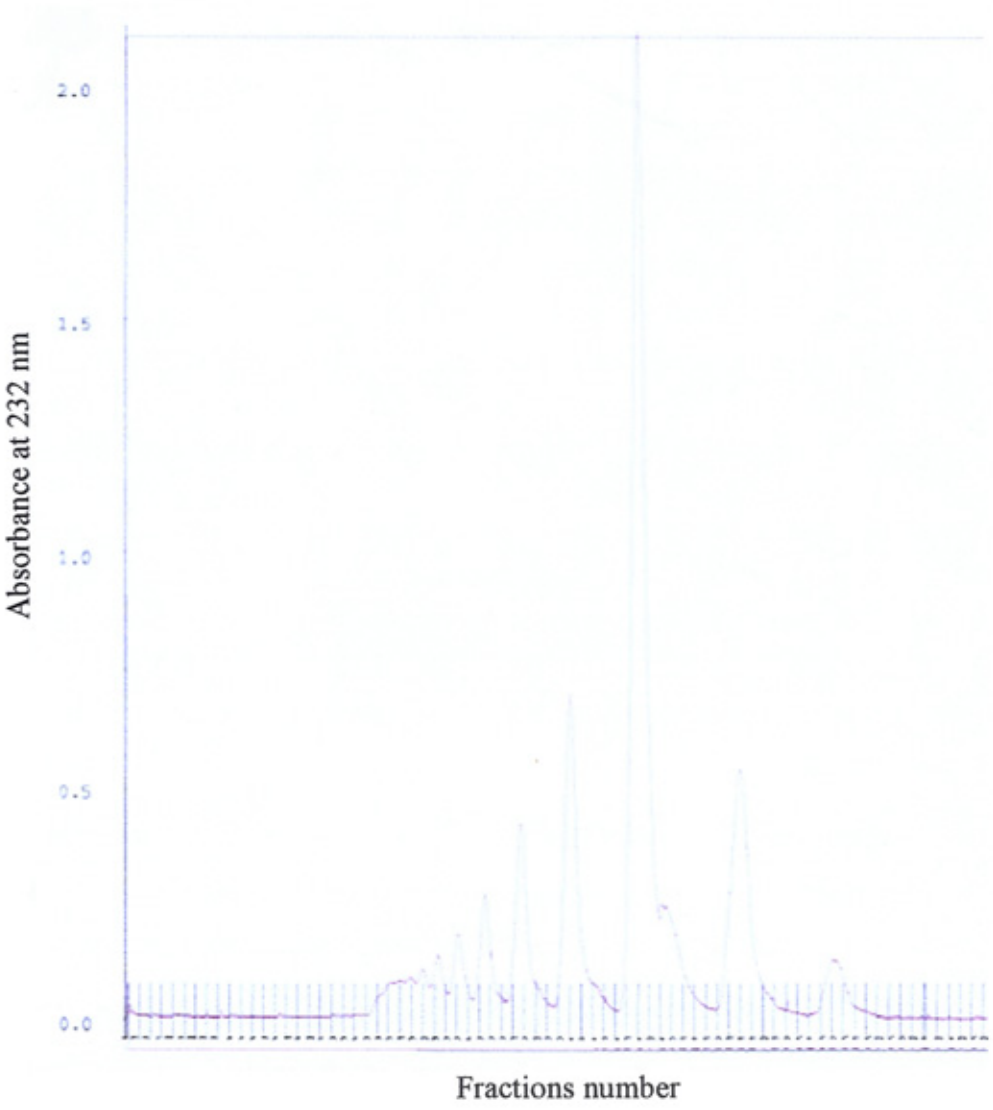

Figure VE: Purification of HA oligosaccharides by size exclusion chromatography. Oligosaccharides of HA (HA was partially digest with the hyaluronate lyase of *S. pyogenes*) were subjected to size exclusion chromatography on a Bio-Gel P-6 column. A sample of 0.5 ml of 20 min digestion (the digestion was lyophilised and dissolved in 0.5 ml of 0.5 M NaCl) was loaded onto the column pre–equilibrated with 0.5 ml NaCl and eluted in 0.5 ml NaCl at a flow rate of 0.1 ml min^{-1}. The eluent was monitored by absorbance at 232 nm using the inline UV spectrophotometer. The fractions numbers are shown on the x-axis. Fractions containing the same oligosaccharides were pooled.

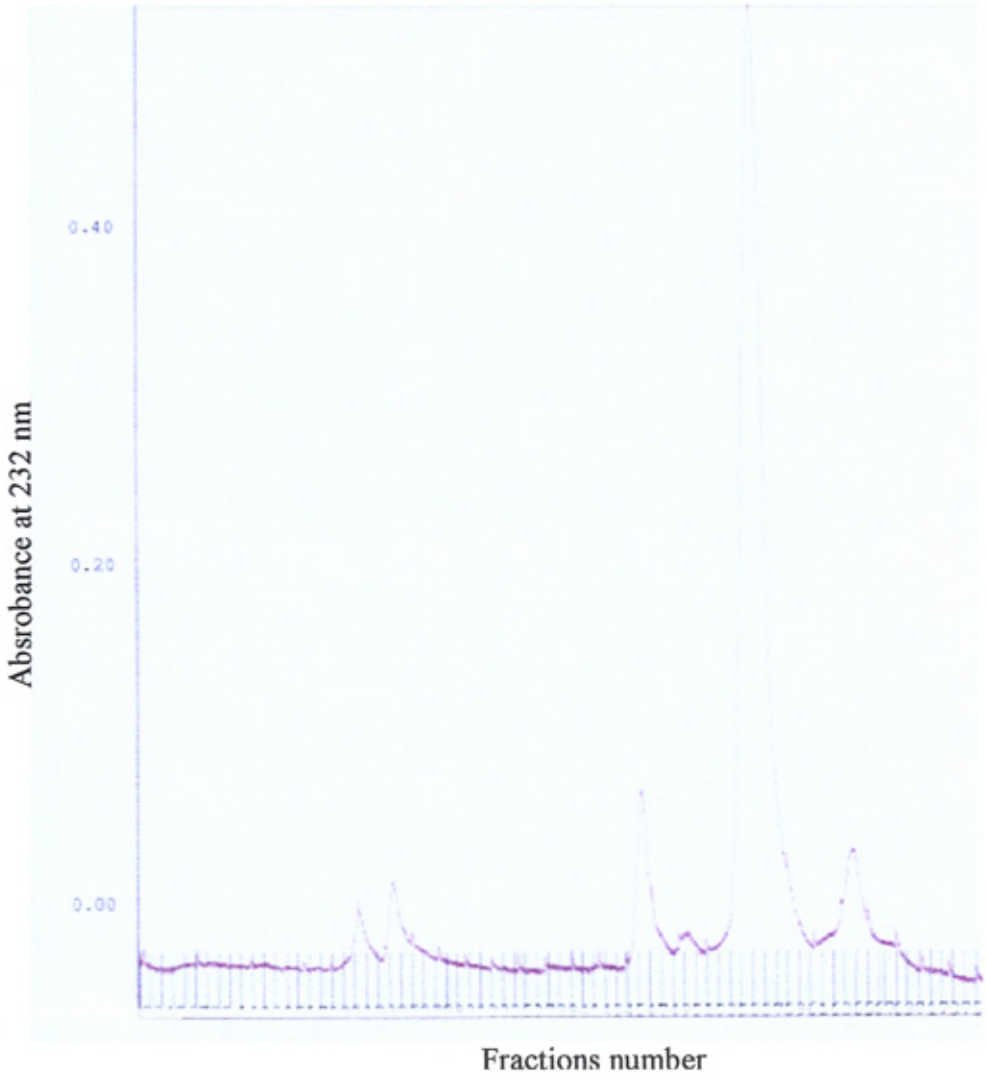

Figure VF: Purification of chondroitin-4-sulphate oligosaccharides by size exclusion chromatography. . Oligosaccharides of chondroitin-4-sulphate (digest with the hyaluronate lyase of *S. coelicolor*) were subjected to size exclusion chromatography on a Bio-Gel P-6 column. A sample of 0.5 ml of 20 min digestion (the digestion was lyophilised and dissolved in 0.5 ml of 0.5 M NaCl) was loaded onto the column pre–equilibrated with 0.5 ml NaCl and eluted in 0.5 ml NaCl at a flow rate of 0.1 ml min^{-1}. The eluent was monitored by absorbance at 232 nm using the inline UV spectrophotometer. The fractions are shown in black sticks. The fractions numbers are shown on the x-axis. Fractions containing the same oligosaccharides were pooled.

Appendix VI

Table VIA: Calculation the k_{cat} of SC1C2.15 toward sodium hyaluronate

conc	rate	M/min	M/min/mg	µM/min	µM/min/mg	µmoles/min	µmoles/min/mg enzyme	µmoles/min/µmole enzyme	1/v	1/s
0.125	0.988	0.0001796	0.149697	179.63636	149696.97	0.0898182	74.848485	6204.9394	0.0001612	8
0.25	1.042	0.0001895	0.1578788	189.45455	157878.79	0.0947273	78.939394	6544.0758	0.0001528	4
0.5	1.291	0.0002347	0.1956061	234.72727	195606.06	0.1173636	97.80303	8107.8712	0.0001233	2
1	1.381	0.0002511	0.2092424	251.09091	209242.42	0.1255455	104.62121	8673.0985	0.0001153	1
2	1.403	0.0002551	0.2125758	255.09091	212575.76	0.1275455	106.28788	8811.2652	0.0001135	0.5
			0		0		0	0	#DIV/0!	
0.125	0.945	0.0001718	0.1431818	171.81818	143181.82	0.0859091	71.590909	5934.8864	0.0001685	8
0.25	1.022	0.0001858	0.1548485	185.81818	154848.48	0.0929091	77.424242	6418.4697	0.0001558	4
0.5	1.275	0.0002318	0.1931818	231.81818	193181.82	0.1159091	96.590909	8007.3864	0.0001249	2
1	1.399	0.0002544	0.2119697	254.36364	211969.7	0.1271818	105.98485	8786.1439	0.0001138	1
2	1.473	0.0002678	0.2231818	267.81818	223181.82	0.1339091	111.59091	9250.8864	0.0001081	0.5
			0		0		0	0	#DIV/0!	
0.125	0.931	0.0001693	0.1410606	169.27273	141060.61	0.0846364	70.530303	5846.9621	0.000171	8
0.25	1.177	0.000214	0.1783333	214	178333.33	0.107	89.166667	7391.9167	0.0001353	4
0.5	1.358	0.0002469	0.2057576	246.90909	205757.58	0.1234545	102.87879	8528.6515	0.0001173	2
1	1.373	0.0002496	0.2080303	249.63636	208030.3	0.1248182	104.01515	8622.8561	0.000116	1
2	1.404	0.0002553	0.2127273	255.27273	212727.27	0.1276364	106.36364	8817.5455	0.0001134	0.5

Table VIB: Calculation the k_{cat} of SC1C2.15 toward chondroitin-4 sulphate

conc	rate	M/min	M/min/mg	µM/min	µM/min/mg	µmoles/min	µmoles/min/mg enzyme	µmoles/min/µmole enzyme	1/v	1/s
0.125	0.314	5.709E-05	0.0237879	57.090909	23787.879	0.0285455	10.194805	845.14935	0.0011832	8
0.25	0.437	7.945E-05	0.0331061	79.454545	33106.061	0.0397273	14.188312	1176.211	0.0008502	4
0.5	0.768	0.0001396	0.0581818	139.63636	58181.818	0.0698182	24.935065	2067.1169	0.0004838	2
1	0.859	0.0001562	0.0650758	156.18182	65075.758	0.0780909	27.88961	2312.0487	0.0004325	1
2	0.9	0.0001636	0.0681818	163.63636	68181.818	0.0818182	29.220779	2422.4026	0.0004128	0.5
			0		0		0	0	#DIV/0!	
0.125	0.316	5.745E-05	0.0239394	57.454545	47878.788	0.0287273	10.25974	850.53247	0.0011757	8
0.25	0.482	8.764E-05	0.0365152	87.636364	73030.303	0.0438182	15.649351	1297.3312	0.0007708	4
0.5	0.712	0.0001295	0.0539394	129.45455	107878.79	0.0647273	23.116883	1916.3896	0.0005218	2
1	0.783	0.0001424	0.0593182	142.36364	118636.36	0.0711818	25.422078	2107.4903	0.0004745	1
2	0.902	0.000164	0.0683333	164	136666.67	0.082	29.285714	2427.7857	0.0004119	0.5
			0		0		0	0	#DIV/0!	
0.125	0.301	5.473E-05	0.022803	54.727273	45606.061	0.0273636	9.7727273	810.15909	0.0012343	8
0.25	0.46	8.364E-05	0.0348485	83.636364	69696.97	0.0418182	14.935065	1238.1169	0.0008077	4
0.5	0.708	0.0001287	0.0536364	128.72727	107272.73	0.0643636	22.987013	1905.6234	0.0005248	2
1	0.813	0.0001478	0.0615909	147.81818	123181.82	0.0739091	26.396104	2188.237	0.000457	1
2	0.834	0.0001516	0.0631818	151.63636	126363.64	0.0758182	27.077922	2244.7597	0.0004455	0.5

Table VIC: Calculation the k_{cat} of SC1C2.15 toward chondroitin-6-sulphate

conc	rate	M/min	M/min/mg	µM/min	µM/min/mg	µmoles/min	µmoles/min/mg enzyme	µmoles/min/µmole enzyme	1/v	1/s
0.125	0.309	5.618E-05	0.0081423	56.181818	8142.2925	0.0280909	4.0711462	337.49802	0.002963	8
0.25	0.398	7.236E-05	0.0104875	72.363636	10487.484	0.0361818	5.2437418	434.70619	0.0023004	4
0.5	0.612	0.0001113	0.0161265	111.27273	16126.482	0.0556364	8.0632411	668.44269	0.001496	2
1	0.74	0.0001345	0.0194993	134.54545	19499.341	0.0672727	9.7496706	808.24769	0.0012372	1
2	0.888	0.0001615	0.0233992	161.45455	23399.209	0.0807273	11.699605	969.89723	0.001031	0.5
			0		0		0	0	#DIV/0!	
0.125	0.286	0.000052	0.0075362	52	7536.2319	0.026	3.7681159	312.37681	0.0032013	8
0.25	0.404	7.345E-05	0.0106456	73.454545	10645.586	0.0367273	5.3227931	441.25955	0.0022662	4
0.5	0.73	0.0001327	0.0192358	132.72727	19235.837	0.0663636	9.6179183	797.32543	0.0012542	2
1	0.759	0.000138	0.02	138	20000	0.069	10	829	0.0012063	1
2	0.886	0.0001611	0.0233465	161.09091	23346.509	0.0805455	11.673254	967.71278	0.0010334	0.5
			0		0		0	0	#DIV/0!	
0.125	0.283	5.145E-05	0.0074572	51.454545	7457.1805	0.0257273	3.7285903	309.10013	0.0032352	8
0.25	0.406	7.382E-05	0.0106983	73.818182	10698.287	0.0369091	5.3491436	443.44401	0.0022551	4
0.5	0.759	0.000138	0.02	138	20000	0.069	10	829	0.0012063	2
1	0.772	0.0001404	0.0203426	140.36364	20342.556	0.0701818	10.171278	843.19895	0.001186	1
2	0.886	0.0001611	0.0233465	161.09091	23346.509	0.0805455	11.673254	967.71278	0.0010334	0.5

Table VID: Calculation the k_{cat} of SC1C2.15 toward potassium hyaluronate

conc	rate	M/min	M/min/mg	µM/min	µM/min/mg	µmoles/min	µmoles/min/mg enzyme	µmoles/min/µmole enzyme	1/v	1/s
0.125	0.145	2.636E-05	0.0109848	26.363636	10984.848	0.0131818	5.4924242	455.32197	0.0021962	8
0.25	0.212	3.855E-05	0.0160606	38.545455	16060.606	0.0192727	8.030303	665.71212	0.0015022	4
0.5	0.289	5.255E-05	0.0218939	52.545455	21893.939	0.0262727	10.94697	907.50379	0.0011019	2
1	0.386	7.018E-05	0.0292424	70.181818	29242.424	0.0350909	14.621212	1212.0985	0.000825	1
2	0.414	7.527E-05	0.0313636	75.272727	31363.636	0.0376364	15.681818	1300.0227	0.0007692	0.5
			0		0			0	#DIV/0!	
0.125	0.134	2.436E-05	0.0101515	24.363636	20303.03	0.0121818	12.181818	1009.8727	0.0009902	8
0.25	0.212	3.855E-05	0.0160606	38.545455	32121.212	0.0192727	19.272727	1597.7091	0.0006259	4
0.5	0.289	5.255E-05	0.0218939	52.545455	43787.879	0.0262727	26.272727	2178.0091	0.0004591	2
1	0.402	7.309E-05	0.0304545	73.090909	60909.091	0.0365455	36.545455	3029.6182	0.0003301	1
2	0.456	8.291E-05	0.0345455	82.909091	69090.909	0.0414545	41.454545	3436.5818	0.000291	0.5
			0		0			0	#DIV/0!	
0.125	0.145	2.636E-05	0.0109848	26.363636	21969.697	0.0131818	13.181818	1092.7727	0.0009151	8
0.25	0.207	3.764E-05	0.0156818	37.636364	31363.636	0.0188182	18.818182	1560.0273	0.000641	4
0.5	0.278	5.055E-05	0.0210606	50.545455	42121.212	0.0252727	25.272727	2095.1091	0.0004773	2
1	0.382	6.945E-05	0.0289394	69.454545	57878.788	0.0347273	34.727273	2878.8909	0.0003474	1
2	0.424	7.709E-05	0.0321212	77.090909	64242.424	0.0385455	38.545455	3195.4182	0.0003129	0.5